Initial Stability of Press-fit Acetabular Components in Total Hip Replacements

Crosnier, Emilie

Award date:
2015

Awarding institution:
University of Bath

Initial Stability of Press-fit Acetabular Components in Total Hip Replacements

Emilie Aurélie Crosnier

Doctor of Philosophy

University of Bath

Department of Mechanical Engineering

February 2015

ACKNOWLEDGEMENTS

I would like to thank everyone who have made this thesis possible. Firstly, Prof Tony Miles and Prof Patrick Keogh for their invaluable guidance and support throughout my PhD. Nick Waywell, Duncan Scrivens and instrumentation for all their help with building the test rigs. I am grateful to the Victoria Wells studentship in collaboration with the Enid Linder Foundation for funding my PhD, and to Stryker for donating the acetabular cups. I would like to thank my friends, both at the University of Bath and around the world, for being there and providing distractions throughout the years. Finally, a special thanks to my family and Patrick, for being fantastic and supportive for far longer than these past few years!

ABSTRACT

The hip joint is subjected to cyclic loading and motion during activities of daily living, which can induce micromotion of total hip replacements. High levels of micromotion inhibit bone formation, and hence osseointegration of cementless implants. Initial stability is therefore crucial to ensure successful osseointegration of cementless acetabular cups. Hence, it is important to be able to measure the micromotion of acetabular cups *in vitro* in order to predict if they will survive once implanted.

There are no standardised methods to measure cup micromotion however there are numerous studies available in the literature. These studies have two main limitations: they only measure cup micromotion in the assumed dominant direction(s) of motion rather than in six degrees of freedom; and they overlook the effect of dynamic hip motion as the hip joint is held in a fixed position. Finally, most of these studies either use cadaveric pelvic bones or synthetic foam blocks with a hemispherical cavity, both of which have their advantages and limitations.

A new robust methodology capable of measuring cup micromotion in six degrees of freedom under cyclic loading and hip motion was developed, as well as a more representative synthetic acetabular model which replicated the structural support in the acetabulum.

A number of investigations were carried out using this protocol. The results indicated that hemispherical cavities used to model the acetabulum overestimate cup stability compared to the more representative model which replicated the natural acetabulum; there was a significant increase in cup micromotion under dynamic hip motion; and clinically relevant micromotions were present in all translations.

This novel protocol provides a better understanding of the behaviour of an implanted press-fit cup and the basis for more representative protocol for future pre-clinical evaluations of new design features that can improve cup fixation, and hence its longevity.

CONTENTS

FIGURES

TABLES

SYMBOLS AND ABBREVIATIONS

BW	Body Weight
CoCr	Cobalt Chrome
DoF	Degrees of Freedom
HA	Hydroxyapatite
LVDT	Linear Variable Differential Transformer
μ	Micro – $x10^{-6}$
SLS	Single Leg Stance
sd	Standard Deviation
θ	Theta – angle in degrees
THR	Total Hip Replacement

1. INTRODUCTION

Total Hip Replacement (THR) is one of the most successful and cost effective orthopaedic surgeries today, with over one million procedures performed worldwide every year [1]. It provides relief from pain and restores the natural function of the hip joint, allowing patients to return to a normal lifestyle. THR is a victim of its own success: with implant survival rates greater than 90% at ten years [2-5], the number of procedures performed constantly increases [6], especially in younger and more active patients [7]. The active life style of these younger patients means that implants need to last longer and under more demanding conditions. Hence, even in the best-case scenario, many younger patients will outlive their implant and may require one or more revision operation in their lifetime [7].

New types of implants are available each year, promising better outcomes and increased longevity compared to their predecessors and competitors. Pre-clinical *in vitro* testing attempts to screen out erroneous design philosophies before they are implanted into patients. However, as past events have shown, even the most pre-clinically tested prostheses can fail catastrophically. Hence, one must question the effectiveness of the standardised protocols performed during pre-clinical testing.

Aseptic loosening has been identified as the leading cause of THR failure, and is more common on the acetabular side than the femoral side [7-9]. The causes of aseptic loosening are multifactorial; however, initial stability of cementless acetabular cups has been highlighted as a crucial prerequisite for the long term survival of THR. High levels of micromotion at the bone-prosthesis interface can inhibit osseointegration, resulting in the premature loosening of the acetabular cup and hence revision surgery [10]. Even though a clear link has been drawn between initial stability and successful osseointegration of the acetabular cups, there is no standardised protocol available to investigate the level of micromotion, and hence the initial stability, of an implanted cementless acetabular cup.

The aim of this thesis was therefore to develop a new pre-clinical test protocol, which can measure the micromotion of cementless acetabular cups under physiological conditions to help predict if they will successfully osseointegrate once implanted. To do so, research was structured around three key aspects.

The first aspect concentrated on the literature review, which included background information on the hip joint and THR and a review of published studies assessing acetabular cup stability. This information was then used to define the physiological conditions within the hip joint that needed to be replicated, and to identify the most appropriate approach for the systematic assessment of acetabular cup micromotion.

The second aspect of this research was to develop a robust methodology for *in vitro* experimental assessment of acetabular cup micromotion. This included the development of a reliable system to measure the micromotion of an acetabular cup, the creation of a physiological acetabular model in which the cup is to be implanted, and the design of a dynamic hip motion simulator to replicate the conditions the hip joint is subjected to during

activities of daily living. The combination of these factors provided the basis for a more representative pre-clinical testing protocol.

The third, and final, aspect involved the experimental assessment of a new acetabular component by comparing it to its commonly used and clinically proven predecessor using the developed test protocol.

2. Background and Literature Review

2.1. Introduction

The hip joint is one of the largest and most important joints in the human body [11, 12]. It plays a key role in activities of daily living such as walking, running, jumping, rising from a chair etc. In addition to this, it bears the weight of the human body and the forces of the strong muscles present in the hip and the leg. The hip joint is also the most flexible joint in the body after the shoulder [12].

There are many factors that can cause degenerative changes to the hip joint, these include age related wear, disease and trauma. These can cause pain and restrict mobility, thereby turning activities of daily living into difficult and painful tasks.

Total hip replacement (THR) surgeries are performed to relieve pain and restore the normal anatomy of the hip joint following wear, disease or trauma, allowing patients to return to a normal lifestyle. THR is a successful procedure, however, implant failures still occur, in particular those associated with the acetabular component, resulting in the need for revision surgery.

In this chapter, the anatomy and biomechanics of the healthy hip joint are described. Total hip replacements are then presented; this includes indications for the procedure, the description of the implants currently used and the most common modes of failure. Finally, published pre-clinical test methodologies and studies investigating the important aspects of the initial stability of acetabular cups are assessed.

2.2. THE NATURAL HIP JOINT

The hip joint is a synovial joint comprising the femoral head and the acetabulum. The femoral head articulates within the acetabulum to form a multi-axis ball-and-socket joint (Figure 2.1). Its main function is to support and transmit the forces between the pelvis and the lower limb [11, 13, 14].

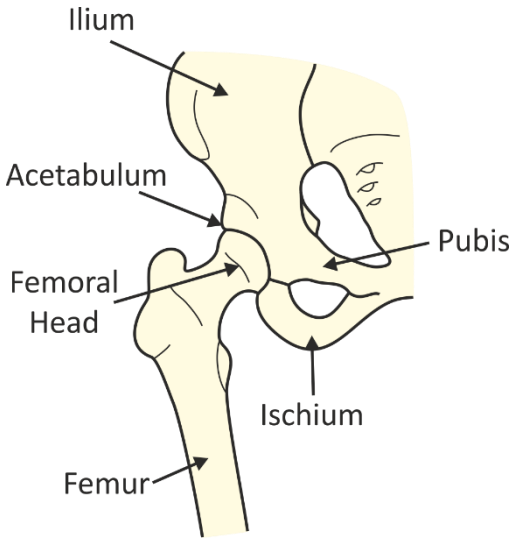

Figure 2.1 – The hip joint

In healthy individuals, a layer of cartilage covers both the femoral head and the acetabulum. The hip joint is surrounded by synovial fluid and surrounded by fibrous tissue forming the capsule. The cartilage acts as a bearing surface, both protecting the bone from damage and distributing the forces experienced during movement to achieve minimal wear over a lifetime. The combination of the cartilage and the synovial fluid, which acts as a lubricant, allows virtually frictionless movements of the hip joint [11, 13].

The hip joint is surrounded by large muscles, which allow for a wide range of motion (Figure 2.2). They include flexor (psoas major and iliacus) and extensor muscles (gluteus maximus and hamstring), abductors (gluteus medius and minimus) and adductors (adductors longus, medius and brevis), and external (obturator internus and externus, gemellus superior and inferior, and quadratus femoris) and internal (tensor fascia latae) rotators [11, 13].

The ligaments in the hip are present to reinforce and stabilise the hip joint as well as prevent excessive range of movement [11]. There are four extracapsular ligaments in the hip joint: the iliofemoral ligament, the ischiofemoral ligament, the pubofemoral ligament and the transverse acetabular ligament; and one intracapsular ligament: the ligamentum teres (Figure 2.3). The iliofemoral ligament is the strongest ligament in the human body and provides considerable constraint to the hip joint [11]. The transverse acetabular ligament binds the ends of the labrum by crossing the acetabular notch [11]. The purpose of the ligamentum teres is to hold the acetabulum to the femoral head together and to prevent further displacement following hip dislocation [11, 13].

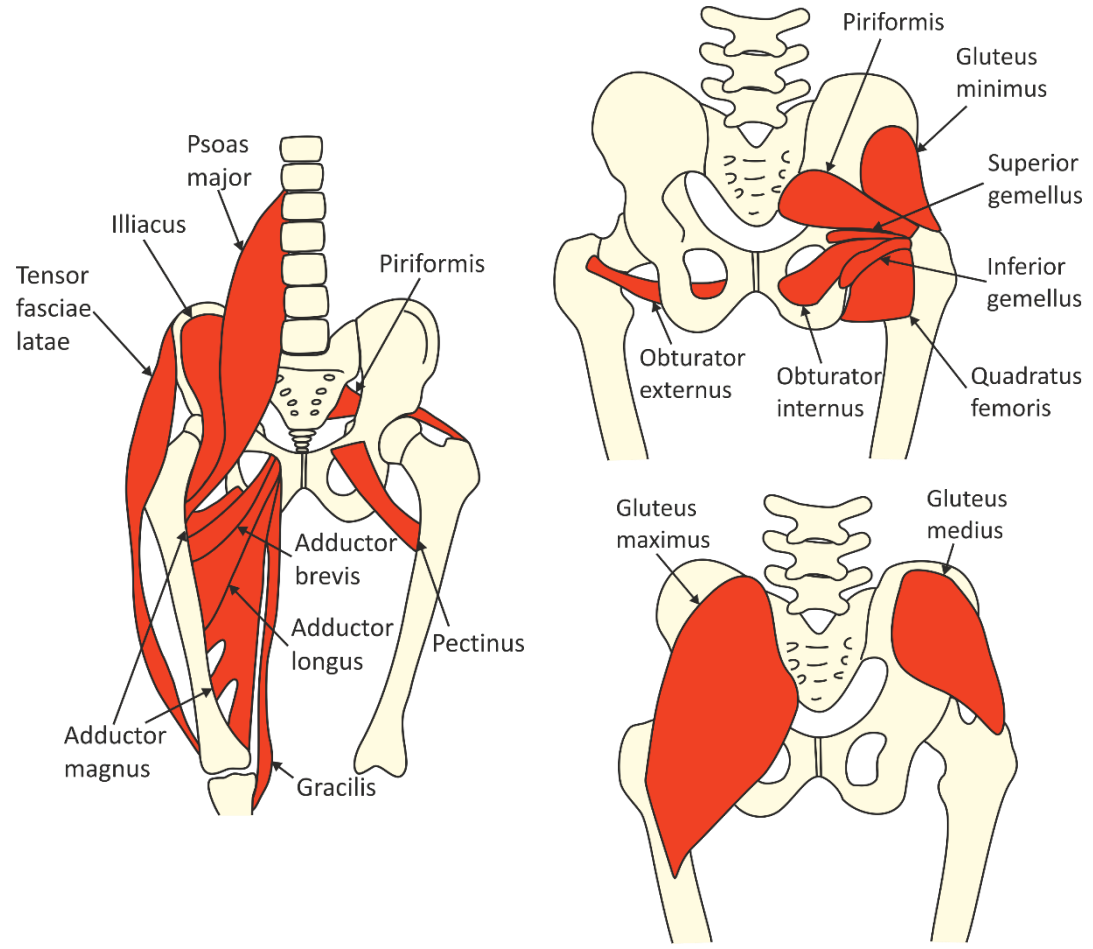

Figure 2.2 – Muscles of the hip joint (illustration modified from [15])

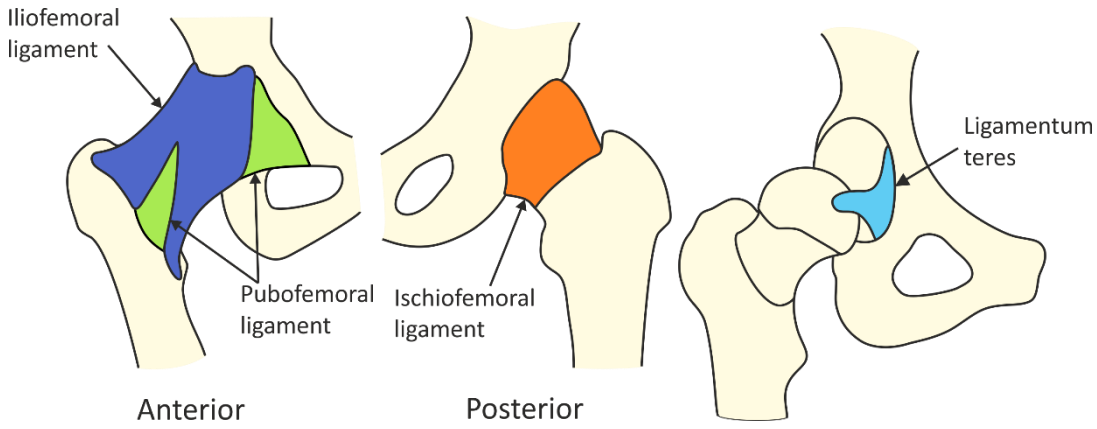

Figure 2.3 – Ligaments of the hip joint (illustrations based on [11])

2.2.1. THE FEMUR

The femur is the longest bone in the body. The femoral head forms two-thirds of a sphere and is the ball section of the hip joint (Figure 2.4). The femoral head is attached to the main body of the femur via the femoral neck. The angle between the femoral neck and shaft is approximately 125°. The distal part of the femur articulates with the tibia and the patella to form the knee joint. The femur is an important attachment site for various muscle groups which allow movement of the hip and knee joints [7, 11].

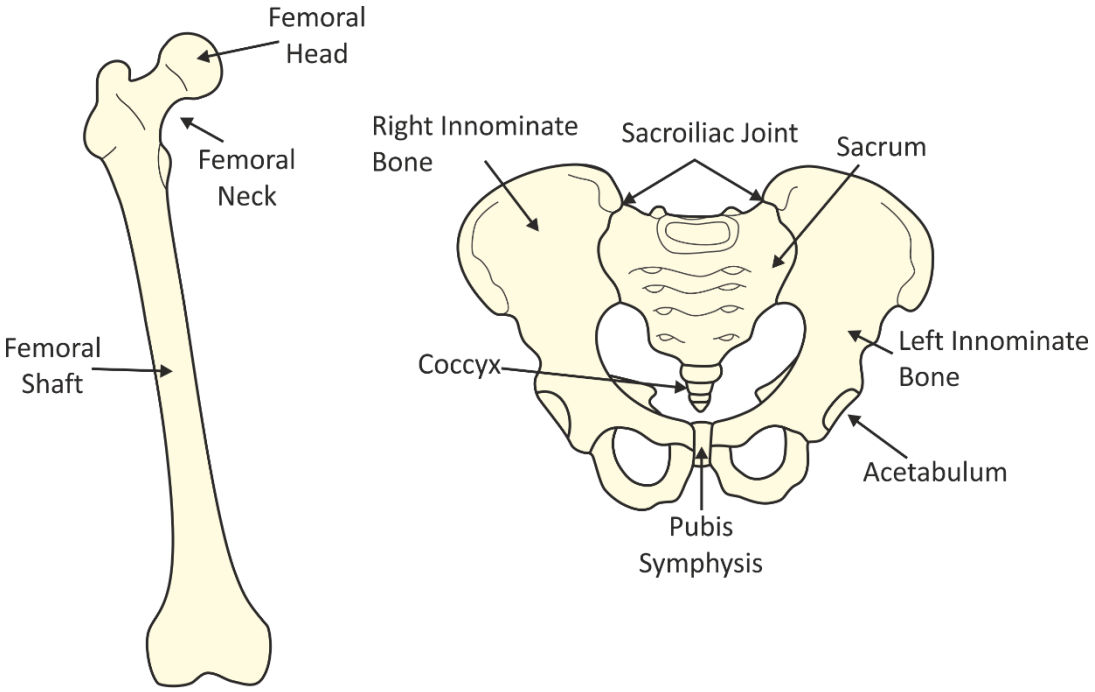

Figure 2.4 – The femur (left) and the pelvis (right)

2.2.2. THE PELVIS

The pelvis is a ring like bone structure that protects internal organs, connects the spine to the lower limbs, and provides attachment sites for important muscles to transmit forces and control movement of the hip joint. The pelvis consists of four bones: the right and left innominate bones, the sacrum and the coccyx (Figure 2.4).

The innominate bones, also known as the pelvic bones or coxal bones, form the anterior part of the pelvis and articulate with the right and left femoral heads at the hip joints (Figure 2.4). The innominate bone is a large, flattened, irregular shaped bone formed from three different bones segments: the ilium, the ischium and the pubis (Figure 2.5). These segments are connected by a tri-radiate (Y-shaped) cartilage in youth and fused as one bone in adults [7, 11]. The ilium forms the upper part of the acetabulum and the large expanded portion above it. The ischium is the lowest and strongest portion of the innominate bone. It includes the posteroinferior part of the acetabulum and the ischial ramus. The pubis includes the anterosuperior part of the acetabulum, the pubic ramus and the pubic symphysis. The ischial ramus and the pubic ramus join inferiorly to form the obturator foramen. The two innominate

bones are united by cartilage at the pubic symphysis to form the front of the pelvis, and join the sacrum at the sacroiliac joints to form the back of the pelvis (Figure 2.4) [7, 11].

The sacrum forms the posterior part of the pelvis and is the connection point between the spine, the two innominate bones and the coccyx (Figure 2.4). At the base of the sacrum is the coccyx, also known as the tailbone. It is an important attachment site for various muscles, tendons and ligaments, such as the gluteus maximus, the anterior and posterior sacrococcygeal ligaments, and some fibres of the sacrospinous and sacrotuberous ligaments. It also acts as a support when sitting [7, 11].

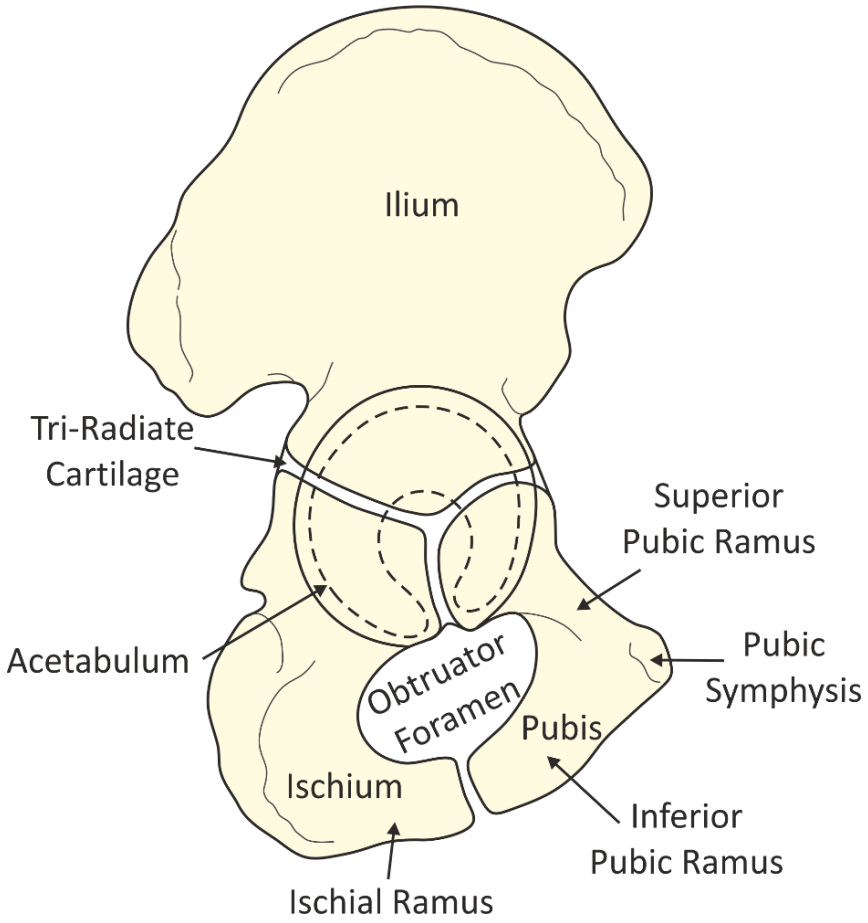

Figure 2.5 – The innominate bone showing the three pelvic bones and the tri-radiate cartilage joining them together

The Acetabulum

The acetabulum is a deep, cup-shaped socket, which articulates with the femoral head to form the hip joint. Its shape is such that, in the unloaded state, there is an incongruent fit between the acetabulum and the femoral head [13, 16-18]. However the acetabulum deforms under load to ensure a congruent fit with the femoral head [13, 16, 17, 19-22]. The acetabulum is orientated laterally, inferiorly, and anteriorly. This orientation is both functionally and clinically important as it increases the range of motion of the hip joint while maintaining its stability [11, 23, 24]. Acetabular inclination ranges between 23° and 59° with an average around 40°- 45°, while acetabular anteversion ranges between 15° and 35° with an average of 20° [13, 23, 24].

Acetabular anteversion differs between gender and is significantly greater in women, with mean values ranging from 15° to 18.5° in men and 19° to 24.1° in women [23, 24].

The weight-bearing surface of the acetabulum is a layer of cartilage that covers the lunate surface (Figure 2.6): a horseshoe-shaped ring made of subchondral bone [11, 14, 25]. This ring breaks inferiorly to form the acetabular notch. The lunate surface forms two facets called the anterior and posterior horns on either sides of the notch [14, 21, 26]. The anterior horn comprises both the ilio-pubic and ischio-pubic branches, whilst the posterior horn is formed of the ilio-ischial branch; it is the larger of the two horns [14]. The inner edge of the cartilage ends abruptly around the acetabular fossa, a rough and non-articulating surface devoid of cartilage and largely covered by the synovial membrane [11, 27]. The outer edge of the cartilage is the uneven rim of the acetabulum, which blends with the labrum without any distinct demarcation [11, 27]. The labrum has two important functions: it manages the transition between the hard acetabular rim and the soft articulating capsule, ensuring a progressive transition of the forces in the hip; and it deepens the acetabular socket, hence preventing dislocation of the hip by retaining the femoral head within the acetabulum [11, 13, 14, 19].

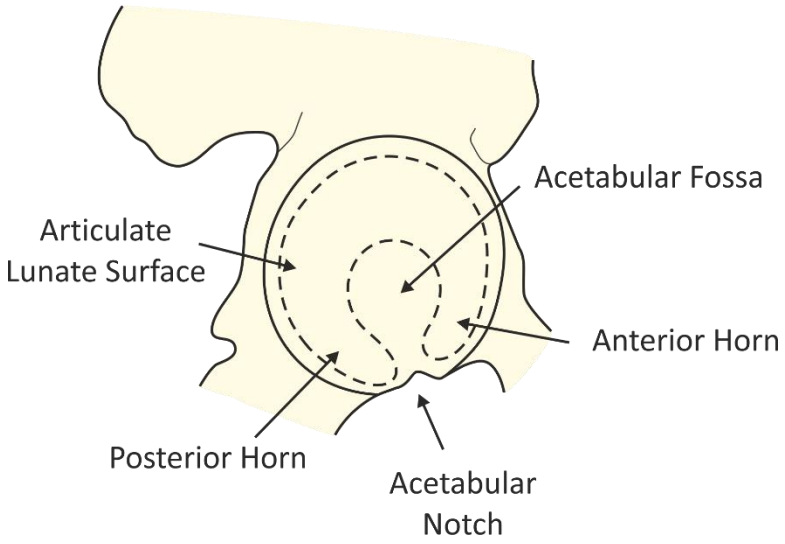

Figure 2.6 – The acetabulum

The rim of the acetabulum is a succession of three peaks and three troughs, resulting in an asymmetric profile [14, 24, 28, 29]. Each trough corresponds to a fusion point between two of the three pelvic bones: they are the anterior ridge (ilium-ischium junction), the posterior ridge (ilium-pubis junction) and the acetabular notch (ischial-pubis junction) [24]. The irregularity of the acetabular rim is the result of the growth and fusion process of the three pelvic bones, which starts prenatally and lasts well beyond puberty [24, 28]. During this period, each bone is subjected to different mechanical constraints, resulting in the bones growing in different directions and in the outwards ossification of the acetabular rim [14, 28]. The length of the process allows the structure of the acetabular rim to properly adapt to its function [28].

The opening width of the acetabular notch depends on the size of the acetabulum, and hence it is reported as an angle rather than a length (Figure 2.7). The opening width ranges between 51° and 68° and is usually wider, shorter and deeper in males than in females [25, 29, 30].

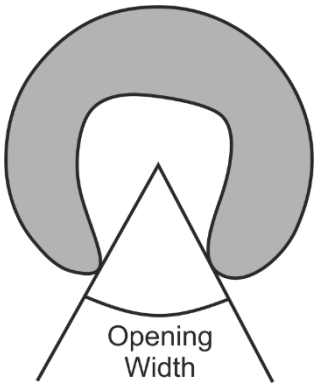

Figure 2.7 – Opening width angle of the acetabular notch (illustration adapted from [30])

2.2.3. Load Transfer in the Hip Joint

Bone closely resembles a sandwich structure, with its core made up of low-density trabecular bone covered by a thin layer of cortical bone [31-35]. The major part of the load is carried by and transferred through the cortical bone while the trabecular bone plays an important role in maintaining the structural form of the bone and preventing the cortical shell from collapsing [31, 33, 34].

Trabecular bone typically has a density ranging between 0.17 g/cm^3 and 0.50 g/cm^3, and a compressive strength ranging between 2 MPa and 50 MPa [36, 37]. The density of cortical bone ranges between 1.20 and 1.95 g/cm^3, its compressive strength ranges between 130 and 220 MPa, and it has a thickness ranging between 0.4 and 4.0 mm [13, 37-39]. These properties were obtained from long bones such as the femur or the tibia, as they are easier to test and their properties are uniformly distributed along the bone.

The mechanical properties of the trabecular and cortical bone within the pelvic bone have not been the focus of much research. Cadaveric studies have reported that these properties vary within the pelvic bone, adjusting to the load and stress distributions present in different locations. Hence, in order to withstand the associated high loads and stresses, the thickest cortical bone and the densest trabecular bone are found in the superior-anterior area of the acetabular wall and along the major path of weight transition up to the greater sciatic notch and the sacroiliac joint [11, 19, 31, 35, 40]. The density of the trabecular bone decreases further away from the acetabulum and is at its lowest in the ischial bone and the interior of the ilium [11, 35, 41]. This results in two thick cortical struts: the anterior and posterior columns, which run along the major path of weight transition within the pelvic bone (Figure 2.8) [21, 40, 42].

The anterior, or ilio-pubic, column is the longer of the two columns and is composed of the entire pubis and a large portion of the ilium, as well as the anterior half of the acetabulum. It extends from the iliac crest, down the iliac wing and through the superior pubis ramus towards the pubis symphysis. The posterior, or ilio-ischial, column is composed mainly of the ischium

and a small part of the ilium. It extends from the posterior iliac body below the greater sciatic notch, down to the ischial body and into the inferior ischio-pubis ramus [17, 42].

The major role of the acetabular columns is to add stability, to distribute forces within the hip joint and to transfer these forces between the acetabulum and the sacroiliac joint [21, 40, 42]. The acetabular columns provide structural support to the anterior and posterior walls of the acetabulum as they are the area of primary load transfer within the acetabulum. This was confirmed by Byers *et al.* [27] who observed the highest levels of wear of acetabular cartilage in those areas.

The columns join above the acetabulum, forming a radiolucent triangle (Figure 2.9) [22, 40]. The radiolucent triangle is a cartilaginous cleft that provides flexibility to the acetabulum, allowing it to deform under load [40]. The shape of the radiolucent triangle is dependent, amongst other factors, on the loading pattern and the orientation of the femoral head [22]. With age, the hip joint becomes more congruent when unloaded [19, 22]. This increase in congruity results in an increased loading of the acetabular roof which results in an increase of the bone density of the normally radiolucent triangle [40]. As the density of the bone between the two columns increases, the acetabulum becomes less flexible [40]. Hence, this radiolucent triangle can be used to identify changes in loading pattern of the hip over time [40].

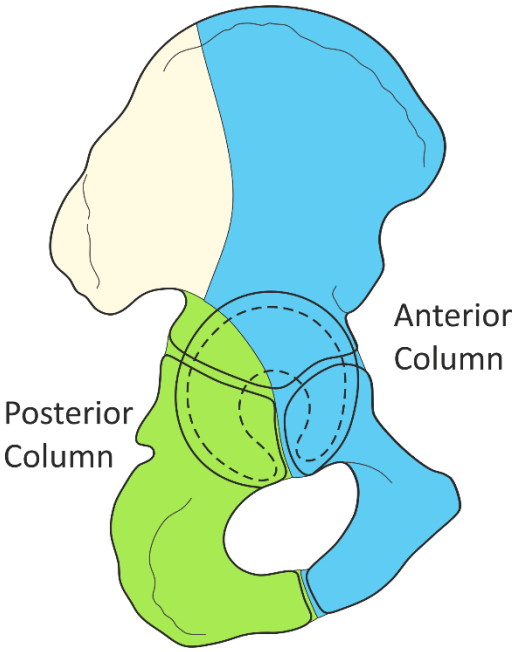

Figure 2.8 – The anterior and posterior acetabular columns

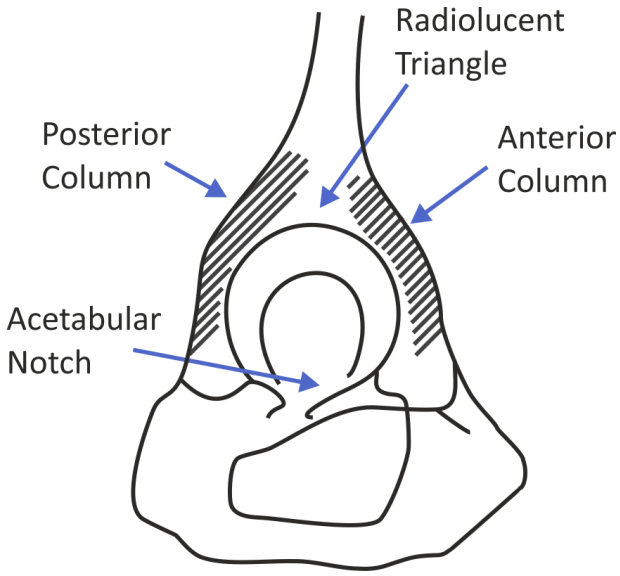

Figure 2.9 – Radiolucent triangle above the acetabulum formed by the acetabular columns

2.3. BIOMECHANICS OF THE HIP

The biomechanics of the hip relates to the forces and motions occurring in the hip joint, including current knowledge of the mechanical behaviour of the hip and lower limbs during activities of daily living.

2.3.1. RANGE OF MOVEMENT OF THE HIP JOINT AND THE GAIT CYCLE

In a normal healthy person, the range of movement of the hip is extensive and occurs in all three planes of motion (Figure 2.10): flexion and extension (sagittal plane), abduction and adduction (coronal plane), and internal and external rotations (transverse plane). The range of motion of the hip is frequently reduced by age and hip deformities [43-46].

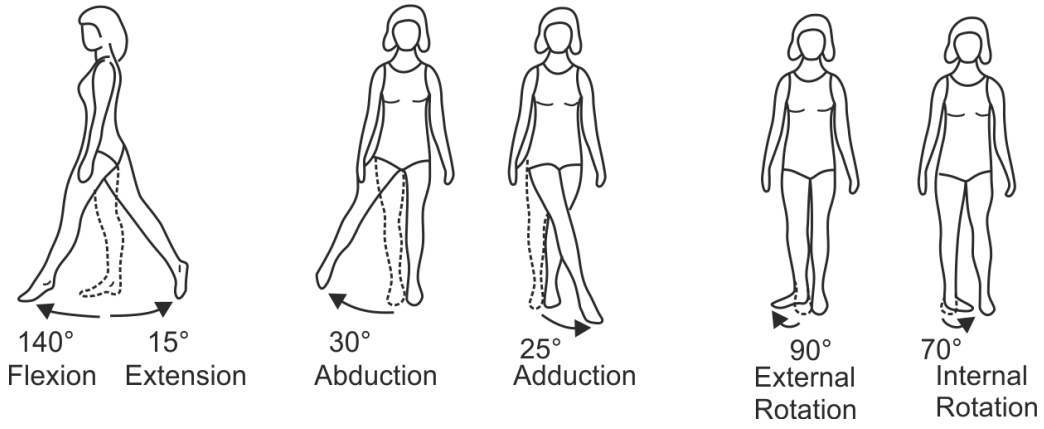

Figure 2.10 – Range of movement of the hip (illustration adapted from Basic Biomechanics of the Musculoskeletal System [13])

The gait cycle refers to the physical range of motion that the body goes through while walking [15, 47]. The number of cycles each hip experiences is roughly around one to two million cycles per year [48-50]. The gait cycle has been widely investigated, especially the effect of different variables (such as age, sex, joint disease etc.) on the pattern of movement of the lower limbs.

The gait cycle comprises the stance phase (around 60% of the gait cycle), and the swing phase (Figure 2.11) [45, 51, 52]. By convention, the description of the gait cycle begins with the heel strike. The foot then flattens on the ground and the pressure transfers from the back of the foot to the front as the body rocks forwards. Finally, the stance phase ends with toe-off, where the heel lifts off the ground and the front of the foot pushes off the ground. The swing phase starts the moment the foot stops touching the ground. The leg then swings forwards. The swing phase ends, along with the gait cycle, when the next heel strike occurs [51, 53].

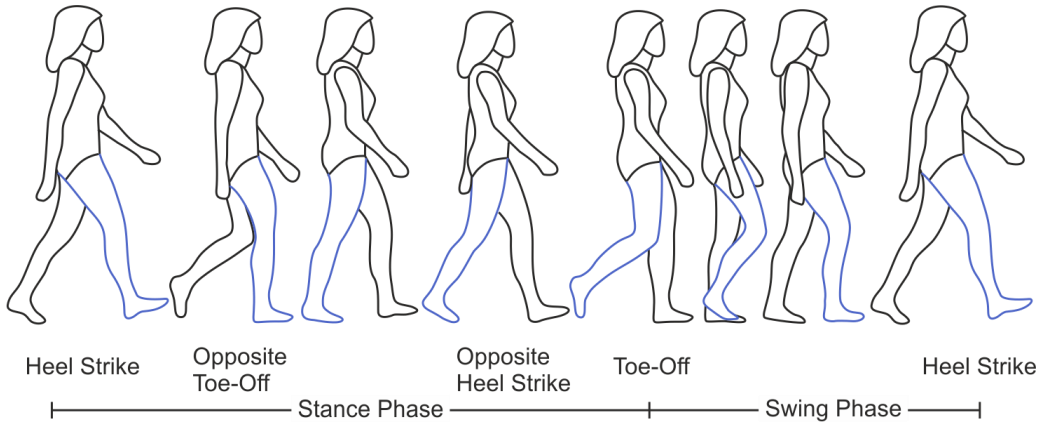

Figure 2.11 – Gait Cycle (illustration adapted from Human Walking [54])

Many studies have measured hip joint motion in all three orthogonal planes during gait. The methods used include groups of three rotational potentiometers to record angular motion [53, 55]; or either interrupted-light photography [45] or video motion analysis systems [46, 51, 52, 56-59] to analyse the displacement of targets fixed to specific anatomic landmarks.

In the sagittal plane, extension of the hip begins just prior to heel strike and gradually increases until shortly before toe-off when the hip begins to flex. Flexion continues just prior to the next heel strike. Flexion-extension is the motion most commonly reported because it is the primary motion during gait [56]. The range of flexion-extension of the hip joint during level walking is around 40°. The data published in the literature show consistent angles for the maximum flexion, maximum extension and hence overall range (Table 2.1).

Table 2.1 – Range of flexion-extension during walking available in the literature

Study	Age Range	Flexion	Extension	Range
Bergmann *et al.* [57]	51-76	26.4°	6.9°	33.3°
Isacson *et al.* [53]	25-35	-	-	30.2°
Johnston and Smidt [55]	23-55	37°	15°	52°
Kadaba *et al.* [51]	18-40	-	-	43.2°
Kerrigan *et al.* [46]	Mean 73	26.4°	14.3°	40.7°
	Mean 28	24.0°	20.4°	44.4°
Murray *et al.* [45]	>65	32°	10°	42°
	<65	33°	13°	46°
Nadeau *et al.* [58]	41-70	30.8°	15.5°	46.3°
Paul [59]	-	31°	11°	42°
Riener *et al.* [52]	24-34	50°	-8°	42°
Mean		**32.3°**	**10.9°**	**42°**

In the coronal plane, adduction begins just after toe-off and gradually continues until the late stance phase. At this stage, abduction begins and is maximised just after toe-off when adduction starts again. The range of abduction-adduction during level walking is about 12° [51, 53, 55, 57, 58].

In the transverse plane, the hip rotates internally just before heel strike. It remains internally rotated until the late stance phase when it rotates externally. The hip remains externally rotated through much of the swing phase until the late swing phase when internal rotation occurs again. The recorded range of rotations is about 13° for level walking [51, 53, 55].

Going up stairs is a common activity of daily living [56, 58]. Even though the general gait cycle profile is very similar for both activities [56, 58, 60], stair climbing has been reported to be mechanically more demanding than level walking as it requires a greater range of hip motion in flexion-extension and places the hip in a more flexed position [52, 56, 58]. The maximum flexion and extension for stair climbing published in the literature varies greatly between studies. The overall average range of flexion-extension is, however, similar between studies and is around 50° (Table 2.2).

Table 2.2 – Range of flexion-extension during stair climbing available in the literature

Study	Age Range	Flexion	Extension	Range
Andriacchi *et al.* [56]	20-34	42°	-3°	39°
Bergmann *et al.* [57]	51-76	56.3°	4.9°	61.2°
Nadeau *et al.* [58]	41-70	60.1°	-4.7°	55.4°
Paul [59]	-	37°	1°	38°
Riener *et al.* [52]	24-34	75°	-12°	63°
Mean		**54°**	**-2.8°**	**51.3°**

2.3.2. Loading of the Hip Joint

The loading pattern that the hip is subjected to during the gait cycle has also been investigated. There are different methods used to measure this loading pattern: indirect and direct measurements. Indirect measurements use force plates and motion recording systems to measure and compare both impact forces and gait cycles between normal and implanted hips. This approach, which was first adopted by Paul [59], consists of experimentally recording the ground reaction forces and the configuration of the lower limb and hip region during a series of gait cycles, and using this information in combination with electromyography (EMG) measurements of phasic muscle activity to calculate the reaction force exerted in the hip joint.

Measuring the reaction force within the hip joint *in vivo* was popularised by Bergmann *et al.* [61] who used an instrumented hip stem with a three-axis load cell combined with a telemetry system to directly assess the load within the hip. One of the main advantages of this method was that measurements could be taken on patients during a wide range of activities of daily living, some of which are impossible to investigate when using force plates and motion recording systems, such as lying down on a bed, or getting into and out of a car or a bathtub. However, the data obtained from these studies do not fully represent the loading experienced by the natural hip as it was replaced by the instrumented implant [62]. Furthermore, *in vivo* measurement methods are expensive, technically complex and offer no benefit to the patient receiving the instrumented implant [61, 63].

Finally, the data obtained with both methods can be used to create mathematical models, which can numerically predict the effect of different factors on the joint reaction force [63]. They are relatively quick to run, inexpensive and do not need test subjects once the model is created. However, they are limited by the many necessary assumptions and simplifications needed, generally resulting in higher resultant forces than those measured [61-63].

The loading pattern of the hip joint varies between activities and subject [59, 61, 63, 64]. Similarly to studies investigating the motion of the hip joint, the loading pattern of the hip joint during gait is widely reported in the literature. It is characterised by a double peak curve, also known as the Paul Cycle (Figure 2.12). The peak loads occur after heel-strike and before toe-off [59, 60]. They are similar in magnitude, with one slightly higher than the other. There is, however, some disagreement regarding which peak has the highest magnitude [59-61, 65, 66]. The peak forces for walking range between 2.5 and 5 times body weight (Table 2.3) [57, 59, 61-63, 65-69]. The hip forces increase with walking speed: an increase of 0.1 mm/s has been reported to result in an increase of approximately 0.2 times body weight [63].

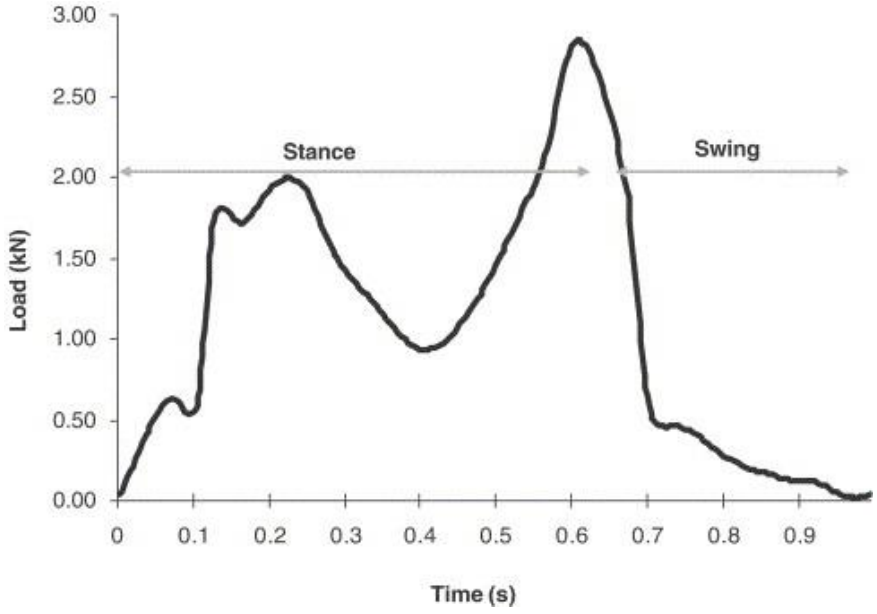

Figure 2.12 – Vertical hip joint reaction force profile during the gait cycle or the Paul Cycle (illustration from [47] with permission)

Stair climbing force profiles are similar to those of walking but have slightly higher peak forces. The maximum hip joint forces reported for stair climbing range between 2.5 and 5.5 times body weight (Table 2.3) [57, 59, 67, 68]. Peak hip forces measured when stumbling are significantly greater than those measured for walking and stair climbing, with forces reaching up to 11 times the body weight (Table 2.3) [61, 68].

Table 2.3 – Summary of hip contact force measurements and/or predictions available in the literature (BW = body weight)

Study	Type of Study	Type of Measurement	Peak Force
Bergmann *et al.* [61]	*In vivo*	Instrumented prosthesis	2.9 – 4.7 BW walking 7.2 – 8.7 BW stumbling
Bergmann *et al.* [67]	*In vivo*	Instrumented prosthesis	3.1 – 4.1 BW walking 3.4 – 5.5 BW upstairs
Bergmann *et al.* [57]	*In vivo*	Instrumented prosthesis, force plate & motion capture system	2.38 BW walking 2.51 BW upstairs
Bergmann *et al.* [68]	*In vivo*	Instrumented prosthesis, force plate & motion capture system	3.9 BW walking 4.2 BW upstairs 11 BW stumbling
Brand *et al.* [63]	*In vivo* + Numerical	Instrumented prosthesis, force plate & motion capture system + mathematical model	2.5 – 3.5 BW walking
Crowninshield *et al.* [65]	Numerical	Mathematical model	3.3-5 BW walking
English and Kilvington [69]	*In vivo*	Instrumented prosthesis	2.7 BW walking
Kotzar *et al.* [62]	*In vivo*	Instrumented prosthesis	2.7 BW walking
Paul [59]	Numerical	Mathematical model	4.9 BW walking 7.2 BW upstairs
Seireg and Arvikar [66]	Numerical	Mathematical model	5.4 BW walking

Loading Pattern within the Acetabulum during Gait

Direct *in vivo* measurements of hip joint loading using instrumented implants also provide information on the position and direction of the resultant force within the hip joint [57]. As the leg moves during the gait cycle, so does the femoral head within the acetabulum. This results in a change in the position and direction of the resultant force within the hip joint (Figure 2.13). As previously mentioned, the hip joint experiences high reaction forces during the stance phase of the gait cycle. At heel strike, the reaction force is on the posterior wall of the acetabulum and directed towards the posterior acetabular column. The path of the load then follows the horseshoe shape of the lunate surface and ends on the anterior wall of the acetabulum and directed towards the anterior acetabular column for toe-off. As previously described, the peak loads experienced by the hip joint during the gait cycle are during heel strike and toe-off. This means that the peak loads experienced by the hip joint during gait are directed into the supportive structures of the acetabular columns.

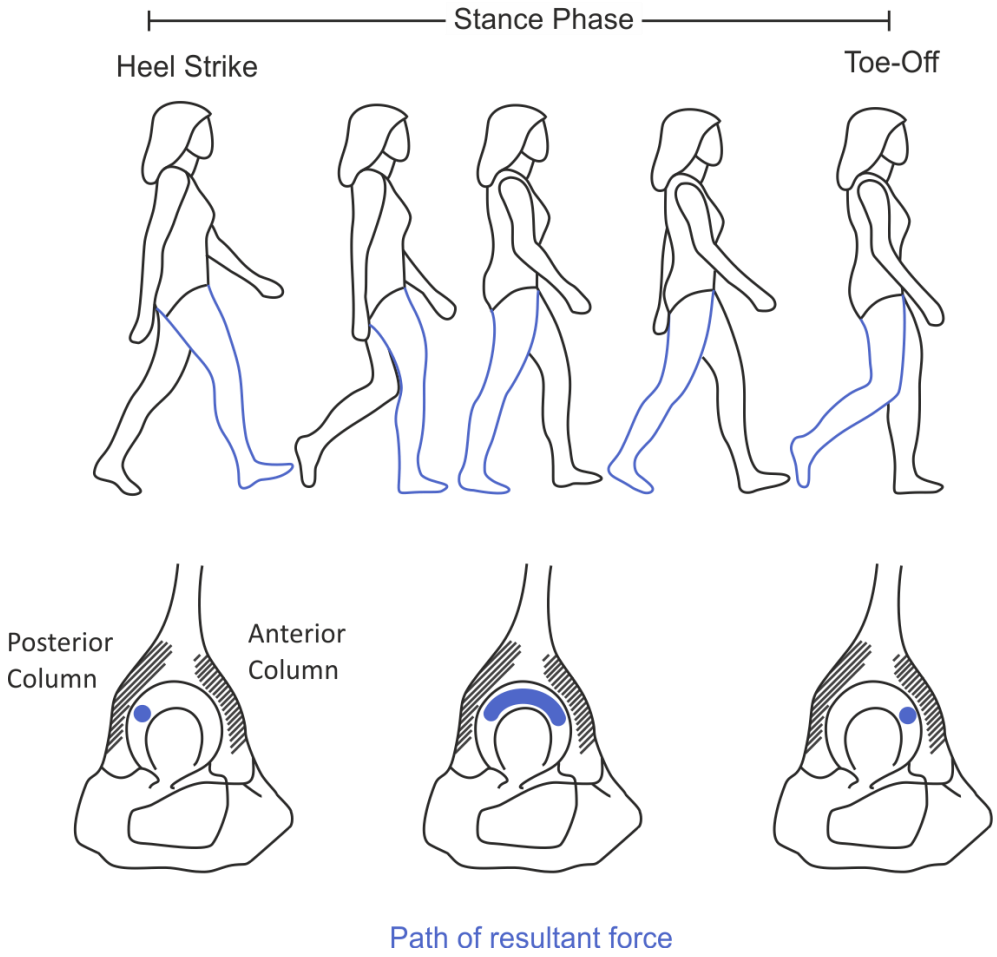

Figure 2.13 – Position and direction of the reaction force within the acetabulum

2.4. TOTAL HIP REPLACEMENTS

Total hip replacement (THR) is a surgical procedure in which the entire natural hip joint is removed and replaced by a man-made prosthetic implant. THR became a common procedure in the 1960s and, following remarkable development and innovations over the years, has become one of the most widely used orthopaedic operations.

2.4.1. INDICATIONS FOR TOTAL HIP REPLACEMENTS

Typically subjected to well over one million cycles a year and forces reaching up to 10 times the body weight, the hip is one of the most heavily loaded joints in the body [49, 50]. With age and use, the joint is susceptible to damage and disease, which can cause pain and restrict mobility, thereby reducing quality of life.

Osteoarthritis is the primary indication for over 80% of all THR [2-5]. Osteoarthritis is the degradation of the joint and occurs when the cartilage present at the bearing surfaces of a joint wears away, resulting in bone rubbing against bone. This causes pain, stiffness and loss of movement of the affected joint [15, 70]. Other primary diagnoses occur with varying frequency in different countries and include acute fractures (3-10%), osteonecrosis (2-4%) and inflammatory arthritis (1-2%) [2-5]. Any disease and condition affecting the hip that causes pain and discomfort to the patient may constitute an indication for THR.

2.4.2. BRIEF HISTORY OF TOTAL HIP REPLACEMENTS

The earliest documented attempts to treat trauma and hip disease date back to the 1790s and consisted of amputation. In the beginning of the 19th century, hip deformities were treated by osteotomy and arthrodesis. These methods involved fusing the hip joint, resulting in a joint with no effective mobility [7].

The 20th century saw the development of modern THR, which was introduced in two major steps. The first step was the development of “Mold Arthroplasty”, also known as “Cup Arthroplasty”, by the surgeon Smith-Petersen in the 1920s. This technique consisted of interposing material in the joint between the femoral head and the acetabulum. He first used glass and then Pyrex after he observed soft tissue ongrowth on an explanted piece of glass. However, these materials fractured easily in the hip so he turned to Vitallium, an alloy of chrome, cobalt and molybdenum, which was unique with regards to its biocompatibility in living tissue. Only half of the surgeries performed using this Vitallium mould (Figure 2.14) successfully relieved pain, however, this was a major step in the development of acetabular cups in THR [7].

The second step was the introduction of endoprostheses in the 1940s, which consisted of a femoral head attached to a short stem and implanted in the intertrochanteric region of the femur (Figure 2.14). These implants were initially made of acrylic but, because of wear issues, they were later made of a cobalt-chrome (CoCr) alloy. This change was one of many modifications made to endoprostheses; however, most of these endoprostheses became loose and failed because of their defective load bearing capacity [71]. The small stem was later replaced by a longer intramedullary stem to give the head more mechanical support [7, 71].

Figure 2.14 – A Smith-Petersen Vitallium mould arthroplasty from 1939 (left); a Wiles stainless steel endoprosthesis from 1938 (centre); a Judet Brothers acrylic endoprosthesis from the late 1940s (right; all pictures from [72] with permission)

In 1938, Philip Wiles performed the first THR by implanting a stainless steel ball-and-socket hip prosthesis, which was attached to the bone with screws and bolts. This prosthesis, as with other similar ones, was prone to mechanical failure. It was not until the 1950s, when Sir John Charnley began his extensive research, that the modern THR was created. His innovations included the use of a dental bone cement called polymethylmethacrylate to anchor the prostheses, and "Low Friction Arthroplasty", which comprised a stainless steel intramedullary stem with a 22 mm diameter femoral head articulating into a high-density polyethylene polymer cup (Figure 2.15). This was a major turning point for orthopaedics as his innovations, which are still used today, could for the first time successfully treat major hip disabilities [7, 73, 74].

Figure 2.15 – A Charnley THR from 1962 (picture from [72] with permission)

2.4.3. Modern Developments in Total Hip Replacements

Using bone cement was initially a very popular method to anchor the prostheses as any errors in bone resection or reaming could be accommodated [71, 74, 75]. The short and mid-term results were excellent with a low rate of complications, failures and revisions. However, the long-term results were less satisfactory; high loosening rates and loss of bone stock were commonly reported in early THR, increasing exponentially after 5 years of implantation and particularly affecting younger patients [7, 71, 74]. These problems were thought to be linked to the use of cement. Exothermic reactions were known to occur during cement polymerisation and methyl methacrylate particles had been discovered in soft tissues surrounding loose implants during revision surgeries. The cause of implant loosening was therefore widely attributed to "Cement Disease" [74, 76-78]. In addition to this, several

studies revealed that methyl methacrylate undergoes ageing in the human body; with time, the cement becomes more rigid and fragile, and is increasingly affected by creep deformation as its elastic modulus decreases [74].

Operative and cementing techniques were continuously improved in the hope of reducing implant loosening. Improvements such as thorough cleaning of the bone surface using brushing and pressurised lavage, control of bleeding, vacuum mixing of the bone cement, and the use of cement guns for the introduction of the cement all have resulted in improvements in cementing techniques [8, 74, 78]. Today, using cement for implant fixation remains a viable option and is widely used for older patients, providing a reproducible and cost-effective technique [8, 75, 79]. Cement still is the most common choice of implant fixation in Sweden (Figure 2.16).

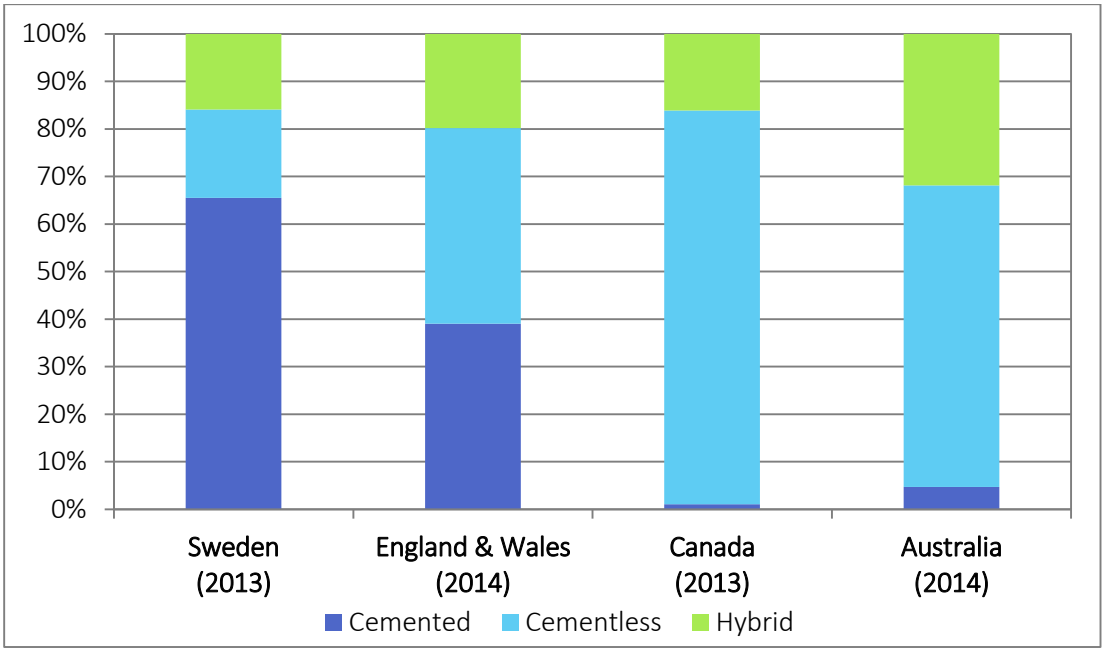

Figure 2.16 – Types of THR fixation used during surgery from different national registries [2-5]. In this case, hybrids include both standard hybrids (cemented stem and cementless cup), and reverse hybrids (cemented cup and cementless stem)

As a response to cement disease, a new anchoring philosophy, cementless fixation, was introduced in the 1980s. This included the development and use of new materials that encourage osseointegration, thereby removing the need for cement in THR [7]. Osseointegration is the biological process in which an implanted prosthesis is integrated with the surrounding bone and is achieved through bone ingrowth or bone ongrowth [7, 71]. Bone ingrowth relies on the bone growing into the porous surface of an implant to secure it, while bone ongrowth is provided by the direct adhesion of the bone to the implant [79-81]].

Implant modularity was another development of THR, which was brought on by cementless fixation, where the femoral head is separate from the stem and the acetabular cup is composed of a shell and a liner (Figure 2.17). Both the stem and the acetabular shell are made of metal, usually CoCr or Titanium alloys, and covered with a porous coating for osseointegration. The head and the liner come in a multitude of materials to form different

bearing couples such as ceramic on polyethylene, ceramic on ceramic, metal on polyethylene and metal on metal. Furthermore, modularity allows the surgeon to decide on the implant parameters, such as head size and liner material, during surgery, as well as change a worn out liner or head without removing a well fixed shell or stem, respectively, during revision surgery [75, 77, 80, 82]. Modular stems are now also used in cemented fixation.

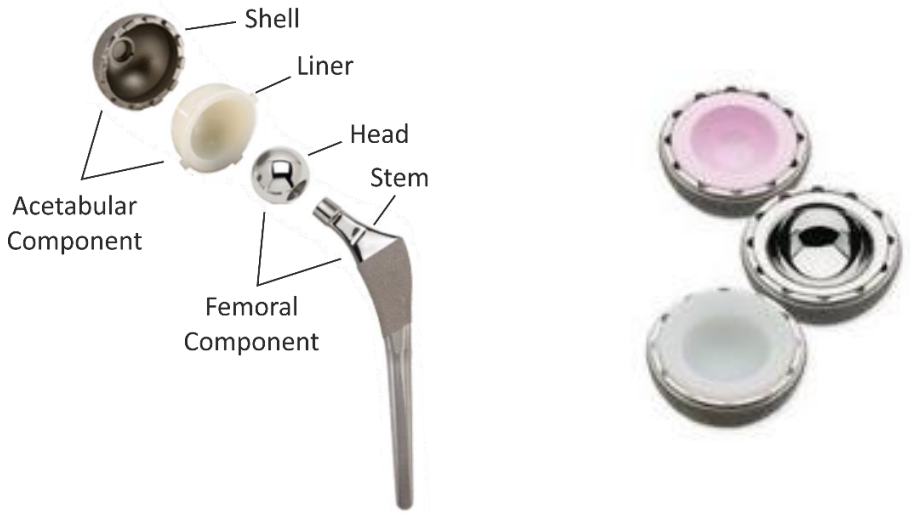

Figure 2.17 – Modular total hip replacement implant (left; picture from [83], edited by author); acetabular cups with a ceramic, a metal and a polyethylene liner (right; picture from [84])

National joint registries and clinical studies have reported a lower percentage of revisions of cementless THR than cemented THR in younger patients (Figure 2.18) [2, 4, 80]. This difference increases with duration of implantation [2, 4, 80]. Hence, cementless fixation has become a popular fixation method for THR (Figure 2.16), especially in younger and more active patients [7, 74].

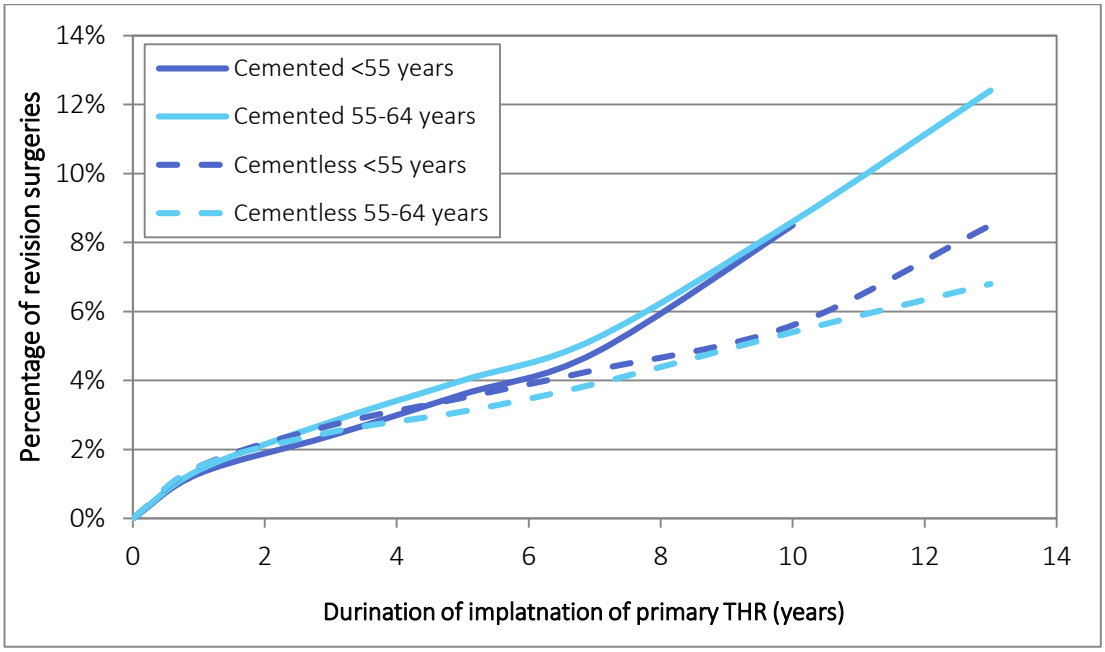

Figure 2.18 – The percentage of revision surgeries on both primary cemented and cementless THR in younger patients with respect to the duration of implantation [2].

Due to the high success rates of cemented implants using modern cementing techniques and the promising results of cementless implants, hybrid fixation is also available. Standard hybrids comprise a cemented femoral stem and a cementless acetabular cup [85], while reverse hybrids comprise a cementless stem and a cemented cup [4]. Hybrid fixations are used in 15% to 30% of all THR (Figure 2.16); however, the type of hybrid used varies between countries. In England and Wales, 85% of hybrid procedures are standard hybrids [4], whilst in Sweden, 87% of these procedures are reverse hybrids [3].

2.4.4. Failure Modes of Total Hip Replacements

THR is a successful surgical procedure with excellent results. According to their national joint registries, the 10 year survivorship of THR in Sweden and in Australia is 95% [3] and 93.2%, [2] respectively, while the National Joint Registry of England and Wales [4] reported a 7 year survivorship of 96.0%.

The small percentage of THR that do fail need to be revised. Furthermore, THRs are being increasingly performed on younger and more active patients who therefore outlive the lifetime of their implant. There are various causes for revision surgeries, none of which are mutually exclusive. The four main causes of revision are osteolysis and aseptic loosening, dislocation or instability, infections, and fractures (Figure 2.19) [2-5].

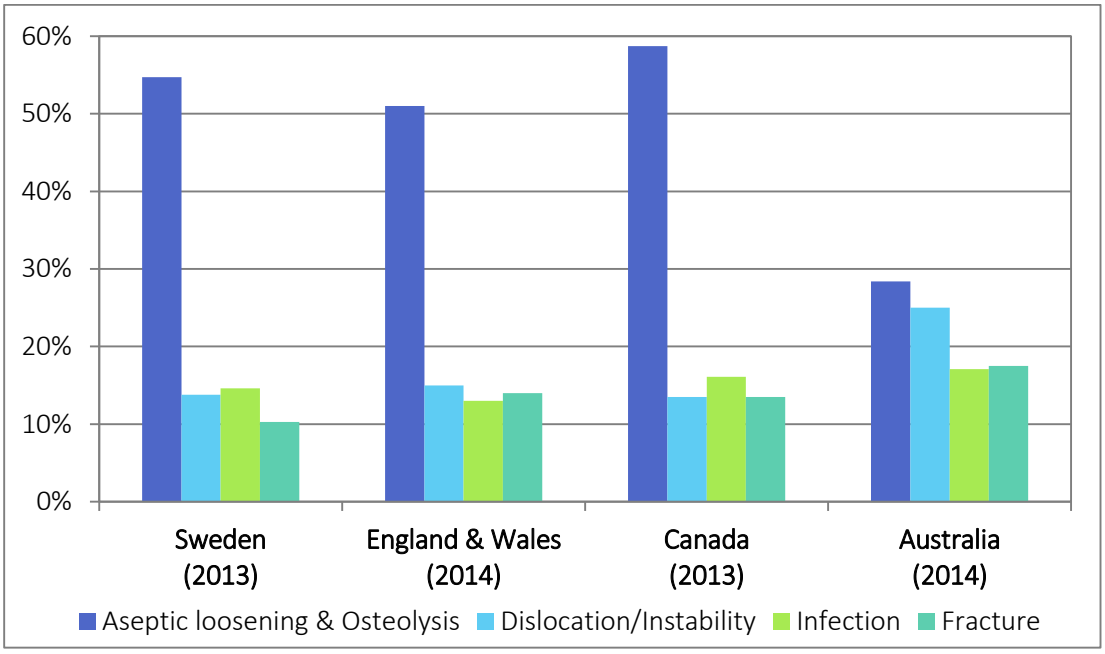

Figure 2.19 – Reasons for revision surgeries from different national registries [2-5]. The Swedish and Australian registers published only the primary reason for revision, while the Canadian, and the English and Welsh registries published all reasons for revision

Osteolysis and aseptic loosening have, for a long time, been the most common failure mode of THR (Figure 2.19) [77, 86]. Osteolysis, or bone resorption, is the dissolution or degeneration of bone tissue around an implant, which reduces the surface contact area between the implant and the bone [15]. When bone resorption reaches a critical amount, the implant becomes loose; this is known as aseptic loosening. Aseptic loosening is asymptomatic for a

long time, with symptoms usually appearing only when large bony defects are present. These defects require complicated reconstructions that increase surgical risk and decrease the chances of survival of the revision implant [9, 87]. Regular clinical and radiographic follow-up are necessary to detect aseptic loosening in its early stages [9, 87].

Studies have recorded promising long-term results in stem fixation using modern cementing techniques and cementless fixation, however, the loosening rate of acetabular components remains high, regardless of the type of fixation [7-9, 88]. Apart from Sweden, where most acetabular cups are cemented, the majority of cups implanted in the rest of the world are cementless, either as part of cementless or hybrid THR procedures. Furthermore, since they are implanted into younger and more active patients, cementless cups also need to withstand higher levels of activity for a longer period of time compared to cemented polyethylene cups [7, 74]. Hence, pre-clinical studies of cementless cups under physiological conditions are crucial.

2.5. ASEPTIC LOOSENING OF ACETABULAR COMPONENTS

Clinically, an acetabular component is considered loose if the implant continuously migrates [9] and/or if radiolucent lines are present in the three Delee and Charnley [89] acetabular zones (Figure 2.20). Radiolucent lines indicate either gaps or the presence of a fibrous membrane between the bone and the implant. Thin and non-progressive radiolucent lines are visible in most individuals and are considered normal. However, if the radiolucent zone is continuously expanding and/or is thicker than 2 mm, then the implant is considered loose and revision surgery is required [80, 89, 90].

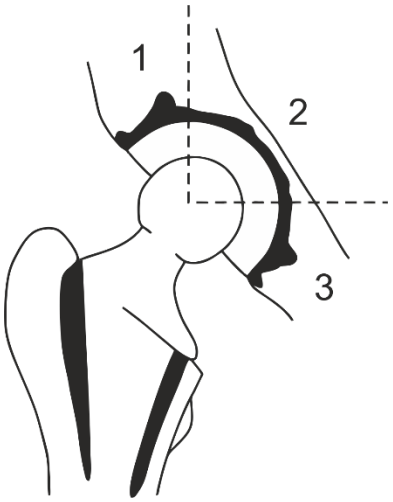

Figure 2.20 – Acetabular zones of loosening according to Delee and Charnley (illustration adapted from [89])

2.5.1. CAUSES OF ASEPTIC LOOSENING

Initially, the cause of implant loosening was widely attributed to cement disease. However, implant loosening and loss of bone stock, two main symptoms of cement disease, were also observed in cementless THR. New roentgenographic and histologic evaluations of loosened prosthesis indicated a pathologic response to foreign materials, such as cement or wear particles. For this reason, cement disease was renamed “Particle Disease” [77, 78, 80].

Wear particles are generated by two surfaces rubbing against one another [91]. In THR, wear particles can originate from two separate places. Most particles are generated at the articulating surface of the joint while fewer, but larger, particles come from non-articulating surfaces such as the backside of the liner, fretting between the screws and the metal shell, fretting of the modular taper junction of the femoral head, and at the bone-cement interface [77, 92-96]. Wear debris can therefore be cement, polyethylene, metal or ceramic particles [76, 78, 91]. Generation of wear particle increases with the number of gait cycles as wear is a function of activity. It is also aggravated by third-body wear caused by trapped wear particles between the liner and the shell, or between the femoral head and acetabular liner [77, 91, 92, 95].

It is widely recognised that the presence of wear debris induces an inflammatory response in the surrounding tissues [77, 97]. Granulomas, macrophages, giant cells and wear debris have

been observed in periprosthetic tissue obtained during revision surgeries, revealing a marked foreign-body reaction [77, 93, 95]. Macrophages resorb bone and release osteoclast-activating agents in response to wear particles [78, 91, 93, 95]. Wear particles also supress the formation of mature functioning osteoblasts [77]; this causes a negative balance between bone resorption and bone formation, resulting in osteolysis. In addition to this, metal particles are also responsible for pseudotumours and metallosis around the implant, usually due to metal hypersensitivity, which results in soft tissue necrosis, implant loosening and pain [93, 98]. The effect of wear debris varies between patients; some show little or no bone resorption in the presence of distinct prosthesis wear while others have marked osteolysis with barely any wear present [77].

Fluid pressure waves also contribute to osteolysis. Joint fluid is present everywhere around the acetabular component, including in the joint capsule, between the liner and the shell in modular cups, and in any gaps present between the implant and the bone; these are known as effective joint spaces [76]. If a modular cup is used, a non-congruent liner suspended on the rim of the shell can deform under cyclic loading caused by gait, resulting in a pumping action called diaphragm pumping (Figure 2.21) [82, 94, 98, 99]. If the locking mechanism between the shell and the liner allows movement or is worn, then the liner will be able to move in and out of the shell, resulting in piston pumping (Figure 2.21) [82, 94, 99, 100]. In both cases, the volume space between the liner and the shell reduces when the cup is loaded and increases again when it is unloaded. This causes the joint fluid present to flow between the liner-shell interface and the bone-implant interface through any screw holes present in the shell, resulting in fluid pressure waves in and around the acetabulum [48, 77, 82, 99]. Piston pumping can also occur if the cup is unstable within the acetabulum; in this case, the gap between the bone and the shell reduces under load, resulting in a rise in pressure of the joint fluid. Hence, under cyclic loading, an unstable cup can also generate fluid pressure waves at the bone-implant interface.

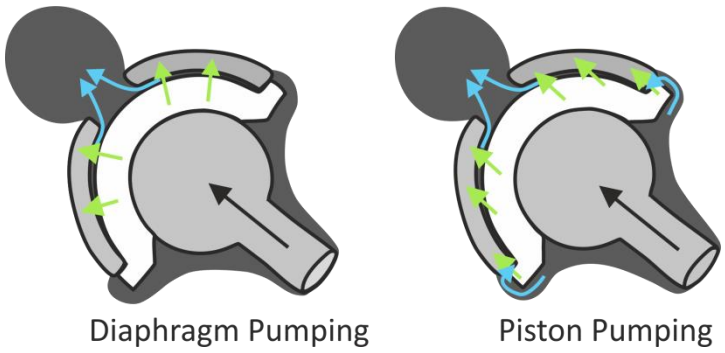

Figure 2.21 – Diagrams illustrating diaphragm pumping and piston pumping when under load. The black arrows are the load; the green arrows are the movement of the liner; and the blue arrows are the path of migration of fluid and particles (illustration adapted from [99])

The presence of small fluid shear can be beneficial as it stimulates osteocytes, hence mediating bone formation [48, 101]. However, high fluid pressures damage and kill osteocytes at the bone-implant interface [48, 91, 101]. This indirectly leads to bone resorption as bone is no longer replenished but is still destroyed [101]. Studies investigating the effect of fluid pressures on cell cultures have reported cell damage with hydraulic pressures of 35 kPa or

more; and bone resorption has been produced by both cyclic and constant pressures in animal models [101-105]. Furthermore, fluid pressure waves can transport wear particles present in the joint fluid to the bone-implant interface (Figure 2.21), contributing to particle disease [48, 77, 78, 82, 99].

Fluid pressure waves and particle disease can be aggravated by implant instability. An unstable cup is prone to both micromotion and migration under cyclic loading [48, 106]. Micromotion is the dynamic movement of the cup in response to cyclic loading of the prosthesis where the cup returns to its original position once the load is removed; whilst migration is the irreversible displacement of the cup as it embeds itself into the acetabulum as a consequence of loading [86]. Studies have reported elevated intracapsular pressure and an increase in wear debris generation in hips with loose components [78, 94, 107, 108].

It is unclear if osteolysis is primarily caused by particle disease or fluid pressure waves [78, 91, 107]. The foreign body response caused by the wear particles present at the bone-implant interface is probably more detrimental than the cell damage caused by high fluid pressure waves. However, these wear particles require access to the bone-implant interface to cause osteolysis. Hence, the only way that particle disease can occur is if fluid pressure waves and pathways are present to pump these wear particles to the bone-implant interface [78, 91, 107, 108]. On the other hand, a fully-fixed implant can inhibit particle ingress [107]. Osseointegration is therefore vital for the long-term survival of the implant.

2.5.2. Prerequisites for Osseointegration

Osseointegration is the biological process in which an implanted prosthesis integrates with the surrounding bone. This process is similar to that of bone healing following a fracture. It includes the formation of a hematoma around the implant immediately after implantation; the development of a provisional bone matrix secreted by osteoblasts directly onto the implant surface a few days after implantation, which develops in to immature bone; and finally the remodelling of the immature bone into mature bone, providing biological fixation of the implant [13, 109, 110]. The bone healing process, and hence osseointegration of an implant, can be impaired by pharmacological agents, such as non-steroid anti-inflammatory drugs and patient specific factors and warfarin, and by patient specific factors, such as osteoporosis, rheumatoid arthritis, advanced age, nutritional deficiency and smoking [109, 110].

As osseointegration is complex process which can take up to several weeks, cementless cups initially rely on primary mechanical fixation [73, 79, 87, 111]. Three conditions must be met for osseointegration to take place: good bony apposition, appropriate surface finish, and stable initial fixation.

Good Bony Apposition

Large gaps between the bone and the acetabular component can compromise the osseointegration of the implant in different ways. Firstly, a gap at the interface means that the bone cells need to create a bridge between the bone and the implant [81, 112]. Secondly, gaps are “effective joint spaces” that allow both fluid pressure waves and the circulation of wear debris, resulting in bone resorption and osteolysis [76]. Researchers are divided on the

definition of a tolerable gap at the bone-implant interface. While some authors have reported that bone ingrowth is possible with gaps at the bone-implant interface up to 2mm [113, 114] and 3mm [7], others have argued that the gaps must be smaller than 0.35mm [115]. However, most agree that the rate and consistency of bone ingrowth is enhanced with smaller gaps. Furthermore, the presence of a bioactive coating, such as hydroxyapatite (HA), enables bigger gaps to be bridged [112].

Appropriate Surface Finish

Surface finish of the outer coating of the acetabular shell provides a scaffold into which bone ingrowth can occur. The pore size of the coating is an important factor; if these are too small, the cells cannot grow into the coating and therefore osseointegration does not occur. On the other hand, if these pores are too big, the coating does not provide the mechanical stability required for the newly grown bone [116, 117]. The optimal pore size is therefore a compromise between the biological and mechanical factors. Studies have shown that the optimal pore size ranges between 100 µm to 400 µm; however this range is dependent on the coating material and type of coating used [7, 81, 116-120].

The most common coating materials are titanium plasma-spray and porous cobalt-chromium alloys; although sintered beads, fibre metal and many others are also available (Figure 2.22) [75, 81, 87]. Bioactive substances, such as HA, can also be sprayed onto the porous coating to stimulate bone ongrowth, hence increasing the chances of successful bone-implant integration [87, 121].

Figure 2.22 – Cementless acetabular cups with different surface finishes and different numbers of screw holes (top) or none (bottom; picture from [87] with permission)

Stable Initial Fixation

Initial stability of acetabular cups is important for osseointegration as high levels of cup micromotion at the bone-implant interface inhibits bone formation and, instead, contributes to the development of a fibrous membrane [78, 81, 87, 122]. The threshold of implant micromotion at which fibrous tissue grows instead of bone tissue has been the subject of many studies [10, 123-125]. The general consensus in the literature is that 40 µm of micromotion and below promotes bone growth, whilst micromotions above 150 µm favours fibrous tissue

formation. A mixture of bone growth and fibrous tissue formation occurs with micromotions between 40 µm and 150 µm. Within this range of implant motion, the proportion of bone ingrowth depends on implant, patient and surgery specific factors [10, 123-125]. Hence, initial stability can be defined as the rigid fixation between the implant and the host bone cavity with minimal levels of micromotion of the implant in order to promote osseointegration. There is a range of mechanical fixation methods that provides initial stability of the acetabular cup. They are based on two distinct fixation philosophies: on-line and press-fit.

On-line fixation is when the acetabulum is reamed to the same diameter as the cup, and the cup is then anchored and stabilised within the acetabulum using spikes, fins (Figure 2.23), or most commonly trabecular bone screws (Figure 2.22) [7, 87]. This technique offers reliable stability and proper seating of the cup within the acetabulum [7, 87, 106].

Figure 2.23 – Tri-spiked acetabular component with a porous coating and polyethylene liner (left; picture from [126] with permission); acetabular component with fins and a ceramic liner (right; picture from [127])

There are a few potential complications associated with the use of bone screws. Firstly, if the screws are not inserted correctly, they can cause irreversible neurovascular injuries [128]. Secondly, screws can acts as a pivot for the cup, which results in its toggling motion under cyclic loading [106, 119, 129]. Finally, screws are also linked to wear debris generation. Fretting between the screw and the metallic shell will produce metallic particles, while the screw heads or the edges of screw holes can damage the liner, especially if it is made of a soft material such as polyethylene [93, 95, 97, 98, 130]. Wear particles can remain at the shell-liner interface, accelerating the generation of wear debris through third body wear [94, 100]. The screw holes can also act as a pathway, allowing particles to migrate to the bone-implant interface, which can trigger particle disease [92, 97, 130]. In order to limit the risk associated with the use of screws, Wasielewski *et al.* [128] identified areas of the acetabulum where screws can be safely used, and some implant manufacturers provide plugs to close any unused screw holes.

The benefits of using cups with spikes or fins include immediate fixation and rotational stability without providing pathways for wear debris like screw holes do [126, 129, 131, 132]. Furthermore, they are less likely to cause neurovascular damage. However, once they are positioned in the acetabulum, any adjustment of the position of the cup is very difficult [126, 131]. Studies have also observed that bone ingrowth occurs less frequently and in smaller amounts in cups using spikes compared to cups using screws [133]. This is partly due to the fact that spikes only provide rotational stability, while screws provide both rotational and axial

stability [134]. Furthermore, Cook *et al.* [133] demonstrated that screws convert torsional forces into compressive forces, thereby increasing the contact area at the bone-implant interface, further promoting bone ingrowth.

Press-fit fixation is obtained when an oversized cup is implanted into an under-reamed acetabular cavity. As the cup is hammered in place, the acetabulum deforms and recoils around the implant, firmly gripping it in place [135, 136]. For a correctly implanted press-fit cup, the contact area between the implant and the host bone should be limited to the rim of the cup [137]. This produces a strong equatorial fit, resulting in high compressive stresses, and hence compressive forces, at the periphery of the acetabulum which stabilises the cup [40, 64, 113, 137, 138]. In addition to this, by limiting the contact area to the rim of the cup, the majority of the load is transmitted through the peripheral cortical bone present at the rim of the acetabulum, recreating the load transfer observed in the natural hip [40, 137, 139]. Another advantage of rim contact between the cup and the bone is that it acts as a seal, preventing debris generated by the bearing surfaces from infiltrating and compromising the bone-implant interface [87, 113, 140].

Obtaining the optimum degree of under-reaming is key. If the press-fit is not sufficient, then the compressive forces holding the cup in place will be too low, compromising the stability of the cup [135, 141]. On the other hand, if the press-fit is too high, complications such as incomplete seating and acetabular fractures can occur [113, 135, 140]. Studies have shown that the ideal press-fit is between 1 to 2 mm, depending on bone quality [106, 135, 141].

Fins, spikes and trabecular bone screws can be used as additional fixation with press-fit cups. There are many opposing reports concerning the use of additional fixation, especially trabecular screws with press-fit cups. The general consensus is that press-fit acetabular cups can be successfully implanted with and without trabecular screw fixation; the decision to use screws depends mainly on the bone quality of the acetabulum, the stability of the inserted acetabular component and the surgeon's preference. However, most studies agree that if press-fit is enough, then trabecular bone screws should be avoided and the screw holes should be plugged to reduce debris generation and remove pathways [93, 97, 140, 142, 143].

2.6. INVESTIGATING CEMENTLESS ACETABULAR CUP STABILITY

Pre-clinical tests are an important stage when developing joint replacement prostheses. Ideally, their aim is to identify if a new implant will survive *in vivo* by subjecting it to a series of tests *in vitro* that replicate *in vivo* conditions prior to clinical trials.

Standardised tests currently available for THR address design specifications, materials, and wear properties of the bearing surfaces, focusing only on the implant itself and its biocompatibility. However, there are no standards to assess both the short and long-term stability of implanted hip prostheses. This is surprising considering that aseptic loosening is the number one cause of failure of THR and that initial stability is crucial for the long-term survival of cementless implants, especially the acetabular cup.

There are numerous studies that have assessed the stability of implanted cementless acetabular cups. This section reviews the different factors that are important when designing a method to assess acetabular cup stability. These include the different measurement methods and systems, the loading protocols, the acetabular cup positioning and the acetabular model in which the cup is implanted.

2.6.1. MEASURING CUP STABILITY

There are many different methods that have been employed to investigate the stability of implanted acetabular cups. These methods can be categorised into two different approaches: load-to-failure tests and micromotion and migration studies.

LOAD-TO-FAILURE STUDIES

Load-to-failure studies are designed to test acetabular components under extreme conditions to investigate their design limits. These methods use standard test equipment and have well-defined end-points, making them relatively straightforward to setup and carry out. There are four commonly used methods in the literature: the torque test, the lever-out test, the pull-out test and the edge-loading test (Figure 2.24).

Failure in rotation of an acetabular cup will occur if the frictional forces at the bone-implant interface are smaller than those generated between the bearing surfaces [144]. The torque test assesses the torsional and rotational stability of acetabular cups by applying a torque parallel to the rim of the implanted shell and measuring the force required to loosen it (Figure 2.24) [131, 135, 141, 144-149].

Another popular method used to test cup stability is edge loading [132, 139, 149-152]. Edge loading occurs *in vivo* during impingement and dislocation [149, 150]. Following implantation, the acetabular shell is loaded axially at its periphery at a constant stroke rate until shear failure occurs. Shear failure is defined as permanent displacement of the shell by 150 µm; it is measured using a displacement sensor positioned on the rim of the shell and on the opposite side of the load (Figure 2.24).

Lever-out tests are used to investigate the initial stability of an acetabular component by levering the shell out of the acetabulum [141, 144, 153-155]. Impingement and articulation

forces caused by resisting rim effects and friction can result in levering-out of an implanted acetabular cup *in vivo* [144]. This is assessed *in vitro* by connecting the shell to a lever arm, usually through the dome screw hole, and loading the lever arm perpendicularly until the shell dislodges itself from the acetabulum (Figure 2.24).

The last method commonly used is a pull-out test where the shell is pulled-out of the socket resulting in a direct distraction (Figure 2.24) [144, 155]. This type of failure is unlikely to occur in THR, however, it replicates the direction of pistoning of the shell within the acetabulum under load, which may provoke cup loosening [155].

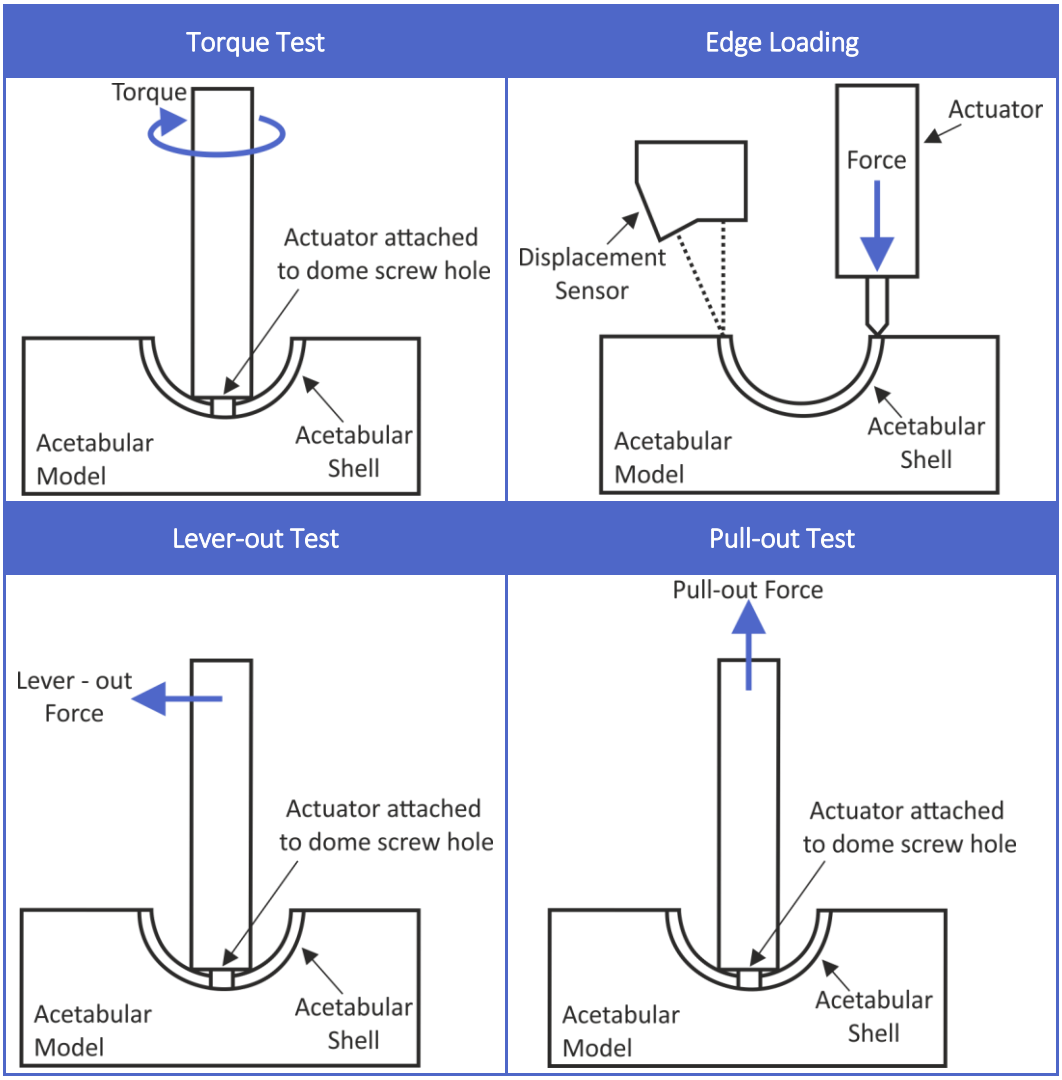

Figure 2.24 – Examples of load-to-failure tests commonly used in the literature

The main limitations of these load-to-failure tests are that they do not give any indication of how the implants function under physiological conditions nor do they recreate normal use of the implant. Furthermore, they only replicate one-off, extreme situations, such as a stumble or a dislocation. They do not investigate the effect of repeated activities of daily living, such as walking, stair climbing or rising from a sitting position. Finally, with the exception of the rim loading tests, none of the tests have a relevant clinical limit. These methods allow comparison of the stability of different cups, but are unable to say what is safe.

Acetabular Cup Micromotion and Migration Studies

Techniques to measure the micromotion and migration of an acetabular cup under dynamic loading have been developed over the past 20 years, with the aim of better understanding how acetabular cups behave *in vivo*. Results from these studies have allowed comparisons between implants and helped identify parameters that affect stability. This information can be used to improve cup fixation and therefore increase the longevity of cementless acetabular cups.

A variety of sensors and instrumentation have been used to measure the motion of acetabular cups *in vitro*. They can be divided into two main measurement philosophies: direct measurements, where sensors such as linear variable differential transformer (LVDT) sensors, eddy current transducers and extensometers are in direct contact with the implant; and indirect measurements, making use of imaging techniques and motion capture systems.

LVDTs and eddy current transducers are commonly used to measure the micromotion of an acetabular component under load [106, 119, 129, 134, 156-160]. LVDTs are electrical transducers that measure linear displacement via an inner core that moves through an inductance coil. There are many positives related to the use of LVDTs: high accuracy, ease of use and low cost. However, LVDTs are relatively large, which limits where they can be positioned, and they usually require large and complex assemblies to locate them during testing. Eddy current sensors are contactless and generate a magnetic field that depends on the distance between the sensor and its target. Similar to LVDTs, the results obtained using eddy current transducers are very accurate, reliable and comparable; furthermore, they tend to be smaller than LVDTs. However, the aluminium targets required to make eddy current transducers work are relatively large, which makes their positioning challenging and limiting, especially when it comes to attaching the aluminium target to either the bone or the acetabular cup.

When measuring the micromotion and migration of acetabular cups, these sensors are either placed in direct contact with the liner or arranged to measure the motion of a target that is rigidly attached to the cup. There are different setups available in the literature that measures the micromotion between the bone and the rim of the acetabular cup (Figure 2.25). These include: six LVDTs divided into two clusters to measure the three translations of both the anteromedial and the posteromedial side the cup [134]; three LVDTs [106] or three eddy current sensors [129, 159, 160] to measure the axial translation of the cup in different locations along its rim; four LVDTs to measure the axial and radial translations of the cup [157]; and six LVDTs positioned in different directions around the rim of the cup to measure its three translational directions [119, 156].

There are some limitations with these setups. Firstly, these methods only measure a few selected directions of motion, either because these directions are assumed to be the dominant direction of motion or because of limitations in placing the sensors. For example, eddy current transducers are only used to measure axial micromotion of the cup because of the difficulty of placing the aluminium targets. Another limitation is the assumption in some of these studies that the cup is a rigid body, and therefore use measurements taken at

different areas along the acetabular rim to determine the overall motion of the cup [119, 156]. It has been shown that the cup deforms under load [161-164] and therefore measurements taken at different areas along the rim of the cup should be considered as independent and not be combined to determine the overall motion of the cup.

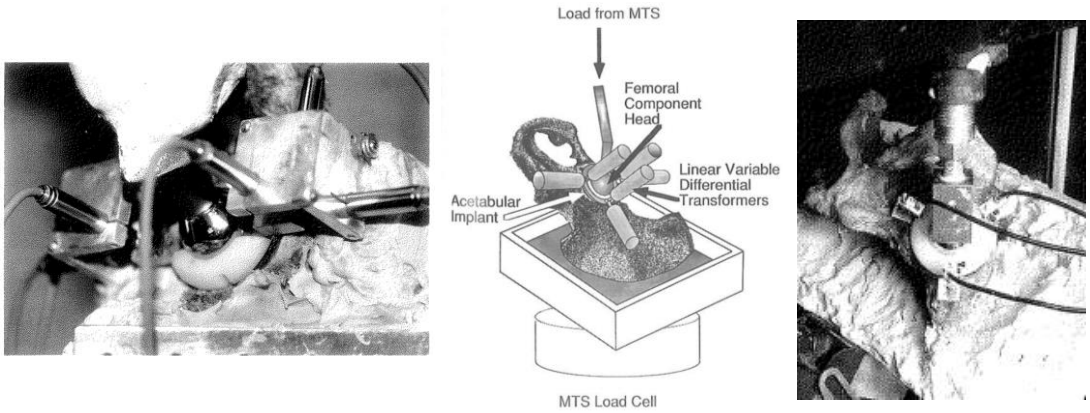

Figure 2.25 – Different setups described in the literature to measure the micromotion of acetabular cups using LVDTs and eddy current transducers (pictures from: [129, 134, 156] with permission).

Extensometers have been used in one study to measure the axial translation and the lateral tilt of the acetabular shell relative to the bone [165]. This method involved modifying the cup in order to attach the extensometers. This may have affected the structural properties of the cup and hence its behaviour once implanted. Furthermore, the accuracy of extensometers was not as good as LVDTs and eddy current transducers.

Recent studies have used imaging techniques or motion capture systems to measure the micromotion and migration of implanted acetabular cups under physiological load [166]. Roentgen stereophotogrammetric analysis (RSA) is commonly used in orthopaedics to determine the position of an implant, but it can only be used under static loading conditions. Therefore, it cannot be used to assess the micromotion of the cup under dynamic loading. However, it can successfully measure the migration of an implanted cup [166, 167]. Infrared diodes have also been used to measure the micromotion and migration of a cup using a 3D digitizer or motion capture systems [168, 169]. Both systems can register movement in terms of a Cartesian co-ordinate system and therefore measure six degrees of freedom (DoF). However, the infrared diodes can be challenging to repeatedly position and attach, introducing errors and variability in the results; furthermore, the levels of micromotion of the cup are at the limit of the measuring range of these systems, resulting in high levels of inaccuracy in the results [168].

There are no *in vitro* methods in the literature that accurately measure micromotion of acetabular components in all six DoF. It can be expected that the micromotion of the cup occur in multiple directions considering that the hip is subjected to cyclic loading and motion during activities of daily living. On the other hand, there are a few *in vitro* methods published in the literature that measure the micromotion in the six DoF of implanted femoral stems [170-175].

One of the most commonly used methods is the system developed by Berzins *et al.* [171] (Figure 2.26), which measures the three translational ranges of motion in the orthogonal axes

and the rotation about these axes via a single point of attachment. This method uses six LVDTs (three superior-inferior, two medial-lateral, and one anterior-posterior) held in a rig attached to the femur (Figure 2.26). A cruciform frame protrudes out of the lateral side of the bone, with one of its ends rigidly attached to the stem and target spheres held on the three other ends. The configuration of the transducers allows them to measure the position of all three spheres. This allows for six independent equations of motion to be generated and therefore the motion in six DoF of the implant to be calculated. This system is widely used in the literature to measure both the micromotion and the migration of implanted femoral stems [170, 174-179].

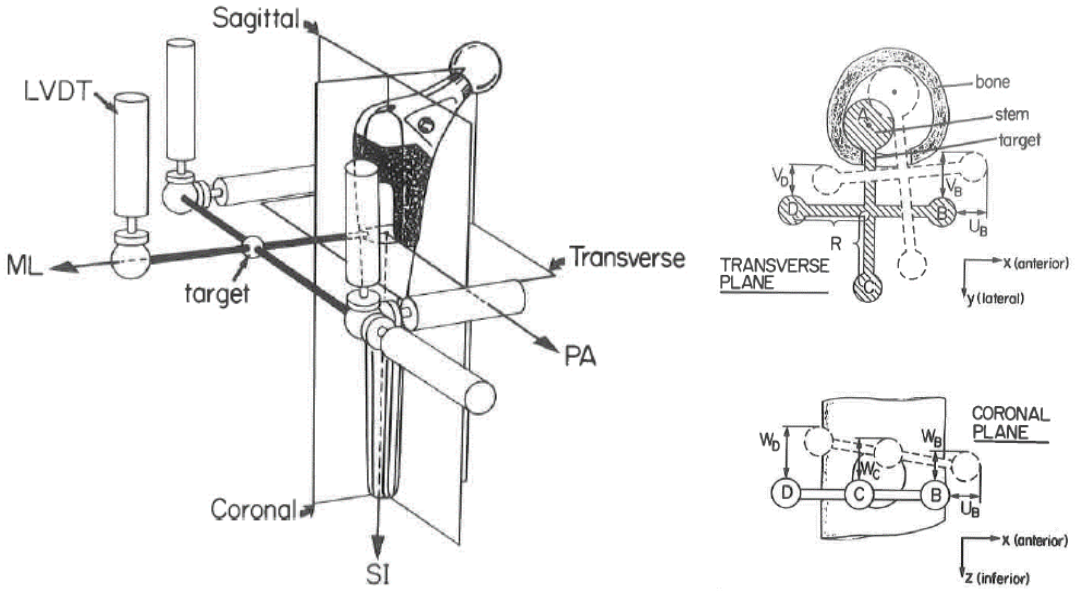

Figure 2.26 – Six DoF measurement setup developed by Berzins et al. [171] (SI = superior-inferior, ML = medial-lateral, PA = posterior-anterior; U_B, V_B, V_D, W_B, W_C, W_D = displacements recorded by LVDTs; illustration from [171] with permission)

The main limitation of this method is in positioning the measurement system. One needs to identify a place where the target can be rigidly attached to the implant, ideally without the need of damaging neither the implant nor the bone, and where the voluminous system with the six LVDTs can be placed without interference. Furthermore, unless the system can be successfully attached to the bone right next to the implant, the system will measure both the micromotion of the implant and the deformation of the bone present between the implant and the system. Despite these limitations, this system can accurately and repeatedly measure the micromotion in all six DoF of an implant without any rigid body assumptions as all the measurements are taken from the same point.

2.6.2. LOADING PROTOCOLS

Studies assessing micromotion or migration of acetabular cups use one of two different loading regimes: either ramp or cyclic loading. Many methods use ramp loading, which involves loading the cup to a maximum load and measuring its displacement [119, 129, 134, 156, 165, 168]. Cyclic loading involves cyclically loading the cup and measuring motion either

during cyclic loading (micromotion) [106, 157, 160, 166, 169] or as the change in position of the cup after cyclic loading (migration) [134].

Cyclic loading is more physiological than ramp loading as the hip undergoes cyclic loading during gait. Hence, the behaviour of an implanted acetabular cup during gait can be better assessed under cyclic loading. The number of cycles employed during cyclic testing varies between studies, from 5 cycles [106] to 100,000 cycles [134]. The frequency of the cyclic loading also varies between studies, ranging from 0.5 Hz [169] to 4 Hz [160]. However, most studies use loading frequencies between 0.5 – 2 Hz as they are representative of walking speeds.

The maximum load used in studies also varies from 100 N to 3.8 kN [106, 119, 129, 134, 156, 157, 160, 165, 166, 168, 169]. Most studies do not give any indication as to why a specific load was chosen [106, 119, 134, 156, 160, 165, 166, 168]. A few studies do indicate the reason for their chosen load: for example, 1.9 kN is equivalent to 2.61 times body weight of a 75 kg person, which represents the average peak load seen in stairs descent [169]; 2.35 kN represents the peak force during single leg stance of an 80 kg person [129]; and 3.8 kN represents around 400% of a 90 kg person [157].

2.6.3. Specimen Positioning

The position of the acetabular cup, and therefore the direction of loading of the hip joint, varies between studies. Some only give an indication of the positioning of the cup when tested, such as: “in the angle of maximum resultant force during the gait cycle” [168]; “in full flexion” [134]; or “in anatomical position” [129]. Others offer more information about the position of the hip during testing. Some of them indicate in which angle the hip was orientated, such as 45° abduction and 0° anteversion [166] or 30° inclination and 20° anteversion [106], whilst others give the position of the hip relative to external features, such as 60° from the vertical [157, 160]. Even though these positions offer the possibility to reproduce the testing protocol, no reasoning behind the chosen position of the hip was given.

A few studies have indicated both the positioning of the hip during testing and what it represented. For example, in one study the hip was positioned in 15° abduction and 10° forwards flexion, which corresponded to single leg stance [165]; and in another the hip was orientated to replicate the peak loads seen during normal walking (6.5° flexion and 7.2° abduction) and descending stairs (9.2° extension and 9.5° abduction) [169].

There are no studies that have investigated the effect of dynamic hip motion, such as that seen during a full gait cycle, on the micromotion and/or migration of an acetabular component. The combined effect of dynamic motion and cyclic loading on implant micromotion and/or migration has been investigated on the femoral side, with results suggesting that implants exhibit significantly higher levels of micromotion under dynamic hip motion compared to static positioning [180, 181].

2.6.4. ACETABULAR MODELS

Stability studies aim to investigate how prostheses behave when implanted and, therefore, require an appropriate acetabular model.

In vitro tests are usually performed on cadaveric pelvic bones because their unique and complex structure is difficult to replicate. However, there are inherent limitations to cadaveric testing. Cadaveric bones are in limited supply and are therefore expensive and difficult to obtain, especially in the quantities needed for pre-clinical tests. Studies have also reported large interspecimen variability in both bone quality and size [131, 151]. Finally, due to the irregular shape of the innominate bone, complex rigs are required to locate and secure them on testing machines, usually resulting in differences in positioning between specimens.

To counter the limitations of using cadaveric bones, many studies have turned to synthetic acetabular models. Foam blocks with a hemispherical cavity are a popular alternative to cadaveric pelvic bones as they are easily reproducible, have similar mechanical properties to bone, and are cheaper and more readily available [149, 151, 154, 182]. Unlike cadaveric bones, the interspecimen variability of these foam blocks is low as they are manufactured with consistent mechanical properties [131, 139, 144, 149].

Most studies investigating the stability of acetabular components use solid, rigid polyurethane biomechanical testing blocks manufactured by Sawbones (Malmö, Sweden) [131, 139 , 141, 144, 146, 150, 182]. Other studies have used EP-Dur polyurethane resin blocks made of modified diphenylmethandiisocyanate (Bayer, Leverkusen, Germany) [154], Pedilen foam (Otto Bock HealthCare, Minneapolis, Minnesota, USA) [149] and Darofoam (Daro, Butler, Wisconsin, USA) [152] to make their acetabular model. These foam blocks come with a variety of mechanical properties, all within the range of trabecular bone properties. These can therefore be used to investigate the stability of different acetabular cups when implanted into different bone qualities.

Some earlier studies have shown through comparison that foam blocks are a good alternative to cadaveric pelvic bones [141, 144, 182]. Furthermore, these studies also reported less variation in results when using foam blocks compared to cadaveric pelvic bones. There are, however, some inherent limitations to the use of foam blocks as acetabular models: only one type of bone is included and the acetabulum is always modelled as a hemisphere, simplifying the acetabulum.

To obtain more clinically relevant results, some studies have introduced more complex acetabular models. These models contain important acetabular and pelvic features in order to recreate a more physiological replica of the acetabulum. The aim of these models was to combine the advantages of both cadaveric bones and foam models [32, 151, 183]. These more complex models have not only been used to determine the stability of acetabular components, but have also been used to investigate other factors, such as internal and surface strains of the pelvis following cup implantation.

Sawbones fourth generation hemipelvis composite bones have been used in previous studies as an acetabular model [160, 169]. These composite bones are specifically made for

mechanical testing by accurately replicating the shape of the pelvis and the physiological properties of real bones. Validation studies comparing fourth generation Sawbones composite bones and cadaveric bones have been performed on the femur [184] and the tibia [185], however none have validated the use of the hemipelvis composite bone as an appropriate acetabular model. These models are also expensive, limited to a single size and, similarly to cadaveric pelvic bones, are difficult to locate for testing purposes.

To replicate the support from the cortical bone around the acetabulum, some studies have used composite cylinders. These feature a thick cylinder made of short glass fibres and epoxy resin filled with large cell rigid polyurethane foam to model the outer cortical bone and the trabecular bone, respectively [166, 167]. These models are easy to manufacture with constant mechanical properties and their simple shapes make them easy to place and locate on test machines. Even though they replicate the cortical support present around the acetabulum, they do not take into account the geometry of the acetabulum, such as the presence of the acetabular notch, which can affect cup fixation.

A more complex composite structure was designed by Jamieson *et al.* [151], which replicated the important anatomic and structural features of the acetabulum. This acetabular model comprised low density polyurethane foam with polymeric reinforcements representing the trabecular bone bed and the periacetabular cortex, respectively (Figure 2.27). In addition to this, anatomical features were also replicated, such as the acetabular notch, an external chamfer of the bony margin, reinforced columns representing the ilium, ischium and pubis, and a bony defect. This model was validated by comparing its stiffness profile to that of seven cadaveric acetabula; however, the validation did not include comparable tests, such as the stability test for which this model was designed. Furthermore, even though this model is easy to place and locate on testing machines and can be reused up to four times, it is still complex to manufacture and expensive [132, 151].

Foam blocks with a hemispherical cavity and two rectangular cavities on opposite sides of the acetabulum (Figure 2.28) have also been used as an acetabular model [161, 163, 186, 187]. This model replicates the pinching effect between the anterior and posterior columns of the acetabular component observed in both clinical and cadaveric investigations [164, 186, 188]. This model was validated using cadaveric pelvic bone by comparing acetabular shell deformation when implanted into both cadaveric pelvic bone and this model. Furthermore, this model is easy to manufacture, has constant mechanical and geometrical properties, and is easy to place on testing machines.

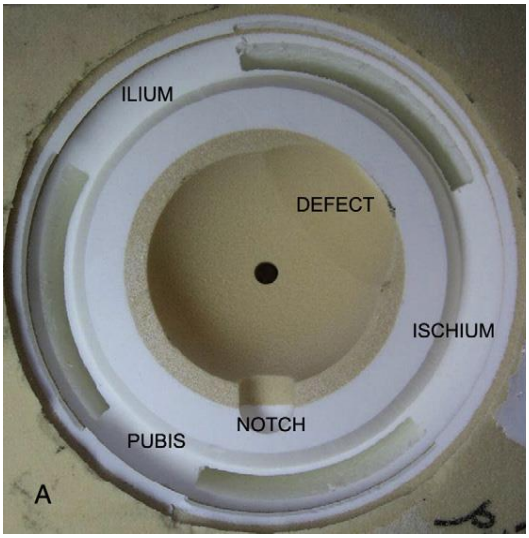

Figure 2.27 – Acetabular model by Jamieson *et al.* (picture from [151] with permission)

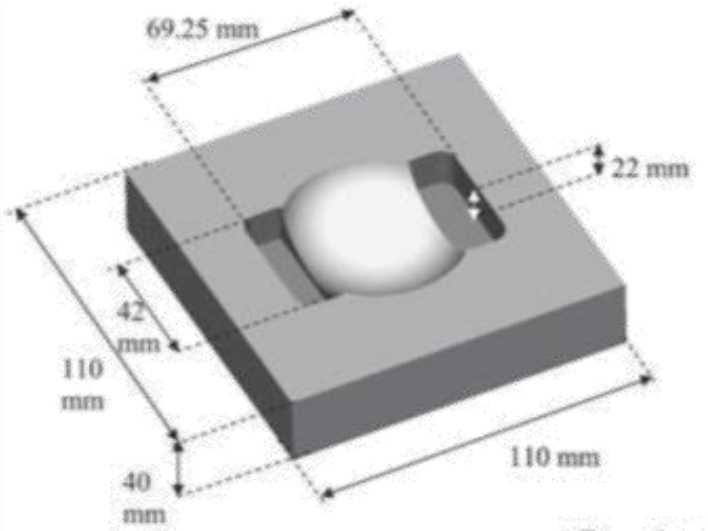

Figure 2.28 – Acetabular model by Jin *et al.* (right; picture from [186] with permission)

2.7. CONCLUSIONS

The hip is a key joint in the human body. It can be worn out or damaged due to the many load bearing cycles and significant forces that it has to withstand over time. THR is an important procedure that removes the pain and restores the function of a diseased hip joint. A brief history of THR has been presented to show how improvements and modern developments have contributed to its increasing success. Today, one of the main reasons of failure of THR is the high loosening rates of acetabular components. Initial stability is a key factor for osseointegration and hence for the success of cementless acetabular component fixation. It is therefore crucial to investigate the stability of acetabular cups and the factors that might affect it in order to reduce the risks of aseptic loosening and therefore further improve the success rate of THR.

There are no standardised methods to assess initial stability of acetabular components when implanted. However, there are numerous studies available in the literature and a review of these has been presented. The main conclusions that can be drawn from this review are that micromotion studies aim to provide a better insight into how cups behave once implanted, however, they do not fully replicate *in vivo* conditions *in vitro* due to three main limitations. Firstly, none of these studies have investigated the motion of acetabular cups in all DoF; instead, they only measure or report a few selected directions of motion that are assumed as dominant. Secondly, these studies are performed quasi-statically where the hip is set at a fixed angle, usually replicating heel strike or single leg stance; but none have taken into account the effect of both cyclic loading and motion the hip is subjected to during activities of daily living. Finally, most of these studies either use cadaveric pelvic bones, which are limited in number and vary in size and properties; or synthetic models with a hemispherical cavity that do not replicate the complex mechanical and structural properties present in and around the acetabulum.

Hence, in order to properly assess the micromotion, and therefore stability, of press-fit acetabular cups, a new test method is required that measure the micromotion of acetabular cups in all six DoF when implanted in an acetabular models that correctly replicate the structural support seen in the acetabulum; and subjected to both physiological loading and hip motion.

3. AIM AND OBJECTIVES

Initial stability of press-fit acetabular components is an important requirement for the long-term success of its fixation and its survival in the human body. A poorly fixed prosthesis is prone to micromotion under physiological loading and hip motion. High levels of micromotion can inhibit bone formation and therefore osseointegration of the implant. This can result in the loosening and the premature revision of the implant.

The aim of this project was to design and develop a robust methodology to assess the micromotion of press-fit acetabular cups under both cyclic loading and dynamic hip motion, which could form the basis for a more representative pre-clinical protocol for the evaluation of new and different cup designs. This aim was achieved through the following four key objectives:

- **Development of a method to measure the micromotion, in six DoF, of an implanted acetabular cup under cyclic loading.** No studies have accurately measured the overall micromotion of acetabular cups in all six DoF. Measuring the six DoF is important to fully understand the motion of the acetabular cup under physiological conditions, and hence its behaviour once implanted.
- **Creation of an acetabular model replicating important anatomic features of the acetabulum.** Currently, most studies investigating the stability of acetabular cups either use cadaveric pelvic bones or synthetic foam blocks with a hemispherical cavity. Both options have their advantages and disadvantages. Creating a more anatomically representative synthetic model offers the ability to simulate the complex behaviour of the acetabulum, as seen with cadaveric testing, whilst keeping the low interspecimen variability and ease of testing of synthetic models.
- **Design of a dynamic rig to model the movement of the hip during common activities of daily living.** Studies assessing acetabular cup stability keep the hip joint in a fixed position throughout testing, usually replicating single leg stance or heel strike. However, dynamic motion of the hip can have an effect on the stability of the cup. Hence, recreating *in vitro* the movement of the hip during common activities of daily living allows for a more physiologically representative test.
- **Assessment of the pre-clinical test protocol.** The pre-clinical test protocol obtained through the combination of these three first objectives was used to investigate the micromotion of an acetabular cup with a new porous coating by comparing it to its clinically successful predecessor.

4. CUP MICROMOTION IN SIX DEGREES OF FREEDOM UNDER SINGLE LEG STANCE

4.1. INTRODUCTION

The hip joint is subjected to cyclic loading and motion during activities of daily living, which can induce micromotion of press-fit acetabular cups. High levels of micromotion inhibit bone formation and hence osseointegration of the cup within the acetabulum. Initial stability of the cup is therefore crucial for its long term survival. The ability to measure the micromotion of a cup in the laboratory and hence determine if it is within the threshold of osseointegration constitutes a desirable tool for the orthopaedic community, as it would give a better insight on how the cup behaves once implanted.

As highlighted in Chapter 2, there are no standardised methods to assess initial stability of implanted acetabular components; however, there are numerous studies available in the literature. These studies have three major limitations: firstly, they only measure and report a selected few directions of motion, often in the direction of assumed dominant motion only, rather than investigate the overall motion of the cup in all six DoF. Secondly, these studies are performed quasi-statically where the hip is set at a fixed angle, usually replicating heel strike or single leg stance. No studies accurately measure the micromotion of acetabular cups in six DoF nor do they investigate the effect of cyclic hip motion on the micromotion of the cups. Finally, most of these studies use cadaveric pelvic bones, which is advantageous as they closely replicate the environment in which the cup is implanted. However, cadaveric bones are expensive, limited in supply and have a high interspecimen variability in both size and mechanical properties. Hence, their use in a pre-clinical testing protocol is not feasible as high numbers of specimens similar in size and properties are required.

This chapter focuses on the measurement of the micromotion of an acetabular component when the hip is held in a fixed position: in this case, single leg stance (SLS). This includes a measurement system devised to measure the micromotion of an acetabular cup in six DoF under cyclic loading and the protocol associated to it, as well as a synthetic acetabular model designed to replicate the structural properties presented in the acetabulum. The dynamic component of this thesis, in which a dynamic hip motion simulator was developed to replicate hip flexion-extension during activities of daily living, is described in the next chapter.

4.2. PROSTHETIC COMPONENTS

A single acetabular component and a femoral head were used throughout the entire development of the test protocol. Common prosthetic components were chosen for clinical relevance.

For the bearing surfaces, metal-on-polyethylene was chosen as it is the most common bearing surface combination in primary THR in the UK, comprising of 60% of all procedures and 29.3% of all procedures involving a cementless acetabular cup (both cementless and hybrid fixation) [4].

For this work, a 28 mm CoCr femoral head was used. There are three common femoral head sizes used in the UK: 32 mm (36%), 28 mm (34%) and 36 mm (27%) [4]. However, when only considering metal-on-polyethylene bearings, the 28 mm femoral head is the most commonly used head size with 44% of all procedures; the larger femoral heads are mostly made of ceramics rather than metal [4].

For the acetabular component, a Trident cup with HA coating (Stryker, Mahwah, NJ, USA), was used (Figure 4.1). The Trident acetabular component is the second most widely used cementless cup in the UK (19%) behind the Pinnacle cup (31%; DePuy, Warsaw, IN, USA) [4].

The Trident acetabular component comprised a 54 mm solid back shell with HA coating and its corresponding polyethylene liner (X3 liner, Stryker). The shell was completely covered with the porous coating and had a screw hole at its dome, called the dome screw hole (Figure 4.1). It is used to connect the cup to the inserter during surgery. This hole is usually closed with a plug before the liner is inserted into the shell.

Figure 4.1 – Trident acetabular cup with HA coating and X3 polyethylene liner

4.3. PROTOCOL TO MEASURE CUP MICROMOTION IN SIX DOF

The first aspect of this pre-clinical test protocol was the development of a measurement system and a protocol to accurately and repeatedly assess the micromotion in six DoF of a press-fit acetabular cup.

4.3.1. MICROMOTION MEASUREMENT SYSTEM

A popular method used to measure the micromotion of femoral stems was adapted to measure the micromotion of the acetabular cup. This method was chosen as it reliably measures all six DoF of an implant from a single point of attachment, hence removing any error created by rigid body assumptions.

The target frame was rigidly attached to the acetabular cup through a rod threaded into the dome screw hole at the apex of the acetabular cup (Figure 4.2). The dome screw hole was chosen as an attachment site for two reasons. Firstly, it allowed the rod and the target frame to be rigidly attached to the cup without modifying the cup, as any modifications could change its mechanical properties and hence its behaviour when implanted. Secondly, since research suggests that press-fit primarily relies on peripheral fixation within the acetabulum, it was assumed that a small hole at the bottom of the acetabular cavity through which the rod passed though would not affect the stability of the cup.

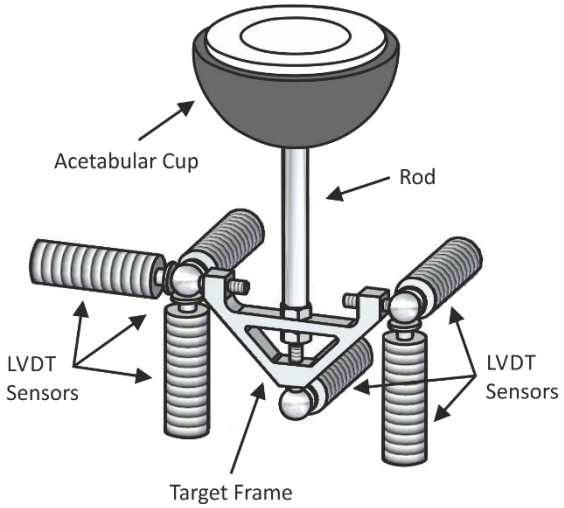

Figure 4.2 – Six DoF measurement system connected to the acetabular component

Six LVDTs (Red Crown model 3441552000 F05; Marposs, Bentivoglio, Italy) were used to measure the displacement of the spheres attached to the target frame (Figure 4.2). These sensors had a measuring range of ±0.5 mm with a linear error ≤3 µm. They were therefore able to detect small displacements in the tens of microns while having a measurement range large enough to accommodate for any migration of the cup during testing. Flat contacts with a diameter of 6 mm were used on the LVDTs to measure the displacement of the target spheres. Flat contacts were chosen over point contacts to make sure that the displacements measured by the LVDTs were only the motion of the cup reflected into the target spheres and not the point contact moving along the radius of the target sphere itself.

The configuration of the LVDTs allowed for six independent equations of motion to be generated (Appendix 1). These equations were expressed in matrix form (Equation 1) which was then used to convert the displacement measured by the six LVDTs into micromotion of the cup in six DoF: three translational ranges in the orthogonal axes (X, Y, Z) and the rotations around these axes (θ_X, θ_Y, θ_Z; Figure 4.3). The translations X, Y and Z corresponded to the anterior-posterior, superior-inferior and medial-lateral motions, respectively. For the rotations, θ_X and θ_Y corresponded to the medial-lateral and the anterior-posterior tilts, respectively, and θ_Z is the medial-lateral rotation.

Equation 1 – Conversion matrix

$$\begin{bmatrix} Z_D \\ Z_B \\ Y_D \\ Y_B \\ Y_C \\ X_B \end{bmatrix} = \begin{bmatrix} 0 & 0 & 1 & 0 & -ED & 0 \\ 0 & 0 & 1 & 0 & EB & 0 \\ 0 & 1 & 0 & EA & 0 & ED \\ 0 & 1 & 0 & EA & 0 & -EB \\ 0 & 1 & 0 & EA + EC & 0 & 0 \\ 1 & 0 & 0 & 0 & -EA & 0 \end{bmatrix} \begin{bmatrix} X_A \\ Y_A \\ Z_A \\ \theta_X \\ \theta_Y \\ \theta_Z \end{bmatrix}$$

Z_D, Z_B, Y_D, Y_B, Y_C, and X_B are the displacements recorded by the sensors, the central matrix is the conversion matrix with EA, EB, EC, and ED being the dimensions of the target mount, and X_A, Y_A, Z_A, θ_X, θ_Y, and θ_Z are the motion in six DoF of the cup.

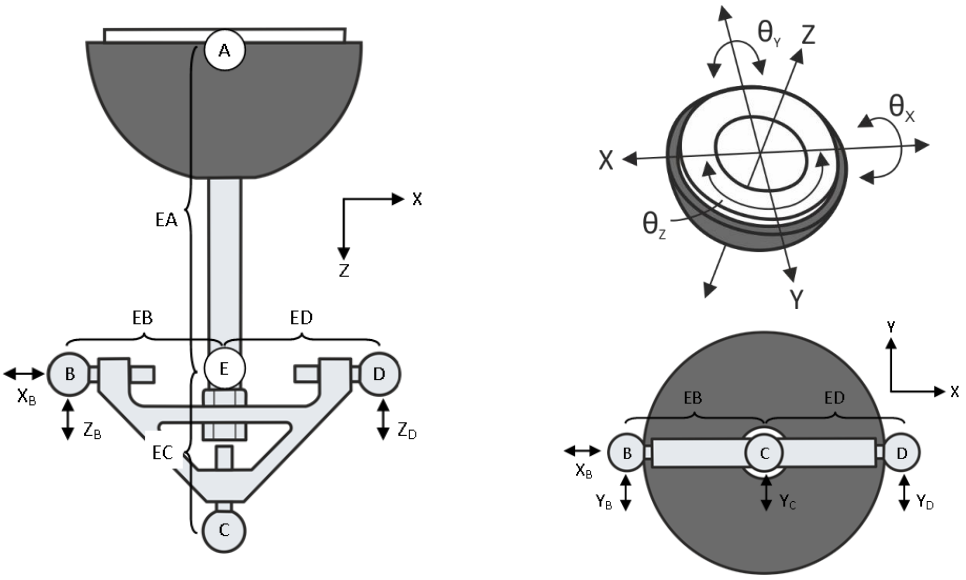

Figure 4.3 – Free body diagram identifying the dimensions and directions of motion used in the conversion matrix (Equation 1)

The target geometry was defined in such a way that the single point in which the micromotion in six DoF was calculated was the centre of rotation of the hip joint. This meant that even though the assumption of the cup behaving as a rigid body was not needed in calculating the micromotions as they were all taken from a single point, it was still assumed that the distance between the dome of the cup and the centre of rotation of the hip remained constant.

System Validation

Before being used to measure the micromotion of the acetabular cup, the system was validated to assess its accuracy and precision to check that it was able to measure the relevant micromotions of the cup in all six DoF. This was done using a Zwick bi-axial hydraulic testing machine (HBT 25-200; Zwick Testing Machines Ltd., Leominster, UK) as it was capable of both axial translation and rotation. The system was mounted on the Zwick and each of the six DoF was assessed independently by applying a known input translation or rotation to the measurement system and measuring the output signal. For each direction of motion, nine data points were taken at intervals of 100 µm or 0.1°; this was repeated five times.

The precision of the system was assessed by comparing the five different sets of data obtained from each repeat, while the accuracy of the system was assessed by determining how close the measured values were from their intended target value. The results showed that the system was very precise, with little variation between each repeat for all directions of motion. The accuracy of the six DoF measurement system was shown to be 20 µm in translations and 0.025° in rotations. The results of the system validation are available in Appendix 2.

It was therefore established that the measurement system was appropriate to measure the micromotion of an implanted acetabular cup. As previously mentioned, micromotions below 40 µm are ideal for tissue formation. Therefore, an accuracy of 10 µm in translations was acceptable. Furthermore, 0.08° of rotation equated to 40 µm of displacement in the direction of the arc of rotation for the 54 mm diameter Trident cup, and hence an accuracy of 0.025° was also acceptable.

4.3.2. Test Protocol

Along with the measurement system described above, a test protocol was developed to assess cup micromotion. This comprised of a method to insert the cup into the acetabular cavity, cyclically load it whilst taking micromotion measurements, and then removing it from the acetabular cavity.

Throughout the development of this micromotion test protocol, Sawbones polyurethane foam blocks (density of 0.48 g/cm³) with a hemispherical cavity were used as an acetabular model. The diameter of these hemispherical cavities were 1 mm smaller than that of the acetabular cup to obtain a 1 mm press-fit fixation of the cup.

Insertion Method

There are many methods described in the literature to insert the acetabular components prior to *in vitro* testing. Most studies use the insertion protocol recommended by the manufacturer, which is impacting the cup in the acetabulum using a mallet until it is fully seated [119, 129, 134, 144, 160, 165, 186]. Whilst this method is perfectly acceptable for surgery, it is user dependent, yielding some degree of variability in the impaction force and number of hammer blows, which can influence the stability of the cementless cup. This can result in high variability in the measured micromotion of the cup, which could mask the effect of the specific factor being investigated on cup micromotion, such as cup geometry, porous coating or fixation method.

To reduce this variability, materials testing machines are commonly used to insert the cup within the acetabulum. The most commonly used method is to load the component up to a pre-defined maximum load, which varies between 980 N and 8 kN depending on the study [131, 139, 141, 146, 149, 151, 152, 163]. On the other hand, both MacKenzie *et al.* [140] and Kim *et al.* [113] used a method to insert the cup in which pulses of 2 kN lasting 0.5s were generated for either 2 cycles or 5 cycles, respectively. Apart from the fact that the cup insertion methods are different between the different studies, these methods provide a controlled process with systematic and repeatable outcomes.

In this study, the cup was inserted into the acetabular model using a single axis hydraulic testing machine (Dartec Series HC10, Zwick Testing Machines Ltd, Leominster, UK)) controlled by the Workshop 96 program (Workshop 96 Toolkit, V2.18, Zwick Testing Machines Ltd, Leominster, UK). After trying the different types of insertion methods described in the literature, the chosen insertion method was similar to that used by MacKenzie *et al.* [140] and Kim *et al.* [113], where a protocol of 5 cycles of loading at a frequency of 1 Hz was performed. During preliminary trials, it was observed that the acetabular cup was not full inserted into the acetabular cavity with a peak load of 2 kN, hence a peak load of 5 kN was used instead [131].

A custom-made fixture, consisting of a disk fitting over the rim of the component, was used to ensure that the load was distributed evenly during implantation (Figure 4.4), and a bull's eye spirit level was balanced on the acetabular rim before and after insertion to ensure proper alignment. As the cup was pre-assembled before insertion, the custom-made fixture applying the uniform load was in contact with the rim of the liner. This provided a greater surface area on which the load was applied. Furthermore, as insertion was done in quasi-static conditions compared the impact of a hammer blow, this should not affect the insertion of the cup or the integrity of the liner.

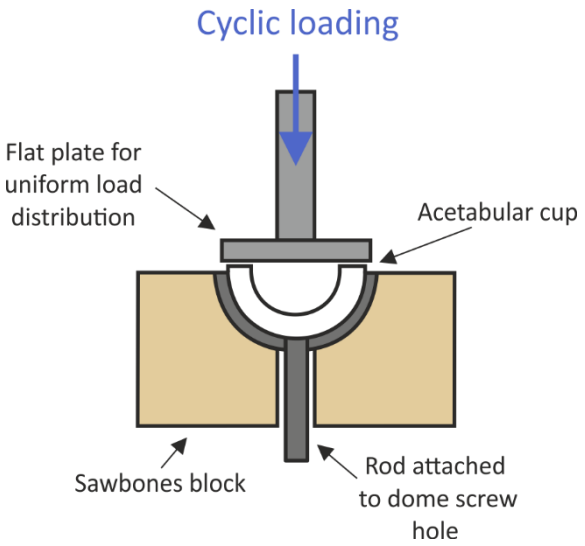

Figure 4.4 – Diagram of the cup insertion method

Micromotion Measurement Method

A test rig was designed to perform the micromotion tests (Figure 4.5); it was made of 10 mm steel plates welded together as previous designs made of aluminium were proven not strong enough to withstand the loads during testing.

In order to allow physiological loading, the 28 mm CoCr femoral head was attached to the actuator of the Dartec, which was positioned at the top of the machine (Figure 4.5). The test rig with the implanted acetabular component and the six DoF measurement system was rigidly attached to the base of the Dartec. This resulted in the hip joint being positioned upside down, with the femoral head at the top and the acetabular cup at the bottom. However, this upside down setup does not affect the interpretation of the results. The cup was inclined at 30° to the horizontal, and loaded vertically with the femoral head; this simulated single leg stance.

The six DoF system and the Sawbones block with the implanted cup were bolted to the top plate of the rig and the target frame was then rigidly attached to the connecting rod using a nut (Figure 4.5). The position of each LVDT was then adjusted to its mid-position to minimise the risk of reaching the end of their stroke during testing. The top plate can be separated from the rest of the rig to make it easier to attach the connecting rod to the target frame and to setup the LVDTs.

The Sawbones block needed to be rigidly attached to the test rig to prevent movement of the block during cyclic loading. Four bolts were used to attach the Sawbones block to the top plate of the test rig, and a block support was positioned below the Sawbones block to provide extra support (Figure 4.5).

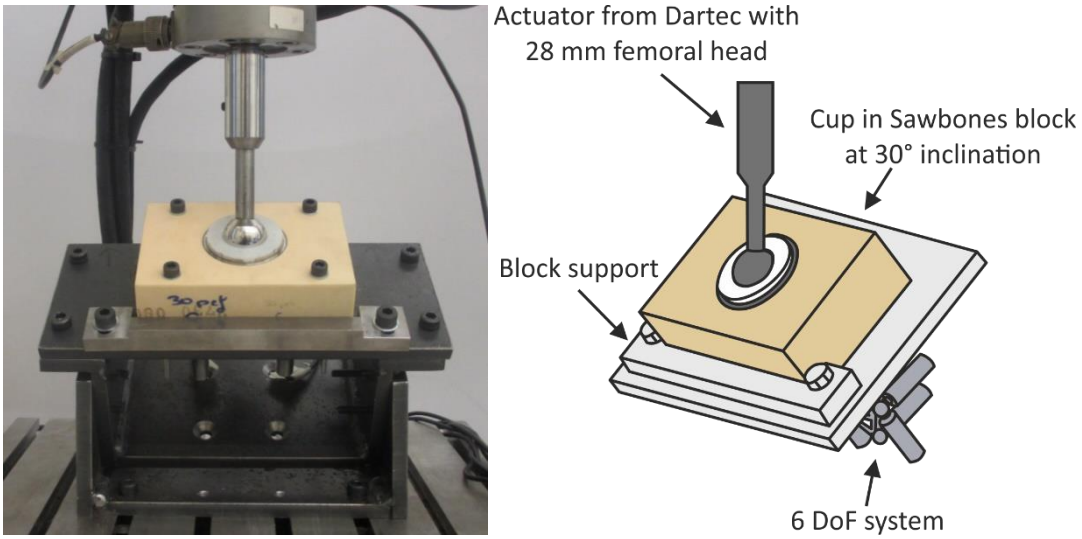

Figure 4.5 – Picture of the micromotion test rig simulating single leg stance (left) and a diagram of the detachable top plate showing the six DoF system underneath the plate (right)

The acetabular cup was cyclically loaded in compression with a sinusoidal wave form between 0.01 kN and 2.0 kN, at a frequency of 1 Hz for 1000 cycles; the tests were executed under load control. The minimum load was set at 0.01 kN to replicate the muscle forces acting on the hip when unloaded. The chosen maximum load was approximately 2.5 times body weight of an

80 kg person, which corresponded to the peak force produced across the hip during gait. A frequency of 1 Hz was used to simulate normal walking speed. These values are in accordance with the British Standards for hip joint simulators (BS 7251-7:1990), which states that the maximum applied load should be at least 1.5 kN and the loading frequency should be between 0.5 Hz and 1 Hz.

Push-out Method

Finally, a uniaxial push-out test was devised to remove the cup from the Sawbones block following the micromotion test. For this, the Sawbones block was inverted and the flat component used to insert the cup was used again to push against the protruding rod at a speed of 0.008mm/s (Figure 4.6). As there are no standards defining the push-out or pull-out rate of an implanted acetabular cup, the chosen speed used is the recommended speed to pull-off a femoral head from its trunnion as defined by the ISO standard ISO 7260-10:2003.

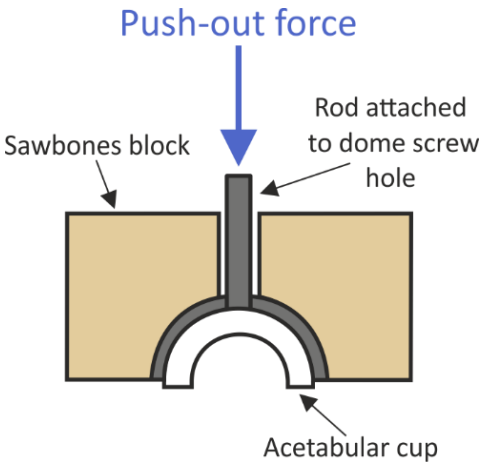

Figure 4.6 – Diagram of the cup push-out test

The acetabular component was not disassembled between each test because repeatedly removing the liner from the shell could damage the liner and its locking mechanism with the shell. This, in turn, could result in micromotion between the liner and the shell, which could affect the behaviour of the cup and the results.

Following push-out, a thin layer of foam incrusted into the porous coating at the rim of the acetabular shell and damage at the periphery of the acetabular cavity were observed (Figure 4.7). The presence of the foam changes the porous coating and may affect the stability of the cup when re-implanted into another block. For this reason, a cleaning procedure was introduced in which the cup was cleaned using a soft nylon brush after every test to remove any foam debris. Visual inspection of the acetabular cup was also performed after every test to ensure that all the foam was removed and that the porous coating of the cup was not scratched or damaged.

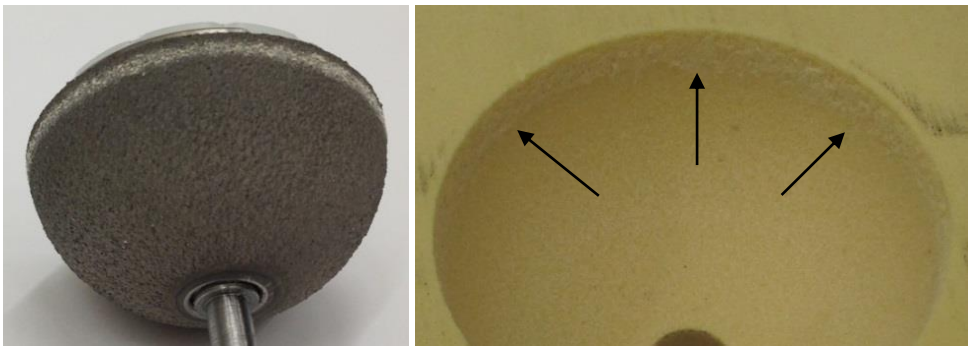

Figure 4.7 – Sawbones foam incrusted into the porous coating at the rim of the acetabular cup (left), and visible damage at the periphery of the acetabular cavity of the Sawbones block (right) after push-out

Data Collection & Processing

A schematic drawing of the test setup showing the components and the connections in instrumentation is shown in Figure 4.8. As previously mentioned, the Dartec was controlled by the Workshop 96 program. A data processing frame with 14 available channels and connected to a PC with LabView software (v. 11.0.1; National Instruments, Austin, TX, USA) was used to record all the data during testing. The load and displacement leads from the Dartec were directly connected to the data processing frame, and three data acquisitions (DAQ) cards were connected to the frame to collect the data from the LVDTs (two LVDTs per card).

For both the cup insertion and the cup push-out tests, only the load and displacement of the Dartec were recorded using a two-channel LabView program. For the micromotion test, an eight-channel LabView program was used to record the data from the Dartec and the six LVDTs. All data were collected in volts with a sampling rate of 100 Hz.

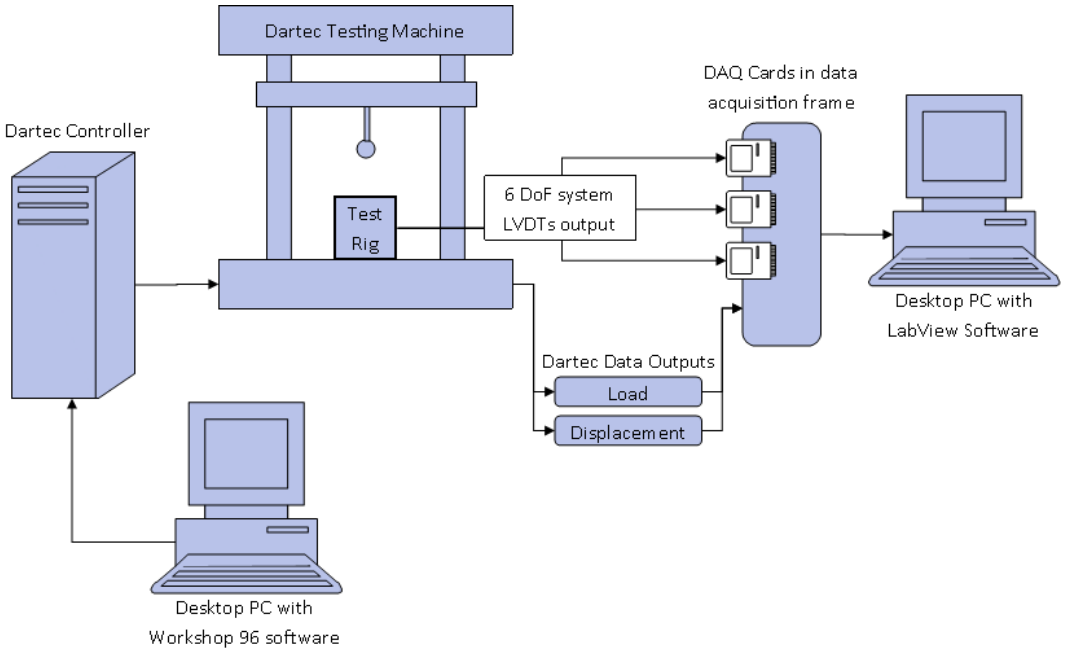

Figure 4.8 – Schematic showing the components and connections in instrumentation

Two Matlab (Matlab 7.13; The MathWorks Inc., Natick, MA, USA) routines were developed to convert the data from volts to their respective unit using predetermined calibrations factors and to extract the most relevant information. The first Matlab code converted the data from the LVDTs to micromotions of the cup in six DoF using the conversion matrix (Equation 1). A Fast Fourier Transform was then used to obtain the amplitude of the micromotion in each direction. The second code identified the push-out force required to extract the cup from the acetabular cavity.

Statistical Method

All statistical analysis was performed using SPSS (IBM, New York, NY, USA). Non-parametric tests with a type I error of $\alpha = 0.05$ (meaning that statistical difference was assumed when $p < 0.05$) were performed.

For paired data, the Friedman and the Wilcoxon signed ranks post hoc tests were used. These were used when comparing different tests performed on the same Sawbones blocks and different translations and rotations during the same test (i.e. are translations in X greater than Y?).

For independent data, the Kruskal-Wallis and the Mann-Whitney post hoc tests were used. These tests were used to assess the difference in micromotion and push-out forces between different tested parameters when new Sawbones blocks were used.

4.4. ACETABULAR MODEL DEVELOPMENT

In order to assess the micromotion of an implanted acetabular cup, an appropriate acetabular model is required. Most studies measuring the micromotion of acetabular cups use cadaveric bone. However, as previously highlighted, using cadaveric bone has its limitations which make it unsuitable for a pre-clinical testing protocol.

Sawbones polyurethane foam blocks are commonly used as a synthetic alternative to cadaveric pelvic bones. There are many advantages in using Sawbones foam blocks: they are easily reproducible, relatively cheap and available in large quantities; their mechanical properties are similar of those of bone; and they are produced with low interspecimen variability. In addition to these advantages, the Sawbones biomechanical testing blocks meet the ASTM F-1839-08 standard as a material for comparative testing of medical devices and instruments [189, 190]. These foam blocks come with a variety of mechanical properties.

Most studies either use high density foam blocks (density of 0.48 g/cm^3, compressive strength of 18 MPa) [182], low density foam blocks (density of 0.24 g/cm^3, compressive strength of 4.9 MPa) [144, 149], or both [131, 139, 141, 150]. These properties are within the range of trabecular bone properties reported in the literature: bone density ranges between 0.17 g/cm^3 and 0.50 g/cm^3, and compressive strength ranges between 2 MPa and 50 MPa [36, 37]. The higher density foam is near the top of the bone density range, simulating normal bone; whilst the lower density foam is near the bottom of this range, simulating weak, e.g. osteoporotic, bone.

Synthetic acetabular models are a good alternative to cadaveric bones, however, they have their limitations, the main one being the simplification of the acetabulum. As previously mentioned, press-fit primarily relies on the strong equatorial fit between the cup and the acetabulum. When Sawbones blocks are used in cup stability investigations, the acetabulum is modelled as a hemispherical cavity, which results in a uniform equatorial fit around the cup. However, the literature suggests that the acetabulum is essentially supported by the anterior and posterior acetabular columns only (Figure 4.9). Both the acetabular notch and the radiolucent triangle play an important role within the pelvis, however, they do not provide any structural support to the acetabulum. Once a cup is implanted into the acetabulum, it is therefore primarily supported by both acetabular columns only, resulting in a pinching effect around the cup, and not a uniform equatorial fit as seen with a hemispherical cavity. Hence, studies using a hemispherical cavity as an acetabular model to predict cup stability do not correctly replicate the *in vivo* environment of the cup and may overestimate its stability. A more accurate model should therefore incorporate the anatomical and structural properties present around the acetabulum and within the pelvis, whilst keeping the low interspecimen variability and ease of use seen in synthetic acetabular models.

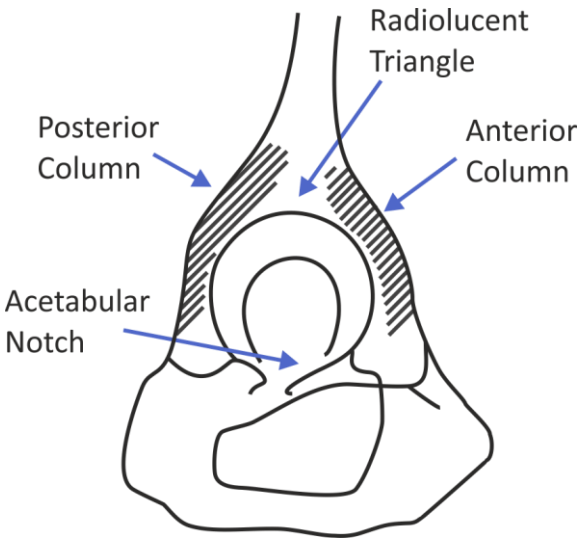

Figure 4.9 – Structural support of the acetabulum within the pelvis

Physiological Acetabular Model

A new acetabular model, similar to the ones used in the literature to assess shell deformation [161, 163, 186, 187], was developed. This model comprised a 53 mm diameter hemispherical cavity (to obtain a 1 mm press-fit), designed with a 0.5 mm offset to ensure that peripheral fixation occurred before the cup bottomed out; and two rectangular cavities, one superiorly and one inferiorly to the acetabulum (Figure 4.10). These cavities model the non-supportive areas present around the acetabulum: the radiolucent triangle and the acetabular notch. Hence, once implanted, the acetabular cup is only supported anteriorly and posteriorly to the acetabulum, recreating the mechanical support of the anterior and posterior columns.

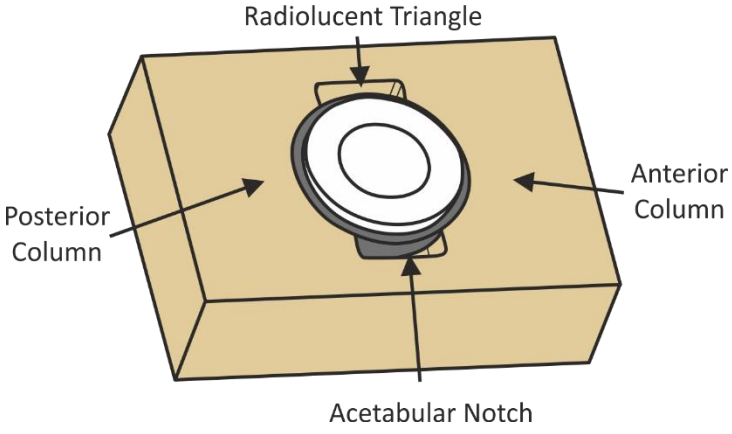

Figure 4.10 – Sawbones block recreating the structural support of the acetabular columns and the non-supportive areas of the radiolucent triangle and the acetabular notch

The width of the acetabular notch was defined as 27 mm, which corresponds to a 60° opening angle [25, 29]. As there were no data available in the literature defining the width of the radiolucent triangle, it was also taken as 27 mm. The width of the radiolucent triangle is most likely smaller than that of the acetabular notch, however, by modelling the radiolucent triangle larger than it should be, this model replicates the worst case scenario by keeping the contact area between the bone and the cup to a minimum. The depth of both these cavities was

14 mm; this depth was the same as those used in similar models described in the literature [161, 163, 186, 187]. A 10 mm diameter hole at the bottom of the acetabular cavity was included to allow the rod connecting the cup to the six DoF measurement system to pass through (Figure 4.11). This model was labelled as the "Physiological" model in this thesis.

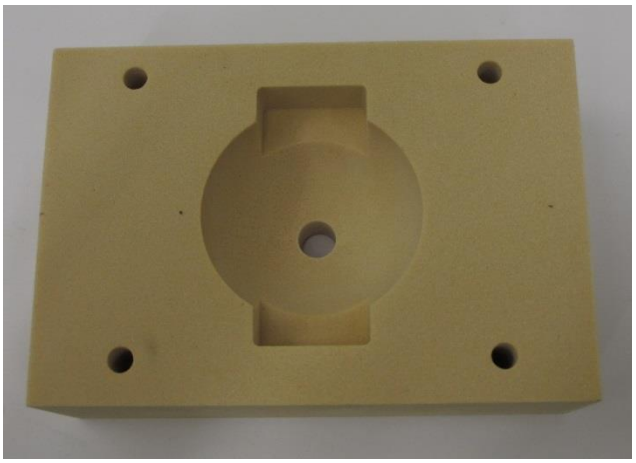

Figure 4.11 – Physiological model

For comparison purposes, an acetabular model with a hemispherical cavity was also designed. For this model, a 53 mm diameter hemispherical cavity was machined into the Sawbones blocks (Figure 4.12). Here again, the acetabular cavity was designed with a 0.5 mm offset to ensure that the cup did not bottom out before peripheral fixation occurred and with a 10 mm hole at the bottom of the acetabular cavity to allow the connection between the cup and the six DoF measurement system. This model was labelled as the "Hemispherical" model in this thesis. The technical drawings of both the physiological and hemispherical acetabular models are available in Appendix 3.

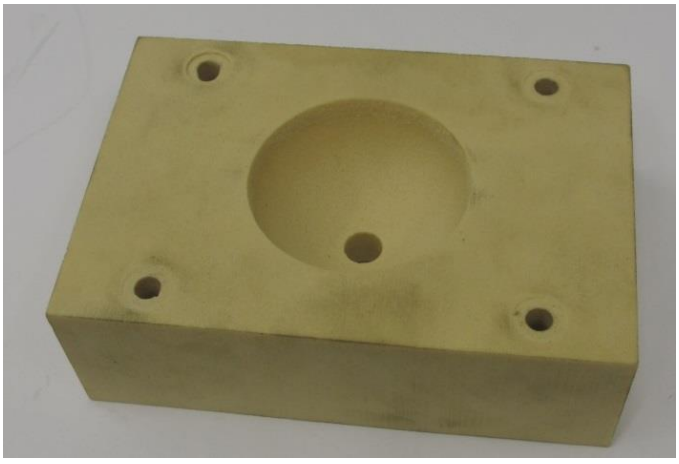

Figure 4.12 – Hemispherical model

Similar to previous studies, a 1 mm press-fit was chosen rather than a 2 mm press-fit to ensure full seating of the cup in the high density hemispherical Sawbones blocks [141, 155, 182]. Furthermore, studies have reported significant variations in dimensions when using reamers, with errors up to 2.9 mm in some cases [112, 140]. The acetabular cavities were therefore

machined using a CNC machine in order to ensure accuracy and reduce variability caused by reaming between each specimen.

The peripheral diameters were then measured using a digitiser (Incise, Renishaw, Wotton-under-Edge, UK) and obtained using a circle fit approximation in a Matlab program prior to testing to confirm the accuracy of the manufacturing. The circle fit method was considered acceptable as a regression study was performed and an R^2 value of 1 was consistently obtained.

Contact Area

Blue layout dye (Kleenscribe layout dye, Starrett, Jedburgh, Scotland, UK) was used to determine the contact area between the cup and the Sawbones block when the cup was implanted into both the hemispherical and the physiological models. Sawbones blocks with a density of 0.48 g/cm³ were used for this investigation. A layer of dye was applied to the acetabular shell and the acetabular cup was then inserted and then removed from the acetabular cavity, leaving a blue stain where the cup came in contact with the foam. The cup was inserted into the acetabular cavities by manually loading the cup with the Dartec until it was fully seated in the acetabular cavity. The cup was then removed using the push-out method.

Peripheral fixation was confirmed for both acetabular models (Figures 4.13 and 4.14) as blue dye was only present around the periphery of the acetabular cavity. Furthermore, if comparing the contact area between the cup and the different acetabular models, it was observed that the depth of contact with the physiological model was about twice that of the hemispherical model (Figure 4.15). The contact area between the acetabular cup and the model was greater with the physiological model compared to the hemispherical model (calculations available Appendix 4). This was because the gaps superior and inferior to the acetabular cavity in the physiological model allowed the foam to deform more when the cup was inserted compared to the hemispherical model, allowing the cup to be imbedded deeper within the cavity and resulting in a greater contact area.

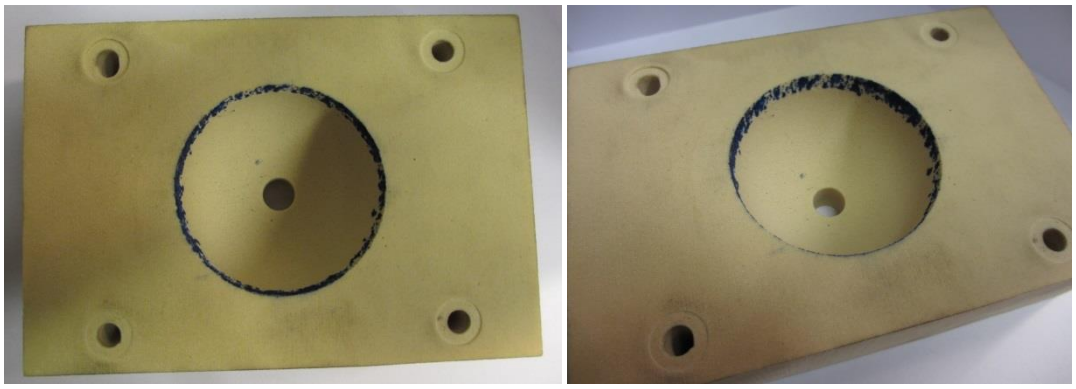

Figure 4.13 – Contact area between the acetabular cup and the hemispherical Sawbones block using layout dye

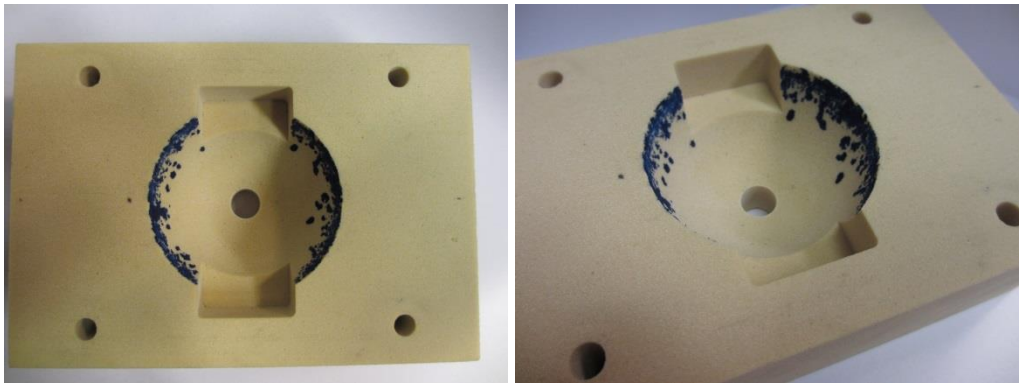

Figure 4.14 – Contact area between the acetabular cup and the physiological Sawbones block using layout dye

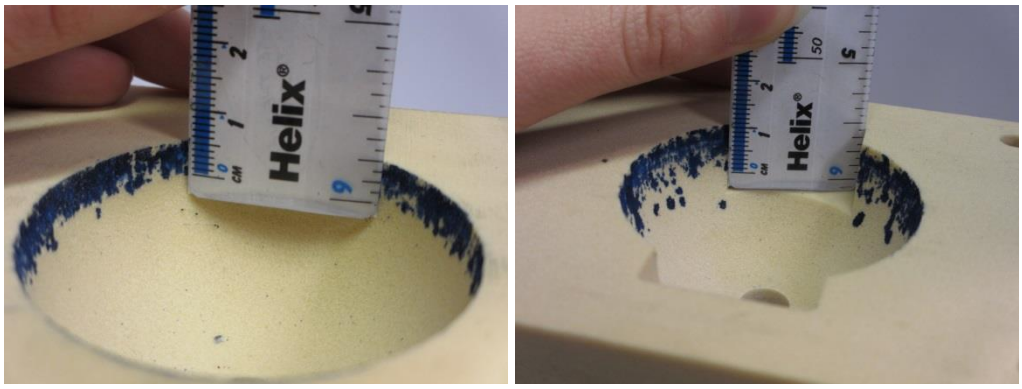

Figure 4.15 – Difference in depth of contact area with hemispherical (left) and physiological (right) acetabular models

4.5. RECYCLABILITY OF THE ACETABULAR COMPONENT AND SAWBONES BLOCKS

Before assessing the difference in acetabular cup stability between the two different acetabular models, it was important to determine if the acetabular component and the Sawbones blocks could be reused. Two recyclability studies were therefore performed using the developed micromotion test protocol. In addition, these recyclability studies were also used to test the protocol itself. Only the hemispherical acetabular model was used for these recyclability studies as it was assumed that the results obtained would be the same regardless of the acetabular model.

To determine if the acetabular component could be reused throughout testing, the micromotion and the push-out forces were compared when the acetabular cup was implanted into five different Sawbones blocks. The results (Figures 4.16 and 4.17) show little variation in both micromotion and push-out forces between each block, with no visible trends of them increasing or decreasing. It was therefore decided that the cup could be reused for all tests, provided that it was cleaned and any foam debris removed between tests.

To determine if the Sawbones blocks could be reused or if new blocks were needed for every test, five blocks were repeatedly tested following the test protocol. The mean peripheral diameter of the acetabular cavity, the micromotion of the cup in six DoF and the push-out force of each repeat were compared to their predecessor using the Wilcoxon signed ranks post hoc test as the samples were paired. It was decided that the two most commonly used densities of Sawbones blocks would be investigated: high density Sawbones blocks with a density of 0.48 g/cm³ and a compressive strength of 18 MPa; and low density Sawbones blocks with a density of 0.24 g/cm³ and a compressive strength of 4.9 MPa. The peak force used to insert the cup into the low density foam block was reduced to 2 kN to prevent damage to the Sawbones block.

The micromotion test protocol was repeated four times on the high density Sawbones blocks, but only three times on the low density Sawbones blocks. The results (Figures 4.18 to 4.23) showed some statistical differences between each repeat. The peripheral diameter increased significantly and the push-out forces tended to decrease with repeated use for both densities. There were only a few statistical differences in micromotion between the repeats; however, this could be due to the high variations in the results caused by the user learning curve. It was therefore decided that, due to the statistical differences present, and the visible damage to the acetabular cavity following push-out (Figure 4.7), only new Sawbones foam blocks would be used for testing.

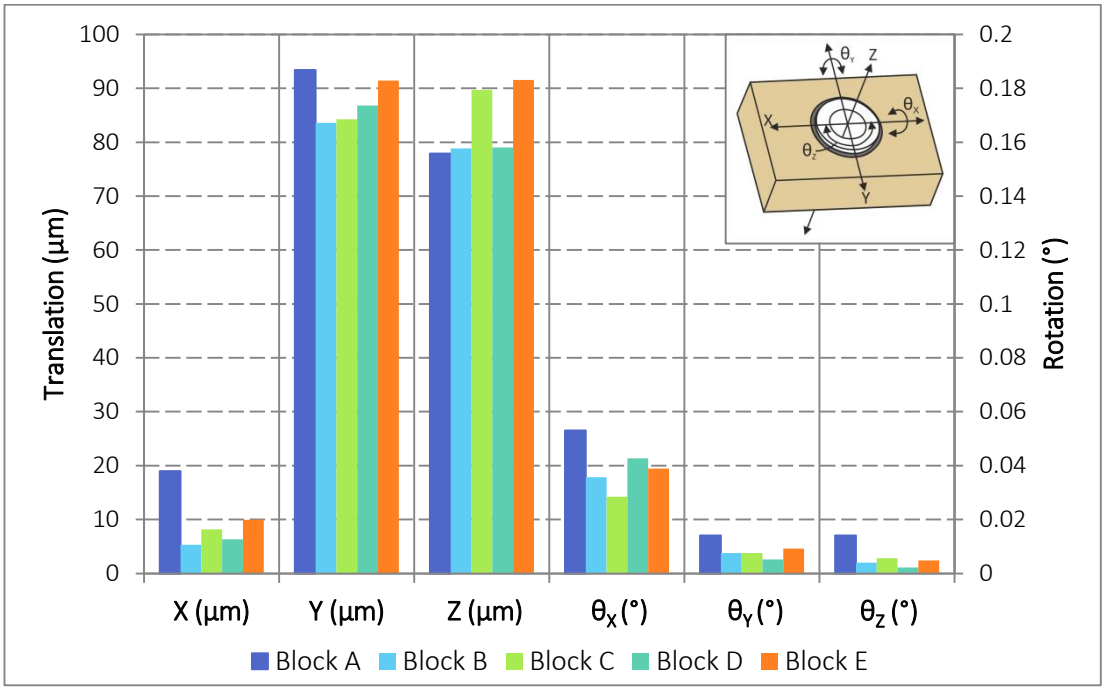

Figure 4.16 – Acetabular cup micromotion in six DoF when implanted into five Sawbones blocks with a hemispherical cavity

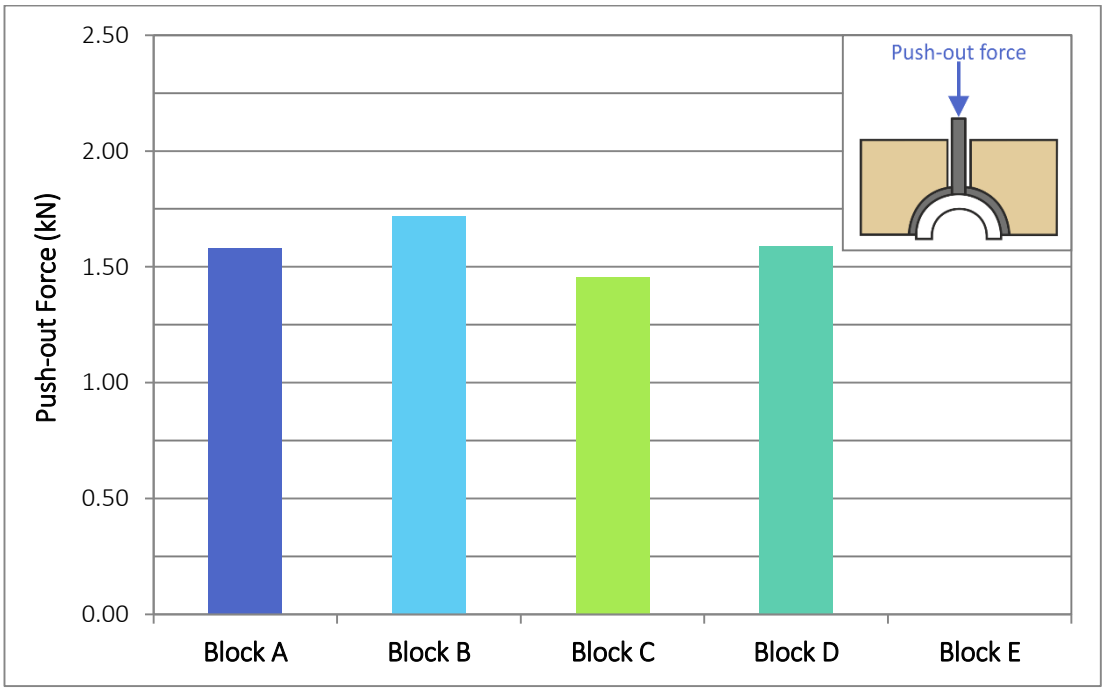

Figure 4.17 – Push-out force required to remove the cup from the five Sawbones blocks with a hemispherical cavity (data from block E is missing due to an error in recording)

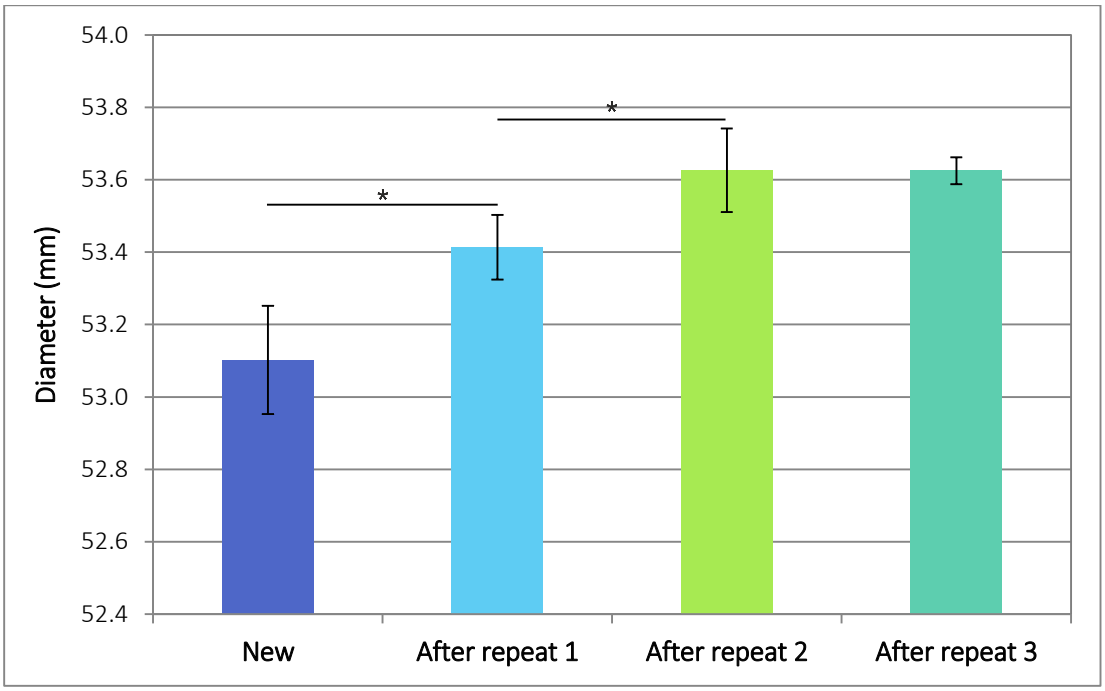

Figure 4.18 – Peripheral diameter of the high density Sawbones blocks with a hemispherical cavity when new and following each consecutive repeat. Values expressed as mean and standard deviation.
*$p < 0.05$ using Wilcoxon signed ranks post hoc test

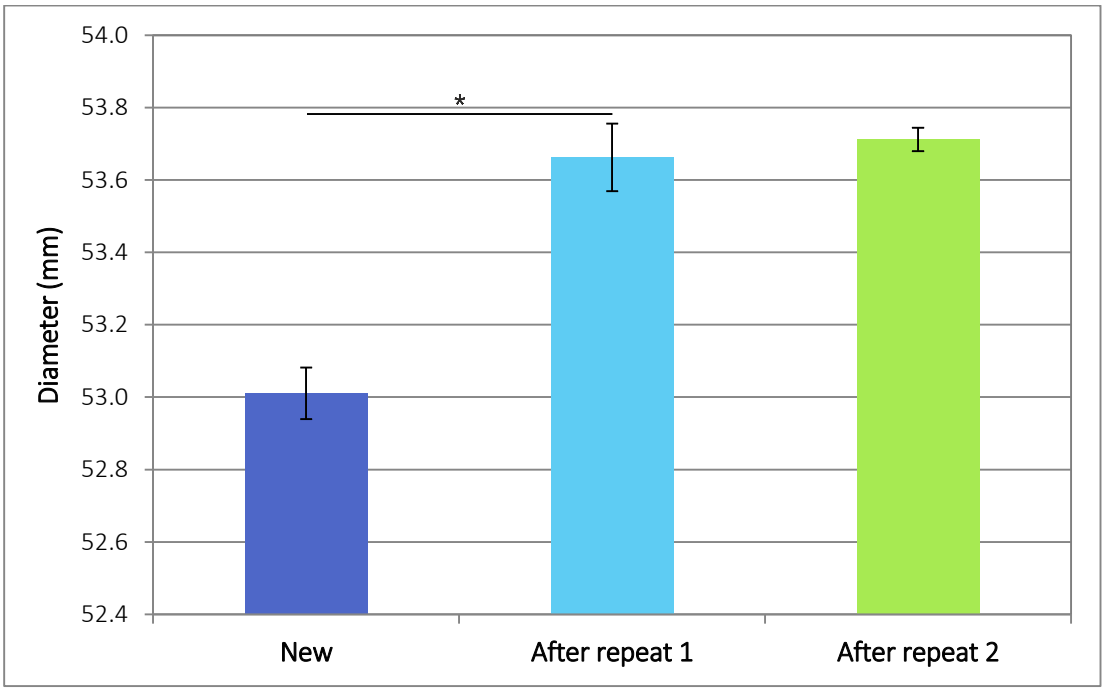

Figure 4.19 – Peripheral diameter of the low density Sawbones blocks with a hemispherical cavity when new and following each consecutive repeat. Values expressed as mean and standard deviation.
*$p < 0.05$ using Wilcoxon signed ranks post hoc test

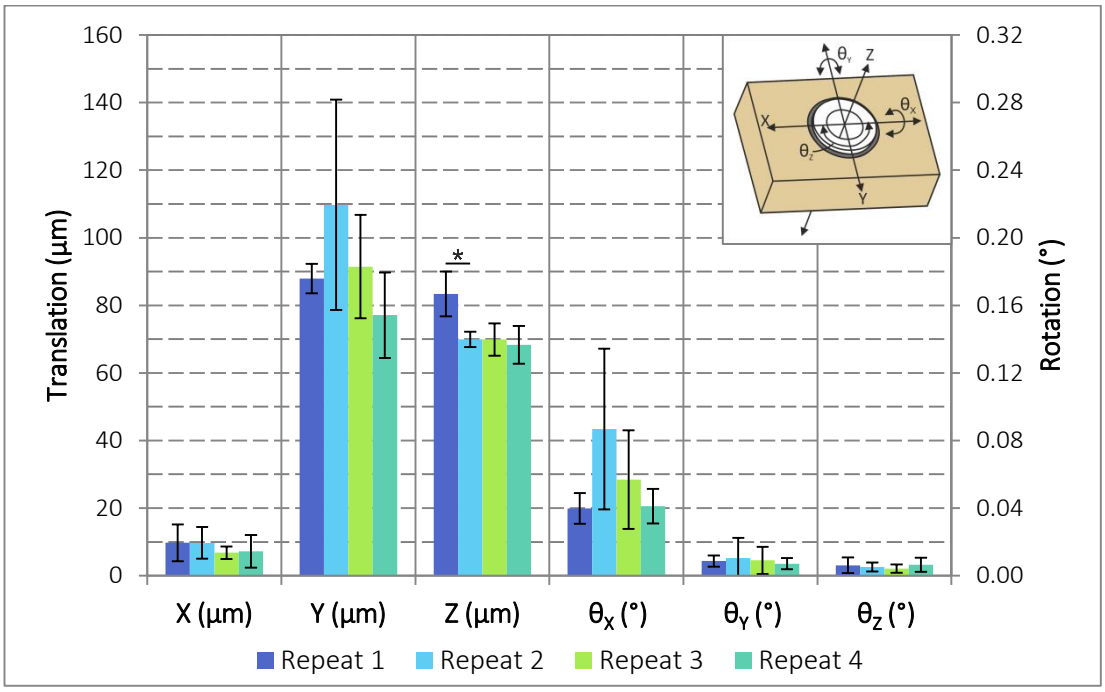

Figure 4.20 – Micromotion in six DoF of the cup during SLS with repeated use of the same high density Sawbones blocks with a hemispherical cavity. (0.08° corresponds to 40 µm). Values expressed as mean and standard deviation. *$p < 0.05$ using Wilcoxon signed ranks post hoc test

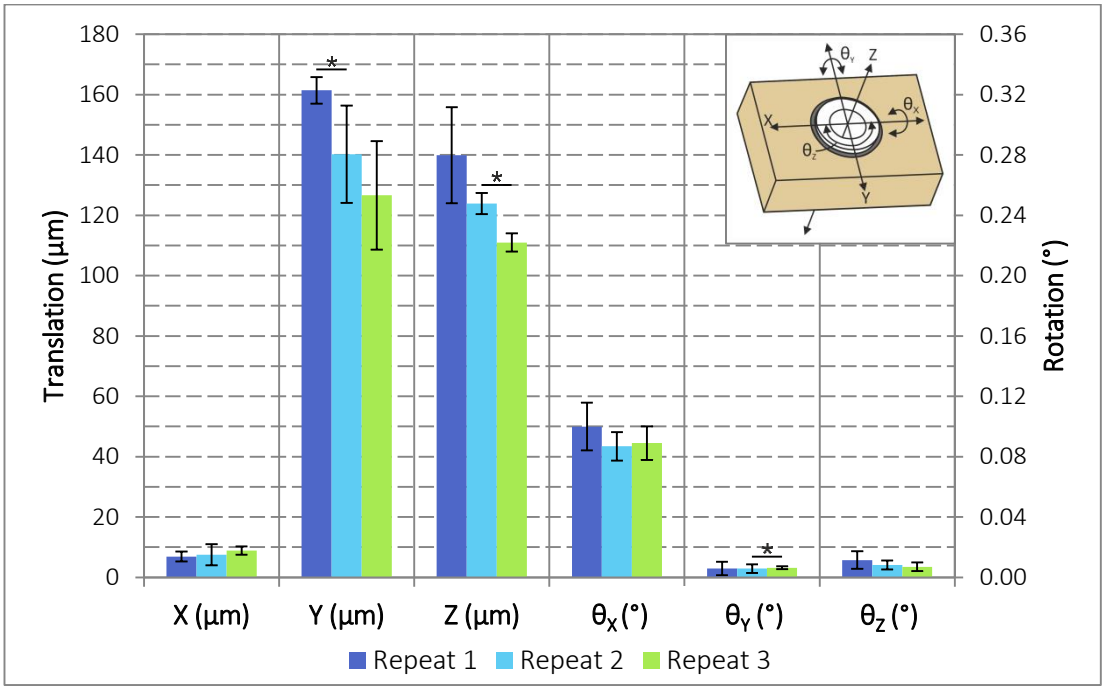

Figure 4.21 – Micromotion in six DoF of the cup during SLS with repeated use of the same low density Sawbones blocks with a hemispherical cavity. (0.08° corresponds to 40 µm). Values expressed as mean and standard deviation. *$p < 0.05$ using Wilcoxon signed ranks post hoc test

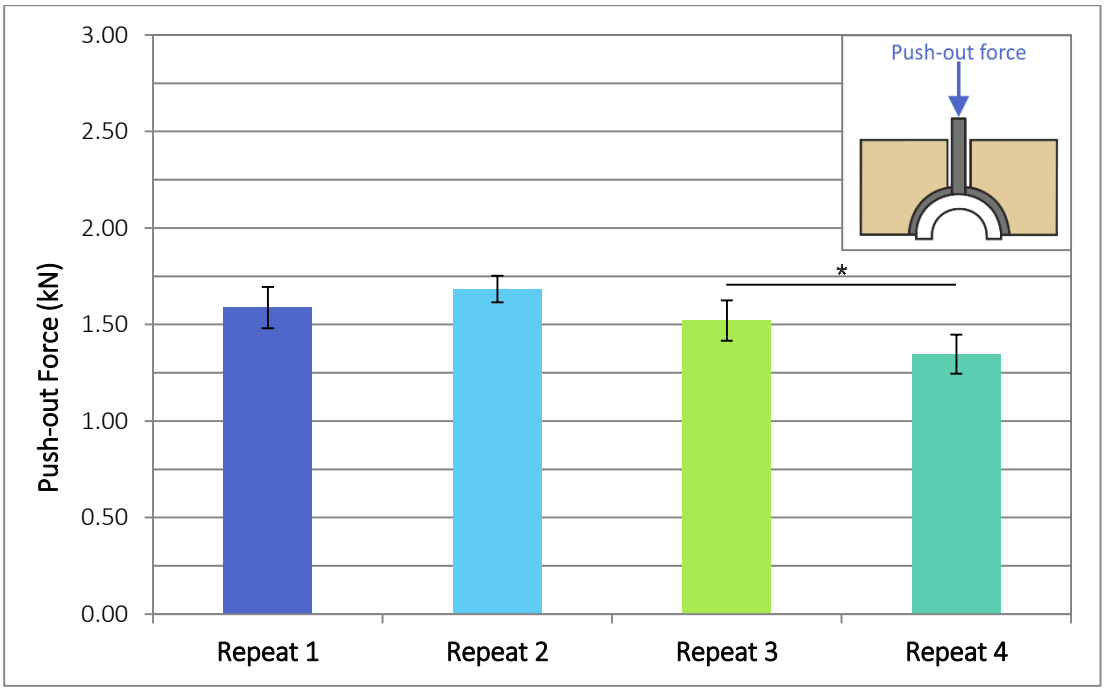

Figure 4.22 – Push-out forces with repeated use of the same high density Sawbones blocks with a hemispherical cavity. Values expressed as mean and standard deviation. *$p < 0.05$ using Wilcoxon signed ranks post hoc test

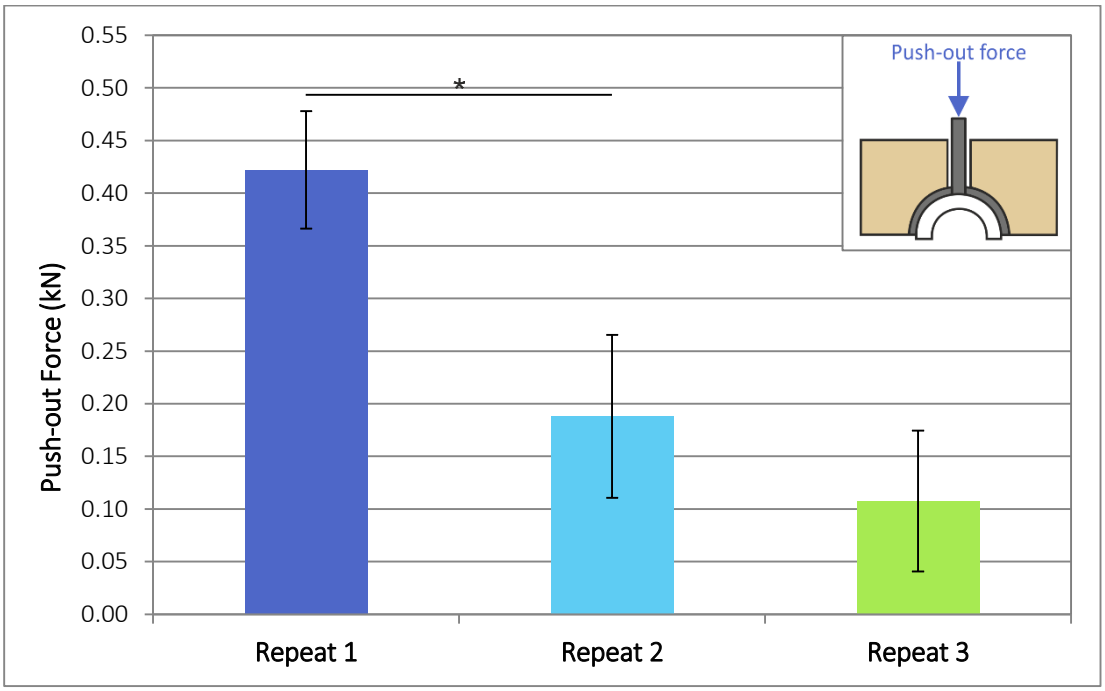

Figure 4.23 – Push-out forces with repeated use of the same low density Sawbones blocks with a hemispherical cavity. Values expressed as mean and standard deviation. *$p < 0.05$ using Wilcoxon signed ranks post hoc test

4.6. TESTING THE PHYSIOLOGICAL ACETABULAR MODEL

The physiological acetabular model was compared to the commonly used hemispherical acetabular model by assessing the differences in cup micromotion and push-out forces between the two acetabular models. These models were manufactured in both the high and the low density Sawbones blocks commonly used in the literature to identify the best acetabular model; hence, the effect of bone density on cup micromotion and push-out forces was also investigated. The findings reported in this section have been published in a peer-reviewed journal [191]; the article is available in Appendix 7.

4.6.1. MATERIALS AND METHOD

The acetabular models were divided into four different groups of six Sawbones blocks each: High Density Hemispherical, High Density Physiological, Low Density Hemispherical and Low Density Physiological.

Elastic deformation of the Sawbones foam near the acetabular cup was observed during the recyclability study. Even though this was observed at the rim of the acetabular model, it can be assumed that this phenomenon occurs along the entire contact surface between the cup and the foam. The six DoF measurement system was attached to a plate below the Sawbones block; hence, the measurements taken are a combination of both cup micromotion and elastic deformation of the Sawbones block. Two extra LVDTs were placed on the Sawbones block 5 mm away from the rim of the acetabular cup (Figure 4.24) to measure the elastic deformation of the foam in the Z direction during cyclic loading (one superiorly and one posteriorly). Ink marks were drawn on the Sawbones blocks to correctly position the LVDTs during the test setup. The LVDTs were positioned 5 mm away from the acetabular rim to ensure that they did not interfere with the cup or the actuator of the Dartec during testing. In the case of the physiological model, only the posterior LVDT was used to measure foam deformation as the measurement site for the superior LVDT was removed to model the radiolucent triangle.

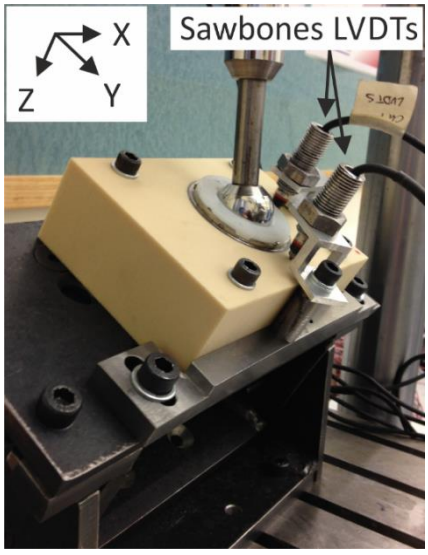

Figure 4.24 – The micromotion test setup showing the position of the LVDTs used to measure Sawbones elastic deformation

For this study, an extra DAQ card was added to the data acquisition frame in order to record the elastic deformation of the foam block and a ten-channel LabView program was used to collect the data (Figure 4.25).

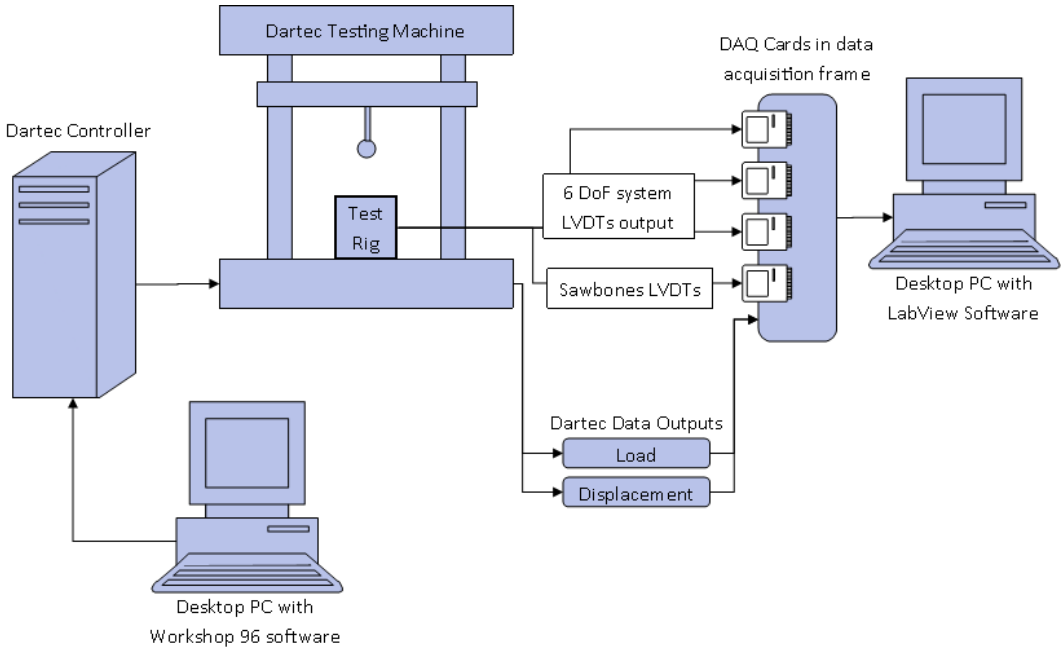

Figure 4.25 – New schematic showing the components and connections in instrumentation including the Sawbones LVDTs

To analyse the Sawbones foam deformation data, an extra function was included to the Matlab routine that calculated the micromotion of the cup in six DoF. Since the elastic deformation of the foam was cyclic due to the nature of the loading, a Fast Fourier Transform was used to obtain the amplitude of the elastic deformation.

For statistical analysis, the Mann-Whitney post hoc test was used to compare the micromotion, the push-out forces and the Sawbones foam deformation between the different acetabular models as the samples were independent. The Wilcoxon signed ranks post hoc test was used to compare the foam deformation at the superior and posterior locations of the same blocks as the samples were paired.

One of the micromotion data files from Low Density Physiological was corrupted during saving; therefore, the number of repeats for this group was five instead of six.

4.6.2. RESULTS

HEMISPHERICAL VERSUS PHYSIOLOGICAL

The general pattern in micromotion of the cup was similar between the different test conditions. Considering that 0.08° in rotations was equivalent to 40 µm of displacement in the direction of the arc of rotation for this cup, the translations were always greater than the rotations (Figures 4.26 and 4.27). In translations, the X micromotions were smaller than the Y

and Z micromotions (Table 4.1). In rotations, the θ_x rotations were generally the largest while θ_Z were always significantly smaller.

There was a change in the general pattern of the cup micromotion when comparing the two different acetabular models, regardless of the bone density (Figures 4.26 and 4.27). In the hemispherical model, the Y micromotion was either significantly greater or not different to the Z micromotion in the high and low density Sawbones blocks, respectively (Table 4.1). However, in the physiological model, the Z micromotion was always significantly greater than Y for both the high and low density Sawbones blocks.

The micromotion of the cup in six DoF was generally greater in the physiological model compared to the hemispherical model. With the high density Sawbones blocks, the X and θ_Y micromotions were significantly greater in the physiological model compared to the hemispherical model (Table 4.2; Figure 4.26). With the low density foam blocks, the Z and θ_X micromotions were significantly greater in the physiological model compared to the hemispherical model (Figure 4.27). An exception to the general trend was the X and θ_Y micromotions that were significantly greater in low density hemispherical model compared to low density physiological model.

When comparing the two different acetabular cavity geometries, the push-out forces were significantly greater in the hemispherical model compared to physiological model for both densities (Table 4.2; Figure 4.28).

Table 4.1 – Results of the statistical analysis comparing the different translations and rotations during the same test conditions. The highlighted numbers represent statistical significance ($p < 0.05$)

		High Density Hemispherical	High Density Physiological	Low Density Hemispherical	Low Density Physiological
Friedman Test	X - Y - Z	0.006	0.016	0.009	0.007
	θ_X - θ_Y - θ_Z	0.004	0.009	0.048	0.007
Wilcoxon Signed Ranks Test	X - Y	0.028	0.116	0.028	0.043
	X - Z	0.028	0.028	0.028	0.043
	Y - Z	0.046	0.046	0.753	0.043
	θ_X - θ_Y	0.034	0.279	0.343	0.039
	θ_X - θ_Z	0.026	0.028	0.046	0.042
	θ_Y - θ_Z	0.039	0.026	0.041	0.038

Table 4.2 – Results of the statistical analysis comparing the physiological model to the hemispherical model with both Sawbones density. The highlighted numbers represent statistical significance ($p < 0.05$)

		X	Y	Z	θ_X	θ_Y	θ_Z	Push-out
Mann-Whitney Test	High Density	0.016	0.078	0.199	0.87	0.034	1.000	0.004
	Low Density	0.006	0.715	0.006	0.041	0.028	0.772	0.006

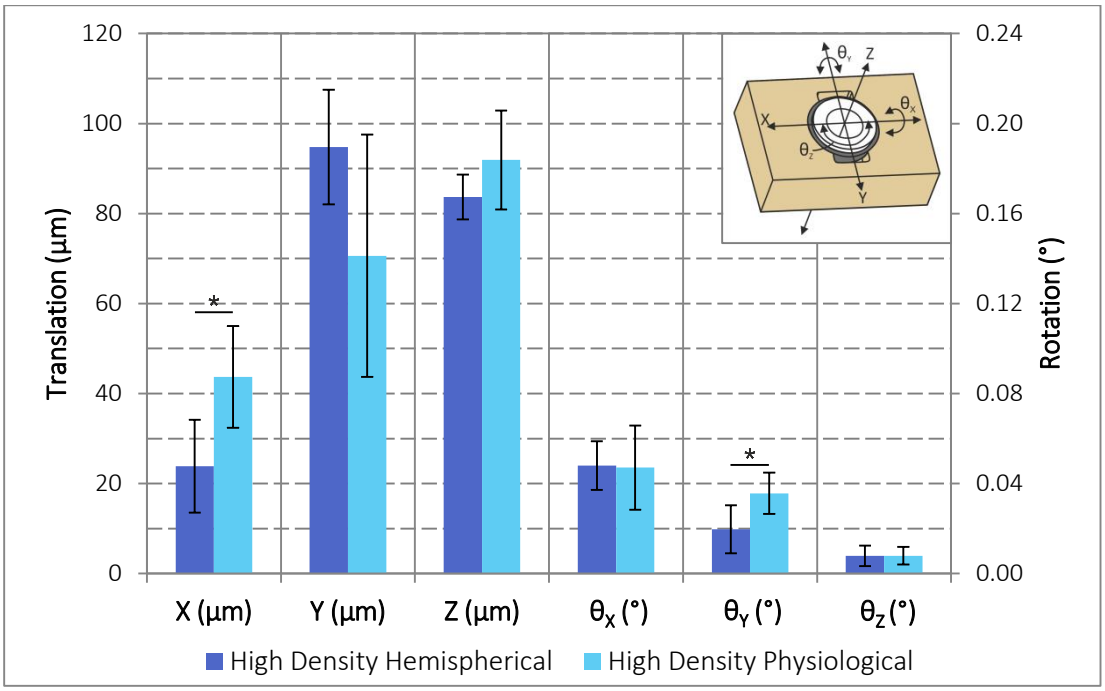

Figure 4.26 – Micromotion of the cup during SLS in both high density hemispherical and physiological Sawbones blocks (0.08° corresponds to 40 µm). Values expressed as mean and standard deviation. *$p < 0.05$ using Mann-Whitney post hoc test

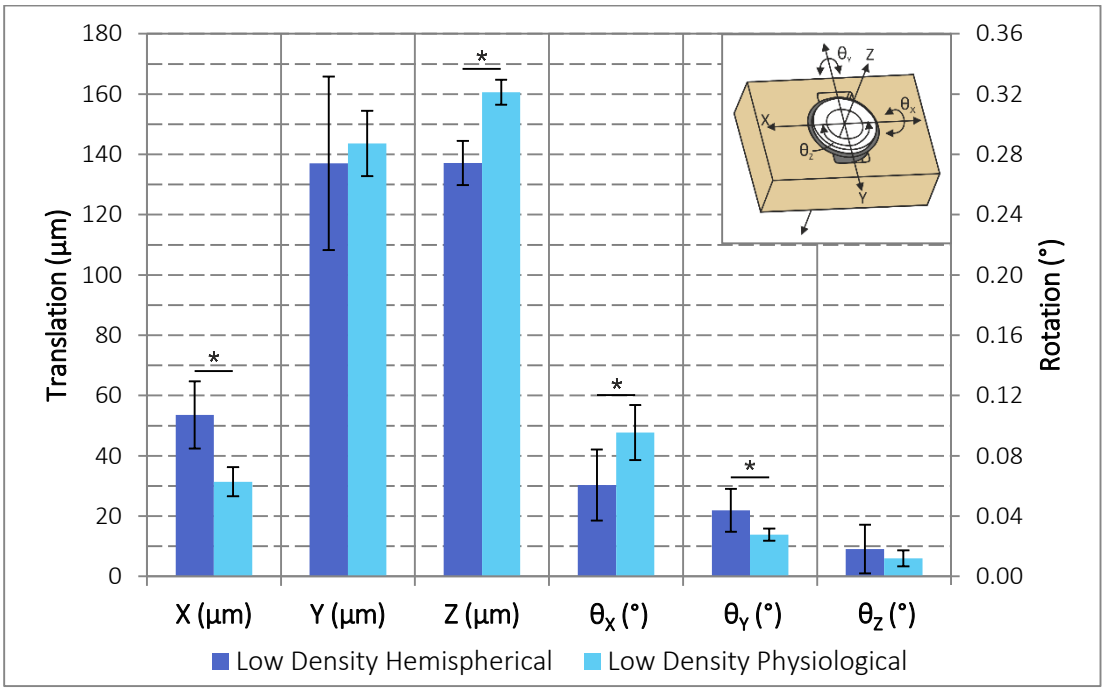

Figure 4.27 – Micromotion of the cup during SLS in both low density hemispherical and physiological Sawbones blocks (0.08° corresponds to 40 µm). Values expressed as mean and standard deviation. *$p < 0.05$ using Mann-Whitney post hoc test

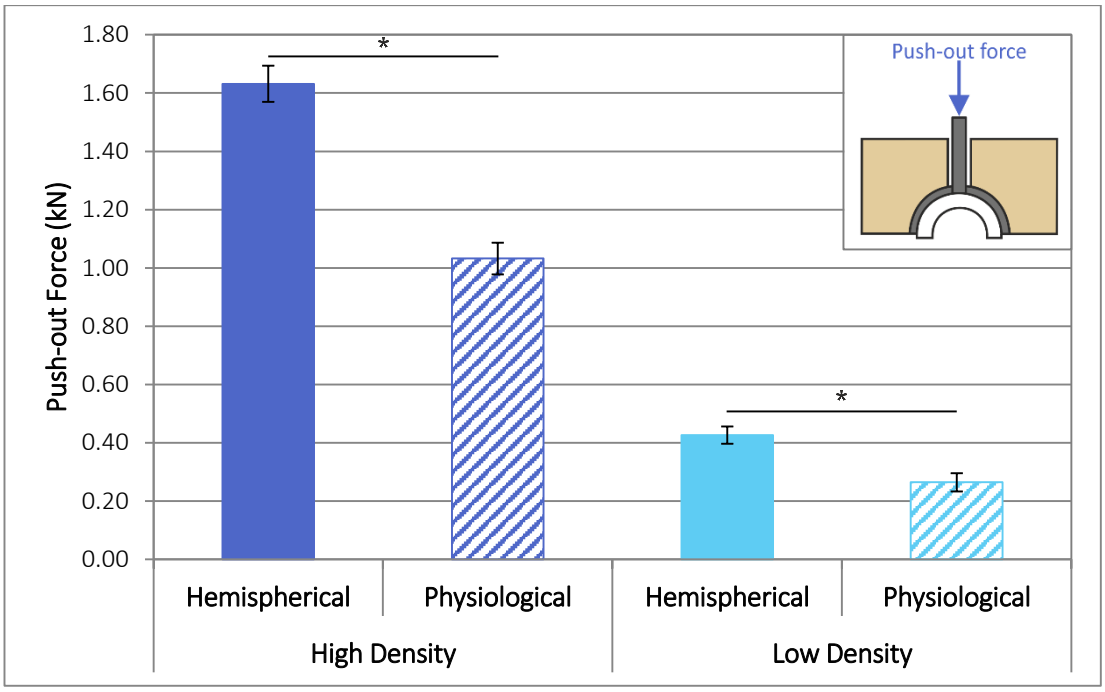

Figure 4.28 – Push-out forces comparing the hemispherical to the physiological acetabular model for both densities. Values expressed as mean and standard deviation. *$p < 0.05$ using Mann-Whitney post hoc test

High versus Low Density Sawbones blocks

The micromotion of the cup was generally greater in the low density compared to the high density Sawbones blocks. In the hemispherical model, the micromotion of the cup was significantly greater in all translations and in θ_Y in the low density blocks compared to the high density blocks (Table 4.3; Figure 4.29). In the physiological model, the Y, Z and θ_X micromotions were significantly greater in the low density blocks compared to the high density blocks (Figure 4.30). The exceptions to this trend was the X micromotions in the physiological model, which was statistically lower in the low density blocks compared to the high density blocks.

When comparing the push-out forces between the two different Sawbones block densities (Figure 4.31), these were significantly greater in the high density blocks compared to the low density blocks for both geometries (Table 4.3).

Table 4.3 – Results of the statistical analysis comparing the high and low density Sawbones blocks with both acetabular models. The highlighted numbers represent statistical significance ($p < 0.05$)

		X	Y	Z	θ_X	θ_Y	θ_Z	Push-out
Mann-Whitney Test	Hemispherical model	0.006	0.025	0.004	0.191	0.014	0.206	0.004
	Physiological model	0.045	0.006	0.006	0.008	0.094	0.226	0.006

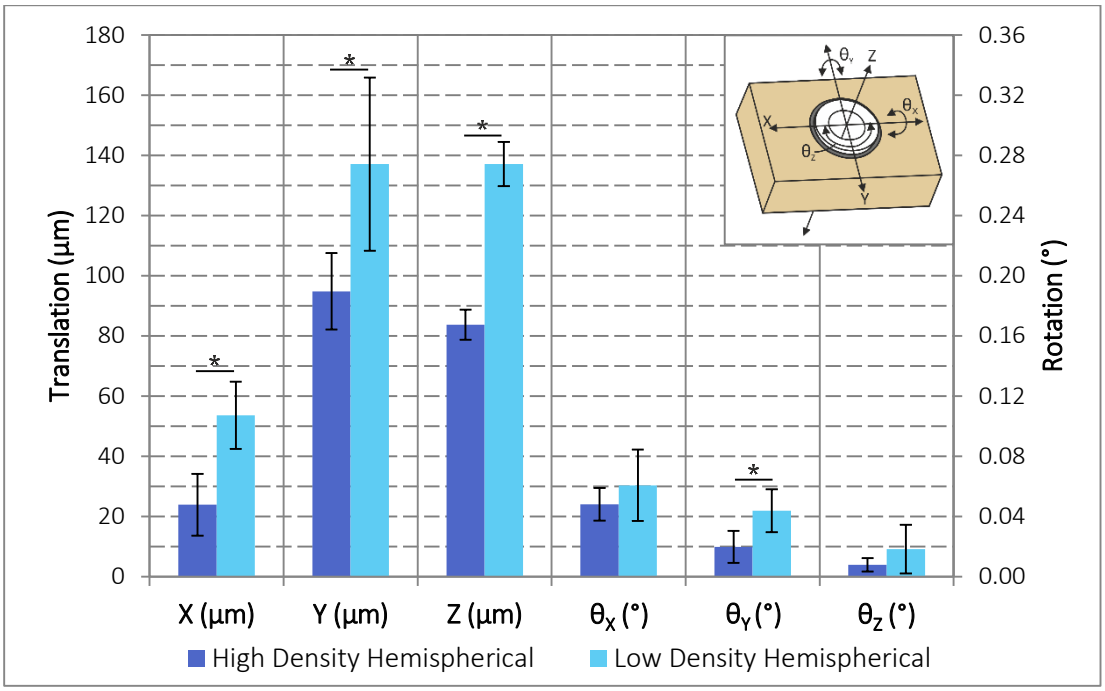

Figure 4.29 – Micromotion of the cup during SLS in both high and low density hemispherical Sawbones blocks (0.08° corresponds to 40 µm). Values expressed as mean and standard deviation. *$p < 0.05$ using Mann-Whitney post hoc test

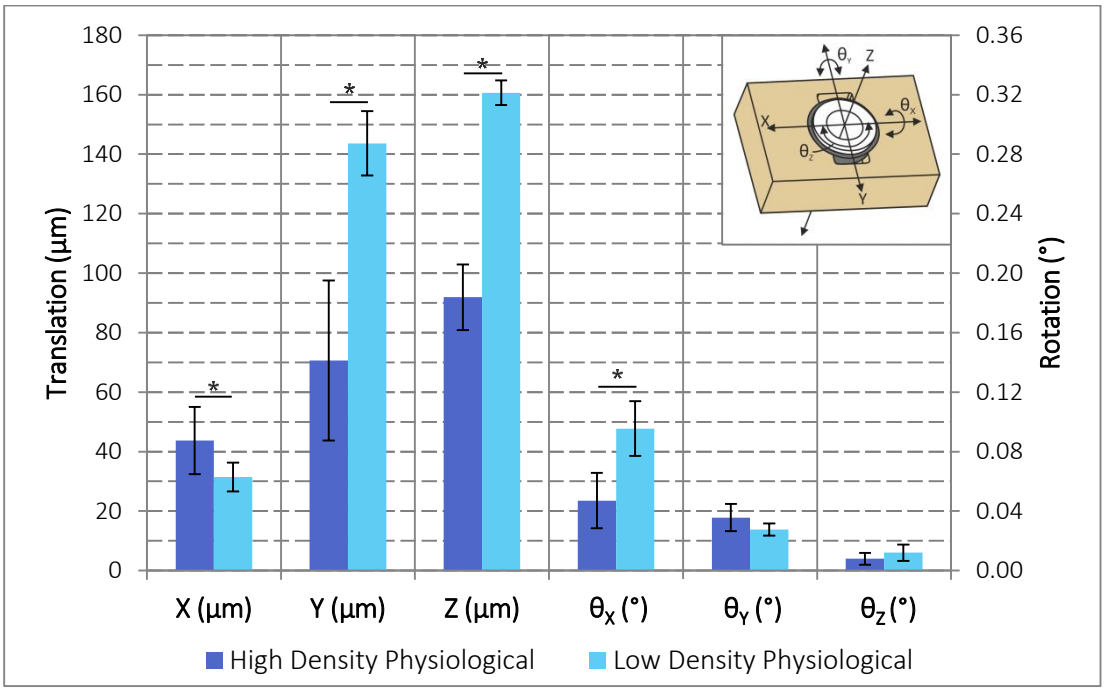

Figure 4.30 – Micromotion of the cup during SLS in both high and low density physiological Sawbones blocks (0.08° corresponds to 40 µm). Values expressed as mean and standard deviation. *$p < 0.05$ using Mann-Whitney post hoc test

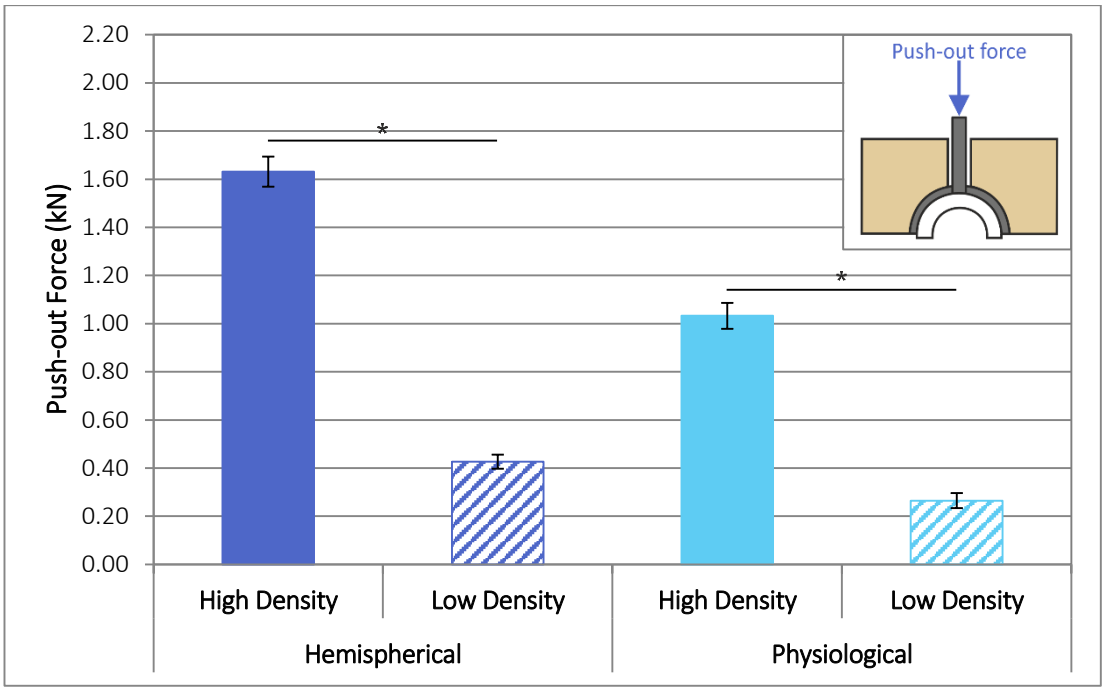

Figure 4.31 – Push-out forces comparing high to low density Sawbones blocks for both acetabular geometries. Values expressed as mean and standard deviation. *$p < 0.05$ using Mann-Whitney post hoc test

Foam Deformation Analysis

There were no significant differences in foam deformation between the posterior and superior measurement sites for both high and low density hemispherical models (Figure 4.32; $p = 0.248$ and $p = 0.173$, respectively). As the foam micromotion at both sites were not significantly different, and as only the posterior LVDT could be used to measure the foam deformation in the physiological models, the comparison of the foam deformation between the different test conditions was performed using the measurements obtained by the posterior LVDT only.

Foam deformation was not statistically different between the hemispherical and the physiological models for both densities (Figure 4.33). However, foam deformation was significantly higher in low density Sawbones blocks compared to high density ones for both geometries (hemispherical: $p = 0.037$, physiological: $p = 0.006$).

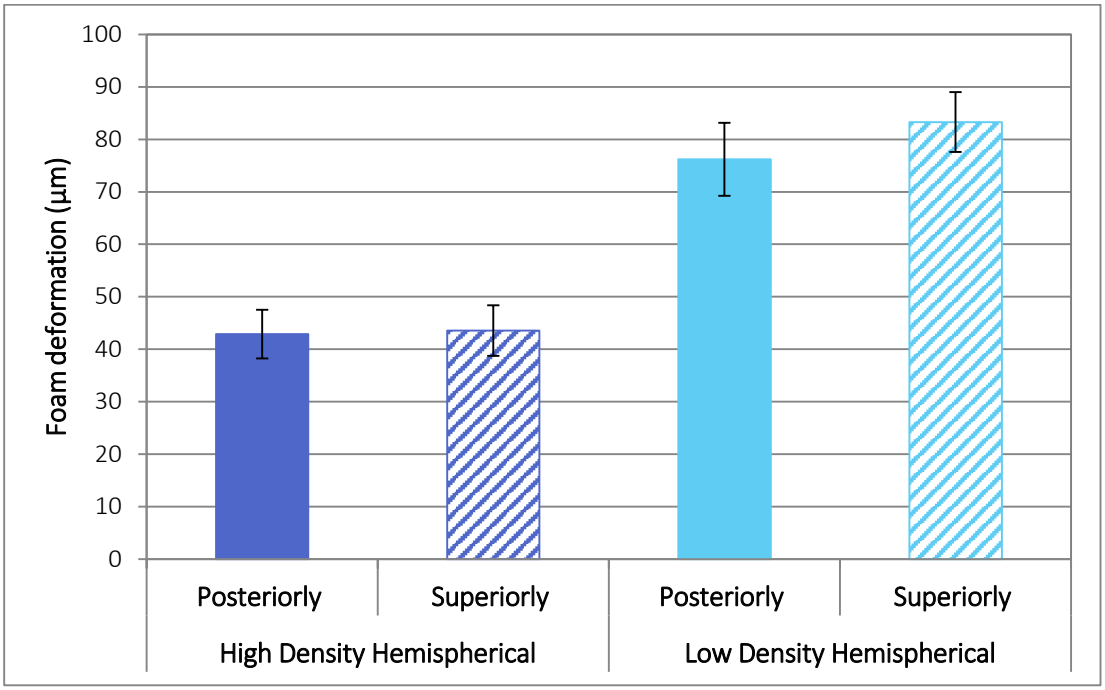

Figure 4.32 – Foam deformation in the posterior and superior locations of both density of the hemispherical models. Values expressed as mean and standard deviation.

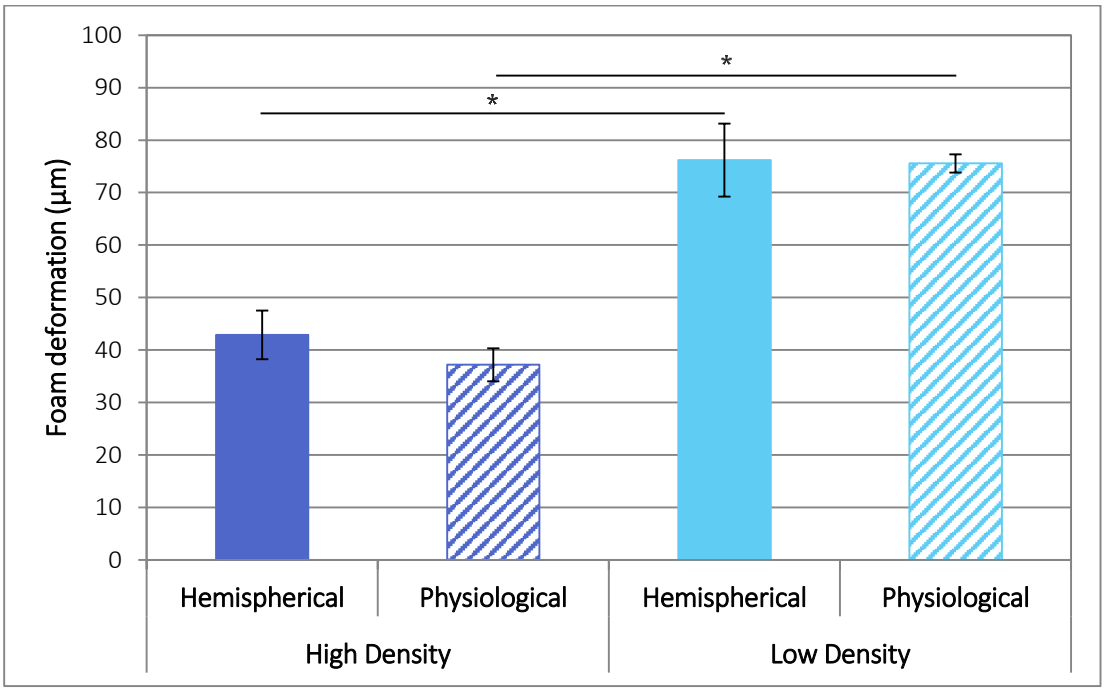

Figure 4.33 – Foam deformation in the posterior side of all four different acetabular models tested. Values expressed as mean and standard deviation. *$p < 0.05$ using Mann-Whitney post hoc test

4.7. DISCUSSION

The aim of this chapter was to discuss the outcome of the design of a robust methodology capable of measuring the micromotion of press-fit acetabular cups in six DoF when subjected to cyclic loading during SLS. The development of this protocol involved addressing two aspects: a system capable of measuring the micromotion of an acetabular cup in six DoF under cyclic loading and its accompanying test protocol; and an acetabular model that incorporated the important physiological and structural features of the acetabulum.

The six DoF measurement system developed for this project was adapted from a proven system commonly used to measure the micromotion of femoral stems [170, 174-179]. One of the major advantages of this system was that all the measurements were taken from a single point of attachment, in this case the dome screw hole. Studies that measure the micromotion of acetabular cups in more than one direction of motion usually take their measurements at different points along the acetabular rim and assume that the cup is a rigid body. However, deformation along the rim of the cup has been reported in the literature [161-164], challenging the rigid body assumption. Hence, taking all the measurements from a single point of attachment is a definite advantage over the other methods as rigid body motion of the cup does not need to be assumed.

The dome screw hole was chosen as an attachment site for two reasons. Firstly, it allowed the connection of the cup to the six DoF measurement system without damaging the cup. Any damage or modification to the cup could change its structural properties which could affect its fixation within the acetabulum. Secondly, as press-fit cups primarily rely on peripheral contact between the cup and the bone, it was assumed that the small hole at the dome of the acetabular cavity required for the connecting rod to pass through would not affect the fixation, and hence the micromotion, of the cup. Peripheral fixation was confirmed with the use of blue dye on the acetabular models used in this thesis (Figures 4.13 and 4.14).

The six DoF measurement system was set up in such a way that the results obtained were a combination of cup micromotion and elastic deformation of the Sawbones blocks. This elastic deformation was measured in the Z direction during the micromotion tests in order to assess its magnitude and variability. The results revealed that Sawbones blocks of the same density exhibited similar levels of deformation regardless of the acetabular geometry. Hence, even though the results obtained are a slight overestimation of the true micromotion of the cup, they are still comparable to one another. On the other hand, Sawbones foam deformation was higher in the low density Sawbones blocks comparted to the high density Sawbones blocks. This was because the low density foam has a lower compressive strength and therefore deformed more than the high density foam when subjected to the same loads.

As it is unknown if the foam deformation was the same throughout the entire acetabular cavity and in the different directions of motion, the measurements obtained were only used to confirm that foam deformation was comparable between test conditions. Measurements of the deformation of the foam under dynamic loading around the entire acetabular cavity was not feasible because placing the additional sensors along the acetabular cavity would affect its mechanical properties and the fixation of the acetabular component, which would affect

the micromotion of the cup. Finite element analyses could be used to determine the full extent of foam deformation; however, this was beyond the scope of this thesis.

The cup insertion method used, which consisted of five sinusoidal cycles with a peak load of 5 kN at a frequency of 1 Hz, was chosen as it allowed the cup to be inserted in the same repeatable manner every time. This method was not strictly clinically relevant as is does not replicate the effect of hammer blows as used during surgery. However, the surgical method is user dependent, and the force and number of hammer blows performed by the same user vary between consecutive implantations. This variability can affect cup fixation, resulting in increased variability in cup micromotion. This increase in variability in the results could mask the effect of the specific factor being investigated, such as cup geometry, porous coating, level of press-fit or cup fixation method. The chosen method, on the other hand, provided a reproducible method to insert the acetabular cup within the acetabulum, and is in line with that used in other published *in vitro* studies [113, 131, 140].

The peak load of 5 kN was chosen following preliminary trials as it ensured that the cup was repeatedly completely embedded within the high density Sawbones blocks with a hemispherical cavity. If another type of acetabular model or cadaveric pelvic bone were to be used, new trials should be performed to check that the peak load is high enough to properly seat the cup into the acetabular cavity. It should also ensure that the load is not too high so as to prevent damage to the acetabular model or the bone. For example, a reduced load of 2 kN was used to insert the cups into the low density Sawbones blocks to prevent damage to the block. The same load was used for the hemispherical model and the physiological model, regardless of the density of the Sawbones block (5 kN for the high density blocks and 2 kN for the low density blocks) to allow comparison between the two acetabular models. The effect of different surgical insertion methods on the micromotion of the cup could be assessed by replacing the insertion protocol used in this thesis with one recommended in the relevant surgical protocol for a specific cup being tested.

The loading profile during the micromotion test was simplified to a sinusoidal wave, as the loading profile of the hip joint during gait (Figure 2.12) was too complex to be replicated by the Dartec. However, the sinusoidal wave profile is a close approximation of the hip loading profile and, as such, has been used in many studies assessing micromotion of acetabular cups [106, 134, 157, 160, 166, 169]. The frequency of the cyclic loading was set at 1 Hz, which simulated normal walking speeds, and the cup was loaded in compression between 0.01 kN and 2.0 kN. The minimum value replicated the effect of the muscle forces maintaining the hip joint together when it is unloaded; and the maximum value represented the average peak load experienced by the hip of an 80 kg person during gait. Furthermore, this loading profile was in accordance with the British Standards for hip joint simulators (BS 7251-7:1990) which is used to assess the wear properties of the bearing surfaces in THR. This standard states that the maximum applied load should be at least 1.5 kN and the loading frequency should be between 0.5 Hz and 1 Hz.

The second objective of this study was to develop an acetabular model which replicated the structural support present in the acetabulum. In addition to this, the acetabular models used for pre-clinical testing should come with consistent properties and shape, and be easy to

position on a testing rig. Most studies measuring cup micromotion use cadaveric pelvic bones [106, 119, 129, 134, 156, 157, 165, 168]. This could be considered as an advantage, however, there are limitations with the use of cadaveric pelvic bones in *in vitro* studies. Cadaveric bones are expensive and limited in supply, have high interspecimen variability in both size and mechanical properties, and are difficult to repeatedly locate on a testing rig [131, 151]. Cadaveric bones are therefore unsuitable for pre-clinical testing as these factors increase the variability of the results, which can, in turn, prevent the identification of specific factors which have a significant effect on cup stability.

Another option for an acetabular model was the polyurethane Sawbones foam blocks, which are primarily used in the load-to-failure tests [131, 139 , 141, 144, 146, 150, 182]. The Sawbones blocks are manufactured with consistent mechanical properties similar to those of bone, they are cheaper than cadaveric bones and their shape make them easy to locate on a testing rig. Furthermore, they are available in a variety of mechanical properties modelling different types of bone. However, the studies that use these blocks model the acetabulum as a hemispherical cavity, simplifying the complex structural properties of the acetabulum and the pelvis. A new acetabular cavity was therefore devised, in which the pinching effect caused by the anterior and posterior acetabular columns, and the non-supportive areas of the acetabular notch and the radiolucent triangle, were replicated. This model is still a simplified version of the acetabulum as the uneven rim geometry of the acetabulum is not included, and only trabecular bone is modelled. A similar model has been validated in another study assessing resurfacing cup deformation by comparing it to cadaveric pelvic bones [186]; however, a cadaveric study should be performed to validate this model for this specific use.

Preliminary studies were performed to assess the reusability of both the acetabular cup and the Sawbones blocks. Damage was expected as the cup was implanted into an under-reamed cavity; and considering that the polyurethane foam is weaker than the metallic acetabular cup, damage was expected on the acetabular model side. This was confirmed during initial observations where foam incrusted into the porous surface of the acetabular cup and damage of the acetabular cavity was observed following push-out (Figure 4.7). The incrusted foam can reduce the stability of the cup, as it can fill the porous surface of the acetabular components, creating a smooth surface and reducing the friction between the cup and the Sawbones block. However, when the cup was cleaned after every test using a soft nylon brush to remove any foam debris, there were no visible trends in the micromotion and push-out forces during repeated use. Hence, only using one cup for all the tests was considered applicable. On the other hand, there were some significant differences in the peripheral diameter of the acetabular cavity, the cup micromotions and the push-out forces with repeated use of the Sawbones blocks, most probably as a result of material being removed from the cavity. The outcome of these preliminary studies suggested that while the acetabular cup can be reliably reused, only new Sawbones blocks should be used for each new test.

Micromotion studies aim to assess the stability of acetabular cups under physiological conditions. One of the main limitations of studies reported in the literature is that they do not accurately measure the micromotion of the cup in all six DoF. Instead, a dominant direction of motion is assumed, usually the translation normal to the face of the acetabular cup, which is equivalent to the Z micromotion in this study [106, 119, 129, 134, 157, 160, 165]. Hence, only

the micromotion in this assumed dominant direction of motion is measured and reported. The results obtained in this study under static SLS conditions show significant levels of micromotion in more than one direction, highlighting the importance of considering all six DoF and not only assuming a dominant direction of motion when measuring cup micromotion.

There was a substantial decrease in stability with the physiological model compared to the hemispherical one, regardless of foam density: the micromotions tended to be higher and the push-out forces were lower (Figures 4.26, 4.27 and 4.28). This decrease in stability can be explained by the change in geometry of the cavity around the rim of the cup. Indeed, as previously discussed, press-fit primarily relies on peripheral fixation, or the interference between the cup and the bone around the rim of the cup. With the hemispherical model, a uniform circumferential force around the cup secured it in place. The presence of the two cavities representing the acetabular notch and the radiolucent triangle in the physiological model reduced the circumferential contact area between the cup and the Sawbones block, resulting in a lower level of force surrounding the periphery of the cup. The presence of these gaps also influenced the change in the direction of the dominant micromotion as less foam was present to resist the load in the Z direction (Figure 4.34). As the physiological model better replicates the environment in which the acetabular cup is implanted into, it can therefore be assumed that studies using hemispherical cavities to model the acetabulum overestimate the stability of acetabular cups.

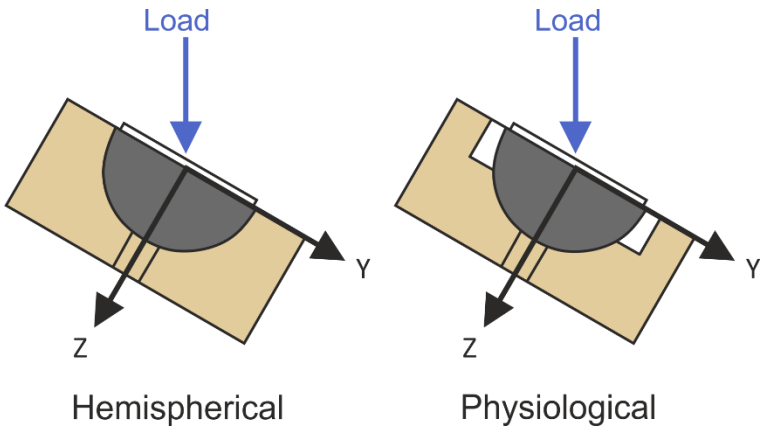

Figure 4.34 – Cross-section view of the hemispherical and the physiological acetabular models showing the direction of the load and the Y and Z micromotions. The white zones on the physiological model show the location of the gaps representing the acetabular notch and the radiolucent triangle.

There were some exceptions with the low density Sawbones blocks where the X and θ_Y micromotions were greater in the hemispherical model compared to the physiological model. This was, however, not the case in the high density foam blocks. The low density foam blocks are weaker and therefore more prone to deformation than the high density blocks. Hence, foam deformation is more likely to occur during insertion, resulting in the cup being embedded deeper within the cavity. This was even more likely in the physiological model as the two extra cavities present allow the foam to deform even more, resulting in a deeper contact area as seen with the layer ink (Figure 4.15). This may have increased the stability of the cup in directions unrelated to the direction of the load, such as X and θ_Y micromotions.

Furthermore, these micromotions were small compared to the ones in the dominant directions of motion; hence, they are unlikely to contribute to implant loosening.

There was a clear decrease in cup stability when it was implanted into the low density Sawbones blocks compared to the high density Sawbones blocks, with most of the micromotions being greater and the push-out forces smaller in the low density Sawbones blocks (Figures 4.29, 4.30 and 4.31). There was an exception to this trend where the X micromotion was higher in the high density physiological model compared to the low density physiological model. Here again, this exception can be explained by the cup embedding itself more in the weaker foam and therefore being more stable in a direction of micromotion that was unaffected by the loading. The lower compressive strength of the low density Sawbones blocks meant that they were more prone to deformation than the high density blocks under the same amount of load, which resulted in smaller compressive stresses around the rim of the implant. Therefore, even if the cup may have embedded itself more into the low density foam block, it was still less stable in the directions of motions affected by loading due to the weaker nature of the foam and the smaller compressive forces holding the cup in place. These smaller compressive forces also made it easier for the cup to be pushed-out of the acetabular cavity, explaining the lower push-out forces measured. Hence, it can be concluded that the cup was less stable in weaker bone compared to normal bone. This finding has been observed in other studies available in the literature assessing cup stability when implanted in both cadaveric bones and Sawbones blocks [131, 139, 141, 155, 157].

4.8. CONCLUSIONS

A system previously used to measure the micromotion in six DoF of femoral stems was adapted for press-fit acetabular cups. The accuracy and precision of the system was proven to be high enough to investigate the small levels of micromotion expected in the press-fit acetabular component whilst having a range big enough to tolerate any migration of the component within the acetabular cavity.

A test protocol was designed to assess the micromotion of a press-fit acetabular component. This involved a method to repeatedly insert the acetabular component within the acetabular cavity; a method to physiologically load the hip joint whilst measuring the micromotion of the acetabular cup; a method to remove the cup from the acetabular cavity without damaging the cup; and finally, a Matlab routine and a statistics protocol to process the raw data into useful information.

A preliminary study to assess the reusability of both the acetabular component and the Sawbones blocks was performed. The results showed no trends or patterns in the micromotion and in the push-out forces when reusing the same acetabular cup, suggesting that it can be reliably reused for testing. On the other hand, assessment of the Sawbones blocks showed that new blocks should be used for each test.

Another important aspect in the development of a new pre-clinical testing protocol to assess the micromotion of acetabular cups was the design of an acetabular model. This model needed to replicate the important structural properties of the acetabulum as well as being easily reproducible, and with low interspecimen variability and ease of use. The physiological model introduced in this study meets all these conditions. This model replicates the structural support of the acetabular columns and the non-supportive areas of the radiolucent triangle and the acetabular notch.

The comparison study between the commonly used hemispherical model and the physiological model showed significantly higher levels of cup micromotion and lower push-out forces with the latter model, suggesting a decrease in stability of the press-fit cup. A similar model to the physiological one used was validated in another study using cadaveric pelvic bones. It was therefore assumed that the micromotions and the push-out from the physiological model were the more realistic ones and hence the simplified hemispherical cavity over-estimated the stability of press-fit cups. It is for this reason that the physiological model was chosen as the acetabular model for the pre-clinical testing protocol.

Another objective of this study was to assess the effect of foam density on cup stability. The results indicated that cups inserted into weaker, e.g. osteoporotic, bone would be more prone to micromotion. Additional fixation methods, such as screws, fins or pegs, or cement are usually recommended for patients with weaker bone. As this thesis concentrates on the stability of press-fit cups without any additional fixations, only the high density Sawbones blocks were assessed from then on.

Furthermore, significant levels of micromotion were observed in all translations. This highlights the need to measure the micromotion of acetabular cups in all directions of motion and not only in the assumed dominant direction of motion.

Finally, the measurements of the foam deformation obtained during cyclic loading showed similar levels of deformation. Therefore, even though the micromotion measured using this system are slight overestimations of the true micromotion of the cup, they are still comparable to one another and conclusions can still be drawn.

5. THE EFFECT OF HIP MOTION ON CUP MICROMOTION

5.1. INTRODUCTION

The previous chapter introduced a protocol to assess cup micromotion in six DoF under cyclic loading and single leg stance. The chapter also described and assessed a physiological acetabular model that aimed to replicate the important structural features present in the acetabulum, whilst keeping the low variability and ease of use of synthetic foam block models.

The hip joint is also subjected to dynamic hip motion during gait. It can be hypothesised that dynamic hip motion has an effect on the micromotion of the cup. However, none of the studies available in the literature assessing cup micromotion have investigated this effect on cup micromotion. On the other hand, two studies have reported significant increases in micromotion of the femoral stem when subjected to dynamic hip motion [180, 181]; the same can be expected on the acetabular side. Hence, one could argue that the methods available in the literature underestimate the stability of implanted acetabular cups.

The aim of this chapter is twofold. Firstly, a dynamic hip motion simulator was developed to replicate *in vitro* the motions that the hip is subjected to during activities of daily living. The combination of this simulator with the six DoF measurement system and physiological acetabular model developed in the previous chapter provided a novel method to assess the micromotion of a press-fit cup under both cyclic loading and dynamic hip motion. The second part of this chapter used this novel test protocol to assess both the effects of dynamic hip motion and the effect of a new porous coating on the micromotion of the cup.

5.2. Development of the Dynamic Hip Motion Simulator

In this section, the specifications for the dynamic hip motion simulator is defined, the rig development is described and finally, the validation work on the simulator is presented.

5.2.1. Rig Specifications

The first stage in developing the dynamic hip motion simulator was to define its specifications. For simplification, it was decided to model the motion of the hip in flexion-extension only, as this is the primary direction of hip motion during gait and many other activities of daily living. Therefore it is the motion that will have the greatest potential to influence cup stability. The activities of daily living that the dynamic hip motion simulator was designed to replicate were level walking, stair climbing and rising from a sitting position. The angles of flexion-extension and the peak load for the different activities of daily living (Table 5.1) were defined based on the data published in the literature and presented in Chapter 2. The rig was also designed to hold a fixed position in flexion to perform static tests in order to assess the effect of dynamic hip motion on cup micromotion.

Table 5.1 – Range of motion and peak load of each activity of daily living to be replicated by the dynamic hip motion simulator

	Flexion	Extension	Range	Peak Load
Walking	30°	10°	40°	2.0 kN
Stair climbing	45°	5°	50°	2.0 kN
Rising from chair	60°	0°	60°	1.5 kN

In order to obtain the double peak loading profile observed in the gait cycle (Figure 2.12), the dynamic hip motion simulator was designed to operate at 0.5 Hz while the Dartec maintained its loading frequency at 1 Hz. Both cyclic loading and hip motion were modelled as a sine wave; this was not the exact replication of the gait profile, however, it is a close approximation. Another important factor was the synchronisation of the load and the hip motion in order to repeatedly obtain peak loads at maximum flexion and extension, which represented heel strike and toe-off, respectively (Figure 5.1).

Finally, the dynamic hip motion simulator was designed so that it could fit on the Dartec and that the six DoF measurement system and the Sawbones blocks could be attached to it in order to be able to assess cup micromotion under dynamic hip motion and cyclic loading.

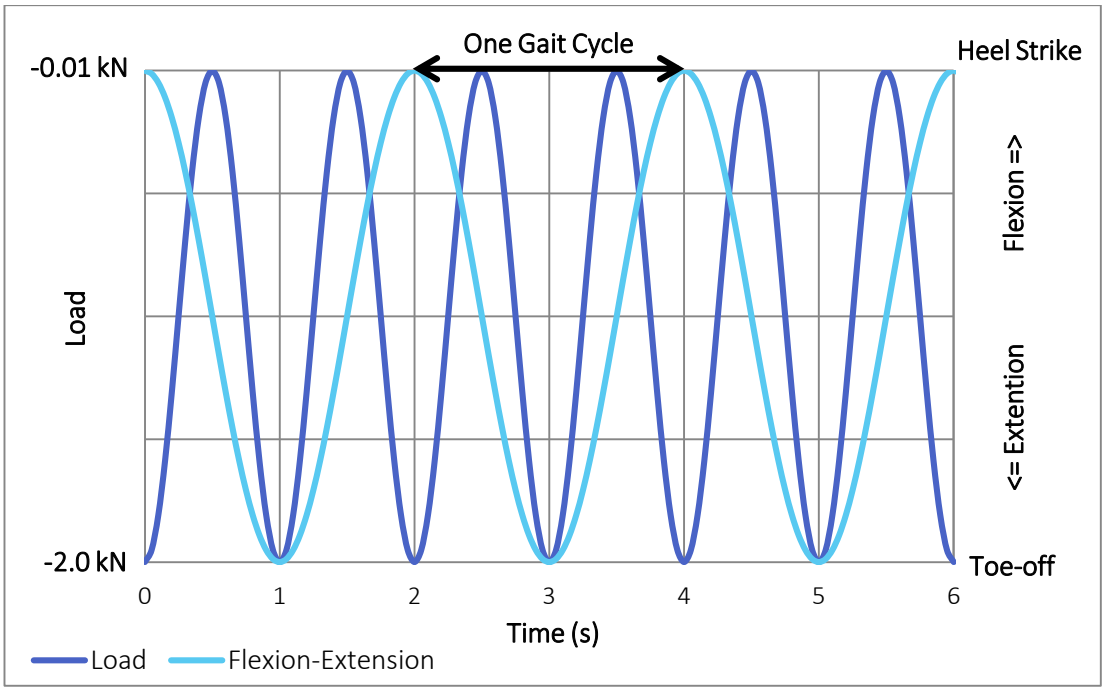

Figure 5.1 – Desired synchronisation between cyclic loading and dynamic hip flexion-extension

5.2.2. Initial Design

The first step in designing the dynamic hip motion simulator was to determine how loading and flexion-extension were going to be generated. In order to correctly simulate hip flexion-extension, the centre of rotation of the dynamic hip motion simulator needed to be aligned with that of the hip joint. It was assumed that the centre of rotation of the acetabular cup, the femoral head and the hip joint were the same.

As the aim of this pre-clinical test was to measure the micromotion of acetabular cups, the position of the acetabular cup, and hence its centre of rotation, was expected to vary throughout the test. Hence, keeping the centres of rotation aligned during testing would be challenging if the acetabular cup with the six DoF system were to be positioned on the dynamic hip motion simulator. On the other hand, the femoral head could be rigidly attached to the dynamic hip motion simulator, keeping both their centres of rotation aligned. However, this would result in two bulky and heavy constructs: one being the dynamic hip motion simulator with the femoral head, and the other being the rig supporting the six DoF system and the Sawbones block with the acetabular cup; one of which would have to be attached to the actuator of the Dartec. Attaching a heavy construct to the actuator of the Dartec was not an option, hence this setup was deemed to be not feasible.

It was therefore decided that the Sawbones block with the acetabular cup and the six DoF system would be placed on the dynamic hip motion simulator, and that, similar to the previous tests, the hip joint would be loaded through a femoral head connected to the Dartec. Considering the issue of the misalignment in centres of rotations caused by the moving acetabular component, the change in position of the centre of rotation of the acetabular component should be small and therefore it should not have a marked effect on the test or results.

5.2.3. Dynamic Hip Motion Simulator Development

The initial development of the dynamic hip motion simulator was carried out under my supervision as a final year project (Duncan Scrivens, Integrated Mechanical and Electrical Engineering (IMEE) MEng, University of Bath) and is summarised in this subsection [192].

The dynamic hip motion simulator was divided into three parts, the moving part, which rotated in flexion-extension and on which the Sawbones block and the six DoF system were attached (called the Sawbones block holder); the motor; and the main body, which held the motor and the Sawbones block holder together. The entire rig was made of 10 mm steel plates to ensure sufficient stiffness to withstand 2 kN of cyclic loading.

Sawbones Block Holder

The Sawbones block holder is the moving part of the dynamic hip motion simulator on which the Sawbones block and the six DoF measurement system were attached (Figure 5.2). In addition, two end plates were added to prevent any buckling of the Sawbones block holder under load. A 12 mm shaft was rigidly connected on both side of the Sawbones block holder which acted as its axis of rotation.

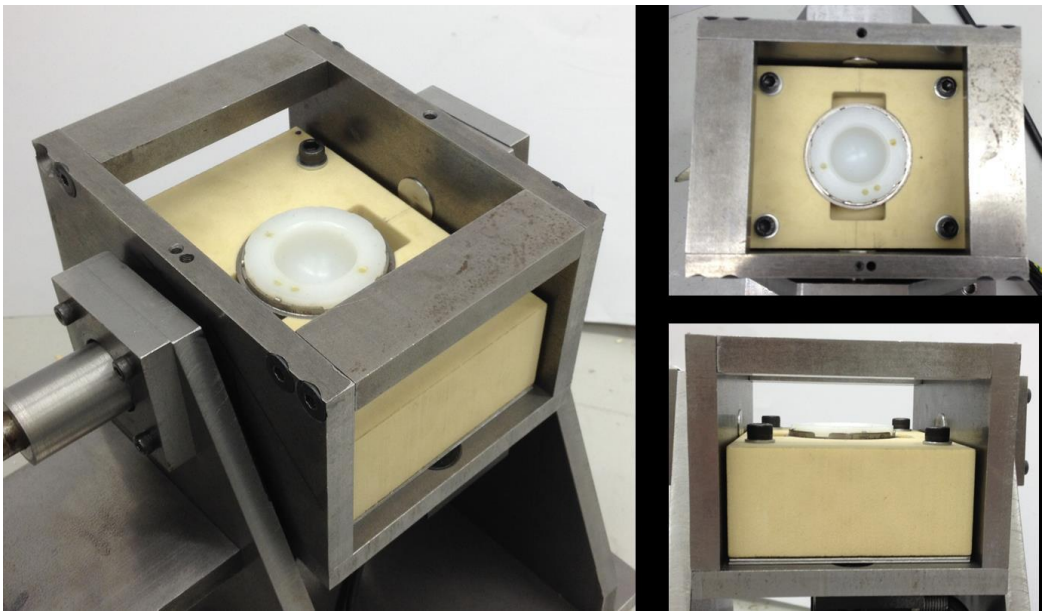

Figure 5.2 – Sawbones block holder (pictures from [192], with permission)

The centre of rotation of the Sawbones block holder was designed to be slightly above that of the hip. This was done to take into account for any errors in the manufacturing of the rig. Shims were then used to raise Sawbones blocks, and therefore the centre of rotation of the hip joint, to align it with the centre of rotation of the rig, providing greater control on the positioning of the cup during testing.

Motor Selection

A permanent magnet, fully enclosed, brushed DC motor (Parvalux PM4D, Parvalux, Bournemouth, UK) and a Parvalux MB gearbox were selected for the dynamic hip motion simulator, with the accompanying control and driver circuit constructed from four major sections: a buffer, scaling and zeroing, an error amplifier and a mini maestro driver circuit. The position input signal was provided by a function generator. In this setup, the signal was a 0.5 Hz sine wave in which the amplitude and the DC offset were used to alter the angles between which the rig oscillated. The shaft of the motor was connected to the shaft of the Sawbones block holder through direct coupling. The angular position of the shaft was fed back via a potentiometer mounted to the motor shaft to the control and driver circuit. A lead from the control and driver circuit was connected to the same data acquisition frame as the LVDTs and the Dartec to record the angular position of the dynamic hip simulator as a voltage (Figure 5.3)

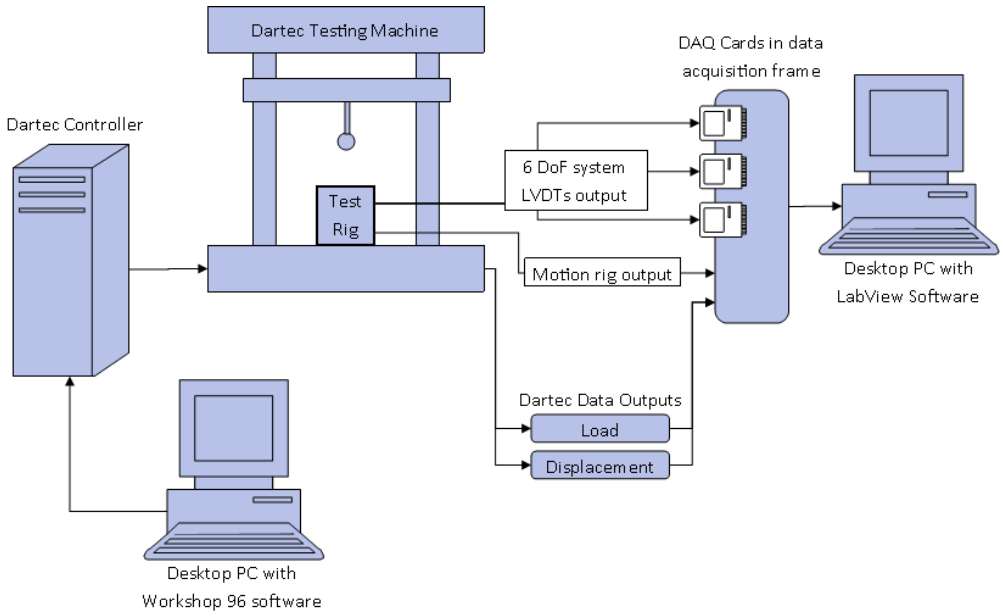

Figure 5.3 – New schematic showing the components and connections in instrumentation including motion rig output

Main Body

A simple frame was designed as the main body of the simulator. Its primary function was to anchor the dynamic hip motion simulator to the Dartec and support both the motor and the Sawbones block holder (Figure 5.4). A 2 mm gap was designed between the Sawbones block holder and the main body to allow free, unimpeded movement of the Sawbones block holder, but still prevent the shaft from bending. Two 12 mm deep groove, single row ball bearings were located within the main body to support the shafts; they provided repeatable low friction rotations and both axial and radial support. The bearings were fully located into the main body and on the shaft through the use of shoulders and circlips.

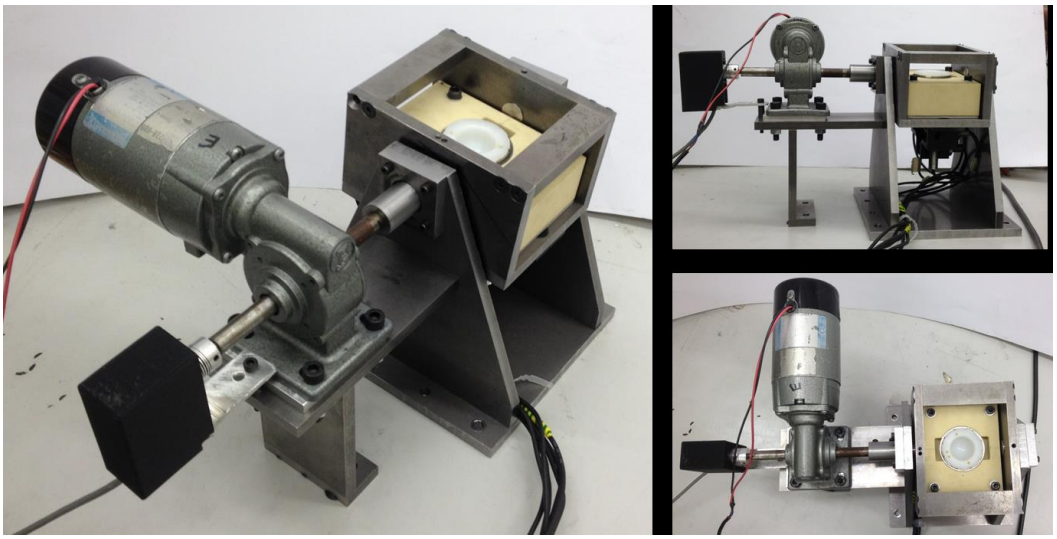

Figure 5.4 – Dynamic hip motion simulator (pictures from [192], with permission)

5.2.4. VALIDATION

Once the dynamic hip motion simulator was built, a series of tests were conducted, with the final year project student, to ensure that the rig was functioning according to the specifications.

POSSIBLE RANGE OF MOTION

The first step of the rig validation was to ensure that the dynamic hip motion simulator could perform the desired ranges of motion at 0.5 Hz as defined in the specifications (Table 5.1). The correct angles of flexion and extension for the selected activities of daily living were set on the dynamic hip motion simulator using a digital inclinometer, and their corresponding output voltage were noted using a single-channel LabView program. The dynamic hip motion simulator was then run at 0.5 Hz for 100 cycles and the output voltage was monitored using the same LabView program; this confirmed that rig could successfully perform the three activities of daily living defined in the rig specifications.

The second step of this validation was to verify that there were no interference between the dynamic hip motion simulator and the Dartec during the modelled activities of daily living. Once the dynamic hip motion simulator was correctly positioned on the Dartec, the three chosen activities of daily living were tested again. The rig could perform both level walking (10° extension to 30° flexion) and stair climbing (5° extension to 45° flexion) without any problem. However, it was decided not to test rising from a chair (0° to 60° flexion) as it was apparent that the end plate on the Sawbones block holder would collide with the Dartec actuator at maximum flexion (60°).

WORST CASE SCENARIO

The aim of this validation test was to verify that the dynamic hip motion simulator could perform both level walking and stair climbing correctly for 1000 cycles when the hip joint was loaded at 2 kN; this represented the worst case scenario. Under these conditions, the frequency of the rotation was maintained, however, there was a clear reduction in the

magnitude of the range of flexion-extension. The fault was attributed to the torque capacity of the motor and gearbox being too low to drive the rig in this scenario. Further investigations suggested that this was caused by friction within the hip joint as both the femoral head and polyethylene liner were hot to the touch after 1000 cycles. Multipurpose grease (Comma Multipurpose Grease, Gravesend, UK) was added at the bearing surfaces to lubricate the hip joint and the same test was performed once more. The dynamic hip motion simulator operated correctly when the hip joint was lubricated and there was no reduction in the range of flexion-extension with the number of cycles. Finally, the dynamic hip motion simulator was operated under both cyclic loading and dynamic hip motion to confirm that the dynamic hip motion simulator can perform under test conditions.

Centre of Rotation

In order to replicate hip flexion-extension, the centre of rotation of the hip joint needed to be aligned to that of the dynamic hip motion simulator. The centre of rotation of the hip joint could be raised by placing shims underneath the Sawbones block. However, as previously mentioned, the location of the centre of rotation of the hip joint moved as a result of cyclic loading. Hence, the centres of rotations were not always aligned during micromotion testing. A preliminary test was devised to identify the best location for the centre of rotation of the hip joint, and hence determine the optimum shim thickness. The results from this test revealed that the best position for the cup was when both centres of rotation were aligned when the cup was loaded at 1.0 kN, which was the midpoint between the high and the low load during cyclic loading.

Synchronisation of Load and Motion

The final step was to synchronise the loading and hip motion in order to achieve peak loads at both maximum flexion and extension (Figure 5.1). The control system of the Dartec would not allow synchronisation with the control system of the dynamic hip motion simulator, therefore it was unable to receive a sine wave to drive the load. Similarly, sine waves could not be taken from the Dartec to drive the dynamic hip motion simulator. Hence, a starting sequence, where both the simulator and the Dartec were manually started one after the other, was investigated.

Initial tests showed that user variability was inevitable with this method; hence, another approach was taken to determine if user variability had any effect on the micromotion of the cup. This was done as a start-stop test where the acetabular cup was subjected to 100 loading cycles, and this was repeated 15 times per set for three sets. As the cup was never removed from the Sawbones block throughout the entirety of this test, it was assumed that the micromotion should be similar for every test. This method, which consisted of starting first the dynamic hip motion simulator and then the Dartec, showed low variability in the cup micromotion and therefore it was assumed that user variability had a negligible effect on the micromotion of the cup. The analysis of this data was performed by Duncan Scrivens; the micromotion of the cup in different directions and the average timing error for one of the three sets are presented in Figures 5.5 and 5.6.

Both sine waves needed to be accurate as small differences in the frequency, even by 0.001 Hz, resulted in shifting the load and motion sine waves out of phase after 1000 loading cycles. Achieving 0.5 Hz accurately with the dynamic hip motion simulator was challenging. The digital function generator displayed the frequency accurately to three decimal places and therefore the loading frequency of the Dartec was changed to match that of the dynamic hip motion simulator before every test. To check that both frequencies were matched, it was decided that the hip joint would be subjected to 200 loading cycles of preconditioning before every test; this was enough to identify any shifting between the load and motion sine waves. In addition, this preconditioning also allowed the user to verify that all the LVDTs were working correctly prior to testing.

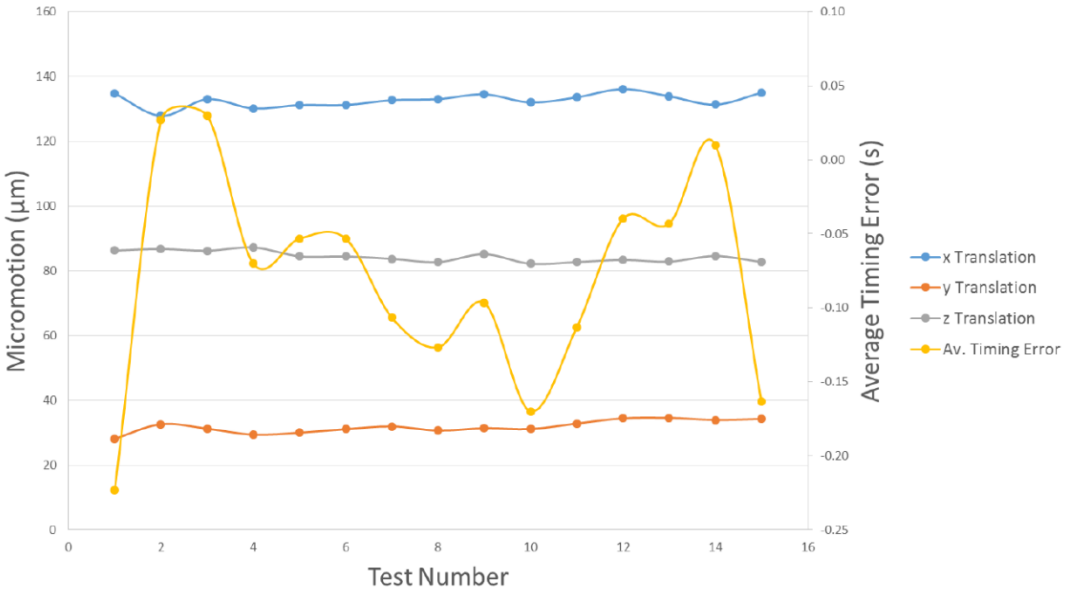

Figure 5.5 – Translations and average timing error recorded during one of the start-stop tests (graph from [192], with permission)

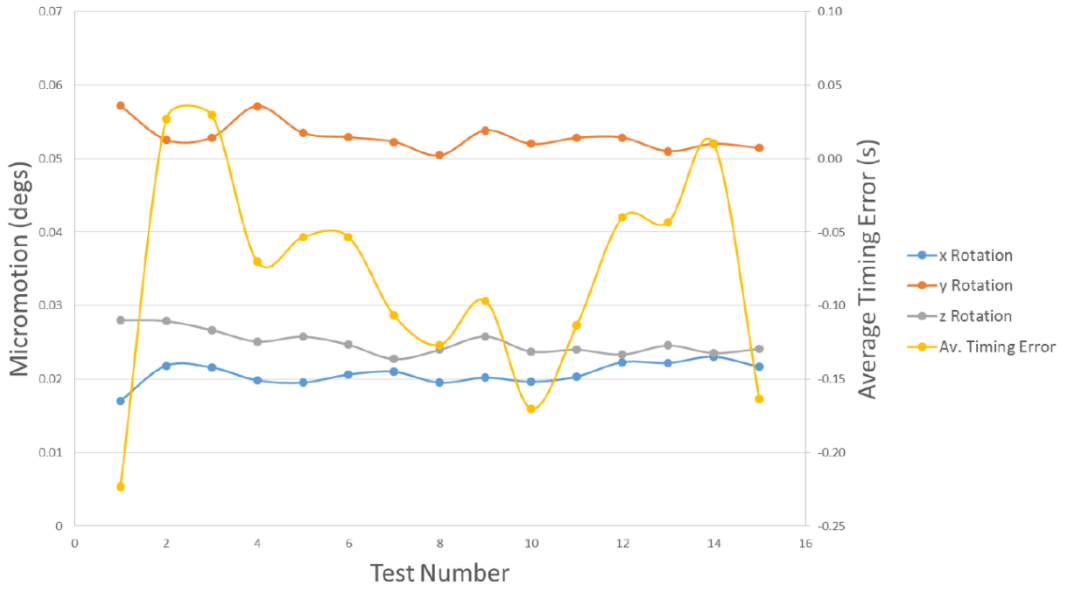

Figure 5.6 – Rotations and average timing error recorded during one of the start-stop tests (graph from [192], with permission)

5.2.5. Changes to Dynamic Hip Motion Simulator

In the natural hip, the path of the load during the gait cycle follows the horseshoe shape along the articular cartilage [57]. However, this was not the case with this setup. Instead, the path of the load followed a straight line long the centre of the acetabular cavity (No inclination in Figure 5.8). To replicate the horseshoe shape loading pattern seen in the hip, cup inclination had to be included.

Surgeons aim to implant the cup at an inclination between 40° and 45° [13, 23, 24]. However, the direction of the load within the hip joint is not vertical, but along the mechanical axis of the hip, which is at 3° from the vertical (Figure 5.7) [193]. Therefore, by taking both of these factors into account, the cup needs to be position at an angle between 43° and 48°; a cup inclination of 45° with respect to the horizontal was therefore chosen.

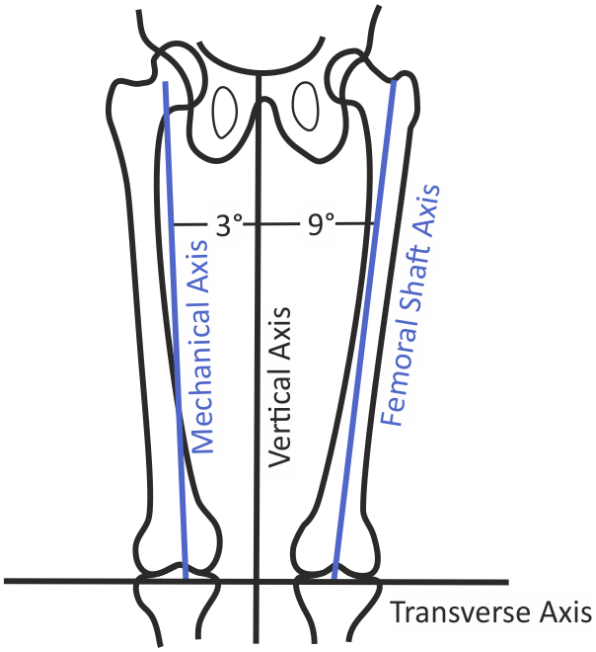

Figure 5.7 – Mechanical and femoral shaft axis of the hip joint with respect to the vertical axis

The second step was to determine where to place the angle plate to replicate the horseshoe shaped loading pattern with the dynamic hip motion simulator. There were two different options to include cup inclination with the current setup. The first option was to place a 45° angle plate below the dynamic hip motion simulator. However, the path of the load with this setup was a shifted version of the original setup: a straight line shifted towards the radiolucent triangle (Option 1 in Figure 5.8). The second option was to place the angle plate on the Sawbones block holder. With this setup, the path of the load followed a horseshoe shape as seen in the natural hip (Option 2 in Figure 5.8).

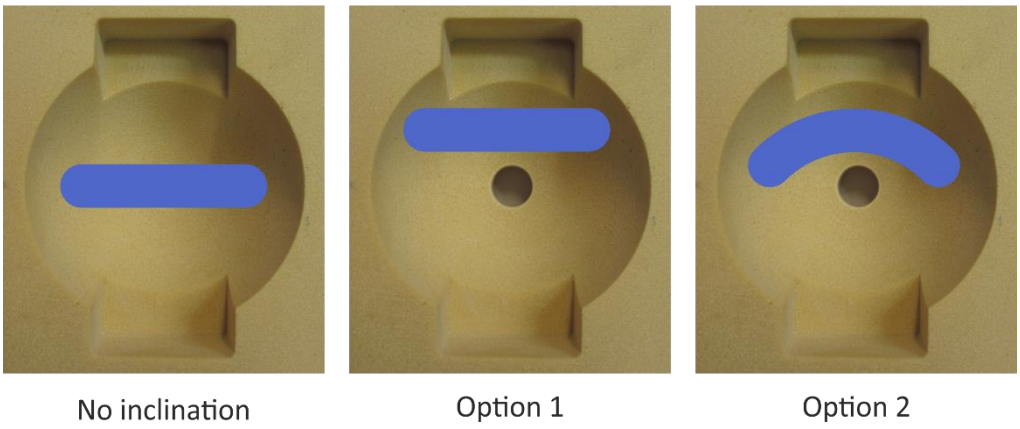

Figure 5.8 – Different loading patterns caused by different options to include cup inclination

Placing an angle plate on the original Sawbones block holder was impossible as the six DoF measurement system would no longer be aligned with the acetabular block. Hence, the Sawbones block holder was redesigned to include an inclination of 45° (Figure 5.9). The top plate, on which the Sawbones block and the six DoF measurement system were attached, was detachable from the rest of the Sawbones block holder in order to facilitate test setups where access to the six DoF measurement system was needed. The six DoF measurement system had to be rotated by 90° due to space constraints and the Matlab code was altered accordingly to keep the directions of micromotion consistent throughout this thesis. Finally, a shim was used to align the centre of rotation of the cup when loaded at 1.0 kN to the centre of rotation of the dynamic hip motion simulator.

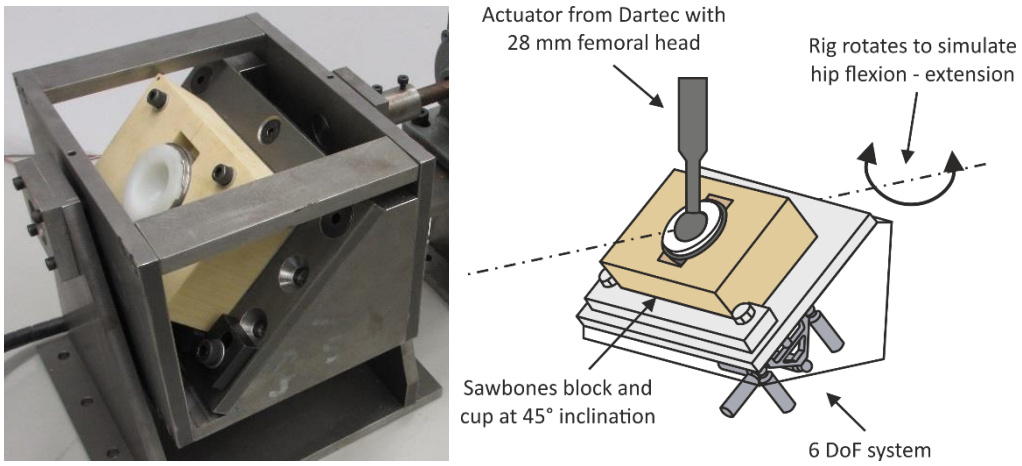

Figure 5.9 – New Sawbones block holder including cup inclination

It was assumed that the modification of the Sawbones block holder did not affect the way the dynamic hip motion simulator performed and therefore only one validation test was redone to verify that both level walking and stair climbing could still be performed on the Dartec. There was no problem with level walking, however, when testing stair climbing, impingement between the liner and the femoral stem occurred at maximum flexion (45°). Indeed, the mounting system used for the femoral head did not replicate the neck shaft angle that would be present if a femoral stem had been used, resulting in the observed impingement. Hence, the maximum flexion during stair climb was reduced to 40° to prevent impingement.

5.3. FINAL TEST PROTOCOL

The test protocol described in Chapter 4 had to be updated to include dynamic hip motion. Below is the test protocol that was used in this study. A detailed protocol of this test methodology and the Matlab codes used to analyse the data are available in Appendices 5 and 6, respectively.

- The Sawbones block was placed on the cup insertion rig and the acetabular cup inserted into the acetabular cavity of the Sawbones block using a standardised protocol of five sinusoidal cycles of 5 kN using the Dartec. A bull's eye spirit level was used before and after loading to check the alignment of the cup.
- The Sawbones block with the cup was removed from the cup insertion rig and bolted on the dynamic hip motion simulator at 45° inclination, lubricated using multipurpose grease, and then aligned with the 28 mm femoral head connected to the Dartec.
- The dynamic hip motion simulator was setup to the desired angles of flexion and extension using a digital inclinometer.
- Once the dynamic hip motion simulator was setup and running, preconditioning started where the hip joint was subjected to 200 sinusoidal load cycles (0.01 kN to 2 kN at 1 Hz). During preconditioning, the user verified that there was no shift between the motion and load cycles, and that all the LVDTs were working correctly.
- Following preconditioning, the micromotion test was started, where hip joint was subjected to 1000 sinusoidal load cycles (0.01 kN to 2 kN at 1 Hz), which is equivalent to 500 steps.
- Once the micromotion test was completed, the Sawbones block with the cup was detached from the dynamic hip motion simulator, placed up-side down on the cup insertion rig for push-out test; the push-out force was recorded.
- The cup was cleaned with a soft nylon brush to remove any foam debris and visual inspection of the porous coating was performed.

Once testing was done, the collected data were analysed using the Matlab routines and SPSS.

This protocol was also used to measure the micromotion of the acetabular cup when kept at a fixed position as the dynamic hip motion simulator is capable of holding its position.

Prior to testing, the peripheral diameter of each Sawbones block was measured using the digitizer (and obtained using the corresponding Matlab routine) to check that they were manufactured to the correct dimension.

5.4. Effect of Dynamic Hip Motion on Cup Micromotion

The second aim of this chapter was to use the developed dynamic hip motion simulator with the six DoF measurement system and the physiological acetabular model to assess both the effects of dynamic hip motion and the effect of a new porous coating on the micromotion of the cup. For this second part, the clinically proven Trident cup with HA coating [4] was compared to the new Tritanium cup (Stryker), which is a Trident cup with a new porous coating designed to improve osseointegration [194]. These acetabular components were chosen as they provide the unique opportunity to compare the effect of a new porous coating on cup stability whilst keeping other variables, such as cup geometry and fixation type, the same.

5.4.1. Materials and Method

The final test protocol was used in this study.

Two new acetabular shells: one Trident cup with HA coating and one Tritanium cup, were obtained with their corresponding polyethylene liners (two X3 liners, Stryker) for this study (Figure 5.10). The shells had an external diameter of 54 mm and the liners were for a 28 mm femoral head.

Figure 5.10 – Trident cup with HA coating (top) and Tritanium cup (bottom)

Each cup was tested under three conditions; static flexion, level walking and stair climbing (Table 5.2) for 500 steps. Each condition was repeated five times, each time with a new Sawbones block (density = 0.48 g/cm^3); hence thirty new Sawbones blocks with the physiological cavity were manufactured for this study. Even though lubrication of the hip joint and preconditioning were not required for the static flexion tests, these were still done for comparison purposes.

Table 5.2 – Testing parameters

	Min Load	Max Load	Loading Frequency	Flexion Angle	Extension Angle	Simulator Frequency
Static Flexion	-0.01 kN	-2.0 kN	1 Hz	30°	n.a.	n.a.
Level Walking	-0.01 kN	-2.0 kN	1 Hz	30°	10°	0.5 Hz
Stair Climbing	-0.01 kN	-2.0 kN	1 Hz	40°	5°	0.5 Hz

For statistical analysis, non-parametric tests with a type I error of $\alpha = 0.05$ were performed. The Friedman and the Wilcoxon signed ranks post hoc tests were used to identify differences between different translations and rotations during the same test conditions. The Kruskal-Wallis and the Mann-Whitney post hoc tests were used to identify differences in micromotion and push-out forces between different test conditions.

5.4.2. Results

Trident Cup with HA Coating

The general pattern in micromotion observed was the same regardless of the test condition (Figure 5.11). Considering that 0.08° in rotation corresponds to 40 µm of displacement, the translations were always greater than the rotations. In translations, the X micromotions were the greatest whilst the Z micromotions were the smallest (Table 5.3). The θ_Y rotations were generally greater than those in θ_X and θ_Z.

The micromotion of the cup was generally greater under dynamic hip motion (both level walking and stair climbing) compared to static flexion (Figure 5.11). The micromotion of the cup was significantly greater in all translations and in θ_Y when subjected to dynamic hip motion compared to static flexion (Table 5.4). The micromotion of the cup was also significantly greater in both X and Z under stair climbing compared to level walking.

There were no significant differences in push-out forces following the different micromotion test conditions with the Trident cup (Table 5.4; Figure 5.12).

Table 5.3 – Results of the statistical analyses comparing the different translations and rotations during the same test condition with the Trident cup. The highlighted numbers represent statistical significance ($p < 0.05$)

		Static Flexion	Level Walking	Stair Climbing
Friedman Test	X - Y - Z	0.007	0.247	0.015
	θ_X - θ_Y - θ_Z	0.015	0.019	0.022
Wilcoxon Signed Ranks Test	X - Y	0.043	0.225	0.043
	X - Z	0.042	0.08	0.043
	Y - Z	0.043	0.176	0.345
	θ_X - θ_Y	0.157	0.041	0.039
	θ_X - θ_Z	0.063	0.458	0.783
	θ_Y - θ_Z	0.039	0.038	0.042

Table 5.4 – Results of the statistical analyses comparing the different test condition with the Trident cup as shown in Figures 5.11 and 5.12. The highlighted numbers represent statistical significance ($p < 0.05$)

		X	Y	Z	θ_X	θ_Y	θ_Z	Push-out
Kruskal-Wallis Test	Static – Walking – Stairs	0.006	0.012	0.002	0.769	0.006	0.099	0.112
Mann-Whitney Test	Static – Walking	0.021	0.009	0.008	0.740	0.005	0.050	0.112
	Static – Stairs	0.009	0.016	0.009	0.650	0.011	0.054	0.321
	Walking - Stairs	0.047	0.463	0.008	0.496	0.521	0.504	0.081

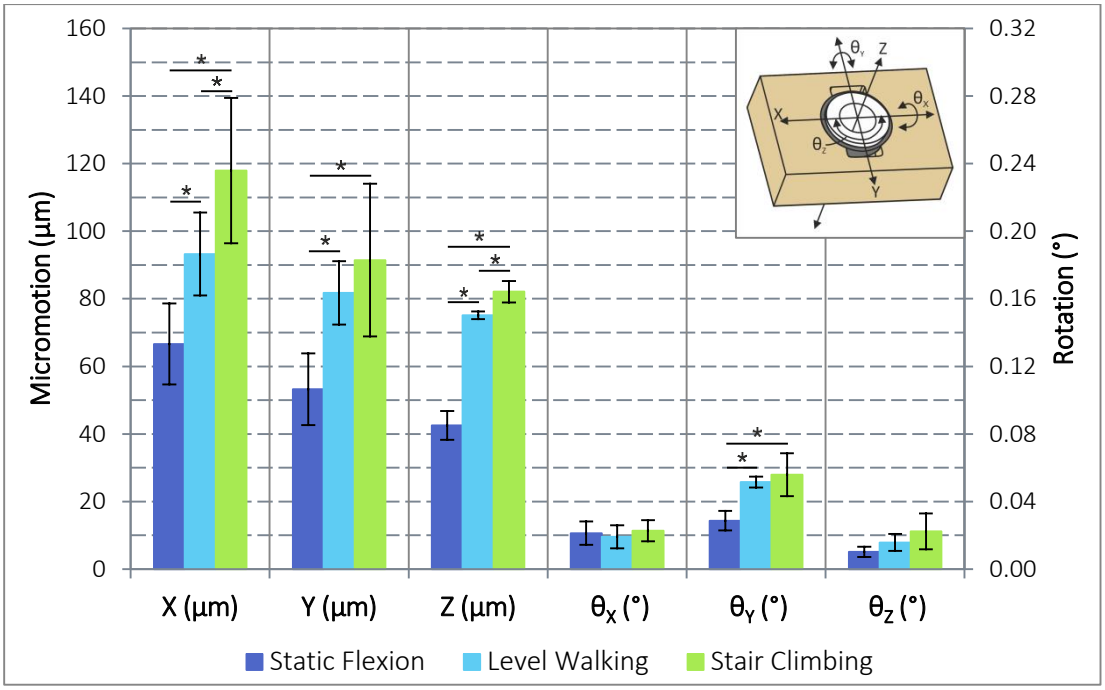

Figure 5.11 – Micromotion in six DoF of the Trident cup under three conditions: static flexion, level walking and stair climbing (0.08° corresponds to 40 µm). Values expressed as mean and standard deviation. *$p < 0.05$ using Mann-Whitney post hoc test

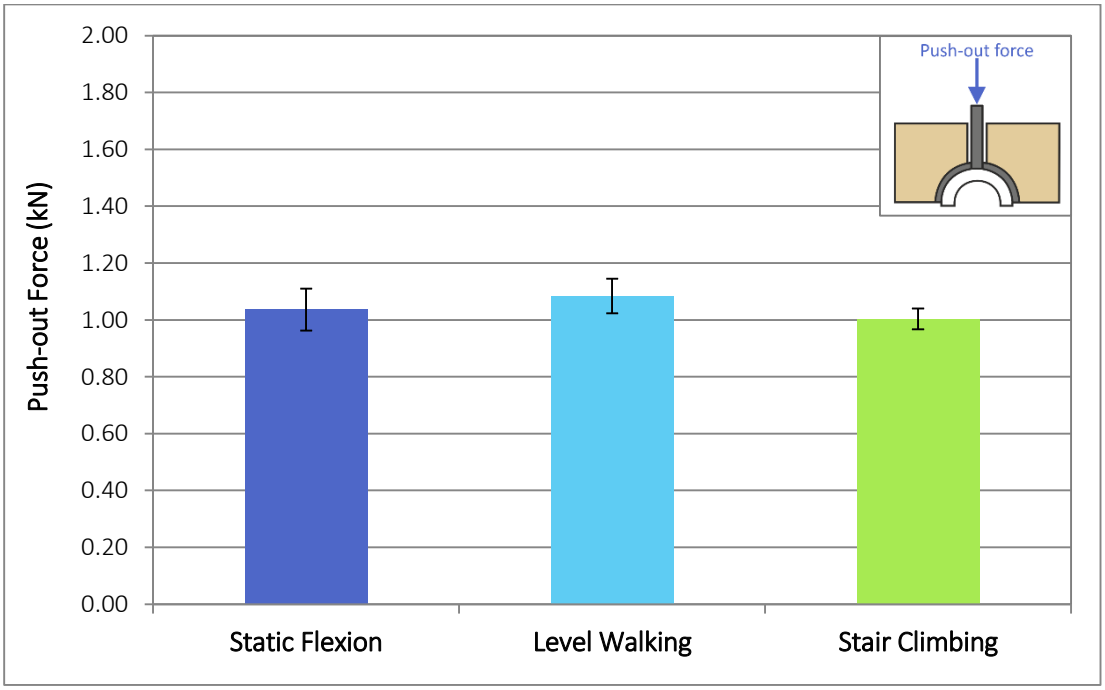

Figure 5.12 – Push-out forces of the Trident cup following micromotion tests. Values expressed as mean and standard deviation

TRITANIUM CUP

The general pattern seen with the Trident cup was also observed with the Tritanium cup (Figure 5.13). Considering that 0.08° in rotation corresponds to 40 µm of displacement, the translations were always greater than the rotations. In the translations, the X micromotions were the greatest whilst the Z micromotions were the smallest (Table 5.5). In the rotations, the θ_Y rotations were generally the greatest whilst those in θ_Z were the smallest.

The micromotion of the cup was significantly greater in all six DoF when subjected to dynamic hip motion (both level walking and stair climbing) compared to static flexion (Table 5.6). Only θ_Y was significantly greater when the cup was subjected to stair climbing compared to level walking.

The push-out forces of the Tritanium cup following the different micromotion test conditions were significantly different to one another (Table 5.6; Figure 5.14). The push-out force following the micromotion test under static flexion was the smallest, whilst the push-out force following stair climbing was the greatest.

Table 5.5 – Results of the statistical analyses comparing the different translations and rotations during the same test condition with the Tritanium cup. The highlighted numbers represent statistical significance ($p < 0.05$)

		Static Flexion	Level Walking	Stair Climbing
Friedman Test	X - Y - Z	0.007	0.022	0.015
	θ_X - θ_Y - θ_Z	0.01	0.007	0.007
Wilcoxon Signed Ranks Test	X - Y	0.043	0.043	0.043
	X - Z	0.043	0.043	0.043
	Y - Z	0.041	0.5	0.225
	θ_X - θ_Y	0.157	0.038	0.038
	θ_X - θ_Z	0.039	0.038	0.038
	θ_Y - θ_Z	0.038	0.039	0.034

Table 5.6 – Results of the statistical analyses comparing the different test condition with the Tritanium cup as shown in Figures 5.13 and 5.14. The highlighted numbers represent statistical significance ($p < 0.05$)

		X	Y	Z	θ_X	θ_Y	θ_Z	Push-out
Kruskal-Wallis Test	Static–Walking–Stairs	0.007	0.006	0.008	0.027	0.002	0.013	0.004
Mann-Whitney Test	Static – Walking	0.009	0.009	0.009	0.031	0.006	0.013	0.015
	Static – Stairs	0.009	0.009	0.009	0.020	0.005	0.013	0.009
	Walking - Stairs	0.251	0.175	0.599	0.549	0.018	1	0.027

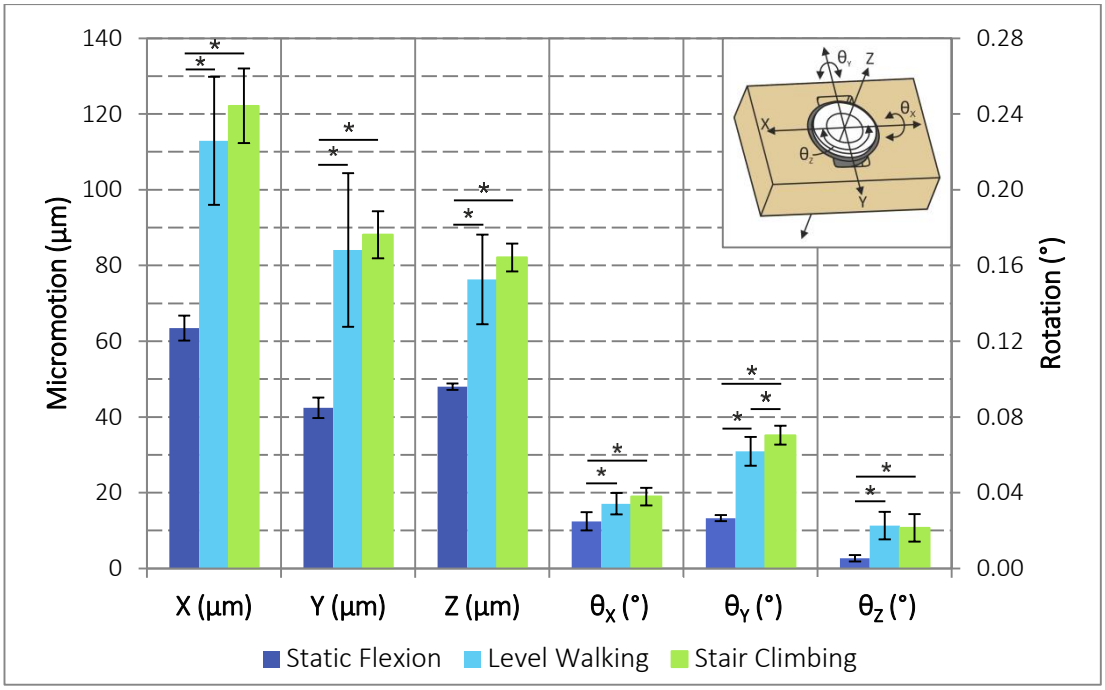

Figure 5.13 – Micromotion in six DoF of the Tritanium cup under three conditions: static flexion, level walking and stair climbing (0.08° corresponds to 40 µm). Values expressed as mean and standard deviation. *p < 0.05 using Mann-Whitney post hoc test

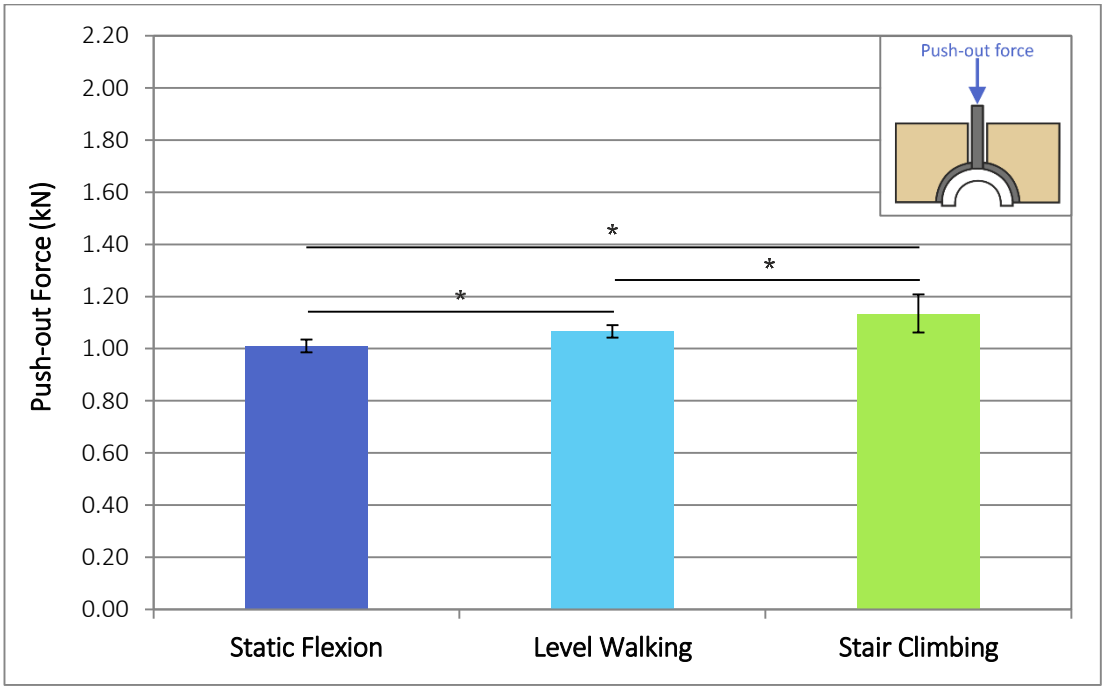

Figure 5.14 – Push-out forces of the Tritanium cup following micromotion tests. Values expressed as mean and standard deviation. *p < 0.05 using Mann-Whitney post hoc test

COMPARING TRIDENT WITH HA COATING TO TRITANIUM

When tested under static flexion, the only significant difference was the Z micromotion which was greater with the Tritanium cup (Table 5.7; Figure 5.15). When subjected to dynamic hip motion simulating level walking, the micromotions of the Tritanium cup in X, θ_X and θ_Y were significantly greater than those of the Trident cup (Figure 5.16). Finally, there were no significant difference in micromotion between both cups when subjected to dynamic hip motion simulating stair climb (Figure 5.17) apart from θ_X which was greater with the Tritanium cup.

There were no significant differences in push-out forces between the two cups following micromotion tests under both static flexion and level walking (Figure 5.18). The push-out force was, however, significantly greater with the Tritanium cup following the micromotion tests under stair climbing condition.

Table 5.7 – Results of the statistical analyses comparing the Trident cup to the Tritanium cup during the different testing conditions as shown in Figures 5.15 to 5.18. The highlighted numbers represent statistical significance ($p < 0.05$)

		X	Y	Z	θ_X	θ_Y	θ_Z	Push-out
Mann-Whitney Test	Static Flexion	0.245	0.071	0.045	0.729	0.606	0.05	0.399
	Level Walking	0.047	0.917	0.11	0.033	0.017	0.339	0.674
	Stair Climbing	0.917	0.754	0.914	0.032	0.083	0.913	0.014

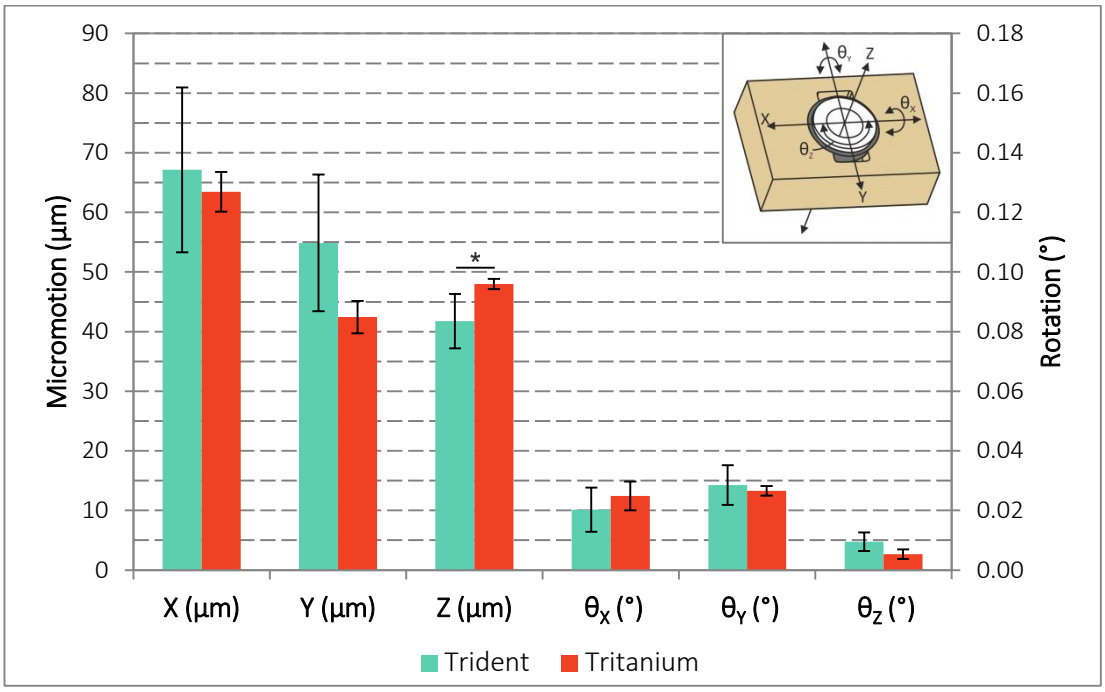

Figure 5.15 – Micromotion in six DoF of both the Trident cup and the Tritanium cup when subjected to static flexion (0.08° corresponds to 40 µm). Values expressed as mean and standard deviation. *$p < 0.05$ using Mann-Whitney post hoc test

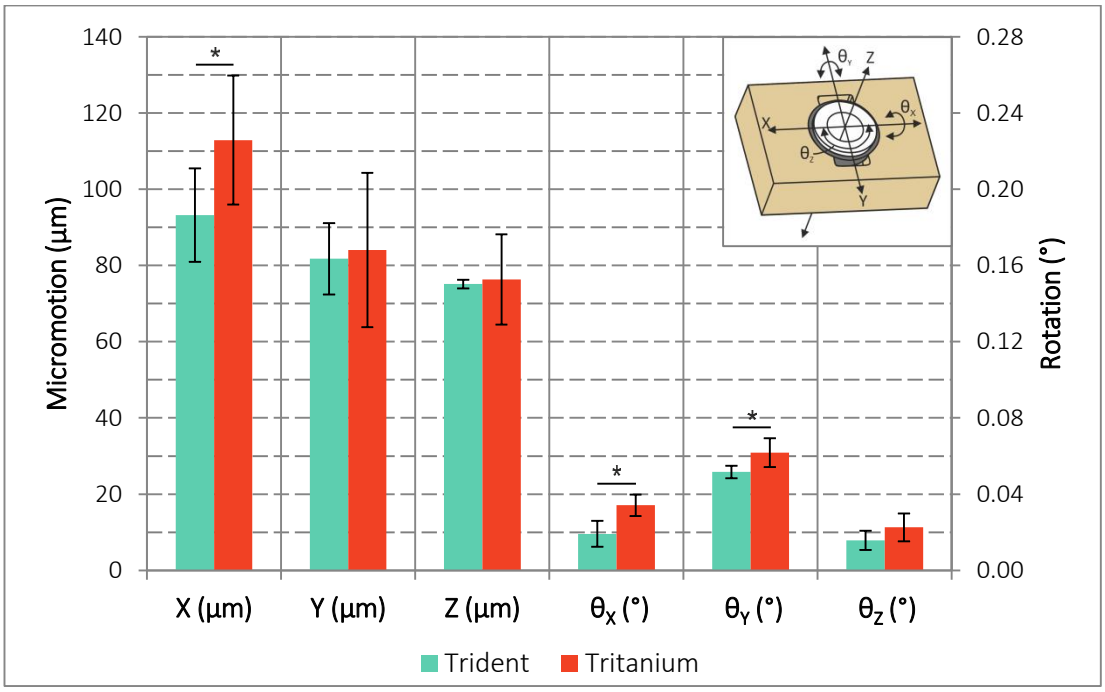

Figure 5.16 – Micromotion in six DoF of both the Trident cup and the Tritanium cup when subjected to level walking (0.08° corresponds to 40 µm). Values expressed as mean and standard deviation. *$p < 0.05$ using Mann-Whitney post hoc test

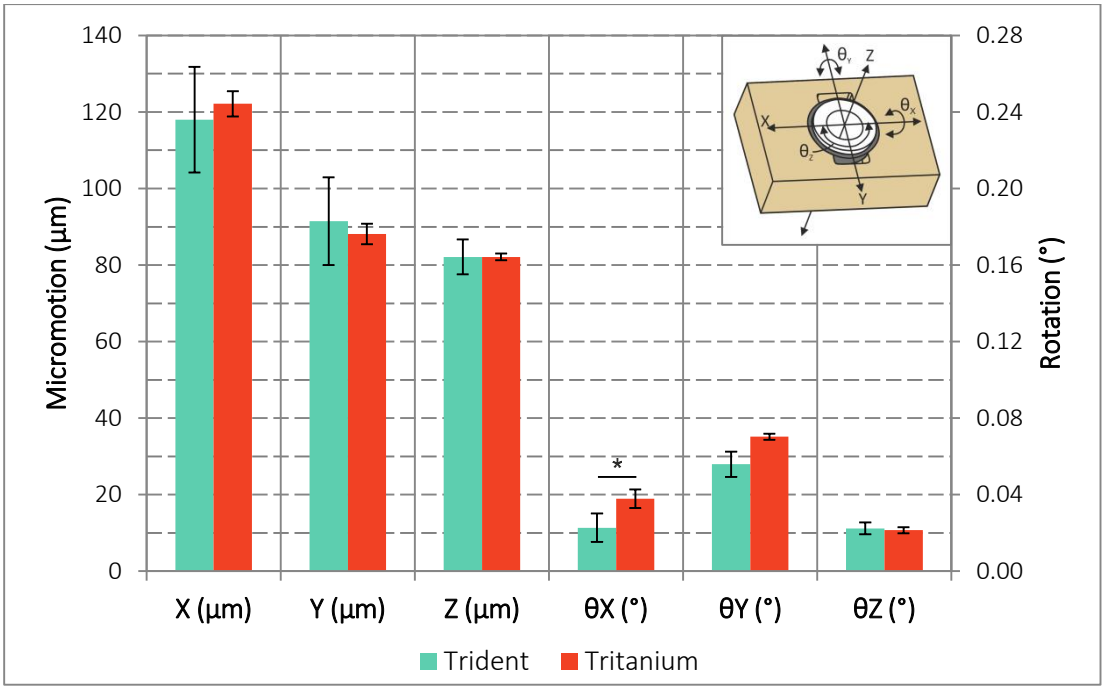

Figure 5.17 – Micromotion in six DoF of both the Trident cup and the Tritanium cup when subjected to stair climbing (0.08° corresponds to 40 µm). Values expressed as mean and standard deviation. *$p < 0.05$ using Mann-Whitney post hoc test

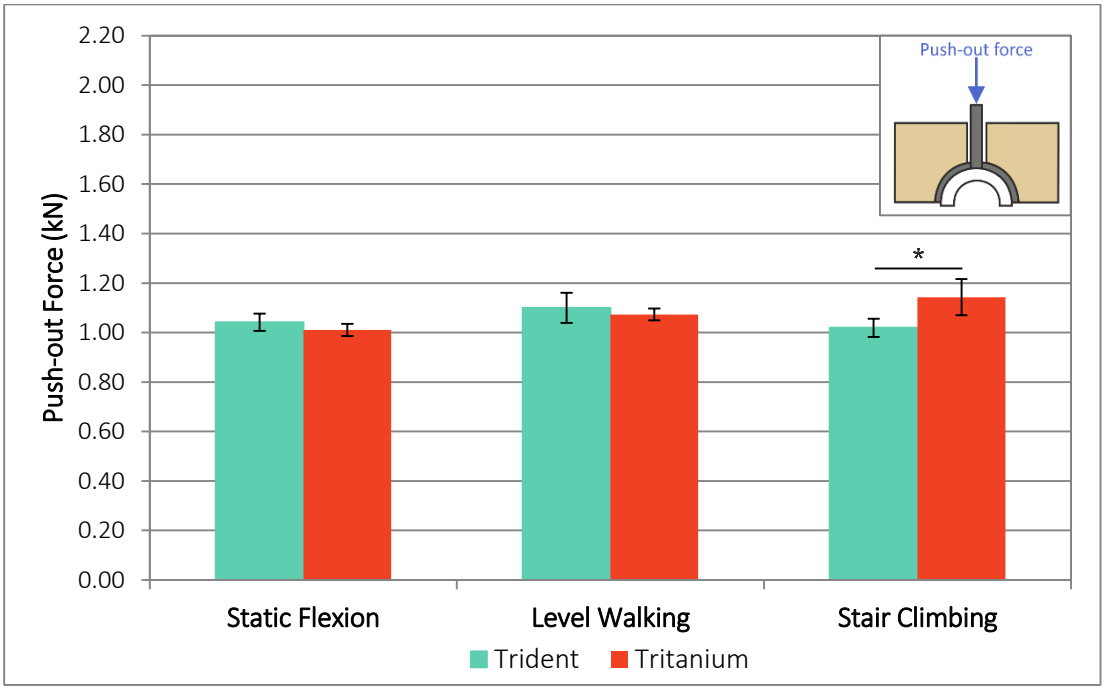

Figure 5.18 – Push-out forces of both the Trident cup and the Tritanium cup following micromotion tests. Values expressed as mean and standard deviation. *$p < 0.05$ using Mann-Whitney post hoc test

5.5. DISCUSSION

There are no studies that have investigated the effect of dynamic hip motion on the stability of press-fit acetabular cups. Two studies have investigated this effect with femoral stems and reported a significant increase in micromotion of the implant under dynamic hip motion [180, 181]. It was therefore hypothesised that dynamic hip motion would also have an effect on the micromotion of acetabular cups.

The dynamic hip motion simulator was designed to replicate the motion of the hip during selected activities of daily living: level walking, stair climbing and rising from a sitting position. Combined with the six DoF measurement system and the physiological acetabular model described in the previous chapter, and set up on the Dartec, this dynamic hip motion simulator allowed the measurement of the micromotion of a press-fit cup under both cyclic loading and hip motion.

The dynamic hip motion simulator only modelled hip flexion-extension, however, as this is the main direction of motion during the selected activities of daily living, it was assumed to be the motion that was most likely to have an effect on cup micromotion. Similar to the loading profile, the flexion-extension profile was modelled as a sinusoidal wave for simplification. The flexion-extension profile of the hip joint closely resembles a sinusoidal wave, and this approximation has been previously used in other studies [180, 181]. The hip was cycled at half the frequency of the load (0.5 Hz) to obtain the double peak load profile of the gait cycle. The load and the hip motion were synchronised to obtain peak load at heel strike and toe-off (Figure 5.1). This had to be done manually as a synchronised automatic start was not possible with the test equipment, which resulted in small variations between the sine waves of the hip motion and the loading cycles. User variability was therefore an inherent problem when manually starting both the load and the motion separately. However, a preliminary study showed that the small errors in timing caused by user variability did not seem to affect the micromotion of the cup (Figures 5.5 and 5.6). Hence, provided that the user is trained correctly, the dynamic hip motion simulator and the Dartec could both be started manually one after the other without compromising the results.

A cup inclination of 45° was included in the dynamic hip motion simulator as it allowed the load to follow a horseshoe-shaped path within the acetabulum under dynamic hip motion. This replicated the path of loading in the natural hip during gait, which follows the horseshoe shape of the lunate cartilage (Figures 2.13 and 5.9).

Some compromises had to be made regarding the activities of daily living assessed. Indeed, rising from a chair could not be modelled because of contact between the Dartec actuator and the dynamic hip motion simulator at high flexion angles. In addition, the maximum hip flexion during stair climb had to be reduced from 45° to 40° due to the impingement between the stem supporting the femoral head and the acetabular liner. The mounting system used for the femoral head did not replicate the neck shaft angle that would be present if a femoral stem had been used, resulting in the observed impingement. However, this new range of motion was still within the published range of motion of the hip during stair climb. Level walking could be performed as specified. Hence, the dynamic hip motion simulator could replicate the

flexion-extension motion of the hip joint during level walking and stair climbing, as well as hold a fixed flexion position to model heel strike. The mounting system used for the femoral head could be replaced with a femoral stem; the correct neck-shaft angle could prevent some of the impingement occurring at high flexion, allowing other activities of daily living to be tested.

Misalignment between the centres of rotation of the hip joint and the dynamic hip motion simulator was inherent in this setup, as the centre of rotation of the hip joint moved during cyclic loading due to the micromotion of the acetabular cup and the deformation of the Sawbones block. The preliminary study investigating this issue demonstrated that the best position for the cup is when both centres of rotation were aligned when the cup was loaded at 1.0 kN. A shim was placed underneath the Sawbones block to raise the acetabular cup (and hence the centre of rotation of the hip joint) to the correct position for the micromotion tests. As the position of the centre of rotation of the hip joint may vary with different factors, such as cup geometry, fixation method, Sawbones block density etc., the location of the centre of rotation of the hip joint when it is loaded to 1.0 kN needs to be identified and aligned with that of the dynamic hip motion simulator using shims underneath the Sawbones blocks prior to any new tests.

Finally, the dynamic hip motion simulator successfully passed an “endurance” scenario test which aimed to determine if it could maintain its frequency and range of motion for 1000 cycles when subjected to 2 kN of load. The hip joint needed to be lubricated as the friction generated between the bearing surfaces when dry was enough to cause a reduction in the range of motion of the dynamic hip motion simulator. The dynamic hip motion simulator also sustained the set frequency and range of motion when tested in combination with cyclic loading.

The second phase of testing described the use of the dynamic hip motion simulator with the six DoF measurement system and the physiological acetabular model to assess the effect of hip motion and two different porous coating on the micromotion of a press-fit acetabular cup. In order to carry this out, the micromotion and push-out force of two press-fit acetabular cups (a Trident cup with HA coating and a Tritanium cup) were assessed under three different conditions: static flexion, level walking and stair climbing. Static flexion, in which the hip joint was kept at 30° flexion throughout the micromotion test, simulated heel strike during level walking. This test condition provided a reference with which to compare the micromotion and push-out forces of the cups when subjected to dynamic hip motions (both level walking and stair climbing). Level walking and stair climbing were chosen as they are both common activities of daily living that patients will undertake relatively soon following surgery, and therefore conditions that the implants must be able to withstand.

As reported in the literature review, the maximum load that the hip joint is subjected to during stair climbing tends to be slightly higher than that of level walking [57, 59, 67, 68]. However, the loading protocol in this study was kept constant for all test conditions to provide a direct interpretation of the differences between stair climbing, level walking and static flexion as a function of the direction in joint reaction force only.

Similarly to the findings in the Chapter 4, significant levels of micromotion were observed in all translations, highlighting the importance of measuring all six DoF and not assuming a dominant direction of motion. Furthermore, the dominant direction of motion assumed in studies published in the literature is usually the translation equivalent to the Z micromotion in this thesis [106, 119, 129, 134, 157, 160, 165]. The results from this study, however, clearly show that the micromotions in X and Y are either similar or significantly greater than in Z during heel strike and in both dynamic hip motions tested (Figures 5.11 and 5.13).

There was a singificant increase in the micromotion of the cup when it was subjected to both level walking and stair climbing compared to static flexion, regardless of the cup tested (Figures 5.11 and 5.13). This observation was also reported in a study investigating the effect of dynamic hip motion on femoral stems [181]. An increase in micromotion of the cup when subjected to dynamic hip motion was expected as the direction of the joint reaction force was no longer static but varied throughout the motion of the hip joint. This change in direction of the joint reaction force can generate toggling motion of the cup, resulting in an increase in cup micromotion in all directions.

The micromotion of the cup also tended to be greater when it was subjected to stair climbing compared to level walking (Figures 5.11 and 5.13). An increase in micromotion with stair climbing compared to level walking was expected. The range of motion was increased within the same time period for stair climbing compared to level walking (frequency kept at 0.5 Hz, but range of motion increased by 5°). This resulted in a greater and faster change in the direction of the joint reaction force during every motion cycle, and hence, in an increase in cup micromotion. The Trident cup was more affected by the increase in range of motion seen between level walking and stair climbing compared to the Tritanium cup. Indeed, the increase in cup micromotion was significant in both X and Z micromotions with the Trident cup, which were both above 40 µm. On the other hand, only the θ_Y rotation, which were below 40 µm, was significantly greater with the Tritanium cup. As there were no significant increase in micromotion between level walking and stair climbing amongst the clinically relevant motions (X, Y, and Z) with the Tritanium cup, it can be hypothesised that changes in range of hip motion had little effect on the stability of this cup.

There were no significant difference, nor any visible trend, in the push-out force of the Trident cup with the different test conditions (Figure 5.12). This indicates that the dynamic hip motion had no effect on the force required to remove the Trident cup from its acetabular cavity. On the other hand, there was a significant increase in push-out force as the range of motion increased with the Tritanium cup (Figure 5.14). A possible explanation for this is that the dynamic hip motion helped to seat the Tritanium cup deeper within the acetabular cavity, resulting in an increase in push-out force. This increase in push-out force suggests that the Tritanium cup was more stable during stair climbing and level walking than static flexion; this is in contradiction to the micromotion results, which suggested the opposite. Hence, push-out or pull-out test may not correctly predict cup stability. Finally, it is important to note that the differences in push-out force between the different test conditions with the Tritanium cup were below 0.1 kN. Hence, it can be argued that, even though there were significant differences in push-out forces between each conditions, these differences may not have any clinical significance.

Another aim of this study was to assess a new acetabular component: the Tritanium cup, by comparing it to its clinically successful predecessor: the Trident cup with HA coating. Only a few significant differences in both micromotion and push-out force were observed between the Trident cup and the Tritanium cup. The Tritanium cup exhibited significantly higher levels of micromotion in Z during static flexion (Figure 5.15); in X, θ_X and θ_Y during level walking (Figure 5.16); and in θ_X during stair climbing (Figure 5.17). Most of these significant differences were below 40 μm, which would have no detrimental effect on cup osseointegration. Furthermore, when assessing push-out forces, the only significant difference observed was an increase in push-out force with the Tritanium cup compared to the Trident cup following stair climbing (Figure 5.18). However, the difference was below 0.1 kN and therefore its clinical significance can be questioned. Hence, the lack of any major differences in results between both cups suggests that the new Tritanium cup exhibits a similar level of stability as the Trident cup.

As discussed in Chapter 2, osseointegration relies on three important prerequisites: good bony apposition, initial stability and an appropriate surface coating. Considering the clinical success of the Trident cup with HA coating, it can be considered that this cup fulfils these three prerequisites when implanted correctly. The Trident cup and the Tritanium cup have the same geometry. Hence, if both cups were to be implanted the same way in the same acetabulum, it can be assumed that both cups would have a similar engagement within the acetabulum and that the contact area between both cups and the bone would be the same. Furthermore, the results from this study suggested that the Tritanium cup was as stable as the Trident cup under similar testing conditions. Hence, the Tritanium cup successfully fulfils two of the three prerequisites for osseointegration: good bony apposition and initial stability. The Tritanium cup is covered with a three dimensional titanium matrix designed to resemble trabecular bone structure. This new coating aims to enhance osseointegration by allowing better bone ingrowth within the shell of the acetabular component [194] compared to the Trident cup. Hence, by matching the Trident cup in two of the three prerequisites for osseointegration, and surpassing it in the third prerequisite, the Tritanium cup should be more likely to promote osseointegration, and therefore further improve on the clinical success of the Trident cup. Good clinical results have been reported in a short-term (3 years) follow up of the Tritanium cup [195], however, long-term follow-up is still required to assess the clinical success of this new porous coating.

5.6. CONCLUSIONS

A dynamic hip motion simulator was designed and built. This simulator replicated flexion-extension cycles of the hip joint to simulate two different activities of daily living: level walking and stair climbing. The dynamic hip motion simulator was designed to run at 0.5 Hz while the loading frequency was kept at 1 Hz in order to obtain the double peak load profile as seen in the natural hip joint. A servo motor was used to drive the dynamic hip motion simulator. The position input was provided by a function generator and its amplitude and the DC offset were used to set the angles between which the dynamic hip motion simulator oscillated.

Preliminary tests were performed to ensure that the dynamic hip motion simulator functioned correctly. Friction of the hip joint under load resulted in a decreased range of motion of the dynamic hip motion simulator; this problem was fixed by lubricating the hip joint with multipurpose grease. The centres of rotation of the hip joint and the dynamic hip motion simulator needed to be aligned; this was challenging as the location of the centre of rotation of the hip joint moved as the cup was subjected to cyclic loading. Hence a compromise had to be made, where the centres of rotations were aligned when the cup was loaded at 1 kN. Finally, synchronising the load and motion cycles was not possible; however, repeated testing of manually starting the dynamic hip motion simulator and then the Dartec showed only small variations in the micromotion of the cup; therefore it was assumed that the micromotion of the cup was not affected by user variability.

The novel pre-clinical testing methodology developed was used to investigate the effect of dynamic hip motion on cup micromotion and to assess a new acetabular component by comparing it to its clinically proven predecessor. The results of this study revealed an increase in micromotion when the cup was subjected to dynamic hip motions compared to static flexion, and clinically relevant levels of micromotion in all translation. These observations highlighted the need to measure the micromotion in six DoF and under dynamic hip motion when assessing cup stability. Finally, the results indicated that the Tritanium cup was as stable as the Trident cup with HA coating. Considering its new coating was designed to favour bone ingrowth, and hence improve osseointegration, the Tritanium cup should be more successful than its predecessor.

6. FINAL DISCUSSION

The assessment of the different aspects of the test rig and test protocol, along with the results from the studies performed in this thesis has been provided in the previous chapters. This chapter therefore concentrates on how the results obtained in this thesis compare to those reported in the literature.

There are two types of study in the literature that investigate cup stability: load-to-failure tests and micromotion studies. Load-to-failure tests are extremely popular when assessing cup stability as they are relatively straightforward and use readily available equipment. The most commonly used ones are the torque test and the edge loading test. Both of these tests assess the ability of the acetabular cup to withstand rotations: θ_X for the torque test and either θ_Y or θ_Z for the edge loading test, depending on where the load is applied along the rim of the cup. The results presented in this thesis show that rotations of the cup are significantly lower than translations, regardless of the test condition. Hence, the stability of acetabular cups is grossly overestimated if only these tests are used. However, they should still be performed during pre-clinical assessment of new acetabular cups as they can indicate if the cup fixation can withstand extreme one-off events, such as those that occur in stumbling and hip dislocation.

Micromotion studies aim to assess the stability of acetabular cups under daily living activities. One of their main limitations is that they do not accurately measure the micromotion of the cup in all six DoF. Instead, a dominant direction of motion is assumed, typically the translation normal to the face of the cup, which is the equivalent to the Z micromotion in this thesis [106, 119, 129, 134, 157, 160, 165]. Hence, only the micromotion in this assumed dominant direction of motion is measured and reported. The results obtained in this thesis clearly show significant levels of micromotion in all translations. Furthermore, the data obtained during simulated heel strike, level walking and stair climbing showed similar or significantly greater levels of micromotion in X and Y compared to Z. This demonstrates that there are significant levels of micromotion in more than one direction of motion, and that the assumed dominant direction of micromotion is not necessarily the actual dominant direction of motion. This highlights the importance of considering all six DoF when investigating cup micromotion.

Clinically relevant levels of micromotion (above 40 µm) were mostly observed in translations in this thesis. However, this should not be taken as an indication to only measure translations and ignore rotations when investigating acetabular cup micromotion. Indeed, there are many factors that could cause an increase in rotations. Bone density is one of them: rotations above 0.08° (which was equivalent to 40 µm in this thesis) have been reported in θ_X in the SLS study with the low density Sawbones blocks. Other factors include: acetabular defects, different implant designs and fixation features, or some activities of daily living such as rising from a chair. Furthermore, only flexion-extension was modelled in this study to assess the effect of dynamic hip motion on cup micromotion. The motion of the hip during activities of daily living also includes ab-adductions, and internal and external rotations, which could increase cup rotations to clinically relevant levels. Hence, if other daily living activities or hip motions are assessed, it is recommended that measurement of the micromotion of the cup in all six DoF must be considered.

Comparing the micromotions obtained in this study with those in the literature is complicated as there are a limited number of studies reported and each have specific testing methods and measurement philosophies. Hence, all the studies assessing micromotion of press-fit cups without additional fixation (pegs, fins, screws…) were considered. The main differences in testing protocols that could affect cup micromotion were: level of press-fit; loading protocol and peak load; acetabular model; and orientation of the hip (Table 6.1). The micromotions reported in these studies were compared to those obtained in this thesis using the high density Sawbones block with the physiological acetabular model; this included the results in SLS and those in heel strike for both the Trident cup with HA coating and the Tritanium cup. Furthermore, in order to limit the effect of load, the micromotions from each study were normalised to the applied load prior to comparison (Figure 6.1).

Table 6.1 – Differences in test protocol in micromotion studies using of press-fit cups

Study	Press-fit	Acetabular model	Loading protocol	Peak load	Hip / Cup Orientation
Stiehl *et al.* [134]	1 mm	Embalmed	Cyclic	1.0 kN	Full extension
Perona *et al.* [129]	2 mm	Fresh-frozen	Ramp	2.4 kN	Anatomical position
Kwong *et al.* [165]	1 mm	Embalmed	Ramp	1.1 kN	Single leg stance
Won *et al.* [106]	1 mm	Fresh-frozen	Cyclic	1.5 kN	30° inclination & 20° anteversion
Pitto *et al.* [160]	2 mm	Sawbones Hemipelvis	Cyclic	2.4 kN	60° to horizontal
von Schulze-Pellengahr *et al.* [157]	Not specified	Macerated	Cyclic	3.8 kN	61° to vertical
Present Study	1 mm	Physiological Sawbones Block	Cyclic	2.0 kN	Single leg stance & heel strike

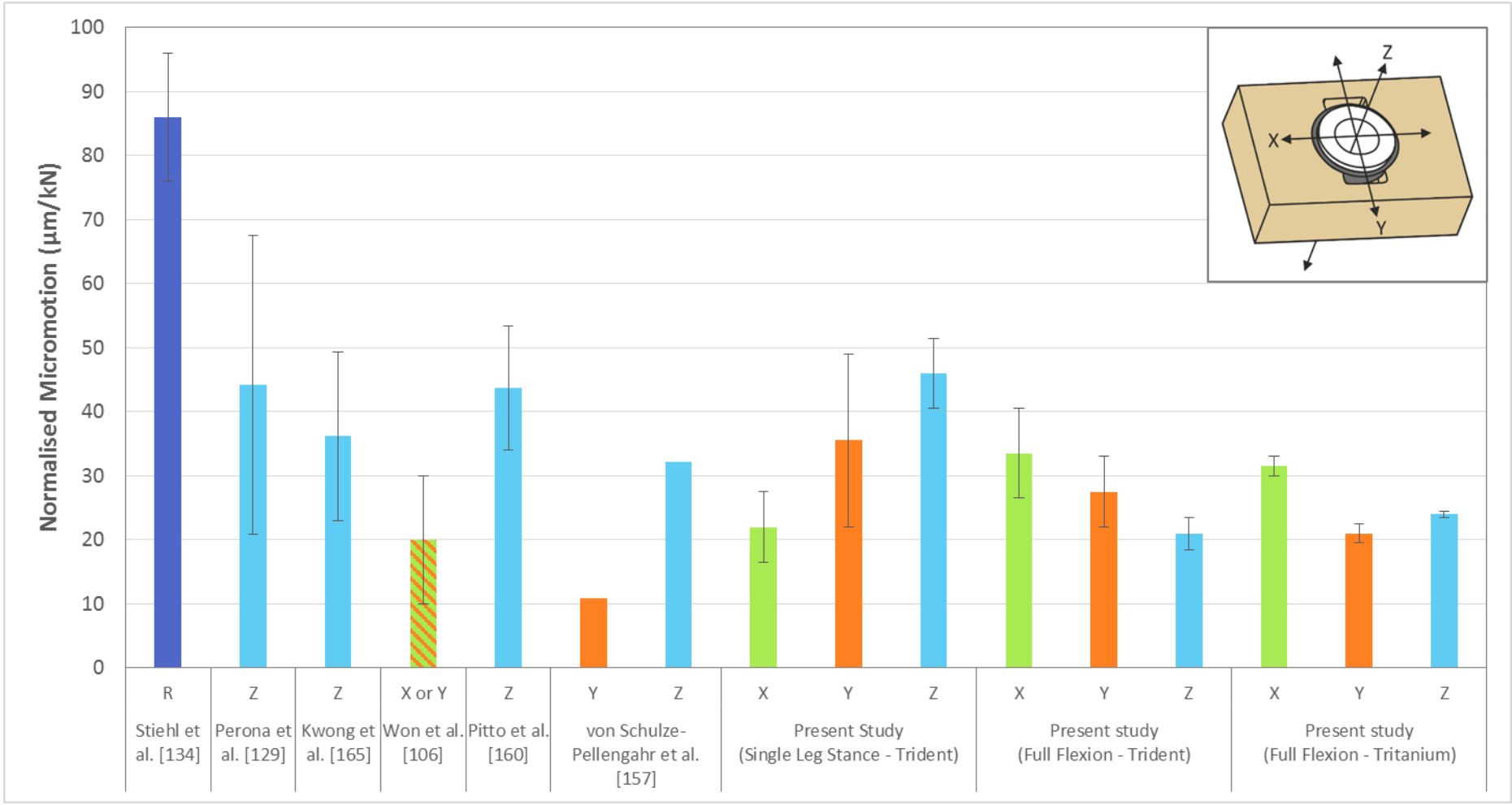

Figure 6.1 – Comparing the micromotions measured during SLS and heel strike in this thesis to studies in the literature (micromotions expressed in terms of mean and standard deviation; bars colour-coded to the direction of motion; R = resultant force)

The micromotions reported in this thesis were similar to those in the literature (Figure 6.1). The only exception to this was the micromotion reported by Stiehl *et al.* [134] which was greater than both the micromotions reported in this thesis and in other studies from the literature. This is because this study reported the micromotion as a resultant of the three translations, which was therefore greater than each individual one.

The Z micromotions reported in this thesis were similar to those reported in the literature, while the X and Y micromotions reported in this thesis tended to be greater than those reported in the literature, especially under heel strike. An explanation for this is the variation in hip orientation between the different studies as the direction in which the cup is loaded dictates the direction in which it will move. This was also the reason for the change in pattern in micromotions observed in this study between SLS and heel strike, where the Z micromotion went from being the largest of the three translations, to the lowest.

Most of the studies selected used cadaveric pelvic bones, either embalmed or fresh-frozen; the only exception was the study by Pitto *et al.* [160] which used composite hemipelvises from Sawbones. The similarity in micromotion between those measured in this study and those published in the literature emphasises the appropriateness of the Sawbones block with the physiological cavity as an acetabular model. Furthermore, the standard deviations were smaller in this thesis compared to those reported in the literature. This reduction in variability in results can be partially attributed to the lower interspecimen variability of the Sawbones blocks compared to that of cadaveric bones. This demonstrates one of the many advantages of using the Sawbones blocks rather than cadaveric bones for pre-clinical tests.

Finally, the push-out method used to remove the acetabular cup from the Sawbones blocks was similar to the pull-out method used by Antoniades *et al.* [155], in which the pull-out force was measured using the Trident cup and foam blocks with hemispherical cavities of similar densities to the high and low density blocks used in the SLS study in Chapter 4 (densities: 0.45 and 0.22 g/cm^3). The mean pull-out force (1.55 kN) was similar to the mean push-out force (1.63 kN; Figure 4.31) with the 1 mm press-fit component implanted into the high density foam blocks. Furthermore, the range of push-out force measured in the SLS study was within the range of the published pull-out force. On the other hand, the mean pull-out force was higher (0.67 kN) than the mean push-out force (0.43 kN) with the low density foam blocks; this was because the cup was inserted with a 2 mm press-fit rather than a 1 mm press-fit.

7. CONCLUSIONS

THR is a successful orthopaedic procedure that aims to relieve pain and restore the natural function of the hip joint, allowing patients to return to their normal lifestyle. Aseptic loosening is the most common mode of failure of THR, accounting for over 50% of all revision surgeries. The acetabular component is particularly affected by aseptic loosening, and, as such, has a higher revision rate compared to femoral stems.

There are many factors that can contribute to aseptic loosening, an important one being initial stability of cementless acetabular components. The long-term survival of cementless cups relies on osseointegration of the implant with the host bone. However, osseointegration is progressive and takes time to occur; in the meantime, the cementless cup must rely on mechanical fixation. The cyclic loading and motion that the hip is subjected to during activities of daily living can induce micromotion of the cup within the acetabulum. High levels of micromotion can inhibit bone formation, and hence osseointegration, of cementless implants. Therefore, initial stability is crucial for the long-term survival of cementless acetabular components.

Even though a clear link between initial stability and successful osseointegration has been identified, there are no standardised pre-clinical protocols to assess the micromotion of cementless cups. There are, however, a number of methods described in the literature. A review of the literature highlighted the need for a new pre-clinical test protocol capable of measuring the micromotion of cementless acetabular cups under both physiological loading and dynamic hip motion.

The aim of this thesis was to better understand the behaviour of the cup once implanted and to provide a method capable of identifying new design features that can improve cup fixation, and therefore its longevity. This aim was achieved through the completion of four key objectives:

- The development of a measurement system capable of measuring the micromotion in six DoF of a press-fit cup subjected to cyclic loading, and its accompanying testing protocol.
- The creation of a synthetic acetabular model replicating the important structural features of the acetabulum.
- The design of a dynamic hip motion simulator to model the flexion-extension motion of the hip joint during common activities of daily living to assess the effect of dynamic hip motion on the micromotion of the cup.
- The assessment of the test protocol encompassing the first three objectives by investigating the effect of a new porous coating on the micromotion of the cup, compared to a clinically proven and commonly used one.

The first objective of this study was to develop a method to measure the micromotion of a press-fit acetabular cup in six DoF when subjected to cyclic loading. This was achieved by adapting a six DoF measurement system which had been previously used to measure the micromotion of femoral stems. This six DoF measurement system was used to determine the micromotion of press-fit cups in six DoF from a single reference point. This removes the need

for rigid body assumptions that are commonly made in other studies where the micromotion of the cup is measured at different locations along the rim of the cup.

Alongside the measurement system, a test protocol was devised to systematically assess the micromotion of press-fit cups. This comprised a cup insertion method, a loading protocol for the micromotion test, and a cup extraction method. Standardised protocols were created for each of these steps to obtain a repeatable and consistent method to measure cup micromotion, and remove any user variability that may affect the results.

The micromotions of a press-fit cup (Trident with HA coating) positioned in SLS, and its push-out force, were measured to compare the more physiologically representative model (physiological) to the commonly used hemispherical cavity. The results showed an increase in micromotion and a decrease in push-out force with the physiological model compared to the hemispherical one, regardless of Sawbones block density. Hence, assuming that the physiological model more closely replicated the environment in which the cup is implanted, it can be concluded that modelling the acetabulum as a hemispherical cavity overestimates the stability of the cup.

For the second objective, each acetabular cavity was manufactured in Sawbones blocks of both high and low density; hence the effect of density on cup stability was also investigated under SLS conditions. A significant increase in cup micromotion and a significant decrease in push-out force were observed with the low density Sawbones blocks compared to the high density ones, regardless of the acetabular model used. This was also observed in other studies investigating the effect of bone density on cup stability. Furthermore, some of the micromotions were above the 150 μm threshold in which osseointegration no longer occurs. This finding suggests that acetabular cups implanted into weaker, i.e. osteoporotic, bone cannot rely solely on press-fit and therefore either require additional fixation, such as trabecular bone screws, or should be replaced with cemented cups.

The third objective of this thesis was to develop a dynamic hip motion simulator to assess the effect of hip flexion-extension on cup micromotion. There are no studies that have investigated this effect on cup micromotion; however, a number have investigated the effect of hip motion on the micromotion of the femoral stem. These studies have reported a significant increase in micromotion under dynamic hip motion, and therefore the same influence could be expected for the acetabular cup.

The developed dynamic hip motion simulator was used in combination with the six DoF measurement system and the physiological acetabular model to assess the effect of dynamic hip motion on cup micromotion. Three different test conditions were simulated: static flexion, in which the hip joint was held at a fixed flexed position simulating heel strike throughout testing, level walking and stair climbing. The study was performed using two different acetabular components: the Trident cup with HA coating and the Tritanium cup. A significant increase in cup micromotion was recorded for both cups when they were subjected to both dynamic hip motions (level walking and stair climbing) compared to static flexion. In addition, the Trident cup had significantly higher levels of micromotion with stair climbing compared to

level walking. The results from this study highlight the importance of including dynamic hip motion when assessing cup micromotion.

The results presented in this thesis show significant levels of micromotion in translations, regardless of the test conditions. This highlights the importance of measuring the micromotions of acetabular cups in all directions of motion and not only in an assumed dominant direction of motion, as is commonly measured and reported in the literature. Furthermore, the results obtained with the dynamic hip simulator show that the dominant direction of motion commonly assumed in the literature (equivalent to the Z translation in this thesis) is not the actual dominant direction of motion. This results in an underestimation of the micromotion of the cup, and hence an overestimation of its stability.

The final objective of this thesis was to determine if the test protocol developed in this thesis was capable of identifying a new design feature that could improve cup fixation. This was achieved by comparing the micromotion of a press-fit cup with a new porous coating (the Tritanium cup) to that of a clinically proven and commonly used press-fit cup (the Trident cup with HA coating). The Trident cup with HA coating is the second most widely used cementless acetabular cup in England and Wales and has had good clinical results. The Tritanium cup is a Trident cup with a new porous coating designed to improve osseointegration by replicating the structure of the trabecular bone with a three dimensional titanium matrix. The system was capable of identifying small but significant difference in micromotion between the two cups. However, the results showed no major difference in micromotion and push-out forces between the two cups. Hence, with similar levels of micromotion and a porous coating designed to improve osseointegration, one can predict that the Tritanium cup should perform as well, if not better, than the Trident cup with HA coating.

In conclusion:

- The design of a pre-clinical test protocol to assess cup micromotion in all six DoF under both cyclic loading and hip motion has been achieved.
- The acetabular model used in this study better replicates the structural properties of the acetabulum and results of the micromotion studies in this thesis using this model are comparable to those in studies using cadaveric pelvic bones.
- In vitro studies investigating cup micromotion should incorporate dynamic hip motion and measure all six DoF as the results showed an increase in micromotion under dynamic hip motion and clinically relevant micromotions in all translations.
- Comparison of the new Tritanium cup with the clinically proven Trident cup with HA coating suggested similar stability between the two cups.
- The new protocol presented in this thesis provides the basis for a more representative protocol for future pre-clinical evaluations of new and different cup designs.

8. FURTHER WORK

8.1. SIMULATOR DEVELOPMENTS

There are a few issues that could be addressed to further strengthen the pre-clinical testing protocol developed in this thesis. Firstly, a femoral stem should be fitted to the Dartec actuator, introducing the femoral neck angle between the stem and the head. By doing so, more activities of daily living could be modelled and tested using the dynamic hip simulator as it would remove the impingement seen during high flexion with the current setup. However, the inclination of the cup and the loading will need to be modified accordingly.

Secondly, there are a couple of control related features with the dynamic motion hip simulator and the Dartec. Firstly, manually synchronising the load and the motion is prone to errors and a method of automatically synchronising the load and motion needs to be developed. Secondly, the frequency of the sine wave generated by the current sine wave generator is not accurate and tends to fluctuate throughout the day and sometimes throughout a test. Even though this fluctuation is small, it can result in significant wave shifts, affecting the synchronisation of the load and motions over the course of a test. A more accurate sine wave generator should therefore be implemented.

With these improvements, the protocol presented in this thesis could be reliably used as a pre-clinical tool for comparison purposes as presented in Chapter 5. However, three extra improvements could also be added to recreate more realistic conditions to assess cup micromotion. The first is the incorporation of both internal and external rotations, and abduction and adduction movements to the dynamic hip motion simulator; this would provide more realistic hip motions and the opportunity to model other activities of daily living in which these movements are dominant. Secondly, the loading pattern could be modified to better resemble that seen in the natural hip joint (Figure 2.12). Finally, a more sophisticated acetabular model could be developed. The current model does not incorporate the different types of bone present in and around the acetabulum, such as the cortical and the subchondral bone. The asymmetric rim profile of the acetabulum could also be modelled.

8.2. FURTHER INVESTIGATIONS

With this novel pre-clinical testing protocol, different factors that may affect acetabular cup fixation and stability can be assessed. These include different cup designs and geometries, different types of cup fixation, different femoral head sizes, surgical techniques, such as reaming and cup positioning, and the presence of acetabular defects or soft tissue at the bone-implant interface.

A cadaveric study should be performed to validate the use of the physiological acetabular model developed in Chapter 4. The physiological model used in this thesis was similar to one reported in the literature, which was validated using cadaveric pelvic bones when assessing acetabular shell deformation. Furthermore, the levels of micromotion of the cup implanted into the physiological acetabular model obtained in this thesis were similar to those published in the literature when the cup was implanted into cadaveric pelvic bones. Both these suggest that the physiological acetabular model is an appropriate model of the acetabulum. However, a cadaveric study should be performed to confirm this by comparing the levels of micromotion of the cup when implanted into the physiological acetabular model and into a cadaveric pelvis under the same testing conditions.

Furthermore, although measuring the global micromotion of an acetabular cup is very useful in understanding its behaviour when implanted in the body, the complete knowledge of the behaviour at the bone-implant interface would also be very beneficial. Full computational models and finite element analysis could be used in combination with the test protocol presented in this thesis to provide a full understanding of the behaviour of the cup when implanted in the human body.

REFERENCES

1. Cotogno, G. and Holzwarth, U., 2012. *Total hip arthroplasty*. Luxembourg: Publications Office of the European Union.

2. Australian Orthopaedic Association National Joint Replacement Registry, 2014, *Annual report*.

3. Swedish Hip Arthroplasty Register, 2013, *Annual report*.

4. National Joint Registry of England and Wales, 2014, *11th annual report*.

5. Canadian Joint Replacement Registry, 2013, *Annual report*.

6. Kurtz, S., Ong, K., Lau, E., Mowat, F. and Halpern, M., 2007. Projections of primary and revision hip and knee arthroplasty in the United States from 2005 to 2030. *J. Bone Joint Surg. Am.*, 89 (4), pp.780-785.

7. Morrey, B.F., 2003. *Joint replacement arthroplasty*. 3rd ed. Edinburgh: Churchill Livingstone.

8. Mulroy Jr, R.D. and Harris, W.H., 1990. The effect of improved cementing techniques on component loosening in total hip replacement. An 11-year radiographic review. *J. Bone Joint Surg. Br.*, 72 (5), pp.757-760.

9. Garcia-Cimbrelo, E. and Munuera, L., 1992. Early and late loosening of the acetabular cup after low-friction arthroplasty. *J. Bone Joint Surg. Am.*, 74 (8), pp.1119-1129.

10. Pilliar, R.M., Lee, J.M. and Maniatopoulos, C., 1986. Observations on the effect of movement on bone ingrowth into porous-surfaced implants. *Clin. Orthop. Relat. Res.*, 208, pp.108-113.

11. Gray, H., Standring, S., Ellis, H. and Berkovitz, B.K.B., 2005. *Gray's anatomy: the anatomical basis of clinical practice*. 39th ed. Edinburgh: Elsevier Churchill Livingstone.

12. Taylor, T. *Hip Joint* [online]. Available from: http://www.innerbody.com/image/skel15.html#full-description [Accessed 6 October 2014].

13. Nordin, M. and Frankel, V.H., 2001. *Basic biomechanics of the musculoskeletal system*. Lippincott Williams & Wilkins.

14. Bonneau, N., Bouhallier, J., Baylac, M., Tardieu, C. and Gagey, O., 2012. Study of the three-dimensional orientation of the labrum: its relations with the osseous acetabular rim. *J. Anat.*, 220 (5), pp.504-513.

15. Farlex. [online]. Available from: http://encyclopedia.thefreedictionary.com/ [Accessed 31 Octobre 2011].

16. Afoke, N., Byers, P. and Hutton, W., 1980. The incongruous hip joint. A casting study. *J. Bone Joint Surg. Br.*, 62-B (4), pp.511-514.

17. Krebs, V., Incavo, S.J. and Shields, W., 2009. The anatomy of the acetabulum: what is normal? *Clin. Orthop. Relat. Res.*, 467 (4), pp.868-875.

18. Goodfellow, J. and Mitsou, A., 1977. Joint surface incongruity and its maintenance: an experimental study. *J. Bone Joint Surg. Br.*, 59-B (4), pp.446-451.

19. Lazennec, J.Y., Laudet, C.G., Guérin-Surville, H., Roy-Camille, R. and Saillant, G., 1997. Dynamic anatomy of the acetabulum: an experimental approach and surgical implications. *Surg. Radiol. Anat.*, 19 (1), pp.23-30.

20. Massin, P., Vandenbussche, E. and Landjerit, B., 1994. Etude expérimentale des déformations du cotyle en charge monopodale [Experimental study of the acetabular wall deformations in unipodal stance]. *Acta Orthop. Belg.*, 60, pp.359-368.

21. Vandenbussche, E., Massin, P., Augereau, B. and Lavaste, F., 1999. Etude cadaverique de la mobilité des cornes acétabulaires de la hanche saine et prothésée par simulation d'appui monopode [Cadaver study of acetabular cup mobility in the healthy hip and prosthesis by monopodal pressure simulation]. *Rev. Chir. Orthop. Reparatrice Appar. Mot.*, 85 (2), pp.136-145.

22. Teinturier, P., Terver, S., Jaramillo, C.V. and Besse, J.P., 1984. La biomécanique du cotyle [Biomechanics of the acetabulum]. *Rev. Chir. Orthop. Reparatrice Appar. Mot.*, 70, pp.41-46.

23. Maruyama, M., Feinberg, J.R., Capello, W.N. and D'Antonio, J.A., 2001. Morphologic features of the acetabulum and femur: anteversion angle and implant positioning. *Clin. Orthop. Relat. Res.*, 393, pp.52-65.

24. Vandenbussche, E., Saffarini, M., Taillieu, F. and Mutschler, C., 2008. The asymmetric profile of the acetabulum. *Clin. Orthop. Relat. Res.*, 466 (2), pp.417-423.

25. Gillard, F.C., Dickinson, A.S., Schneider, U., Taylor, A.C. and Browne, M., 2013. Multi-pelvis characterisation of articular cartilage geometry. *Proc. Inst. Mech. Eng. H*, 227 (12), pp.1255-1264.

26. Govsa, F., Ozer, M.A. and Ozgur, Z., 2005. Morphologic features of the acetabulum. *Arch. Orthop. Trauma Surg.*, 125 (7), pp.453-461.

27. Byers, P.D., Contepomi, C.A. and Farkas, T.A., 1970. A post mortem study of the hip joint. Including the prevalence of the features of the right side. *Ann. Rheum. Dis.*, 29 (1), pp.15-31.

28. Vandenbussche, E., Saffarini, M., Deloge, N., Moctezuma, J.-L. and Nogler, M., 2007. Hemispheric cups do not reproduce acetabular rim morphology. *Acta Orthop.*, 78 (3), pp.327-332.

29. Köhnlein, W., Ganz, R., Impellizzeri, F.M. and Leunig, M., 2009. Acetabular morphology: implications for joint-preserving surgery. *Clin. Orthop. Relat. Res.*, 467 (3), pp.682-691.

30. Tillmann, B., 1969. Die Beanspruchung des menschlichen Hüftgelenks [The Stress of the Human Hip Joint]. *Z. Anat. Entwicklungsgesch*, 128 (4), pp.329-349.

31. Dalstra, M. and Huiskes, R., 1995. Load transfer across the pelvic bone. *J. Biomech.*, 28 (6), pp.715-724.

32. Jacob, H.A.C., Huggler, A.H., Dietschi, C. and Schreiber, A., 1976. Mechanical function of subchondral bone as experimentally determined on the acetabulum of the human pelvis. *J. Biomech.*, 9 (10), pp.625-627.

33. Fabeck, L., Descamps, P., Bourgois, R. and Dhem, A., 1994. Contribution a l'étude des contraintes du bassin en charge. Rôle de la branche pubienne et de l'os spongieux [Deformation of the acetabulum during weight-bearing. Influence of the pubic ramus and the quality of trabecular bone]. *Rev. Chir. Orthop. Reparatrice Appar. Mot.*, 80 (3), pp.181-187.

34. Vasu, R., Carter, D.R. and Harris, W.H., 1982. Stress distributions in the acetabular region - I. Before and after total joint replacement. *J. Biomech.*, 15 (3), pp.155-164.

35. Dalstra, M., Huiskes, R., Odgaard, A. and van Erning, L., 1993. Mechanical and textural properties of pelvic trabecular bone. *J. Biomech.*, 26 (4–5), pp.523-535.

36. Cowin, S.C., 2001. *Bone mechanics handbook*. 2nd ed. Boca Raton, FL: CRC Press.

37. Helgason, B., Perilli, E., Schileo, E., Taddei, F., Brynjólfsson, S. and Viceconti, M., 2008. Mathematical relationships between bone density and mechanical properties: a literature review. *Clin. Biomech.*, 23 (2), pp.135-146.

38. Mow, V.C., Ratcliffe, A. and Woo, S.L.Y., 1990. *Biomechanics of diarthrodial joints*. Springer-Verlag.

39. Anderson, A.E., Peters, C.L., Tuttle, B.D. and Weiss, J.A., 2005. Subject-specific finite element model of the pelvis: development, validation and sensitivity studies. *J. Biomech. Eng.*, 127 (3), pp.364-373.

40. Dorr, L.D., Bechtol, C.O., Watkins, R.G. and Wan, Z., 2000. Radiographic anatomic structure of the arthritic acetabulum and its influence on total hip arthroplasty. *J. Arthroplasty*, 15 (7), pp.890-900.

41. Pedersen, D.R., Crowninshield, R.D., Brand, R.A. and Johnston, R.C., 1982. An axisymmetric model of acetabular components in total hip arthroplasty. *J. Biomech.*, 15 (4), pp.305-315.

42. Tang, J. and Richardson, M.L. *The column principle* [online]. Available from: http://uwmsk.org/acetabularfx/column.html [Accessed 24 November 2011].

43. Hageman, P.A. and Blanke, D.J., 1986. Comparison of gait of young women and elderly women. *Phys. Ther.*, 66 (9), pp.1382-1387.

44. Öberg, T., Karsznia, A. and Öberg, K., 1993. Basic gait parameters: reference data for normal subjects, 10-79 years of age. *J. Rehabil. Res. Dev.*, 30, pp.210-210.

45. Murray, M.P., Kory, R.C. and Clarkson, B.H., 1969. Walking patterns in healthy old men. *J. Gerontol.*, 24 (2), pp.169-178.

46. Kerrigan, D.C., Lee, L.W., Collins, J.J., Riley, P.O. and Lipsitz, L.A., 2001. Reduced hip extension during walking: healthy elderly and fallers versus young adults. *Arch. Phys. Med. Rehabil.*, 82 (1), pp.26-30.

47. Stewart, T.D. and Hall, R.M., 2006. (iv) Basic biomechanics of human joints: hips, knees and the spine. *Curr. Orthop.*, 20 (1), pp.23-31.

48. Konttinen, Y.T., Zhao, D., Beklen, A., Ma, G., Takagi, M., Kivelä-Rajamäki, M., Ashammakhi, N. and Santavirta, S., 2005. The microenvironment around total hip replacement prostheses. *Clin. Orthop. Relat. Res.*, 430, pp.28-38.

49. Schmalzried, T.P., Szuszczewicz, E.S., Northfield, M.R., Akizuki, K.H., Frankel, R.E., Belcher, G. and Amstutz, H.C., 1998. Quantitative assessment of walking activity after total hip or knee replacement. *J. Bone Joint Surg. Am.*, 80 (1), pp.54-59.

50. Silva, M., Shepherd, E.F., Jackson, W.O., Dorey, F.J. and Schmalzried, T.P., 2002. Average patient walking activity approaches 2 million cycles per year: pedometers under-record walking activity. *J. Arthroplasty*, 17 (6), pp.693-697.

51. Kadaba, M.P., Ramakrishnan, H.K. and Wootten, M.E., 1990. Measurement of lower extremity kinematics during level walking. *J. Orthop. Res.*, 8 (3), pp.383-392.

52. Riener, R., Rabuffetti, M. and Frigo, C., 2002. Stair ascent and descent at different inclinations. *Gait Posture*, 15 (1), pp.32-44.

53. Isacson, J., Gransberg, L. and Knutsson, E., 1986. Three-dimensional electrogoniometric gait recording. *J. Biomech.*, 19 (8), pp.627-635.

54. Rose, J., Gamble, J.G. and Adams, J.M., 2006. *Human walking*. Lippincott Williams & Wilkins Philadelphia.

55. Johnston, R.C. and Smidt, G.L., 1969. Measurement of hip-joint motion during walking evaluation of an electrogoniometric method. *J. Bone Joint Surg. Am.*, 51 (6), pp.1083-1094.

56. Andriacchi, T., Andersson, G., Fermier, R., Stern, D. and Galante, J., 1980. A study of lower-limb mechanics during stair-climbing. *J. Bone Joint Surg. Am.*, 62 (5), pp.749-757.

57. Bergmann, G., Deuretzbacher, G., Heller, M., Graichen, F., Rohlmann, A., Strauss, J. and Duda, G.N., 2001. Hip contact forces and gait patterns from routine activities. *J. Biomech.*, 34 (7), pp.859-871.

58. Nadeau, S., McFadyen, B.J. and Malouin, F., 2003. Frontal and sagittal plane analyses of the stair climbing task in healthy adults aged over 40 years: what are the challenges compared to level walking? *Clin. Biomech.*, 18 (10), pp.950-959.

59. Paul, J.P., 1976. Force actions transmitted by joints in the human body. *Proc. R. Soc. London Ser. B*, 192 (1107), pp.163-172.

60. Taylor, S.J.G., Perry, J.S., Meswania, J.M., Donaldson, N., Walker, P.S. and Cannon, S.R., 1997. Telemetry of forces from proximal femoral replacements and relevance to fixation. *J. Biomech.*, 30 (3), pp.225-234.

61. Bergmann, G., Graichen, F. and Rohlmann, A., 1993. Hip joint loading during walking and running, measured in two patients. *J. Biomech.*, 26 (8), pp.969-990.

62. Kotzar, G.M., Davy, D.T., Goldberg, V.M., Heiple, K.G., Berilla, J., Brown, R.H. and Burstein, A.H., 1991. Telemeterized in vivo hip joint force data: a report on two patients after total hip surgery. *J. Orthop. Res.*, 9 (5), pp.621-633.

63. Brand, R.A., Pedersen, D.R., Davy, D.T., Kotzar, G.M., Heiple, K.G. and Goldberg, V.M., 1994. Comparison of hip force calculations and measurements in the same patient. *J. Arthroplasty*, 9 (1), pp.45-51.

64. Ong, K.L., Lehman, J., Notz, W.I., Santner, T.J. and Bartel, D.L., 2006. Acetabular cup geometry and bone-implant interference have more influence on initial periprosthetic joint space than joint loading and surgical cup insertion. *J. Biomech. Eng.*, 128 (2), pp.169-175.

65. Crowninshield, R.D., Johnston, R.C., Andrews, J.G. and Brand, R.A., 1978. A biomechanical investigation of the human hip. *J. Biomech.*, 11 (1–2), pp.75-85.

66. Seireg, A. and Arvikar, R.J., 1975. The prediction of muscular load sharing and joint forces in the lower extremities during walking. *J. Biomech.*, 8 (2), pp.89-102.

67. Bergmann, G., Graichen, F. and Rohlmann, A., 1995. Is staircase walking a risk for the fixation of hip implants? *J. Biomech.*, 28 (5), pp.535-553.

68. Bergmann, G., Graichen, F., Rohlmann, A., Bender, A., Heinlein, B., Duda, G.N., Heller, M. and Morlock, M., 2010. Realistic loads for testing hip implants. *Biomed. Mater. Eng.*, 20 (2), pp.65-75.

69. English, T.A. and Kilvington, M., 1979. In vivo records of hip loads using a femoral implant with telemetric output (a prelimary report). *J. Biomed. Eng.*, 1 (2), pp.111-115.

70. NHS. *Hip Replacements* [online]. Available from: http://www.nhs.uk/conditions/hip-replacement/pages/introduction.aspx [Accessed 23 January 2012].

71. Ling, R.S.M., 1989. Sir John Charnley memorial lecture: mechanical factors in implant fixation. *Curr. Orthop.*, 3 (3), pp.168-175.

72. Reynolds, L.A. and Tansey, E.M., 2007. *Early development of total hip replacement*. London: Wellcome Trust Centre for the History of Medicine at UCL.

73. Callaghan, J.J., Rosenberg, A.G. and Rubash, H.E., 2007. *The adult hip*. 2nd ed. Philadephia: Lippincott Williams & Wilkins.

74. Jones, L.C. and Hungerford, D.S., 1987. Cement disease. *Clin. Orthop. Relat. Res.*, 225, pp.192-206.

75. Sakellariou, V.I. and Sculco, T., 2013. Acetabular options: notes from the other side. *Semin. Arthroplasty*, 24 (2), pp.76-82.

76. Schmalzried, T.P., Jasty, M. and Harris, W.H., 1992. Periprosthetic bone loss in total hip-arthroplasty - polyethylene wear debris and the concept of the effective joint space. *J. Bone Joint Surg. Am.*, 74A (6), pp.849-863.

77. MacInnes, S.J., Gordon, A. and Wilkinson, J.M., 2012. Risk factors for aseptic loosening following total hip arthroplasty. *Pain*, 2 (29), pp.275-294.

78. Mjöberg, B., 1994. Theories of wear and loosening in hip prostheses: wear-induced loosening vs loosening-induced wear–a review. *Acta Orthop. Scand.*, 65 (3), pp.361-371.

79. Blaha, J.D. and Tanifuji, O., 2011. Options for acetabular component fixation. *Semin. Arthroplasty*, 22 (2), pp.85-89.

80. Watt, I., Boldrik, S., van Langelaan, E. and Smithuis, R., 2006. *Hip - Total hip arthroplasty. Normal and abnormal findings* [online]. Available from: http://www.radiologyassistant.nl/en/431c8258e7ac3#a432fb175726ec [Accessed 5 Decembre 2011].

81. Kienapfel, H., Sprey, C., Wilke, A. and Griss, P., 1999. Implant fixation by bone ingrowth. *J. Arthroplasty*, 14 (3), pp.355-368.

82. Young, A.M., Sychterz, C.J., Hopper, R.H. and Engh, C.A., 2002. Effect of acetabular modularity on polyethylene wear and osteolysis in total hip arthroplasty. *J. Bone Joint Surg. Am.*, 84-A (1), pp.58-63.

83. Exactech. *Components of a hip replacement* [online]. Available from: https://www.exac.com/Plone/canada/patients-caregivers-en-ca/joint-replacement-surgery/hip-replacement/components-hip-replacement [Accessed 22 August 2014].

84. Which Medical Device. *Pinnacle acetabular cup system* [online]. Available from: http://www.whichmedicaldevice.com/by-manufacturer/86/254/pinnacle-acetabular-cup-system [Accessed 22 August 2014].

85. Cook, S.D., Thomas, K.A., Barrack, R.L. and Whitecloud III, T.S., 1992. Tissue growth into porous-coated acetabular components in 42 patients effects of adjunct fixation. *Clin. Orthop. Relat. Res.*, 283, pp.163-170.

86. Hao, S., Taylor, J.T., Bowen, C.R., Gheduzzi, S. and Miles, A.W., 2010. Sensing methodology for in vivo stability evaluation of total hip and knee arthroplasty. *Sens. Actuators A*, 157 (1), pp.150-160.

87. Effenberger, H., Imhof, M., Richolt, J. and Rehart, S., 2004. Zementfreie Hüftpfannen [Current concepts of cementless acetabular cups]. *Orthopäde*, 33 (6), pp.733-750.

88. Hailer, N.P., Garellick, G. and Kärrholm, J., 2010. Uncemented and cemented primary total hip arthroplasty in the Swedish hip arthroplasty register. *Acta Orthop.*, 81 (1), pp.34-41.

89. Delee, J.G. and Charnley, J., 1976. Radiological demarcation of cemented sockets in total hip replacement. *Clin. Orthop. Relat. Res.*, 121, pp.20-32.

90. Goldring, S.R., Schiller, A.L., Roelke, M., Rourke, C.M., O'Neil, D.A. and Harris, W.H., 1983. The synovial-like membrane at the bone-cement interface in loose total hip replacements and its proposed role in bone lysis. *J. Bone Joint Surg. Am.*, 65 (5), pp.575-584.

91. Aspenberg, P. and Van der Vis, H., 1998. Migration, particles, and fluid pressure. A discussion of causes of prosthetic loosening. *Clin. Orthop. Relat. Res.*, 352, pp.75-80.

92. Schmalzried, T.P., Brown, I.C., Amstutz, H.C., Engh, C.A. and Harris, W.H., 1999. The role of acetabular component screw holes and/or screws in the development of pelvic osteolysis. *Proc. Inst. Mech. Eng. H*, 213 (2), pp.147-153.

93. Hirakawa, K., Jacobs, J.J., Urban, R. and Saito, T., 2004. Mechanisms of failure of total hip replacements: lessons learned from retrieval studies. *Clin. Orthop. Relat. Res.*, 420, pp.10-17.

94. Manley, M.T. and Serekian, P., 1994. Wear debris: an environmental issue in total joint replacement. *Clin. Orthop. Relat. Res.*, 298, pp.137-146.

95. Lamerigts, N., Buma, P. and Slooff, T., 2000. Bone resorption processes around stable and aseptic loosened total hip arthroplasties: a review of the literature. *Acta Orthop. Belg.*, 66, pp.9-24.

96. Goldberg, J.R., Gilbert, J.L., Jacobs, J.J., Bauer, T.W., Paprosky, W. and Leurgans, S., 2002. A multicenter retrieval study of the taper interfaces of modular hip prostheses. *Clin. Orthop. Relat. Res.*, 401, pp.149-161.

97. Huk, O.L., Bansal, M., Betts, F., Rimnac, C.M., Lieberman, J.R., Huo, M.H. and Salvati, E.A., 1994. Polyethylene and metal debris generated by non-articulating surfaces of modular acetabular components. *J. Bone Joint Surg. Br.*, 76-B (4), pp.568-574.

98. Collier, J.P., Mayor, M.B., Jensen, R.E., Surprenant, V.A., Surprenant, H.P., McNamar, J.L. and Belec, L., 1992. Mechanisms of failure of modular prostheses. *Clin. Orthop. Relat. Res.*, (285), pp.129-139.

99. Walter, W.L., 2005. Mechanisms for pumping fluid through cementless acetabular components with holes. *J. Arthroplasty*, 20 (8), pp.1042-1048.

100. Bloebaum, R.D., Mihalopoulus, N.L., Jensen, J.W. and Dorr, L.D., 1997. Postmortem analysis of bone growth into porous-coated acetabular components. *J. Bone Joint Surg. Am.*, 27 (65), pp.1013-1022.

101. Aspenberg, P. and Van der Vis, H., 1998. Fluid pressure may cause periprosthetic osteolysis: particles are not the only thing. *Acta Orthop. Scand.*, 69 (1), pp.1-4.

102. Evans, C., Mylchreest, S., Mee, A., Berry, J. and Andrew, J., 2006. Cyclic hydrostatic pressure and particles increase synthesis of 1, 25-dihydroxyvitamin D 3 by human macrophages in vitro. *The international journal of biochemistry & cell biology*, 38 (9), pp.1540-1546.

103. Fahlgren, A., Bostrom, M.P., Yang, X., Johansson, L., Edlund, U., Agholme, F. and Aspenberg, P., 2010. Fluid pressure and flow as a cause of bone resorption. *Acta Orthop.*, 81 (4), pp.508-516.

104. Sampathkumar, K., Jeyam, M., Evans, C. and Andrew, J., 2003. Role of cyclical pressure and particles in the release of M-CSF, chemokines, and PGE2 and their role in loosening of implants. *J. Bone Joint Surg. Br.*, 85 (2), pp.288-291.

105. Skoglund, B. and Aspenberg, P., 2003. PMMA particles and pressure—a study of the osteolytic properties of two agents proposed to cause prosthetic loosening. *J. Orthop. Res.*, 21 (2), pp.196-201.

106. Won, C.H., Hearn, T.H. and Tile, M., 1995. Micromotion of cementless hemispherical acetabular components. Does press-fit need adjunctive screw fixation? *J. Bone Joint Surg. Br.*, 77 (3), pp.484-489.

107. Manley, M.T., D'Antonio, J.A., Capello, W.N. and Edidin, A.A., 2002. Osteolysis: a disease of access to fixation interfaces. *Clin. Orthop. Relat. Res.*, 405, pp.129-137.

108. Robertson, O., Wingstrand, H., Kesteris, U., Jonsson, K. and Önnerfält, R., 1997. Intracapsular pressure and loosening of hip protheses. *Acta Orthop Scand*, 68 (3), pp.231-234.

109. Alghamdi, H.S., van den Beucken, J.J.J.P. and Jansen, J.A. Osteoporosis – fracture healing and osseointegration. *Drug Discovery Today: Disease Models*, (0).

110. Mavrogenis, A., Dimitriou, R., Parvizi, J. and Babis, G., 2009. Biology of implant osseointegration. *J Musculoskelet Neuronal Interact*, 9 (2), pp.61-71.

111. Hodey, J., 2001. *Measurment of long term stability and micromotion of a hip stem*. Final Year Project. Department of Mechnical Engineering, University of Bath.

112. Macdonald, W., Carlsson, L.V., Charnley, G.J., Jacobsson, C.M. and Johansson, C.B., 1999. Inaccuracy of acetabular reaming under surgical conditions. *J. Arthroplasty*, 14 (6), pp.730-737.

113. Kim, Y.S., Brown, T.D., Pedersen, D.R. and Callaghan, J.J., 1995. Reamed surface topography and component seating in press-fit cementless acetabular fixation. *J. Arthroplasty*, 10, Supplement 1 (0), pp.S14-S21.

114. Sandborn, P.M., Cook, S.D., Spires, W.P. and Kester, M.A., 1988. Tissue response to porous-coated implants lacking initial bone apposition. *J. Arthroplasty*, 3 (4), pp.337-346.

115. Carlsson, L., Röstlund, T., Albrektsson, B. and Albrektsson, T., 1988. Implant fixation improved by close fit Cylindrical implant – bone interface studied in rabbits. *Acta Orthop. Scand.*, 59 (3), pp.272-275.

116. Klenke, F.M., Liu, Y., Yuan, H., Hunziker, E.B., Siebenrock, K.A. and Hofstetter, W., 2008. Impact of pore size on the vascularization and osseointegration of ceramic bone substitutes in vivo. *J. Biomed. Mater. Res.*, 85A (3), pp.777-786.

117. Bobyn, J.D., Pilliar, R.M., Cameron, H.U. and Weatherly, G.C., 1980. The optimum pore size for the fixation of porous-surfaced metal implants by the ingrowth of bone. *Clin. Orthop. Relat. Res.*, 150, pp.263-270.

118. An, Y.H. and Draughn, R.A., 2000. *Mechanical testing of bone and the bone-implant interface*. Boca Raton, London: CRC Press.

119. Zivkovic, I., Gonzalez, M.H. and Amirouche, F., 2010. The effect of under-reaming on the cup/bone interface of a press fit hip replacement. *J. Biomech. Eng.*, 132 (4), pp.041008.

120. Nilles, J.L., Coletti, J.M. and Wilson, C., 1973. Biomechanical evaluation of bone-porous material interfaces. *J. Biomed. Mater. Res.*, 7 (2), pp.231-251.

121. Röhrl, S.M., Nivbrant, B., Ström, H. and Nilsson, K.G., 2004. Effect of augmented cup fixation on stability, wear, and osteolysis: a 5-year follow-up of total hip arthroplasty with RSA. *J. Arthroplasty*, 19 (8), pp.962-971.

122. Hori, R.Y. and Lewis, J.L., 1982. Mechanical properties of the fibrous tissue found at the bone-cement interface following total joint replacement. *J. Biomed. Mater. Res.*, 16 (6), pp.911-927.

123. Burke, D., Bragdon, C. and O'Connor, D., 1991. Dynamic measurement of interface mechanics in vivo and the effect of micromotion on bone ingrowth into a porous surface device under controlled loads in vivo. *ORS*, Anaheim, USA.

124. Jasty, M., Bragdon, C., Burke, D., O'Connor, D., Lowenstein, J. and Harris, W.H., 1997. In vivo skeletal responses to porous-surfaced implants subjected to small induced motions. *J. Bone Joint Surg. Am.*, 79 (5), pp.707-714.

125. Engh, C.A., O'Connor, D., Jasty, M., McGovern, T.F., Bobyn, J.D. and Harris, W.H., 1992. Quantification of implant micromotion, strain shielding, and bone resorption with porous-coated anatomic medullary locking femoral prostheses. *Clin. Orthop. Relat. Res.*, (285), pp.13-29.

126. Klaassen, M.A., Martínez-Villalobos, M., Pietrzak, W.S., Mangino, G.P. and Guzman, D.C., 2009. Midterm survivorship of a press-fit, plasma-sprayed, tri-spike acetabular component. *J. Arthroplasty*, 24 (3), pp.391-399.

127. Lima Corporate. *Lima product primary cups* [online]. Available from: http://www.lima.it/product-primary_cups-5-30.html [Accessed 22 August 2014].

128. Wasielewski, R.C., Cooperstein, L.A., Kruger, M.P. and Rubash, H.E., 1990. Acetabular anatomy and the transacetabular fixation of screws in total hip arthroplasty. *J. Bone Joint Surg. Am.*, 72 (4), pp.501-508.

129. Perona, P.G., Lawrence, J., Paprosky, W.G., Patwardhan, A.G. and Sartori, M., 1992. Acetabular micromotion as a measure of initial implant stability in primary hip arthroplasty: an in vitro comparison of different methods of intial acetabular component fixation. *J. Arthroplasty*, 7 (4), pp.537-547.

130. Yamaguchi, M., Bauer, T.W. and Hashimoto, Y., 1999. Deformation of the acetabular polyethylene liner and the backside gap. *J. Arthroplasty*, 14 (4), pp.464-469.

131. Baleani, M., Fognani, R. and Toni, A., 2001. Initial stability of a cementless acetabular cup design: experimental investigation on the effect of adding fins to the rim of the cup. *Artif. Organs.*, 25 (8), pp.664-669.

132. Huber, W.O. and Noble, P.C., 2014. Effect of design on the initial stability of press-fit cups in the presence of acetabular rim defects: experimental evaluation of the effect of adding circumferential fins. *Int. Orthop.*, 38 (4), pp.725-731.

133. Cook, S.D., Barrack, R.L., Thomas, K.A. and Haddad Jr, R.J., 1988. Quantitative analysis of tissue growth into human porous total hip components. *J. Arthroplasty*, 3 (3), pp.249-262.

134. Stiehl, J.B., MacMillan, E. and Skrade, D.A., 1991. Mechanical stability of porous-coated acetabular components in total hip arthroplasty. *J. Arthroplasty*, 6 (4), pp.295-300.

135. Curtis, M.J., Jinnah, R.H., Wilson, V.D. and Hungerford, D.S., 1992. The initial stability of uncemented acetabular components. *J. Bone Joint Surg. Br.*, 74-B (3), pp.372-376.

136. Mathieu, V., Michel, A., Flouzat Lachaniette, C.H., Poignard, A., Hernigou, P., Allain, J. and Haiat, G., 2013. Variation of the impact duration during the in vitro insertion of acetabular cup implants. *Med. Eng. Phys.*, 35 (11), pp.1558-1563.

137. Widmer, K.H., Zurfluh, B. and Morscher, E.W., 2002. Load transfer and fixation mode of press-fit acetabular sockets. *J. Arthroplasty*, 17 (7), pp.926-935.

138. Janssen, D., Zwartelé, R.E., Doets, H.C. and Verdonschot, N., 2010. Computational assessment of press-fit acetabular implant fixation: the effect of implant design, interference fit, bone quality, and frictional properties. *Proc. Inst. Mech. Eng. H*, 224 (1), pp.67-75.

139. Small, S.R., Berend, M.E., Howard, L.A., Rogge, R.D., Buckley, C.A. and Ritter, M.A., 2013. High initial stability in porous titanium acetabular cups: a biomechanical study. *J. Arthroplasty*, 28 (3), pp.510-516.

140. MacKenzie, J.R., Callaghan, J.J., Pedersen, D.R. and Brown, T.D., 1994. Areas of contact and extent of gaps with implantation of oversized acetabular components in total hip arthroplasty. *Clin. Orthop. Relat. Res.*, (298), pp.127-136.

141. Adler, E., Stuchin, S.A. and Kummer, F.J., 1992. Stability of press-fit acetabular cups. *J. Arthroplasty*, 7 (3), pp.295-301.

142. Iorio, R., Puskas, B., Healy, W.L., Tilzey, J.F., Specht, L.M. and Thompson, M.S., 2010. Cementless acetabular fixation with and without screws. *J. Arthroplasty*, 25 (2), pp.309-313.

143. Roth, A., Winzer, T., Sander, K., Anders, J.O. and Venbrocks, R.-A., 2006. Press fit fixation of cementless cups: how much stability do we need indeed? *Arch. Orthop. Trauma Surg.*, 126 (2), pp.77-81.

144. Macdonald, W., Carlsson, L.V., Charnley, G.J. and Jacobsson, C.M., 1999. Press-fit acetabular cup fixation: principles and testing. *Proc. Inst. Mech. Eng. H*, 213 (1), pp.33-39.

145. Goriainov, V., Jones, A., Briscoe, A., New, A. and Dunlop, D., 2014. Do the cup surface properties influence the initial stability? *J. Arthroplasty*, 29 (4), pp.757-762.

146. Kaneko, K., Inoue, Y., Yanagihara, Y., Uta, S., Mogami, A. and Iwase, H., 2000. The initial fixation of the press-fit acetabular shell – clinical observation and experimental study. *Arch. Orthop. Trauma Surg.*, 120 (5-6), pp.323-325.

147. Ohlin, A. and Balkfors, B., 1992. Stability of cemented sockets after 3–14 years. *J. Arthroplasty*, 7 (1), pp.87-92.

148. Volz, R.G. and Wilson, R.J., 1977. Factors affecting the mechanical stability of the cemented acetabular component in total hip replacement. *J. Bone Joint Surg. Am.*, 59 (4), pp.501-504.

149. Saleh, K.J., Bear, B., Bostrom, M., Wright, T. and Sculco, T.P., 2008. Initial stability of press-fit acetabular components: an in vitro biomechanical study. *Am. J. Orthop.*, 37 (10), pp.519-522.

150. Hsu, J.-T. and Lin, D.-J., 2009. Effects of screw eccentricity on the initial stability of the acetabular cup in artificial foam bone of different qualities. *Artif. Organs.*, 34 (1), pp.E10-E16.

151. Jamieson, M.L., Russell, R.D., Incavo, S.J. and Noble, P.C., 2011. Does an enhanced surface finish improve acetabular fixation in revision total hip arthroplasty? *J. Arthroplasty*, 26 (4), pp.644-648.

152. Markel, D.C., Hora, N. and Grimm, M., 2002. Press-fit stability of uncemented hemispheric acetabular components: a comparison of three porous coating systems. *Int. Orthop.*, 26 (2), pp.72-75.

153. Meneghini, R.M., Meyer, C., Buckley, C.A., Hanssen, A.D. and Lewallen, D.G., 2010. Mechanical stability of novel highly porous metal acetabular components in revision total hip arthroplasty. *J. Arthroplasty*, 25 (3), pp.337-341.

154. Olory, B., Havet, E., Gabrion, A., Vernois, J. and Mertl, P., 2004. Comparative in vitro assessment of the primary stability of cementless press-fit acetabular cups. *Acta Orthop. Belg.*, 70 (1), pp.31-37.

155. Antoniades, G., Smith, E.J., Deakin, A.H., Wearing, S.C. and Sarungi, M., 2013. Primary stability of two uncementedacetabular components of different geometry: hemispherical or peripherally enhanced? *Bone Joint Res.*, 2 (12), pp.264-269.

156. Hadjari, M.H., Hollis, J.M., Hofmann, O.E., Flahiff, C.M. and Nelson, C.L., 1994. Initial stability of porous coated acetabular implants: the effect of screw placement, screw tightness, defect type, and oversize implants. *Clin. Orthop. Relat. Res.*, 307, pp.117-123.

157. von Schulze-Pellengahr, C., Burkner, A., Lichtinger, T., Teske, W., Fottner, A., Wegener, B. and Vogel, T., 2011. Fuhrt Osteoporose zu einer Reduktion der Primarstabilitat zementfreier Huftpfannen? [Does osteoporosis lead to reduction the primary stability of cementless hip cups?]. *Orthopäde*, 40 (7), pp.607-613.

158. Williams II, V.G., Whiteside, L.A., White, S.E. and McCarthy, D.S., 1997. Fixation of ultrahigh-molecular-weight polyethylene liners to metal-backed acetabular cups. *J. Arthroplasty*, 12 (1), pp.25-31.

159. Pitto, R.P., Bohner, J. and Hofmeister, V., 1997. Einflußgrößen der Primärstabilität acetabulärer Komponenten. Eine In-vitro-Studie [Factors influencing initial stability of uncemented acetabular components. An in-vitro study]. *Biomed. Tech. (Berl).* 42 (12), pp.363-368.

160. Pitto, R.P., Willmann, G. and Schramm, M., 2001. Primärstabilität modularer acetabulärer Komponenten. Eine In-vitro-Vergleichsstudie mit Pfanneneinsätzen aus Polyethylen und Keramik [Initial stability of modular acetabular components. Comparative in-vitro study with polyethylene and ceramic liners]. *Biomed. Tech. (Berl).* 46 (4), pp.109-112.

161. Schmidig, G., Patel, A., Liepins, I., Thakore, M. and Markel, D.C., 2010. The effects of acetabular shell deformation and liner thickness on frictional torque in ultrahigh-molecular-weight polyethylene acetabular bearings. *J. Arthroplasty*, 25 (4), pp.644-653.

162. Miller, A., Su, E., Bostrom, M.G., Nestor, B. and Padgett, D., 2009. Incidence of ceramic liner malseating in Trident® acetabular shell. *Clin. Orthop. Relat. Res.*, 467 (6), pp.1552-1556.

163. Meding, J.B., Small, S.R., Jones, M.E., Berend, M.E. and Ritter, M.A., 2013. Acetabular cup design influences deformational response in total hip arthroplasty. *Clin. Orthop. Relat. Res.*, 471 (2), pp.403-409.

164. Bone, M.C., Dold, P., Flohr, M., Preuss, R., Joyce, T.J., Deehan, D. and Holland, J., 2013. A novel method for measuring acetabular cup deformation in cadavers. *Proc. Inst. Mech. Eng. H*, 227 (12), pp.1341-1344.

165. Kwong, L.M., O'Connor, D.O., Sedlacek, R.C., Krushell, R.J., Maloney, W.J. and Harris, W.H., 1994. A quantitative in vitro assessment of fit and screw fixation on the stability of a cementless hemispherical acetabular component. *J. Arthroplasty*, 9 (2), pp.163-170.

166. Bolder, S.B.T., Schreurs, B.W., Verdonschot, N., van Unen, J.M.J., Gardeniers, J.W.M. and Slooff, T.J.J.H., 2003. Particle size of bone graft and method of impaction affect initial stability of cemented cups. *Acta Orthop. Scand.*, 74 (6), pp.652-657.

167. Bolder, S.B.T., Verdonschot, N., Schreurs, B.W. and Buma, P., 2002. Acetabular defect reconstruction with impacted morsellized bone grafts or TCP/HA particles. A study on the mechanical stability of cemented cups in an artificial acetabulum model. *Biomaterials*, 23 (3), pp.659-666.

168. Kluess, D., Souffrant, R., Mittelmeier, W., Wree, A., Schmitz, K.-P. and Bader, R., 2009. A convenient approach for finite-element-analyses of orthopaedic implants in bone contact: modeling and experimental validation. *Comput. Methods Programs Biomed.*, 95 (1), pp.23-30.

169. Gililland, J.M., Anderson, L.A., Henninger, H.B., Kubiak, E.N. and Peters, C.L., 2013. Biomechanical analysis of acetabular revision constructs: is pelvic discontinuity best treated with bicolumnar or traditional unicolumnar fixation? *J. Arthroplasty*, 28 (1), pp.178-186.

170. Clements, J.P., Gheduzzi, S., Zweymuller, K., Litner, F., Schmotzer, H., Learmonth, I.D. and Miles, A.W., 2005b. An in-vitro cadaveric biomechanical evaluation of the SL Plus hip stem - comparison of long and short term stability. *ORS*, Washington, USA.

171. Berzins, A., Sumner, D.R., Andriacchi, T.P. and Galante, J.O., 1993. Stem curvature and load angle influence the initial relative bone-implant motion of cementless femoral stems. *J. Orthop. Res.*, 11 (5), pp.758-769.

172. Britton, J.R., Lyons, C.G. and Prendergast, P.J., 2004. Measurement of the relative motion between an implant and bone under cyclic loading. *Strain*, 40 (4), pp.193-202.

173. Gilbert, J.L., Bloomfeld, R.S., Lautenschlager, E.P. and Wixson, R.L., 1992. A computer-based biomechanical analysis of the three-dimensional motion of cementless hip prostheses. *J. Biomech.*, 25 (4), pp.329-340.

174. Maher, S.A., Prendergast, P.J. and Lyons, C.G., 2001. Measurement of the migration of a cemented hip prosthesis in an in vitro test. *Clin. Biomech.*, 16 (4), pp.307-314.

175. Jameson, T.M., Gheduzzi, S., Miles, A.W., Schmotzer, H. and Clements, J.P., 2007. Clinically relevant in-vitro hip stem stability studies in composite models. *EFORT*, Florence, Italy.

176. Britton, J.R. and Prendergast, P.J., 2005. Preclinical testing of femoral hip components: an experimental investigation with four prostheses. *J. Biomech. Eng.*, 127 (5), pp.872-880.

177. Gheduzzi, S., Clements, J.P., Webb, J.C.J., Schmotzer, H., Learmonth, I.D. and Miles, A.W., 2005. In-vitro post-operative stem stability using composite and cadaveric models. *ORS*, Washington, USA.

178. Clements, J.P., Gheduzzi, S., Heal, J., Learmonth, I.D. and Miles, A.W., 2003. Measurement of the micromotion and migration of an uncemented stem in an in-vitro test. *IASTED International Conference BioMECH*, Rhodes, Greece.

179. Gheduzzi, S. and Miles, A.W., 2007. A review of pre-clinical testing of femoral stem subsidence and comparison with clinical data. *Proc. Inst. Mech. Eng. H*, 221 (1), pp.39-46.

180. Liu, C., Green, S.M., Watkins, N.D., Gregg, P.J. and McCaskie, A.W., 2003. A preliminary hip joint simulator study of the migration of a cemented femoral stem. *Proc. Inst. Mech. Eng. H*, 217 (2), pp.127-135.

181. Clements, J.P., 2006. *Design and development of pre-clinical hip stem stability testing methods*. Ph.D. University of Bath.

182. Fritsche, A., Bialek, K., Mittelmeier, W., Simnacher, M., Fethke, K., Wree, A. and Bader, R., 2008. Experimental investigations of the insertion and deformation behavior of press-fit and threaded acetabular cups for total hip replacement. *J. Orthop. Sci.*, 13 (3), pp.240-247.

183. Noble, P.C., 1995. *The biomechanics of the acetabulum and acetabular replacement*. Ph.D. University of Strathclyde.

184. Cristofolini, L., Viceconti, M., Cappello, A. and Toni, A., 1996. Mechanical validation of whole bone composite femur models. *J. Biomech.*, 29 (4), pp.525-535.

185. Cristofolini, L. and Viceconti, M., 2000. Mechanical validation of whole bone composite tibia models. *J. Biomech.*, 33 (3), pp.279-288.

186. Jin, Z.M., Meakins, S., Morlock, M.M., Parsons, P., Hardaker, C., Flett, M. and Isaac, G., 2006. Deformation of press-fitted metallic resurfacing cups. Part 1: experimental simulation. *Proc. Inst. Mech. Eng. H*, 220 (2), pp.299-309.

187. Bishop, N. and Morlock, M., 2008. The risk of acetabular cup turn-out due to friction moments. *J. Biomech.*, 41, pp.S326.

188. Squire, M., Griffin, W.L., Mason, J.B., Peindl, R.D. and Odum, S., 2006. Acetabular component deformation with press-fit fixation. *J. Arthroplasty*, 21 (6, Supplement), pp.72-77.

189. F1839-08e2: 2008. *Standard specification for rigid polyurethane foam for use as a standard material for testing orthopedic devices and instruments*. ASTM.

190. Sawbones. *Solid rigid polyurethane foam* [online]. Available from: http://www.sawbones.com/products/bio/testblocks/solidfoam.aspx [Accessed 29/06/2012].

191. Crosnier, E.A., Keogh, P.S. and Miles, A.W., 2014. A novel method to assess primary stability of press-fit acetabular cups. *Proc. Inst. Mech. Eng. H*, 228 (11), pp.1126-1134.

192. Scrivens, D., 2014. *Design, build & test of an in vitro rig to measure acetabular cup micromotion whilst applying dynamic cyclic loading observed during activites of daily living*. MEng, Final Year Project. University of Bath.

193. Wheeless III, C.R., 1996. *Wheeless' textbook of orthopaedics*. Duke University Medical Center's Division of Orthopedic Surgery, Data Trace Internet Publishing.

194. Stryker. *Stryker Tritanium acetabular shell* [online]. Available from: http://www.stryker.com/en-us/products/Orthopaedics/HipReplacement/Acetabular/TritaniumAcetabularShell/index.htm [Accessed 26/01/2015].

195. Naziri, Q., Issa, K., Pivec, R., Harwin, S.F., Delanois, R.E. and Mont, M.A., 2013. Excellent results of primary THA using a highly porous titanium cup. *Orthopedics*, 36 (4), pp.e390-394.

APPENDIX 1. CONVERSION MATRIX

As described in this thesis, the configuration of the LVDTs allows for six independent equations of motion to be generated. These equations can be expressed in the matrix form, which can be used in a Matlab routine to convert the micromotion obtained by the six LVDTs into motion in the six degrees of freedom. The method used to obtain the matrix form of these equations is described below.

Below is the free body diagram of the acetabular cup with the target sphere rigidly attached to the dome of the cup. The arrows show the location and direction of each LVDT. The movements towards the LVDTs were defined as positive translation and the rotations were defined in accordance to the right-hand system convention.

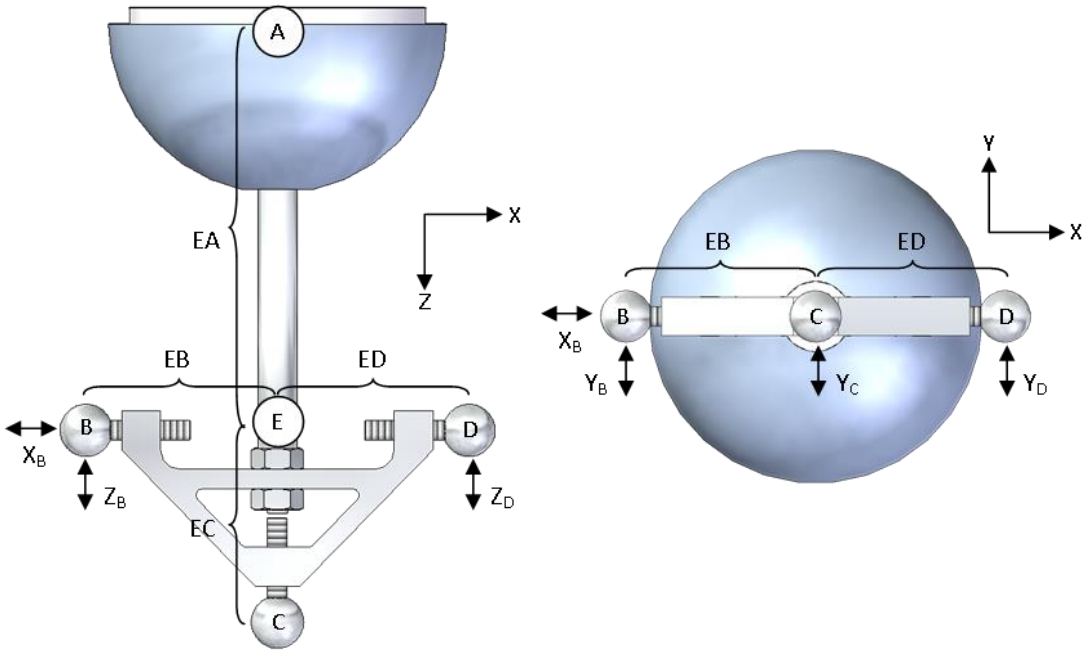

Free body diagram

It was considered that the angles of rotation (θ_x, θ_y, and θ_z) were small therefore:

$$\sin\theta \approx \theta \qquad \text{and} \qquad \cos\theta \approx 1$$

X ROTATION

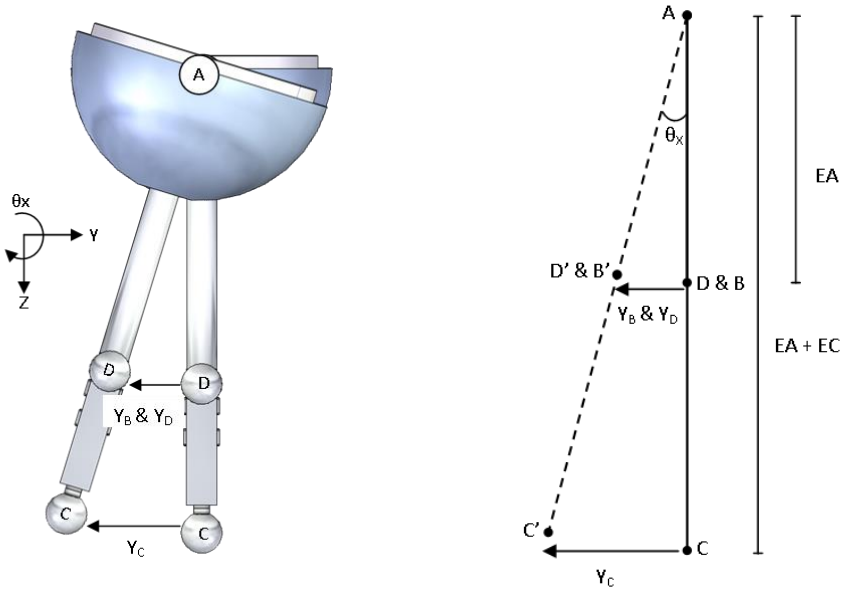

Illustration and FBD of a positive rotation along X axis.

The X rotation is measured by sensors Y_B, Y_D and Y_C:

$$Y_B = -EA \sin\theta_X \approx (-EA)\theta_X$$

$$Y_C = -(EA + EC) \sin\theta_X \approx \big(-(EA + EC)\big)\theta_X$$

$$Y_D = -EA \sin\theta_X \approx (-EA)\theta_X$$

Y ROTATION

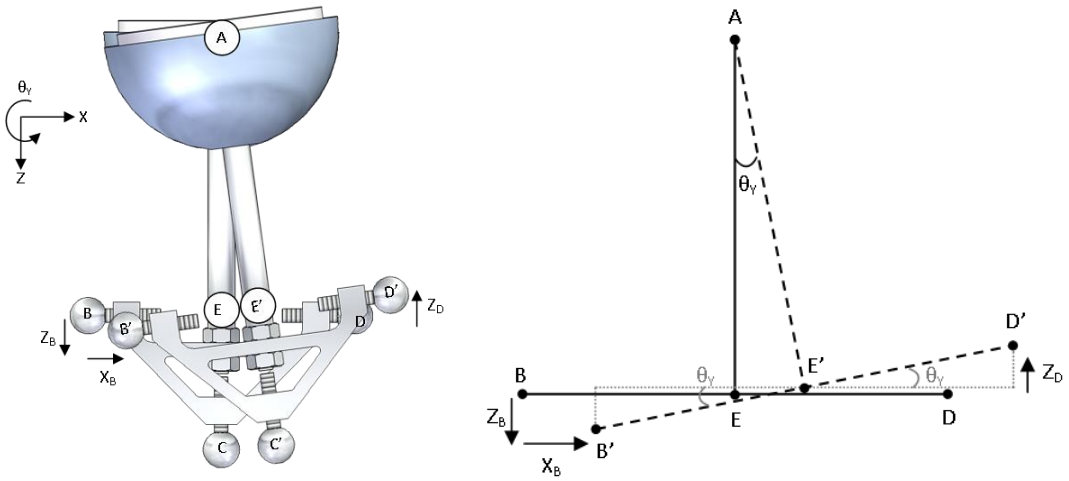

Illustration and FBD of a positive rotation along Y axis.

The Y rotation is measured by sensors X_B, Z_B and Z_C:

$$X_B = EB - (E'B'\cos\theta_Y - E'A\sin\theta_Y) = EB - (E'B' - EA\sin\theta_Y) \approx (EA)\theta_Y$$

$$Z_B = E'B'\sin\theta_Y - (EA - E'A\cos\theta_Y) = E'B'\sin\theta_Y - EA(1-\cos\theta_Y) \approx (EB)\theta_Y$$

$$Z_D = -\big(E'D'\sin\theta_Y + (EA - E'A\cos\theta_Y)\big) = -\big(E'D'\sin\theta_Y + EA(1-\cos\theta_Y)\big) \approx (-ED)\theta_Y$$

Z ROTATION

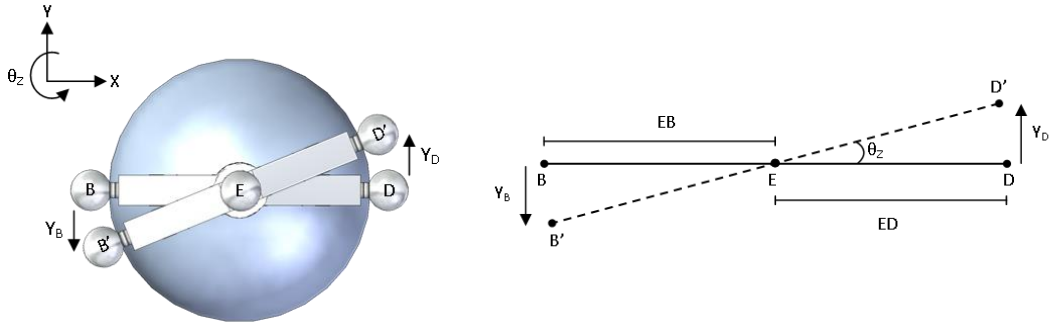

Illustration and FBD of a positive rotation along Z axis

The Z rotation is measured by sensors Y_B and Y_D:

$$Y_B = -EB'\sin\theta_Z \approx (-EB)\theta_Z$$

$$Y_D = ED'\sin\theta_Z \approx (ED)\theta_Z$$

CONVERSION MATRIX

Using the free body diagram and the equations obtained above for each rotation, the six independent equations of motions were obtained:

$$
\begin{aligned}
X_B &= X_A + (EA)\theta_Y \\
Y_B &= Y_A + (-EA)\theta_X + (-EB)\theta_Z \\
Y_C &= Y_A + \big(-(EA + EC)\big)\theta_X \\
Y_D &= Y_A + (-EA)\theta_X + (ED)\theta_Z \\
Z_B &= Z_A + (EB)\theta_Y \\
Z_D &= Z_A + (-ED)\theta_Y
\end{aligned}
$$

Finally, the matrix form of these equations used in the Matlab routine is:

$$
\begin{bmatrix} \mathrm{X_B} \\ \mathrm{Y_B} \\ \mathrm{Y_C} \\ \mathrm{Y_D} \\ \mathrm{Z_B} \\ \mathrm{Z_D} \end{bmatrix} = \begin{bmatrix} 1 & 0 & 0 & 0 & \mathrm{EA} & 0 \\ 0 & 1 & 0 & -\mathrm{EA} & 0 & -\mathrm{EB} \\ 0 & 1 & 0 & -(\mathrm{EA} + \mathrm{EC}) & 0 & 0 \\ 0 & 1 & 0 & -\mathrm{EA} & 0 & \mathrm{ED} \\ 0 & 0 & 1 & 0 & \mathrm{EB} & 0 \\ 0 & 0 & 1 & 0 & -\mathrm{ED} & 0 \end{bmatrix} \begin{bmatrix} \mathrm{X_A} \\ \mathrm{Y_A} \\ \mathrm{Z_A} \\ \theta_\mathrm{X} \\ \theta_\mathrm{Y} \\ \theta_\mathrm{Z} \end{bmatrix}
$$

where the first column is the motion measured by the LVDT sensors, the central matrix is the conversion matrix, and the last column is the motion of the cup in six degrees of freedom.

APPENDIX 2. VALIDATION OF THE SIX DOF MEASUREMENT SYSTEM

The Matlab code used to analyse this data is in Appendix 6.

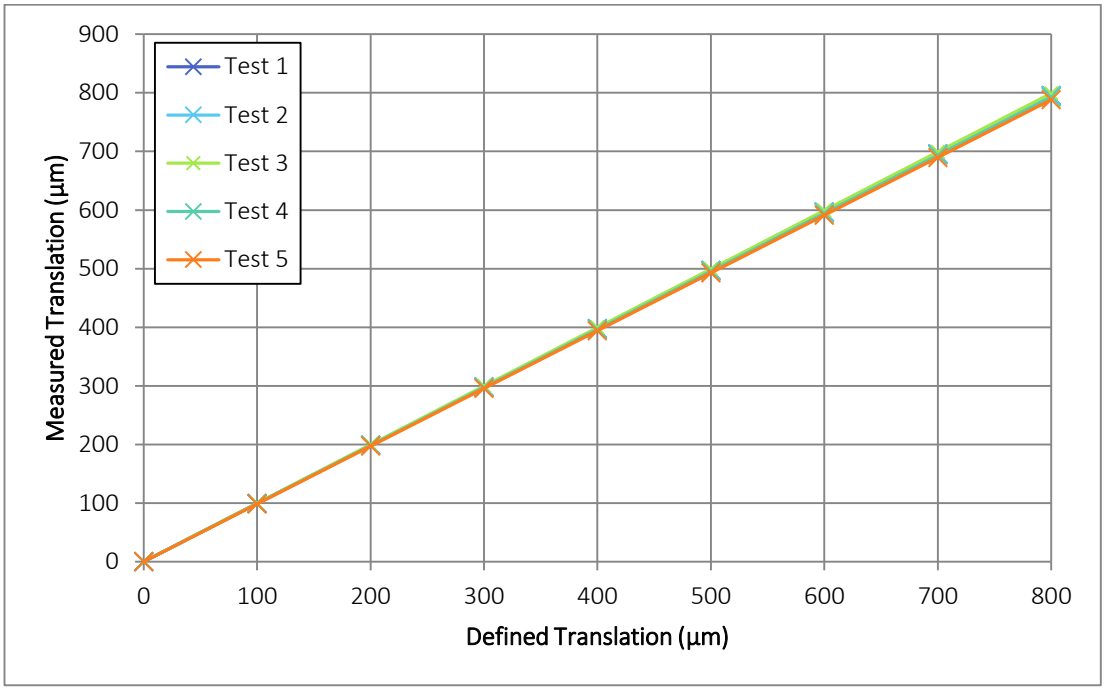

Translation along the X axis

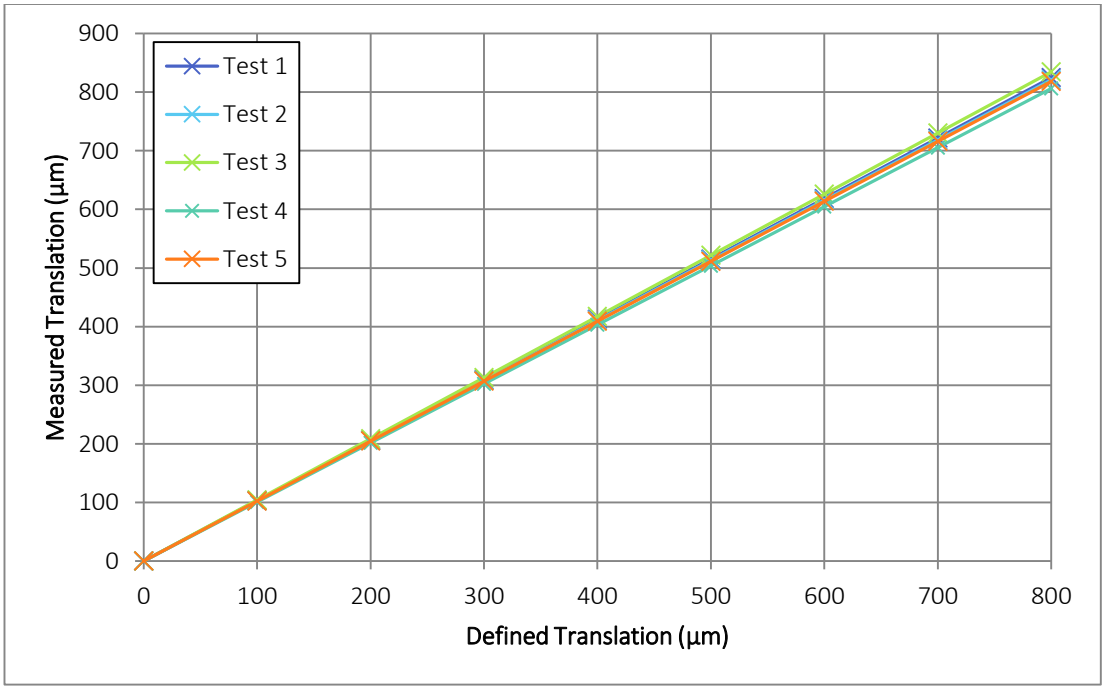

Translation along the Y axis

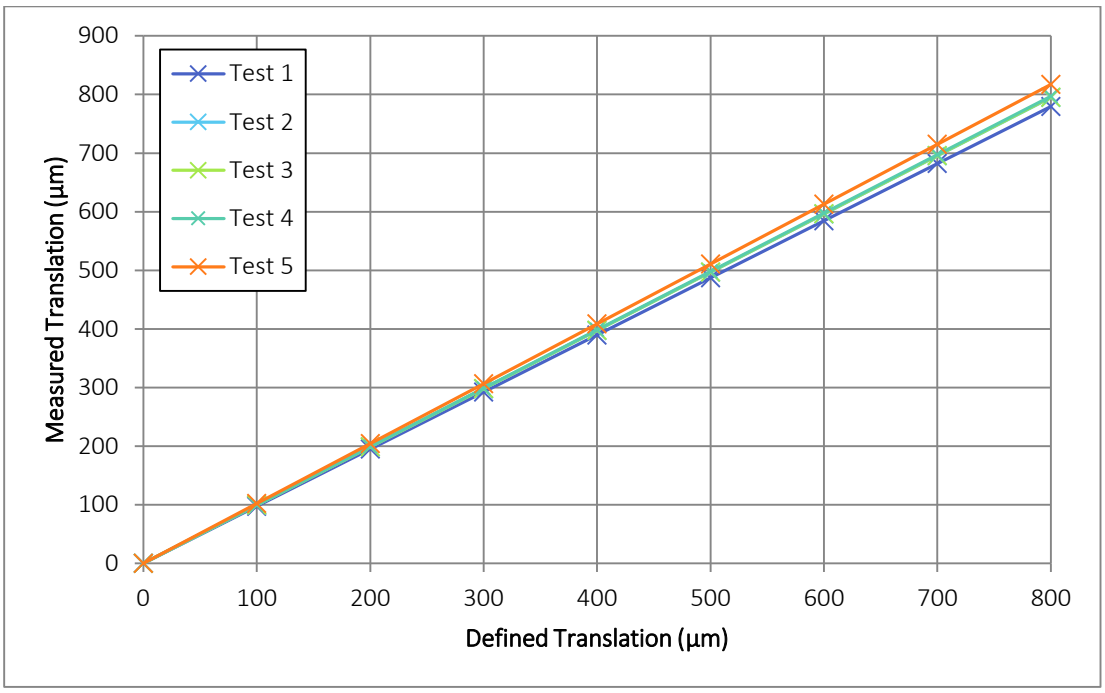

Translation along the Z axis

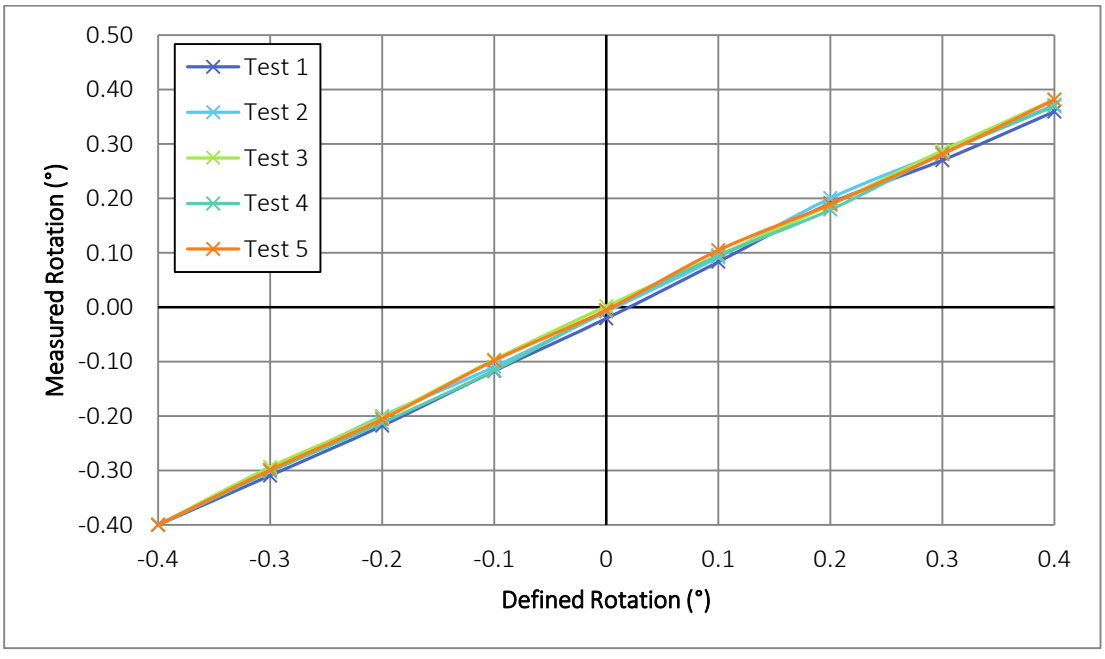

Rotation along the X axis

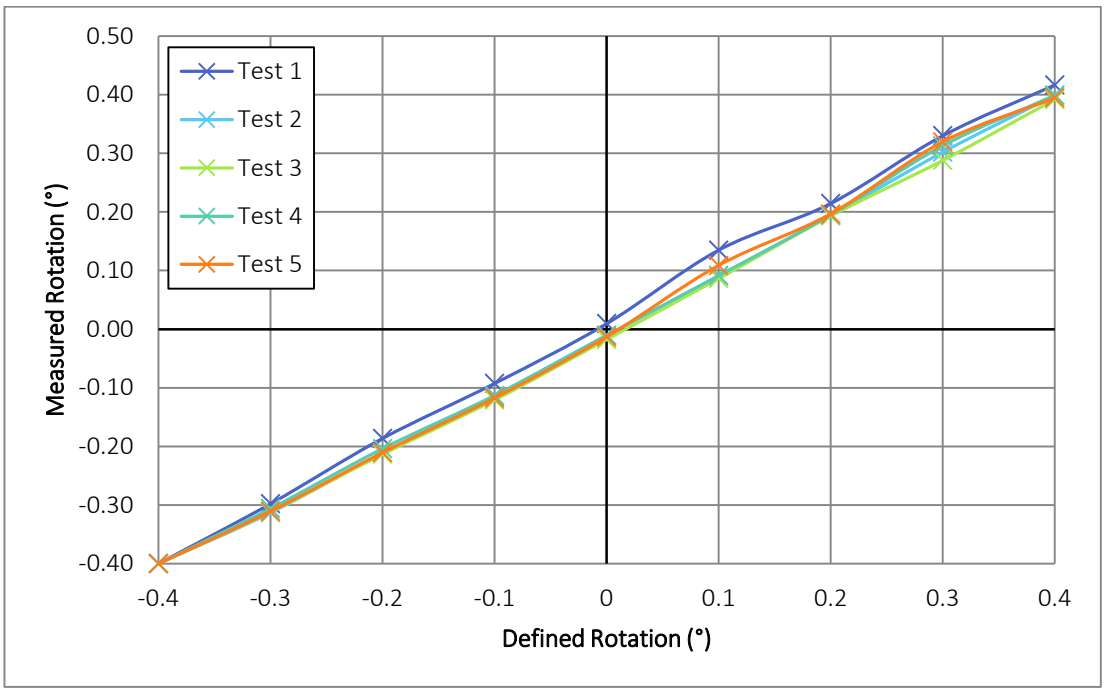

Rotation along the Y axis

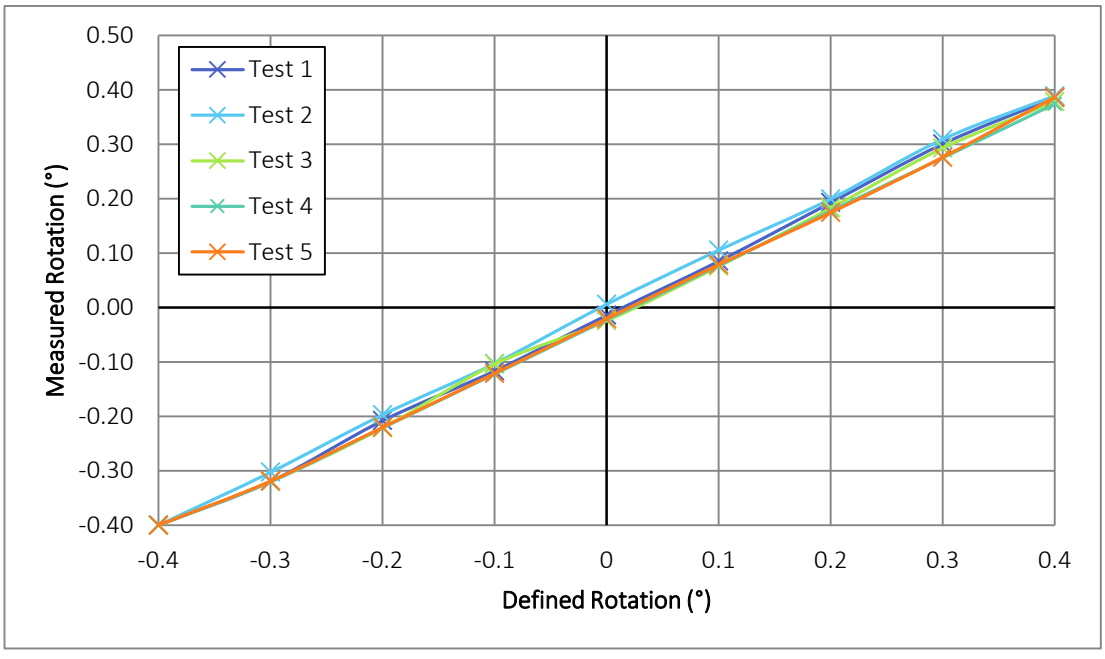

Rotation along the Z axis

APPENDIX 3. SCHEMATICS OF THE SAWBONES BLOCKS

HEMISPHERICAL MODEL

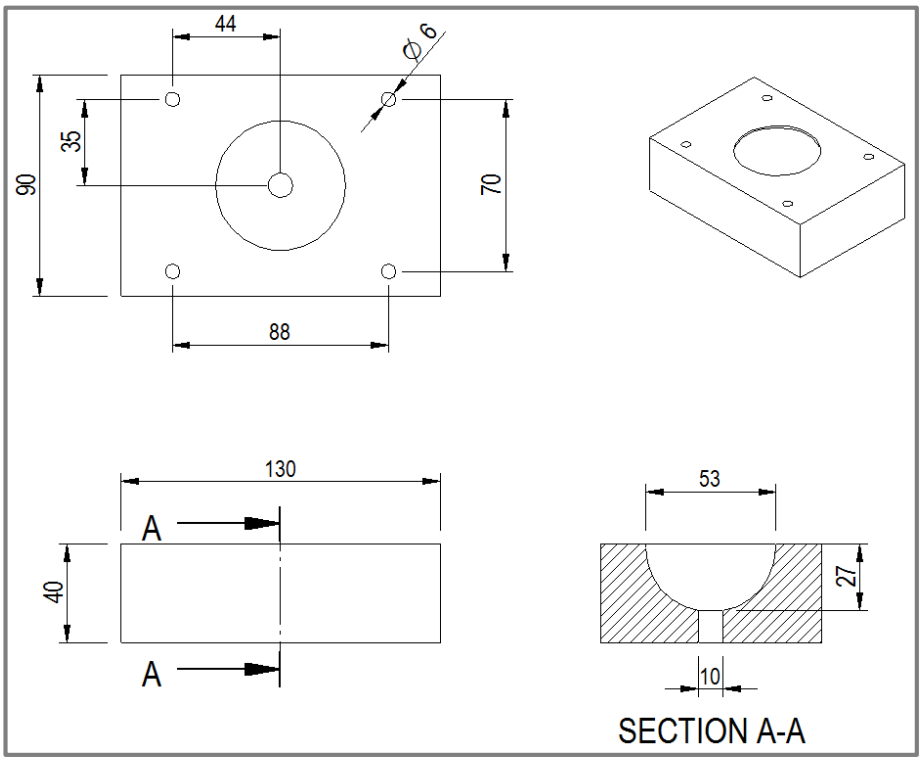

PHYSIOLOGICAL MODEL

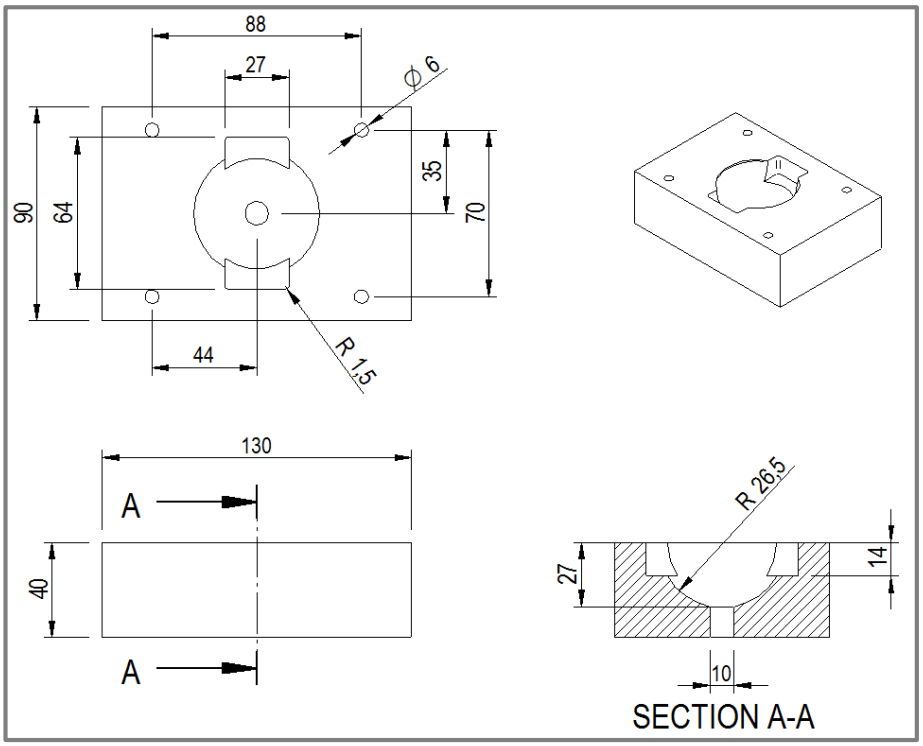

APPENDIX 4. CONTACT AREA CALCULATIONS

HEMISPHERICAL MODEL

The contact depth is taken as 5 mm.

Geometry:

A hemispherical cavity with a radius of 26.5 mm and 0.5 mm deep.

Contact area of the offset (modelled as a rectangle)

$$Width = depth\ of\ offset = 0.5\ mm$$

$$Length = circumference\ of\ hemisphere = 2 \times 26.5 \times \pi$$

$$Surface\ area = 0.5 \times (2 \times 26.5 \times \pi) = 83.25\ mm^2$$

Contact area of ring on hemisphere:

$$Surface\ area\ of\ hemisphere\ =\ 2 \times \pi \times r^2\ =\ 2 \times \pi \times 26.5^2 = 4412.37\ mm^2$$

$$Surface\ area\ of\ spherical\ cap = 2 \times \pi \times r \times h = 2 \times \pi \times 26.5 \times (26.5 - 4.5) = 3663.10\ mm^2$$

$$Surface\ area\ of\ ring = 4412.37 - 3663.10 = 749.27\ mm^2$$

Total contact area:

$$Contact\ area = contact\ area\ of\ offset + contact\ area\ of\ ring = 83.25 + 749.27 = 832.5\ mm^2$$

Total contact area with the hemispherical model is about 830 mm^2.

PHYSIOLOGICAL MODEL

The contact depth is taken as 9 mm

Geometry:

Similar to the hemispherical model with two cavities

Percentage of area in contact with the cup:

Width of each gap is 27 mm at the periphery of the cavity which corresponds to 61.25° per gap and 122.5° for both gaps.

$$\frac{(360 - 122.5)}{360} = \frac{237.5}{360} = 65.97\%$$

Hence, only 66% of the Sawbones foam is in contact with the cup.

Contact area of the offset:

$$Surface\ area = \left(0.5 \times (2 \times 26.5 \times \pi)\right) \times 0.66 = 54.92\ mm^2$$

Contact area of ring:

$$Surface\ area\ of\ hemisphere\ =\ 2 \times \pi \times r^2\ =\ 2 \times \pi \times 26.5^2 = 4412.37\ mm^2$$

$$Surface\ area\ of\ spherical\ cap = 2 \times \pi \times r \times h = 2 \times \pi \times 26.5 \times (26.5 - 8.5) = 2997.08\ mm^2$$

$$Surface\ area\ of\ ring = 4412.37 - 2997.08 = 1415.29\ mm^2$$

$$Surface\ area\ in\ contact\ with\ cup = 1415.29 \times 0.66 = 933.70\ mm^2$$

Total contact area:

$$Contact\ area = contact\ area\ of\ offset + contact\ area\ of\ ring = 54.92 + 933.70 = 988.62\ mm^2$$

Total contact area with the physiological model is about 990 mm^2.

APPENDIX 5. FINAL TESTING PROTOCOL

INCISE

Set up Incise
- Install and load stylus: z-minus_31_3000µm_ruby-ball
- Home machine
- Calibrate Incise

Sawbones Blocks
- Draw mark on Sawbones 5 mm away from cavity edge on right-hand side
- Place block on Incise stand (mark on right-hand side)
- Screw block in place
- Place stand with block on Incise (check everything is aligned)

Measurement
- Place ruby ball head on mark (with manual movement)
- Move head in relative X direction by -8
- Move head by in relative Z direction by -2
- Start scan: Scanning => Scan Object => Scan Profile => OK (do not move stylus)

End of Measurement
- Export profile in ASCII format
  - Saving format: *30pcf*_incise_*0_HA1*
- Move ruby ball away from block (manually) and remove stand with block
- Unscrew block from stand and restart protocol with another block

SET-UP

LVDT sensors
- Calibrate each LVDT (if needed)
- Screw LVDTs in frame

Acetabular Cup
- Insert liner inside shell of acetabular cup
- Tightly screw the rod inside the dome of the acetabular cup

Data collection computer
- Check LVDT cards are in the computer and connect LVDTs
- Connect Load and Displacement channels from Dartec to computer
- Connect Motion rig channel to computer (note channel used)
- Turn on computer and open LabView program

Dartec
- Turn on Dartec according to the "Dartec Test Machine" guide

CUP INSERTION PROTOCOL

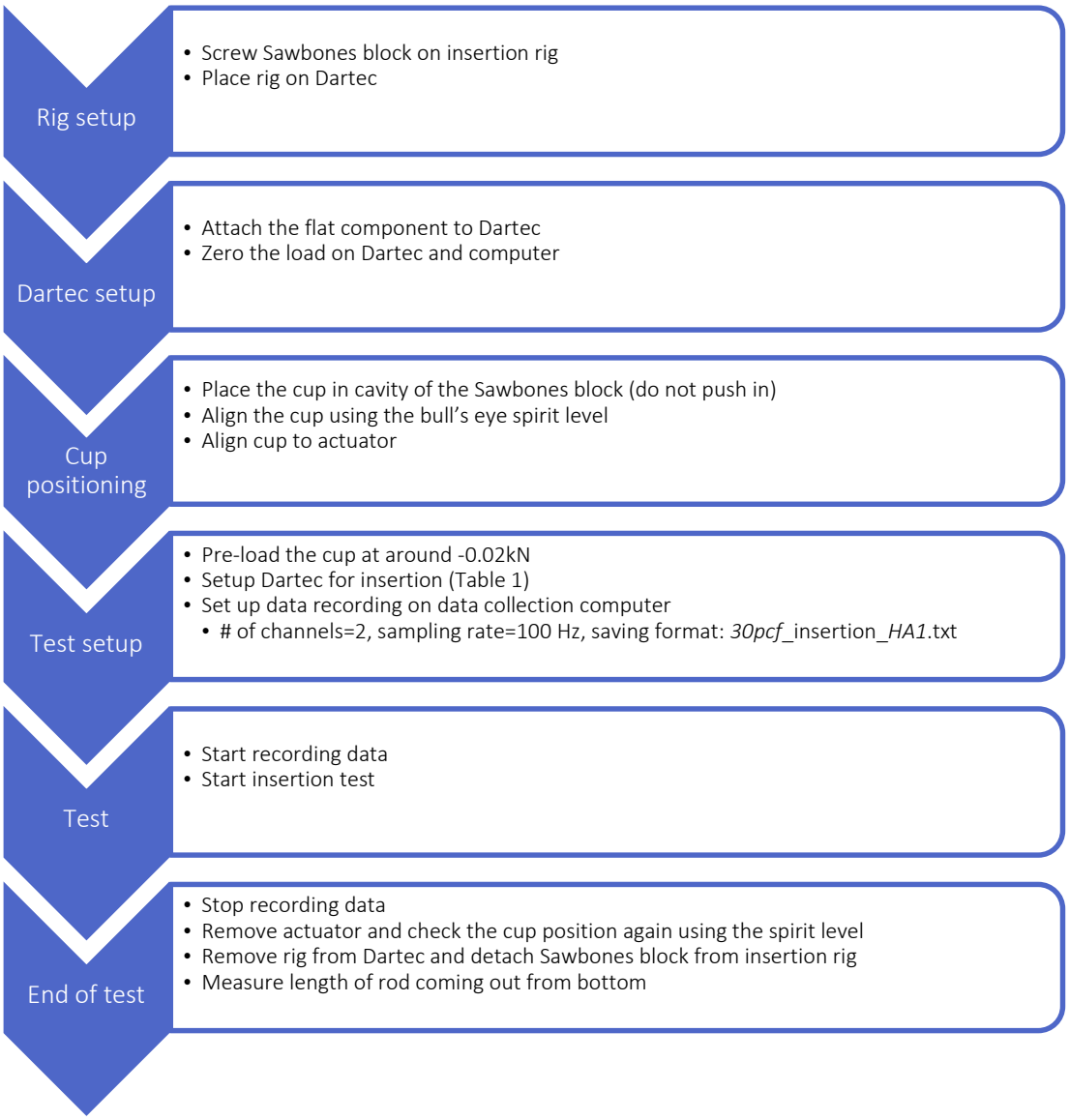

Table 1 – Dartec settings for cyclic loading

Test	Control Mode	Min Load	Max Load	Frequency	Wave Type	# of Cycles
Insertion	Load	-0.01kN	-5.0kN	1Hz	Sine	5
Preconditioning	Load	-0.01kN	-5.0kN	1Hz*	Sine	200
Micromotion Test	Load	-0.01kN	-5.0kN	1Hz*	Sine	1'000

* Frequency can be modified to synchronise with motion rig during dynamic testing.

MICROMOTION PROTOCOL

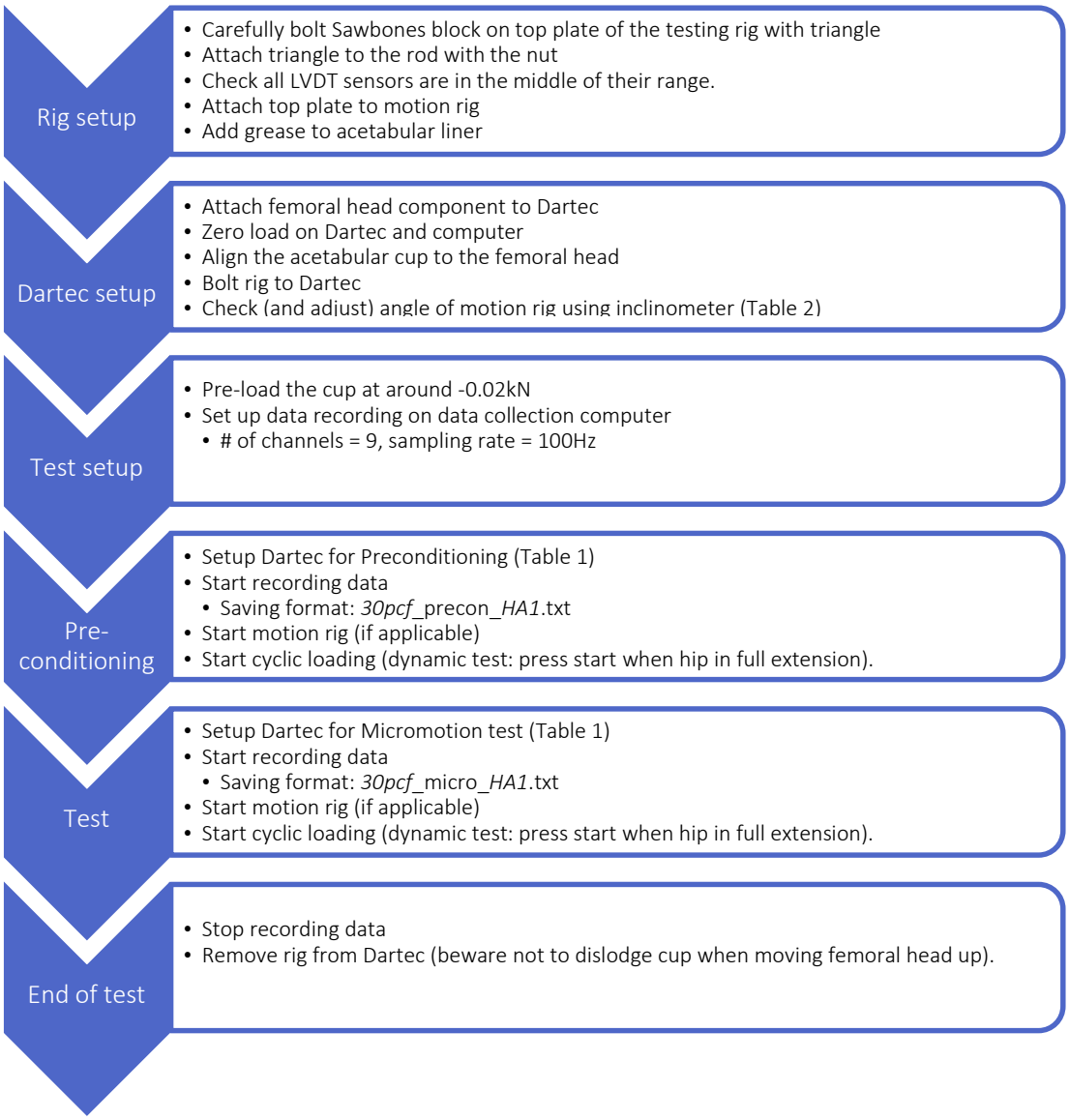

Table 2 – Motion rig settings

	Frequency	Hip Flexion	Hip Extension
Heel strike	NA	30°	NA
Walk	0.5 Hz	30°	10°
Stairs	0.5 Hz	40°	5°

CUP PUSH-OUT PROTOCOL

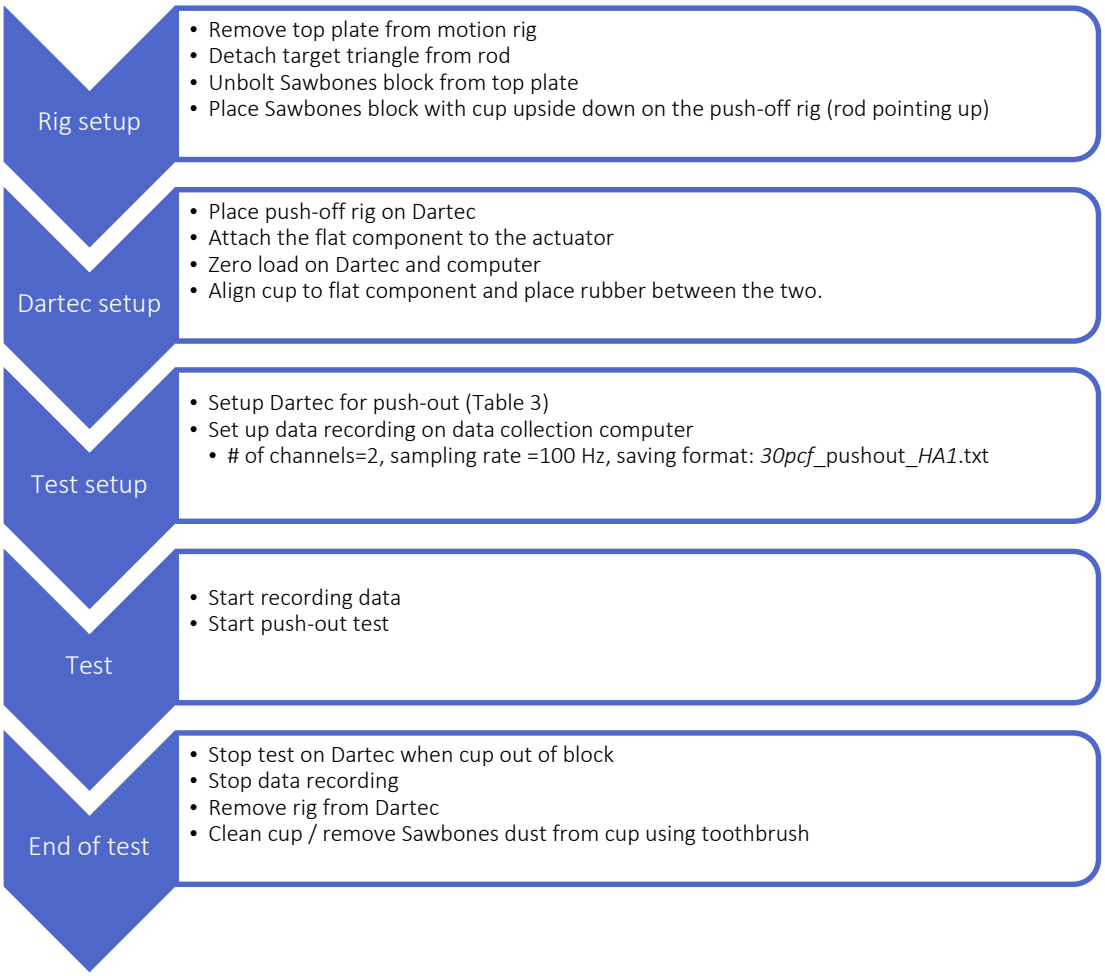

Table 3 – Dartec settings for push-out

Control Mode	Rate	Stop
Stroke	0.008mm/s	Manual

APPENDIX 6. MATLAB CODES

Incise

```
function[Data]=Incise(~)
% Analyses the data obtained by the Incise to obtain the peripheral diameter of the acetabular model.
%
% Emilie Crosnier
% University of Bath 03/09/2013

% Create a folder for output data.
mkdir('H:\Dos\Matlab\Output\');

% Select folder with datafiles to analyse.
folder_name=uigetdir;
cd(folder_name);
filenames=dir('*.asc');

% Work through the different routines
[Data]=RawData(filenames, folder_name)
[Data]=circfit(Data);
[Data]=Output_Diameter(Data);
```

```
function [Data]=RawData(filenames, folder_
name)
% Determine the x and y values to use
%
% Input: list of files to be analysed
% Output: X and Y data without wings.
%
% Emilie Crosnier
% University of Bath 03/09/2013

% Loop through each data file.
for k=1:length(filenames)

  % Open datafile and import data.
  cd(folder_name);
  datafile=filenames(k).name;
  A=importdata(datafile,' ',1);

  % Remove .txt format from filename.
  datafile=strrep(datafile,'.asc','');

  % Define x and y data points.
  x=A.data(:,1);
  y=A.data(:,2);
  % Remove wings
  x(2500:3600,:)=[];
  x(500:1500,:)=[];
  y(2500:3600,:)=[];
  y(500:1500,:)=[];

  % Place data in output structure.
  Data(k).filename=datafile;
  Data(k).x=x;
  Data(k).y=y;

  % Clear all values of loop.
  clear x y xmin ymin X Y dia data
end
```

```
function  [Data] = circfit(Data)
% [xc yx R] = circfit(x,y)
%
% Fits a circle  in x,y plane in a more accurate(less prone to ill condition) procedure than circfit2 but using more memory
% x,y are column vector where (x(i),y(i)) is a measured point
%
% Result is centre point (yc, xc) and radius R an optional output is the vector of coefficient a describing the circle's equation
%
% x^2+y^2+a(1)*x+a(2)*y+a(3)=0
%
% By: Izhak Bucher 25/oct/1991,
%
%%%%%
%
% Method modified to obtain centre point and radius of circle.
%
% Emilie Crosnier
% University of Bath 03/09/13

% Find number of data sets to run through
S=size(Data,2);

% Loop through each data file.
for k=1:S
```

```
 % Define x and y
 x=Data(k).x;
 y=Data(k).y;

 % Perform circfit function to obtain centre point.
 a=[x y ones(size(x))]\[-(x.^2+y.^2)];
 xc = -.5*a(1);
 yc = -.5*a(2);
 R  =  sqrt((a(1)^2+a(2)^2)/4-a(3));

 % Calculate diameter
 dia=R*2;

 % Make centre point = 0,0.
 xs=x-xc;
 ys=y-yc;

 % Plot graph
 plot(x,y)
 hold on
 plot(xc,yc,'g.')
 rectangle('position',[xc-R,yc-R,R*2,R*2],...
   'curvature',[1,1],'linestyle','-','edgecolor','r');
 hold off

 % Place data in output structure
 Data(k).xs=xs;
 Data(k).ys=ys;
 Data(k).diameter=dia;
end
```

```
function[Data]=Output_Diameter(Data)
% Prints diameter using data analysed from Incise.
%
% Input: structure with filenames and diameters.
% Output: output diameters in test file.
% Emilie Crosnier
% University of Bath 03/09/2013

% Find the number of data set to run through:
S=size(Data,2);

% Create file in which data points will be printed.
fid=fopen(['H:\Dos\Matlab\Output\Diameter.txt'],'wt');

% Create line of labels.
fprintf(fid,'%0s\t
%12s\n','name','diameter');

% Loop through each data file
for k=1:S

 % Print data in micromotion file.
 fprintf(fid,'%6s\t
%12.8f\n',Data(k).filename,
Data(k).diameter);

end
% close text file
fclose(fid);
```

Cup Motion

```
function[Data]=Cup_Motion(~)
% Analyses the data obtain by the LVDT sensors to obtain the micromotion and migration of the acetabular cup.
%
% Emilie Crosnier
% University of Bath 21/11/13

% Select folder with datafiles to analyse
folder_name=uigetdir;
cd(folder_name);
filenames=dir('*.txt');

% Define the number of cycles to analyse
nc=input('Number of cycles to analyse = ');

% Define sampling frequency.
sf=input('Sampling frequency (Hz)= ');

% Define loading frequency.
lf=input('Loading frequency (Hz)= ');

% Define motion frequency.
mf=lf/2;

% Define Target Geometry (in m).
ea=0.0711;
eb=0.0295;
ec=0.0314;
ed=0.0295;
```

```
% Define LVDT calibration factors (m/voltage).
m1=0.1003e-3;
m2=0.0999e-3;
m3=0.1009e-3;
m4=0.1006e-3;
m5=0.0975e-3;
m6=0.099e-3;
ms=0.1144e-3;
mb=0.0997e-3;

% Define Dartec calibration factors.
L=1;
D=10;

% Create a folder for output data.
mkdir('H:\Dos\Matlab\Output\');

% Analyse data.
[Data]=Input_Data(filenames,folder_name,nc,sf,lf)
[Data]=Conv_Matrix(Data,ea,eb,ec,ed,m1,m2,m3,m4,m5,m6);
[Data]=Micromotion(Data,sf,lf,mf,nc);
[Data]=Bone_Micromotion(Data,ms,mb,sf);
% Create output files and graphs.
[Data]=Dartec_Output(Data,L,D);
[Data]=Output_Bone(Data);
[Data]=Output_Micromotion(Data);
[Data]=Output_Graphs(Data);
```

```
function[Data]=Input_Data(filenames,folder_name,nc,sf,lf)
% Analyses the data obtain by the LVDT sensors to obtain the micromotion and migration of the acetabular cup.
%
% Inputs: filenames = list of files to be analysed; folder_name = folder with files to analyse; nc = number of cycles to analyse; sf = sampling frequency.
% Outputs: Data = structure with filenames and LVDT raw data.
%
% Emilie Crosnier
% University of Bath 21/11/13

% Loop through each data file.
for k=1:length(filenames)

 % Open datafile and import data.
 cd(folder_name);
 datafile=filenames(k).name;
 A=importdata(datafile,'\t',10);

 % Remove .txt format from filename
 datafile=strrep(datafile,'.txt','');

 % Select data
 volts=A.data;

 % Find the number of measurements.
 n=size(volts,1);

 % Change load from negative to positive (Load=1st column)
 volts(:,7)=volts(:,7)*-1;

 % Find the load peaks (use 1.5kN as minimum height).
 [pks,locs]=findpeaks(volts(:,7),'minpeakheight',1.5);

 % Find the number of peaks found.
 m=size(locs,1);

 % Find the first peak and define as xmin
 for i=1:m
  a=locs(i,1);
  b=locs(i+1,1);
  if b-a>=50
   xmin=b;
   break
  elseif b-a<50
  end
 end

 % Calculate number of points per cycle
 ppc=1/lf;

 % Calculate end point
 xmax=xmin+nc*sf*ppc;
 xmax=round(xmax);

 % Remove value before starting point and after end point
 volts(xmax:n,:)=[];
 volts(1:xmin-1,:)=[];

 % Place data in output structure
 Data(k).filename=datafile;
 Data(k).LVDT=volts(:,1:6);
```

```
  Data(k).Dartec=volts(:,7:8);
  Data(k).Motion=volts(:,9);
%  Data(k).Bone=volts(:,9);

  % Clear all values of loop.
  clear volts n xmin xmax pks locs ppc
end
```

```
function[Data]=Conv_Matrix(Data,ea,eb,ec,ed,m1,m2,m3,m4,m5,m6)
% Converts voltages recorded by LVDT sensors into translations and rotations of the cup
%
% Inputs: Data = voltages recorded by LVDT to analyse.
% Outputs: Data = adds translations and rotations of the cup in data matrix.
%
% Emilie Crosnier
% University of Bath 22/02/13

% Find number of data sets to run through
S=size(Data,2);

% Loop through each data file.
for k=1:S

  % Create matrix with needed data.
  volts=Data(k).LVDT;

  % Transpose the LVDT data to work with the matrix geometry.
   volts=volts';

  % Re-order rows to allow for LVDT labelling and multiply with calibration factor.
  v(1,:)=u(6,:)*m6;
  v(2,:)=u(2,:)*m2;
  v(3,:)=u(5,:)*m5;
  v(4,:)=u(3,:)*m3;
  v(5,:)=u(4,:)*m4;
  v(6,:)=u(1,:)*m1;

  % LVDTs 2 and 6 are in opposite sense to the co-ordinate axes therefore they need to be inverted.
  v(1:2,:)=-v(1:2,:);

  % Find the number of measurements
  n=size(v,2);

  % Define conversion matrix with factors that allow for unequal geometry
  geo=[0 0 1 0 -ed 0;
    0 0 1 0 eb 0;
    0 1 0 -ea 0 ed;
    0 1 0 -ea 0 -eb;
    0 1 0 -(ea+ec) 0 0;
    1 0 0 0 ea 0];

  % Perform inverse matrix operation on each column of the data to obtain translations and rotations.
  for i=1:n;
    micro(:,i)=geo\v(:,i);
  end

  % Convert translation rows from meters to micrometres.
  newmicro(1:3,:)=1e6*micro(1:3,:);

  % Convert rotations rows from radians to
  % degrees
  newmicro(4:6,:)=(180/pi)*micro(4:6,:);

  % Transpose matrix for correct format
  tmicro=newmicro';

  % Place data in output structure
  Data(k).Converted=tmicro;

  % Clear all values of loop.
  clear volts u v n micro i newmicro tmicro
end
```

```
function[Data]=Micromotion(Data,sf,lf,mf,nc)
% Using Fast Fourier Transforms to calculate the amplitude of the micromotion in
%
% Inputs: Data = matrix with translations and rotations of the cup
% Outputs: Data = adds amplitude of micromotion of the cup (both translation and rotation) in data matrix.
%
% Emilie Crosnier
% University of Bath 22/02/13
% Find number of data sets to run through
```

```
S=size(Data,2);

% Loop through each data file.
for k=1:S

 % Create matrix with needed data.
 M=Data(k).Converted;

 % Find the number of measurements.
 n=size(M,1);

 % Find number of columns
 N=size(M,2);

 % Create output Matrix
 amp=[1:6];

 % Calculate amplitude of micromotion using Fast Fourier Transforms.

 for i=1:N

  % fft each vector and work out the magnitude of the micromotion.
  x_fft=fft(M(:,i));
  x_pwr=x_fft.*conj(x_fft)/n;

  % Find max peak around 0.5Hz and 1Hz.
  P1=round((n*lf)/sf);
  P2=round((n*mf)/sf);

  % Bin of interest (at loading and motion frequency)
  bin1=max(x_pwr(P1-5:P1+5));
  bin2=max(x_pwr(P2-5:P2+5));

  % Amplitude (at both frequencies)
  micro_x1=sqrt(4*bin1/n)*2;
  micro_x2=sqrt(4*bin2/n)*2;

  %Sum of amplitudes
  micro_x=micro_x1+micro_x2;

  amp(1,i)=micro_x;
 end

 % Switch X and Y because of new motion setup
 amp(:,[1 2])=amp(:,[2 1]);

 % Place data in output structure
 Data(k).Micromotion=amp;

 % Clear all values of loop.
 clear M n N amp x_fft x_pwr P1 P2 bin1 bin2 micro_x1 micro_x2 micro_x
end
```

```
function[Data]=Bone_Micromotion(Data, ms,mb, sf)
% Converts voltages recorded by the LVDT sensors attached on the bone into displacement.
%
% Input: Data = voltages recorded by LVDT sensors on the bone.
% Output: Data = micromotion of the bone during testing.
%
% Emilie Crosnier
% University of Bath 21/11/13

% Find number of data sets to run through
S=size(Data,2);

% Loop through each data file.
for k=1:S

 % Create matrix with needed data.
 volts=Data(k).Bone;

 % Multiply with calibration factor.
 M(:,1)=volts(:,1)*ms*1e6;
 M(:,2)=volts(:,2)*mb*1e6;

 % Find the number of measurements.
 n=size(M,1);

 % Calculate amplitude of micromotion using Fast Fourier Transforms.
 % fft each vector and work out the magnitude of the micromotion.
 s_fft=fft(M(:,1));
 s_pwr=s_fft.*conj(s_fft)/n;

 b_fft=fft(M(:,2));
 b_pwr=b_fft.*conj(b_fft)/n;

 % Bin of interest (1Hz)
 bin=1+((n*1)/sf);

 % Amplitude at 1Hz
 micro_s=sqrt(4*s_pwr(bin)/n)*2;
 micro_b=sqrt(4*b_pwr(bin)/n)*2;
```

```
  % Create Matrix for amplitudes.
  amp(1,1)=micro_s;
  amp(1,2)=micro_b;

% Place data in output structure
  Data(k).Bone_Micromotion=amp;
  % Clear all values of loop.
  clear volts M s_fft b_fft s_pwr b_pwr bin
micro_s micro_b amp
end
```

```
function[Data]=Dartec_Output(Data,L,D)
% Converts voltages recorded by the
Dartec into displacement and load, and
prints out the data into a text file.
%
% Input: Data = voltages recorded by
Dartec.
% Output: Data = load and displacement of
the Dartec.
%
% Emilie Crosnier
% University of Bath 15/07/13

% Find number of data sets to run through
S=size(Data,2);

% Loop through each data file.
for k=1:S

  % Create matrix with needed data.
  volts=Data(k).Dartec;

  % Multiply with calibration factor.
  v(:,1)=volts(:,1)*L;
  v(:,2)=volts(:,2)*D;
  v(:,3)=Data(k).Motion;

  % Create file in which data will be printed.

fid=fopen(['H:\Dos\Matlab\Output\',Data(
k).
filename,'.txt'],'wt');

  % Print labels in micromotion file.
  fprintf(fid,'%0s\t  %12s\t  %12s\n','Load
(kN)','Displacement (mm)','Motion (V)');

  % Print data in micromotion file.
  fprintf(fid,'%12.8f\t                %12.8f\t
%12.8f\n',v);

  % close text file
  fclose(fid);

  % Clear all values of loop.
  clear volts v
end
```

```
function[Data]=Output_Bone(Data)
% Creates an output file with all the
amplitudes of micromotion.
%
% Inputs: Data = amplitudes of the
micromotion in the 6 degrees of freedom.
% Outputs: Output text file with amplitude
of micromotion
% Emilie Crosnier
% University of Bath 21/11/13

% Find number of data sets to run through
S=size(Data,2);

% Create file in which data will be printed.
fid=fopen('H:\Dos\Matlab\Output\Bone
Micromotion.txt','wt');

% Create line of labels.
fprintf(fid,'%0s\t
%18s\n','Name','Micromotion Side',
'Micromotion Bottom');

% Loop through each data file.
for k=1:S

  % Print data in micromotion file.
  fprintf(fid,'%6s\t                %12.8f\t
%12.8f\n',Data(k).
filename,Data(k).Bone_Micromotion);

end
% close text file
fclose(fid);
```

```
function[Data]=Output_Micromotion(Dat
a)
% Creates an output file with all the
amplitudes of micromotion.
%
% Inputs: Data = amplitudes of the
micromotion in the 6 degrees of freedom.
```

```
% Outputs: Output text file with amplitude
of micromotion
%
% Emilie Crosnier
% University of Bath 22/02/13

% Find number of data sets to run through
S=size(Data,2);

% Create file in which data will be printed.
fid=fopen('H:\Dos\Matlab\Output\Micro
motion.txt','wt');

% Create line of labels.
fprintf(fid,'%0s\t %18s\t %12s\t %12s\t
%12s\t %12s\t
%12s\n','Name','x','y','z','0x','0y','0z');

% Loop through each data file.
for k=1:S

 % Print data in micromotion file.
 fprintf(fid,'%6s\t %12.8f\t %12.8f\t
%12.8f\t %12.8f\t %12.8f\t
%12.8f\n',Data(k).filename,Data
(k).Micromotion);

end
% close text file
fclose(fid);
```

```
function[Data]=Output_Graphs(Data)
% Creates graphs of the micromotion.
%
% Inputs: Data = amplitudes of the
micromotion and migration in the 6
degrees of freedom.
% Outputs: Output graphs of the
micromotion and migration
%
% Emilie Crosnier
% University of Bath 22/02/13

% Find number of data sets to run through
S=size(Data,2);

% Loop though each data file
for k=1:S

 % Create vector with micromotion data
 x=Data(k).Converted(:,1);
 y=Data(k).Converted(:,2);
 z=Data(k).Converted(:,3);
 X=Data(k).Converted(:,4);
 Y=Data(k).Converted(:,5);
 Z=Data(k).Converted(:,6);

 % Find the number of values.
 n=size(x,1);

 % Calculate time data
 for i=1:n;
  t(i,1)=(i-1)/100;
 end

 % Define size of plotting area.
 figure('units','centimeters','position',[3  2
45 24]);

 % Use defined size as print size.
 set(gcf,'PaperPositionMode','auto');
 % Plot micromotion and migration graphs
 [A]=subplot(2,3,1);
 plot(t,x,'k')
 axis tight
 xlabel('time (s)')
 ylabel('displacement (um)')
 title('X Translation')
 grid on

 [A]=subplot(2,3,2);
 plot(t,y,'k')
 axis tight
 xlabel('time (s)')
 ylabel('displacement (um)')
 title('Y Translation')
 grid on

 [A]=subplot(2,3,3);
 plot(t,z,'k')
 axis tight
 xlabel('time (s)')
 ylabel('displacement (um)')
 title('Z Translation')
 grid on

 [A]=subplot(2,3,4);
 plot(t,X,'k')
 axis tight
 xlabel('time (s)')
 ylabel('rotation (rads)')
 title('X Rotation')
 grid on
```

```
[A]=subplot(2,3,5);
plot(t,Y,'k')
axis tight
xlabel('time (s)')
ylabel('rotation (rads)')
title('Y Rotation')
grid on

[A]=subplot(2,3,6);
plot(t,Z,'k')
axis tight
xlabel('time (s)')
ylabel('rotation (rads)')
title('Z Rotation')
grid on

 % Save graph as jpeg

saveas(A,['H:\Dos\Matlab\Output\',Data(k
).
filename,'.jpg']);

 % Close plot
 close;

 % Clear all values
 clear datafile x y z X Z Y xs ys zs Xs Zs Ys n
i t A
end
```

Push-out

```
function[Data]=Pushout_Force(~)
% Analyses the data to obtain the push-out
force of the cup.
%
% Emilie Crosnier
% University of Bath 16/08/2013

% Create folder for output data.
mkdir('H:\Dos\Matlab\Output\');

% Select folder with datafiles to analyse
folder_name=uigetdir;
cd(folder_name);
filenames=dir('*.txt');

% Work through the different routines
[Data]=MaxForce(filenames,
folder_name);
[Data]=Output_Force(Data);
```

```
function[Data]=MaxForce(filenames,
folder_name)
% Analyses the data to obtain the push-out
force of the cup.
%
% Input: Raw data from the Instron.
% Output: structure with filenames and
maximum push-out force
%
% Emilie Crosnier
% University of Bath 16/08/2013

% Loop through each data file.
for k=1:length(filenames)

 % Open datafile and import data.
 cd(folder_name);
 datafile=filenames(k).name;
 A=importdata(datafile,'\t',10);

 % Remove .txt format from filename
 datafile=strrep(datafile,'.txt','');

 % Find maximum force.
 force=min(A.data(:,1));

 % Multiply force by calibration factor.
 cforce=force*-1.01;

 % Place data in output structure
 Data(k).filename=datafile;
 Data(k).force=cforce;

 % Clear all values of loop.
 clear force
end
```

```
function[Data]=Output_Force(Data)
% Analyses the data to obtain the push-out
force of the cup.
%
% Input: structure with filenames and
maximum push-out force.
% Output: output push-out force
%
% Emilie Crosnier
```

```
% University of Bath 16/08/2013

% Find the number of data set to run through:
S=size(Data,2);

 % Create file in which data points will be printed.
fid=fopen(['H:\Dos\Matlab\Output\Push-out Force.txt'],'wt');

% Create line of labels.
fprintf(fid,'%0s\t %12s\n','name','Force');

% Loop through each data file
for k=1:S

  % Print data in micromotion file.
  fprintf(fid,'%6s\t %12.8f\n',Data(k).filename, Data(k).force);

end
% close text file
fclose(fid);
```

Validation – 6DoF Measurement

```
function[Data]=Validation(~)
% Routine to test the validation data of 6 degree of freedom system
%
% Emilie Crosnier
% University of Bath 23/04/13

% Select folder with datafiles to analyse
folder_name=uigetdir;
cd(folder_name);
filenames=dir('*.txt');

% Define Target Geometry (in m).
ea=0.0538;
eb=0.0297;
ec=0.0295;
ed=0.0297;

% Define LVDT calibration factors (m/voltage).
m1=0.1004e-3;
m2=0.0999e-3;
m3=0.1008e-3;
m4=0.1008e-3;
m5=0.0985e-3;
m6=0.0991e-3;

% Work through different routines.
[Data]=Validation_Mean(filenames,folder_name);
[Data]=Conv_Matrix(Data,ea,eb,ec,ed,m1,m2,m3,m4,m5,m6);
[Data]=Validation_Output(Data,folder_name);
```

```
function[Data]=Validation_Mean(filenames,folder_name)
% Obtains the mean of each LVDT.
%
% Inputs: filenames = list of files to be analysed; folder_name = folder with files to analyse
% Outputs: Data = filenames and mean of each LVDT.
%
% Emilie Crosnier
% University of Bath 22/03/13

% Loop through each data file.
for k=1:length(filenames)

  % Open datafile and import data.
  cd(folder_name);
  datafile=filenames(k).name;
  A=importdata(datafile,'\t',10);

  % Remove .txt format from filename
  datafile=strrep(datafile,'.txt','');

  % Select only LVDT data.
  volts=A.data(:,3:8);

  % Calculate mean voltage of each LVDT
  m=mean(volts(:,1:6));

  % Place data in output structure
  Data(k).LVDT=m;
  Data(k).filename=datafile;
  clear datafile volts m A
end
```

```
function[Data]=Conv_Matrix(Data,ea,eb,ec,ed,m1,m2,m3,m4,m5,m6)
% Converts voltages recorded by LVDT sensors into translations and rotations of the cup
%
% Inputs: Data = voltages recorded by LVDT to analyse.
% Outputs: Data = adds translations and rotations of the cup in data matrix.
%
% Emilie Crosnier
% University of Bath 22/02/13

% Find number of data sets to run through
S=size(Data,2);

% Loop through each data file.
for k=1:S

 % Create matrix with needed data.
 volts=Data(k).LVDT;

 % Transpose the LVDT data to work with the matrix geometry.
  volts=volts';

 % Re-order rows to allow for LVDT labelling and multiply with calibration factor.
 v(1,:)=u(6,:)*m6;
 v(2,:)=u(2,:)*m2;
 v(3,:)=u(5,:)*m5;
 v(4,:)=u(3,:)*m3;
 v(5,:)=u(4,:)*m4;
 v(6,:)=u(1,:)*m1;

 % LVDTs 2 and 6 are in opposite sense to the co-ordinate axes therefore they need to be inverted
 v(1:2,:)=-v(1:2,:);

 % Find the number of measurements
 n=size(v,2);

 % Define conversion matrix with factors that allow for unequal geometry
 geo=[0 0 1 0 -ed 0;
  0 0 1 0 eb 0;
  0 1 0 -ea 0 ed;
  0 1 0 -ea 0 -eb;
  0 1 0 -(ea+ec) 0 0;
  1 0 0 0 ea 0];

 % Perform inverse matrix operation on each column of the data to obtain translations and rotations.
 for i=1:n;
  micro(:,i)=geo\v(:,i);
 end

 % Convert translation rows from meters to micrometres.
 newmicro(1:3,:)=1e6*micro(1:3,:);

 % Convert rotations rows from radians to degrees.
 newmicro(4:6,:)=(180/pi)*micro(4:6,:);

 % Transpose matrix for correct format
 tmicro=newmicro';

 % Place data in output structure
 Data(k).Converted=tmicro;

 % Clear all values of loop.
 clear volts u v n micro i newmicro tmicro
end
```

```
function[Data]=Validation_Output(Data,folder_name)
% Creates output files with the mean, standard deviation and standard error of the validation data
%
% Inputs: 6 degrees of freedom data
% Outputs: Output text files with mean, standard deviation and standard error
%
% Emilie Crosnier
% University of Bath 23/04/13

% Find number of data sets to run through
S=size(Data,2);


% Create Matrices
M0=zeros(1,6);
M1=zeros(1,6);
M2=zeros(1,6);
M3=zeros(1,6);
M4=zeros(1,6);
M5=zeros(1,6);
```

```
M6=zeros(1,6);
M7=zeros(1,6);
M8=zeros(1,6);

% Loop though each data file.
for k=1:S

 % Open data to sort
 M=Data(k).Converted;
 datafile=Data(k).filename;

 % Displacement measured
 if(datafile(10:12)=='0.0')
  M0=[M0;M];
 elseif(datafile(10:12)=='0.1')
  M1=[M1;M];
 elseif(datafile(10:12)=='0.2')
  M2=[M2;M];
 elseif(datafile(10:12)=='0.3')
  M3=[M3;M];
 elseif(datafile(10:12)=='0.4')
  M4=[M4;M];
 elseif(datafile(10:12)=='0.5')
  M5=[M5;M];
 elseif(datafile(10:12)=='0.6')
  M6=[M6;M];
 elseif(datafile(10:12)=='0.7')
  M7=[M7;M];
 elseif(datafile(10:12)=='0.8')
  M8=[M8;M];
 else
  error('Error in number');
 end
end

% Remove first line of zero
M0(1,:)=[];
M1(1,:)=[];
M2(1,:)=[];
M3(1,:)=[];
M4(1,:)=[];
M5(1,:)=[];
M6(1,:)=[];
M7(1,:)=[];
M8(1,:)=[];
% Create vector with measurement taken
A=[0.0; 0.1; 0.2; 0.3; 0.4; 0.5; 0.6; 0.7; 0.8];

% Create output matrix of mean
Output_Mean(:,1)=A;

% Calculate the mean voltage for each displacement measured and place in output matrix (remove mean if looking at individual results).
Output_Mean(1,2:7)=mean(M0(:,1:6));
Output_Mean(2,2:7)=mean(M1(:,1:6));
Output_Mean(3,2:7)=mean(M2(:,1:6));
Output_Mean(4,2:7)=mean(M3(:,1:6));
Output_Mean(5,2:7)=mean(M4(:,1:6));
Output_Mean(6,2:7)=mean(M5(:,1:6));
Output_Mean(7,2:7)=mean(M6(:,1:6));
Output_Mean(8,2:7)=mean(M7(:,1:6));
Output_Mean(9,2:7)=mean(M8(:,1:6));

% Create output matrix of standard deviation
Output_std(:,1)=A;

% Calculate the standard deviation for each displacement measured and place in output matrix.
Output_std(1,2:7)=std(M0(:,1:6));
Output_std(2,2:7)=std(M1(:,1:6));
Output_std(3,2:7)=std(M2(:,1:6));
Output_std(4,2:7)=std(M3(:,1:6));
Output_std(5,2:7)=std(M4(:,1:6));
Output_std(6,2:7)=std(M5(:,1:6));
Output_std(7,2:7)=std(M6(:,1:6));
Output_std(8,2:7)=std(M7(:,1:6));
Output_std(9,2:7)=std(M8(:,1:6));

% Create output folder
mkdir(folder_name,'Validation_Output');

% Define folder to save files.
cd('Validation_Output');

% Print mean in file
fid=fopen('Mean.txt','wt');

fprintf(fid,'%12s\t %12s\t %12s\t %12s\t %12s\t %12s\t %12s\t %12s\n','','x','y','z','0x','0y','0z');

fprintf(fid,'%12.8f\t %12.8f\t %12.8f\t %12.8f\t %12.8f\t %12.8f\t %12.8f\n',Output_Mean');

fclose(fid);

% Print standard deviation in file
fid=fopen('Std.txt','wt');
```

```
fprintf(fid,'%12s\t %12s\t %12s\t %12s\t
%12s\t                                %12s\t
%12s\n','','x','y','z','0x','0y','0z');

fprintf(fid,'%12.8f\t    %12.8f\t    %12.8f\t
%12.8f\t          %12.8f\t          %12.8f\t
%12.8f\n',Output_std');

fclose(fid);
```

APPENDIX 7. PUBLICATIONS

POSTER PRESENTATION – BORS ANNUAL MEETING, BATH, UK, 23-24 JUNE 2014

A Novel Method to Measure Micromotion of Acetabular Cups After Total Hip Replacement

E.A. Crosnier*, P.S. Keogh*, A.W. Miles*
*University of Bath, Bath, UK.

centre for orthopaedic biomechanics

Introduction

Initial stability is an important prerequisite for press-fit acetabular cups. A poorly fixed cup is prone to micromotion under physiological loading. If micromotion is above 150 µm, osseointegration is inhibited resulting in implant loosening [1].

Most methods used to assess the stability of cups are static, load-to-failure tests, which do not replicate *in vivo* conditions. Furthermore, these studies use foam models with a spherical cavity, which do not take into account the structural properties associated with the posterior and anterior columns of the acetabulum.

The aim of this study was to demonstrate that using simplified hemispherical cavities as an acetabular model over-estimates the stability of press-fit cups.

Materials and Methods

A cementless acetabular cup (54 mm Trident, Stryker, Mahwah, NJ, USA) was press-fitted into reamed polyurethane foam blocks (Sawbones, Malmö, Sweden; density = 0.48 g/cm³). Two acetabular cavity geometries were investigated: the first was a spherical cavity (Spherical, n = 6) and the second a more physiological geometry (Physiological, n = 6). The pinching effect of the acetabular columns, and the non-supportive areas of the acetabular notch and the radiolucent triangle (Figure 1) was modelled in Physiological [2].

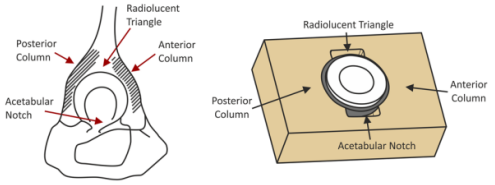

Figure 1 – Important anatomical features of the acetabulum labelled on both the pelvic bone (left) and the Physiological blocks used in this study (right).

Two methods were used to assess the primary stability of the cup. The first method measured the micromotion of the acetabular cup in six degrees of freedom when loaded under physiological conditions at 30° from the horizontal (1 Hz, 1000 cycles, 2.0 kN peak load) (Figure 2). The second method measured the peak failure load during uniaxial push-out following the above cyclic loading.

For statistical analysis, Wilcoxon signed ranks tests with a type I error probability of α = 0.05 were performed (SPSS, IBM, NY, USA).

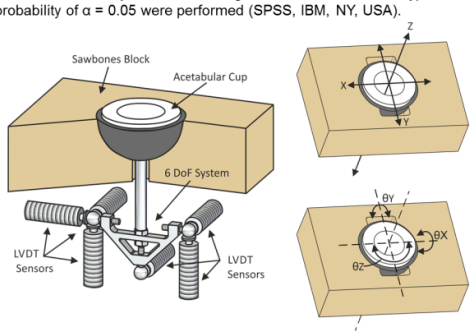

Figure 2 – Left: Setup to measure the six degree of freedom of the acetabular cup. Right: Six degrees of freedom of the acetabular cup.

Results

In general, there was a trend towards greater micromotion with Physiological compared to Spherical. However, the differences were statistically significant in the Z direction only (Figure 3). There was also a change in the relative direction of the micromotion: the motion in the Z direction became greater than the motion in the Y direction for Physiological compared to Spherical.

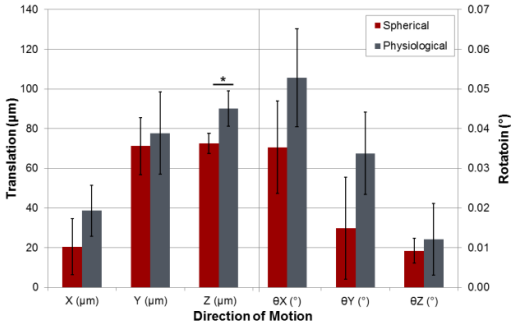

Figure 3 – Micromotion in six degrees of freedom of the cup under cyclic loading (1 Hz, 1000 cycles, 2.0 kN peak force) (mean ± sd). *Statistically significant difference ($p < 0.05$).

The peak push-out force was significantly greater for Spherical than Physiological (Figure 4).

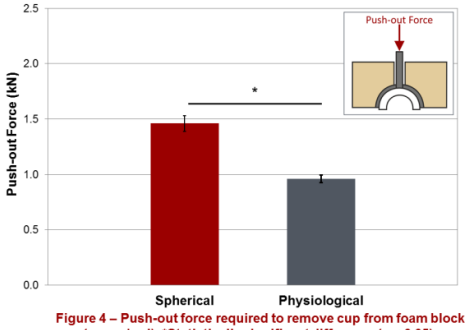

Figure 4 – Push-out force required to remove cup from foam block (mean ± sd). *Statistically significant difference ($p < 0.05$).

Discussion and Conclusions

The micromotions, which were always below 150 µm, obtained in this study were similar to published cadaveric results [3].

The differences in micromotion and in push-out force between Spherical and Physiological show that the geometry of the acetabular cavity has an important effect on the stability of the acetabular cup. The results suggest that the cup was less stable in Physiological than in Spherical. Studies using a spherical cavity therefore may over-estimate the stability of press-fit cups.

The novel measurement method used in this study, combined with the physiological acetabular model, provides an insight into how a cup behaves *in vivo*. With further development, this protocol could become a key method for pre-clinical testing.

UNIVERSITY OF BATH

References:
[1] Pilliar *et al.*, 1986, Clin Orthop Relat Res, 208
[2] Jin *et al.*, 2006, Proc IMechE Part H, 220
[3] Kwong *et al.*, 1994, J Arthroplasty, 9

Corresponding Author: E.A.Crosnier@bath.ac.uk, Department of Mechanical Engineering, University of Bath, Bath, BA2 7AY, UK

INITIAL STABILITY OF ACETABULAR CUPS UNDER PHYSIOLOGICAL CONDITIONS: COMPARING HEEL STRIKE TO THE FULL GAIT CYCLE

*Crosnier, E.A., *Keogh, P.S., *Miles, A.W.
*Centre for Orthopaedic Biomechanics, Department of Mechanical Engineering, University of Bath, UK

Introduction

The hip joint is subjected to cyclic loading during activities of daily living which can induce micromotion at the bone-implant interface of uncemented acetabular cups. Osseointegration, which is essential for long term implant survival, will occur when micromotion at this interface is below 40 µm and may occur up to 150 µm [1].

To date, studies investigating the micromotion of press-fit cups only report micromotion in one direction. Standard methods also maintain a static cup position throughout testing; usually at the angle of maximum resultant force during gait. Current methods therefore do not take into account the effect of dynamic motion of the hip on micromotion of the cup, nor do they investigate all six degrees of freedom (DoF) of motion.

The aim of this study was to assess press-fit cup micromotion in six DoF under physiological loading when heel strike is modelled compared to walking.

Materials and Methods

A cementless acetabular cup (Trident, Stryker) was implanted into polyurethane foam blocks (Sawbones, density=0.48 g/cm³) with a 1 mm press-fit. The blocks were manufactured to replicate important anatomical features of the acetabulum. A six DoF measurement system was rigidly attached to the bottom of the cup through the dome screw hole and micromotion was measured using six LVDT sensors (Figure 1).

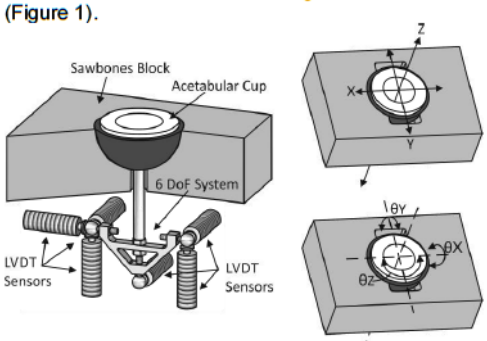

Figure 1 – Six DoF measurement system

The acetabular cup was orientated at 45° inclination. The micromotion of the cup was measured under two conditions: the first represented heel strike with the cup held statically at 30° flexion; the second simulated gait by dynamically flexing and extending the hip (30° flexion to -10° extension; 0.5 Hz) [2]. For all conditions, the cup was cyclically loaded to a peak load of 2.0 kN for 500 steps at 1 Hz. The loading cycles were synchronised with the flexion-extension movement in order to achieve a loading peak at both simulated heel strike and toe-off positions.

For statistical analysis, Mann-Whitney test were performed ($p < 0.05$).

Results

The X, Y, Z and θY micromotions were significantly greater when the cup was subjected to dynamic motion compared to static heel strike (Figure 2). There were no differences in θX and θZ micromotions. In all cases, the micromotion was less that 150 µm.

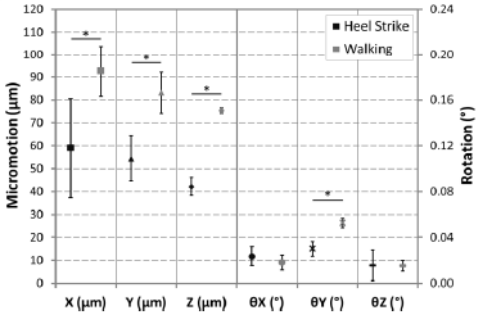

Figure 2 – Micromotion in six DoF of the cup for both heel strike and gait. Values expressed as mean and standard deviation.

Discussion

This study is the first to measure the micromotion in six DoF of a press-fit acetabular cup under both physiological loading conditions and dynamic hip motion. The results indicate that, compared to static tests, the micromotion of the cup increased under dynamic hip motion. The results also showed that all DoF need to be considered when investigating micromotion of the cup as substantial micromotion was seen in more than one direction.

Conclusion

Future pre-clinical tests investigating micromotion of press-fit acetabular cups should include dynamic motion and measure all DoF of the cup.

References

[1] Pilliar et al., 1986, Clin. Orthop. Relat. Res., 208
[2] Bergmann et al., 2001, J. Biomech., 34

Acknowledgement

This study was supported by the Victoria Wells PhD Studentship in collaboration with the Enid Linder Foundation.

Affiliations

*Emilie Crosnier, Department of Mechanical Engineering, University of Bath, Bath BA2 7AY, UK;
E.A.Crosnier@bath.ac.u

Bath Biomechanics Symposium: Current Issues and Future Opportunities in Orthopaedic Research
15th September 2014 University of Bath

PODIUM PRESENTATION – ISTA ANNUAL CONGRESS, KYOTO, JAPAN, 24-27 SEPT. 2014

Six degree of freedom assessment of micromotion of press-fit acetabular cups should be carried out under dynamic hip motion

E.A. Crosnier*, D.E. Scrivens*, P.S. Keogh*, A.W. Miles*

* Centre for Orthopaedic Biomechanics, Department of Mechanical Engineering, University of Bath, Bath, UK

Introduction

The hip joint is subjected to cyclic loading during activities of daily living and this can induce micromotion at the bone-implant interfaces of uncemented implants. Osseointegration, which is essential for long term implant survival, will occur when micromotion at these interfaces is below 40µm and may occur up to 150µm [1].

Studies investigating the micromotion of press-fit acetabular cups only report micromotions in one direction. Standard methods also maintain a static cup position throughout testing; usually at the angle of maximum resultant force during gait. Current methods therefore do not take into account the effect of motion of the hip on micromotion of the cup, nor do they investigate all six degree of freedom (DoF) of motion.

The aim of this study was to assess press-fit cup micromotion in six DoF under physiological loading when the cup is held statically and moved in flexion-extension.

Methods

A cementless acetabular cup (Trident, Stryker) was implanted into polyurethane foam blocks (Sawbones, density = 0.48g/cm³) with a 1mm press-fit. The blocks were manufactured to replicate important anatomical features, which model the acetabulum (Figure 1). A six DoF measurement system was rigidly attached to the bottom of the cup through the dome screw hole and micromotion was measured using six LVDT sensors (Figure 2).

The micromotion of the cup was measured under three conditions. Firstly, the cup was tested statically at 30° flexion, representing heel strike during gait; secondly, under dynamic motion simulating gait (30° flexion to -15° extension; 0.5Hz); and finally, under dynamic motion simulating stair climb (45° flexion to -15° extension; 0.5Hz) [2]. For all conditions, the cup was cyclically loaded to a peak load of 2.0kN for 1000 cycles at 1Hz. The loading cycles were synchronised with the flexion-extension movement in order to achieve a loading peak at both heel strike and toe-off positions.

Results

During all of the tests, micromotions in the medial-lateral and anterior-posterior directions, and the resultant of the anterior-posterior tilt, were above 40 µm (Figure 2). When tested statically, the micromotions in the medial-lateral and in the anterior-posterior directions were similar in magnitude. However, when the cup was subjected to dynamic motion, the micromotion in the anterior-posterior direction increased substantially in magnitude. It was at its highest during simulated stair climb. The anterior-posterior tilt also increased substantially under dynamic motion.

Discussion and Conclusions

This study is the first to measure the micromotion in six DoF of a press-fit acetabular cup under both physiological loading conditions and dynamic hip motion. The results indicate that, compared to static tests, the micromotion of the cup increases under dynamic hip motion. Results also showed that all DoF need to be considered when investigating micromotion of the cup as substantial micromotion was seen in more than one direction. Moving forwards, future pre-clinical tests investigating micromotion of press-fit acetabular cups should include dynamic motion and measure all DoF of the cup.

References

[1] Pilliar *et al.,* 1986, Clin. Orthop. Relat. Res., 208

[2] Bergmann *et al.,* 2001, J. Biomech., 34

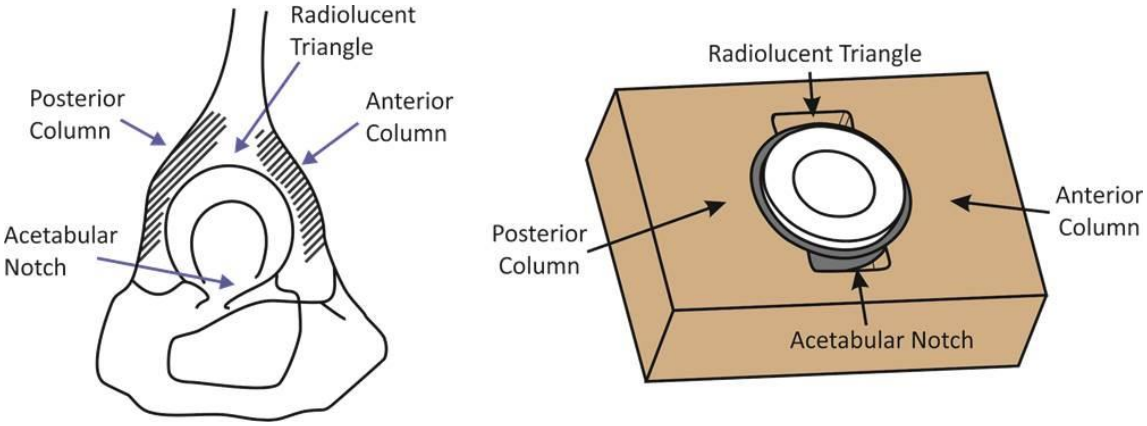

Figure 1 – Important anatomical features of the acetabulum labelled on both the pelvis (left) and the polyurethane foam blocks used in this study (right).

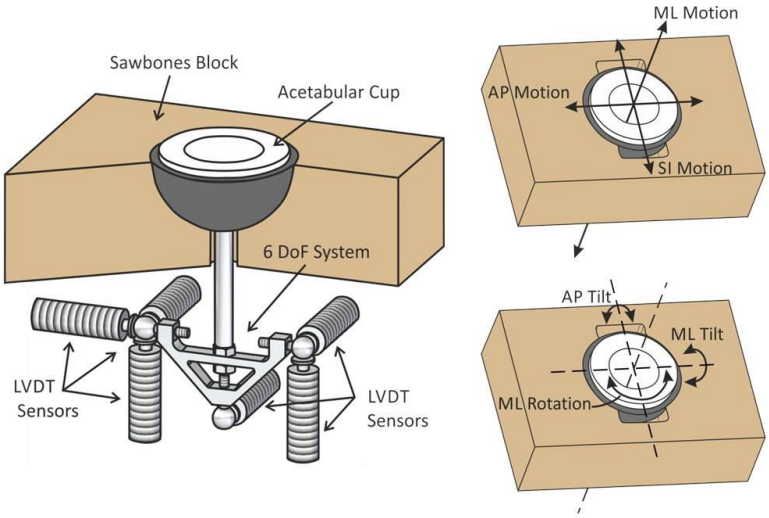

Figure 2 – Left: Setup to measure the six degree of freedom (DoF) of the acetabular cup. Right: 6 DoF of cup (AP = anterior-posterior, ML = medial-lateral, SI = superior-inferior)

JOURNAL ARTICLE

- Crosnier, E.A., Keogh, P.S., Miles, A.W., 2014. A novel method to assess primary stability of press-fit acetabular cups. *Proc. Inst. Mech. Eng. H*, 228(11), 1126-1134.